



This work is protected by copyright and other intellectual property rights and duplication or sale of all or part is not permitted, except that material may be duplicated by you for research, private study, criticism/review or educational purposes. Electronic or print copies are for your own personal, non-commercial use and shall not be passed to any other individual. No quotation may be published without proper acknowledgement. For any other use, or to quote extensively from the work, permission must be obtained from the copyright holder/s.



This work is protected by copyright and other intellectual property rights and duplication or sale of all or part is not permitted, except that material may be duplicated by you for research, private study, criticism/review or educational purposes. Electronic or print copies are for your own personal, non-commercial use and shall not be passed to any other individual. No quotation may be published without proper acknowledgement. For any other use, or to quote extensively from the work, permission must be obtained from the copyright holder/s.

**Exploring the erythrocyte invasion–blocking effect of modified
heparin and heparin mimetics in the human malaria parasite**

Plasmodium falciparum

Muqdad Kareem Hmoud

PhD Thesis

Keele University

October, 2019

ABSTRACT

Despite the efforts in malaria eradication and elimination, malaria still poses a global challenge to health that, through the spread of antimalarial resistance, highlights an urgent need for new approaches for malaria treatment. Heparin and sulphated glycosaminoglycans (GAGs) have been reported to have inhibition activity against intraerythrocytic stages of *P.falciparum in vitro* by (i) disrupting rosette formation, (ii) reversing cytoadhesion to human endothelial cell lines and (iii) blocking merozoite invasion. The extracellular form merozoites are the target of sulphated GAG inhibitors and, given relative ease of access to this stage and its essential activity in propagating an infection, an attractive target of drug development. However, due to the anticoagulation property and potential risk of heparin-induced thrombocytopenia, heparin's development as a potential adjunct therapy was halted.

A rapid and scalable *in vitro* evaluation of the inhibitory activity of sulphated GAGs is a challenge using standard fluorescent assays of parasite growth as the dyes interact with the large negatively charged sulphated GAGs. In this study, we report the development of a robust and scalable luciferase-based assay, including the preparation of a new transgenic *P.falciparum* parasite strain, to determine whether sulphated GAGs have potential growth inhibition activity. Two distinct *P.falciparum* strains (Dd2^{luc} & NF54^{luc}) were also used to explore the staging of the inhibition activity during the reinvasion process. This study uses GAGs from a range of sources; chemically modified heparins, low molecular weight heparins, and GAGs from animal, plant, marine and microbial sources.

Sulphated GAGs inhibitors with good invasion-blocking potency (EC₅₀ ranging between 2-10µg/ml) have been identified and their anticoagulation activity was shown to be reduced

compared with unfractionated heparin. The staging of the effect of these compounds shows that they appear to have a profound effect on merozoite egress from an infected erythrocyte-inducing what is called here a clustered merozoite phenotype. This inhibitory effect hasn't been recognized in previous studies for these GAGs, with only one other report of merozoite egress inhibition by unfractionated heparin available. This thesis highlights routes forward towards developing potent GAG inhibitors of merozoite release and the potential of a number of GAGs identified in this study as chemical tools to study the biology of merozoite egress from the erythrocyte. This study also discusses the implications in developing heparin mimetic with low or no anticoagulation activity, to be used as an adjunct therapy for the treatment of severe malaria.

CONTENTS

Abstract	II
Contents	IV
Abbreviations	IX
Acknowledgement	XIV
Chapter one: Introduction	1
1.1 The burden of malaria.....	1
1.2 <i>P.falciparum</i> life cycle.....	3
1.3 Clinical features of malaria.....	9
1.4 Malaria treatment.....	15
1.5 Malaria prevention.....	17
1.6 Inhibition of <i>P.falciparum</i> merozoite invasion/egress by GAGs inhibitors.....	20
1.7 Glycosaminoglycans.....	25
17.1 Heparan and heparin sulphate.....	26
1.7.2 Dermatan sulphate / Chondroitin sulphate.....	27
1.7.3 Keratan sulphate (KS).....	28
1.7.4 Hyaluronan (Hyaluronic acid)	29
1.8 A role for GAGs in mediating <i>P.falciparum</i> pathogenicity.....	29
1.9 Objectives of this study.....	30
Chapter two: Materials and Methods	31
2.1 Materials	31
2.2 Material stock(reagents).....	31
2.3 List of equipment	34

2.4 Cell culture materials.....	35
2.4.1 Preparation of complete and incomplete <i>P. falciparum</i> cell culture medium.....	35
2.4.2 Preparation of human serum and erythrocytes.....	35
2.5 <i>P.falciparum</i> cell culture methods.....	36
2.5.1 <i>In vitro</i> intraerythrocytic continuous culture of <i>P.falciparum</i>	36
2.5.2 Sorbitol-synchronisation of <i>P. falciparum</i> culture.....	36
2.5.3 Storage of <i>P. falciparum</i> culture.....	37
2.6 Transfection and monitoring of luciferase expression.....	38
2.7 Isolation of DNA from <i>P.falciparum</i>	39
2.7.1 Phenol-chloroform DNA extraction method.....	39
2.7.2 QIAamp® DNA extraction method.....	40
2.8 Assays of growth inhibition in intraerythrocytic <i>P. falciparum</i>	41
2.8.1 Multiwell plate based assays of growth inhibition in <i>P. falciparum</i>	41
2.8.2 Luciferase Assay.....	42
2.8.3 Malaria Sybr Green I fluorescence (MSF) Assay	43
2.8.4 Flow cytometry based assays of growth inhibition in <i>P. falciparum</i>	43
2.9 Monitoring the time course of <i>P.falciparum</i> intraerythrocytic development in the presence of GAGs.....	46
2.10 Molecular Methods.....	48
2.10.1 Plasmid DNA transformation of <i>Escherichia coli</i>	47
2.10.2 Plasmid DNA minipreparation from <i>E. coli</i>	47
2.10.3 Maxi plasmid DNA preparations from <i>E. coli</i>	48
2.10.4 Restriction digests	49
2.10.5 Agarose gel electrophoresis and imaging	49
2.10.6 Purification of DNA fragments from agarose gel.....	50

2.10.7 DNA ligations.....	51
2.10.8 Polymerase chain reaction (PCR)	51
2.10.9 Quantitative real-time PCR (qRT-PCR).....	52
2.10.10 Probe preparation for southern blotting.....	53
2.10.11 Southern blotting.....	54
2.11 Prothrombin time (PT) assay.....	56
2.12 Activated thromboplastin time (aPTT) assay.....	56
Chapter three: Generation and validation of NF54^{luc} transgenic parasite strain expressing a trophozoite stage-specific luciferase reporter.....	57
3.1 Introduction	57
3.2 Results.....	61
3.2.1 Comparison of plate-based fluorescence versus bioluminescence assays of intraerythrocytic growth inhibition using glycosaminoglycans.....	61
3.2.2 Generation the NF54 ^{luc} transgenic parasite.....	63
3.2.3 Validation of the NF54 ^{luc} transgenic parasite.....	67
3.2.4 NF54 ^{luc} transgenic parasites do not appear to lose the reporter plasmid following a period of drug-selection removal.....	73
3.2.5 NF54 ^{luc} transgenic parasites appear likely to maintain episomal plasmid after removal of drug selection pressure.....	76
3.2.6 Stage-specific inhibition of <i>in vitro</i> growth in NF54 ^{luc} using heparin.....	81
3.3 Discussion.....	83

Chapter Four: Investigating the erythrocyte invasion-blocking potential of Low Molecular Weight Heparins (LMWH).....	88
4.1 Introduction.....	88
4.2 Results.....	96
4.2.1 Low molecular weight heparins (LMWHs) inhibit intraerythrocytic parasite growth <i>in vitro</i>	96
4.2.2 Correlating the Luciferase growth assay data with flow cytometry Growth Inhibition Assays (GIA).....	102
4.2.3 LMWHs inhibit parasite growth by blocking erythrocyte invasion.....	106
4.2.4 Exploring the inhibition of erythrocytic rupture and merozoite release by LMWH and heparin	110
4.3 Discussion.....	114
Chapter five: Investigation <i>in vitro</i> the growth inhibitory and invasion blocking effects of heparin mimetics in <i>P.falciparum</i>	126
5.1 Introduction.....	126
5.2 Results.....	132
5.2.1 Sulphated polysaccharides and chemically modified heparin inhibit <i>P.falciparum</i> growth <i>in vitro</i>	132
5.2.2 Determination of EC ₅₀ for the most potent inhibitors of growth.....	140
5.2.3 Exploring the stage-specificity of growth inhibition by CMH9 and sulphated GAGs.....	142
5.2.4 Assessing the anticoagulation activity of CMH9 and sulphated GAGs.....	145
5.2.5 Initial evaluation of the anti-plasmodial activity of marine-derived glycosaminoglycans.....	157
5.3 Discussion.....	164

Chapter Six: Overall discussion and perspectives	178
References.....	187
Appendix I (Chapter five)	216
Appendix II (Chapter five)	219

ABBREVIATIONS

ACTs	Artemisinin Combination Therapies
aPT	Activated Partial Thromboplastin
aPTT	Activated Partial Thromboplastin Time
bp	Base Pair
BSA	Bovine Serum Albumin
BSD	Blasticidin S Hydrochloride
CI	Confidence Intervals
CM	Cerebral Malaria
CMH	Chemically Modified Heparin
CO ₂	Carbon Dioxide
CQ	Chloroquine
CQS	Chloroquine Sensitive
CSA	Chondroitin Sulphate A
CSC	Chondroitin Sulphate
DNA	Deoxyribonucleic Acid
DHFR	Dihydrofolate Reductase
hDHFR	Human Dihydrofolate Reductase
EC ₅₀	50% Effective Concentration
EBA-175	Erythrocyte Binding Antigen-175
EDTA	Ethylene Diamine Tetra Acetic Acid
EtBr	Ethidium Bromide

FSC	Forward Scatter
FV	Food Vacuole
FTIR	Fourier Transform Infrared Spectroscopy
G6PDH	Glucose-6-Phosphate Dehydrogenase
GAGs	Glycosaminoglycans
GIA	Growth Inhibition Assay
GLURP	Glutamate-Rich protein
gp	Glycophorin
gDNA	Genomic DNA
GM	Genetically Modified
GSK	GlaxoSmithKline
Hb	Haemoglobin
HCl	Hydrochloric Acid
HCT	Haematocrit
HIT	Heparin Induce Thrombocytopaenia
HIV	Human Immunodeficiency Virus
Hrs	Hours
HTA	Human Tissue Authority
HTS	High Throughput Screening
ICM	Immune Clusters Merozoites
IE	Infected Erythrocytes
iRBCs	Infected Red Blood Cells
IRS	Indoor Residual Spraying
ISTM	Institute for Science and Technology in Medicine

ITNs	Vector controls Insecticide Treated Nets
L	litres
Lab	Laboratory
LAH	Low anticoagulant heparin
LB	Luria Broth
LMWHs	Low molecular weight heparin
Luc	Luciferase
M	Molar
mGAGs	Marine Glycosaminoglycans
mins	minutes
mL	millilitre
mM	millimolar
MSF	Malaria Sybr Green I Fluorescence
MSPs	Merozoite Surface Protein
MW	Molecular weight
MMV	Medicines for Malaria Venture
N ₂	Nitrogen
NaCl	Sodium Chloride
NaOH	Sodium Hydroxide
nM	nanomolar
O ₂	Oxygen
ORh+	Type-O-Rhesus Positive
<i>P.falciparum</i>	<i>Plasmodium falciparum</i>
<i>Pfpcna</i>	Proliferating Cell Nuclear Antigen

PBS	Phosphate Buffer Saline
PCA	Principal Component Analysis
PCR	Polymerase Chain Reaction
<i>Pf</i> ACT1	<i>Plasmodium falciparum</i> Actin I
<i>Pf</i> EMP1	<i>P. falciparum</i> Erythrocyte Membrane Protein 1
<i>Pf</i> HRP2	<i>P. falciparum</i> Histidine-Rich Protein 2
pLDH	Parasite lactate Dehydrogenase
PMH	Porcine Mucosal Heparin
PV	Parasitophorous Vacuole
PVM	Parasitophorous Vacuole Membrane
qPCR	Quantitative Polymerase Chain Reaction
RBCs	Human Red Blood cells
RLU	Relative Light Units
RNA	Ribonucleic Acid
RT	Room Temperature
RT-PCR	Real-Time Polymerase Chain Reaction
sdH ₂ O	Sterile Distilled Water
Sec	Seconds
TCAMS	Tres Cantos Antimalarial Compound Set
U/mL	Unit Per Millilitre
UTR	Untranslated Region
v/v	Volume per volume
-ve	Negative Control
+ve	Positive Control

w/v	Weight Per Volume
WBCs	White Blood Cells
WHO	World Health Organization
A	Alpha
β	Beta
γ	Gamma
κ	Kappa
μl	Microlitre
μM	Micromolar
$^{\circ}\text{C}$	Degrees Celsius

Acknowledgements

All praise is due to **Allah** without whom nothing is possible.

Foremost, I would like to express my deepest gratitude and sincere thanks to my supervisor Prof. Paul Horrocks for his continuous support, his patience, motivation and immense knowledge passed on to me. His guidance helped me throughout my research and writing of this thesis. I could not imagine having a better mentor as my supervisor. An endless thanks to my inspirational supervisor, a great scientist, who taught me how to be a scientist.

Also, my thanks to my advisor Dr Mark Skidmore for his support and for his contribution in the development and synthesis of compounds that are the subject of my thesis. I would also like to gratefully acknowledge the supply of materials and data from colleagues in Dr Skidmore's team, particularly Courtney Mycroft-West, Lynsay Cooper and Antony Devlin. I also thank Dr Helen Price for her support and guidance during weekly seminars and for help during my research that she was always ready to offer.

I would thank all my fellow PhD students and postdoctoral researchers, past and present, within the Horrocks Lab and in the wider Institute for Science and Technology in Medicine and School of Life Sciences for their help and cooperation.

I gratefully acknowledge and thank with a deep sense of respect my sponsor and my uncle Mr Fayadh Hassan for his priceless support and encouragement during my research and my whole life. I would also like to thank my uncle Dr Jassim Almusawi for his support during my study.

I also acknowledge with heartiest gratitude my mother, who spent her life waiting to see this moment, and to my father, who without him, I will not be, and to my brother. Thanks to my family for their boundless love, endless support and encouragement.

My thanks also goes to my three little stars whose enlighten my life; Shams, Zahraa and Ali. Endless thanks to my wonderful wife- no words can appreciate her priceless support - I can't imagine how I could reach my goal and finish my PhD without her.

Finally, I would thank all my friends in Iraq for their support and encouragement.

Chapter one: General Introduction

1.1 The burden of malaria

Malaria is one of the most impactful infectious diseases that has shaped human life. It is a parasitic protozoan vector-transmitted disease that belongs to the Apicomplexan phylum, transmitted by *Anopheles* mosquitos to a vertebrate host (White et al., 2014). Malaria is endemic in over 87 countries worldwide, with some 219 million cases causing 435,000 deaths in 2017 (WHO 2018). The geography of malaria disease extends from the tropical areas of South American countries to South-east Asia with 90% of malaria cases reported in Sub-Saharan Africa; 85% of deaths are in the same endemic area, mostly involving children under five years old (White et al., 2014) (Figures 1.1 and 1.2). To control malaria infection and decrease the mortality rate, novel approaches are needed such as the development of more active antimalarial drugs that address the increase in drug resistance, effective insecticides and the development of an effective vaccine (Hill., 2011). Five major parasite species cause malaria infection; *P. falciparum*, *P. vivax*, *P. malaria*, *P.ovale*, and *P. knowlesi* (Kantele & Jokiranta., 2011). *P. falciparum* presents the most virulent parasite among the rest of the *Plasmodium* species, it is responsible for the majority of malaria deaths and the main cause of severe malaria which is a multi-organ infection that leads to complicated consequences such as cerebral malaria, severe anaemia, jaundice, acidosis, pulmonary oedema, renal dysfunction/kidney injuries and low birth weight in pregnant women.

P.falciparum distribution intersects with *P.vivax* geographically in endemic areas where the infection spreads. *P.vivax*, however, is not typically found in West Africa due to inability to infect Duffy-Blood-Group negative reticulocyte where this trait is predominant in this area

(Mandal., 2014). It is estimated that 25% of reported cases outside Africa caused by *P.vivax* (Price et al., 2007). That makes *P. vivax* widely spread geographically although being less lethal than *P.falciparum* (Guerra, Snow, & Hay, 2006). *P. falciparum* is responsible for 80% of malaria deaths (severe malaria) with the majority occurring in children under five years worldwide (WHO, 2018).

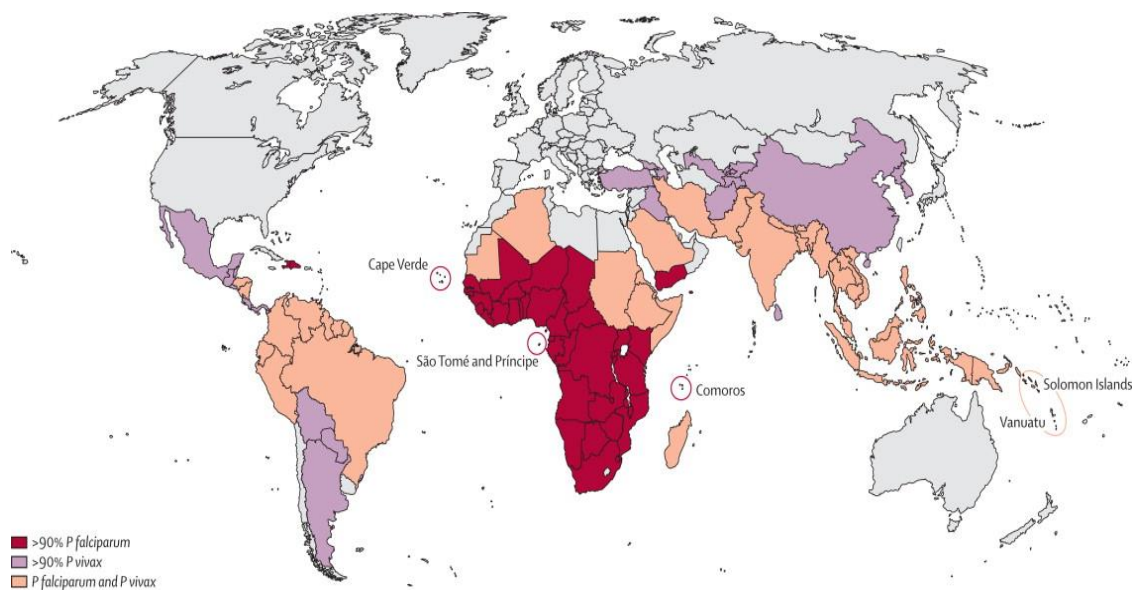


Figure 1.1 Map illustrating the endemic areas of *P.vivax* and *P.falciparum* (Source: Feachem et al., 2010).

Malaria is also a travel-associated disease, imported from endemic areas to non-endemic areas and carried through the tourist, non-government aid or armed forces personnel (Genton et al., 2008). The severity of the disease depends on factors such as age and immune status. (Mandal, 2014).

The main vector of malaria infection is mosquitoes of *Anopheles* genus. There are over 400 *Anopheles spp.* although only 25 of them have been found to be good vectors of malaria (Sinka et al., 2012). *Anopheles gambiae* in Africa is an excellent example of a vector for malaria

transmission to humans and are characterised as tolerant to habitat changes having longevity, surviving in highly dense tropical areas and reproducing rapidly (White et al., 2014).

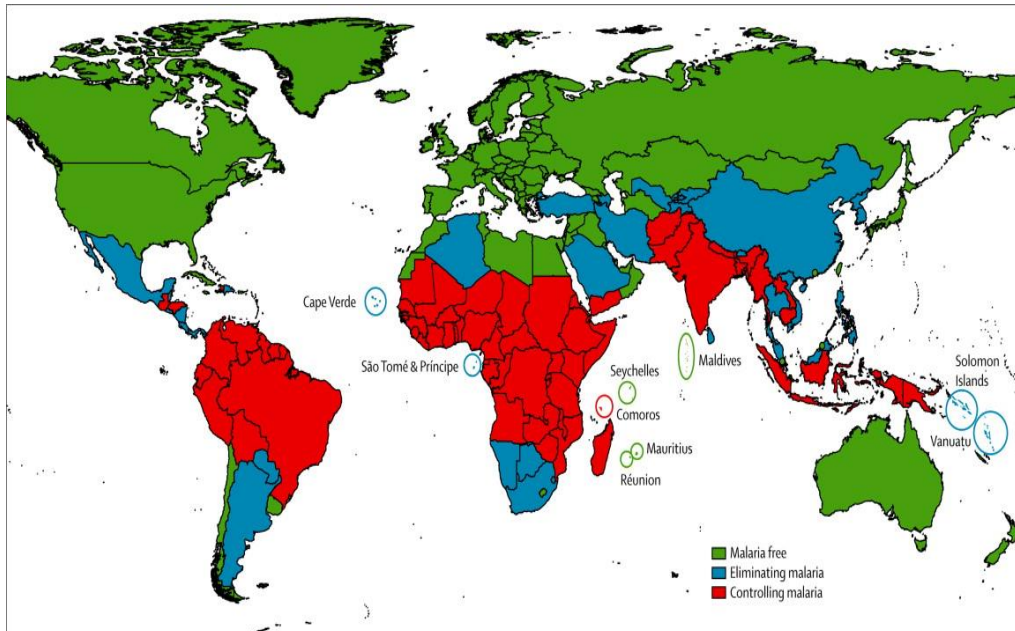


Figure 1.2 Map illustrating the distribution of malaria around the world (Source: Cotter et al., 2013).

1.2 *P. falciparum* life cycle

The life cycle of *P. falciparum* requires a vertebrate host and mosquito vector to survive and to complete its cycle (White et al., 2014). The journey of the parasite (illustrated in Figure 1.3) starts as a sporozoite transmitted from the mosquito bite to human skin, with a few hundred sporozoites injected into the bloodstream where they migrate to infect hepatocytes and to start the first part of the asexual stages of infection. At the pre-erythrocytic (intrahepatic) stage no clinical symptoms occur, making early diagnosis of the disease challenging (Arama & Troye-Blomberg., 2014).

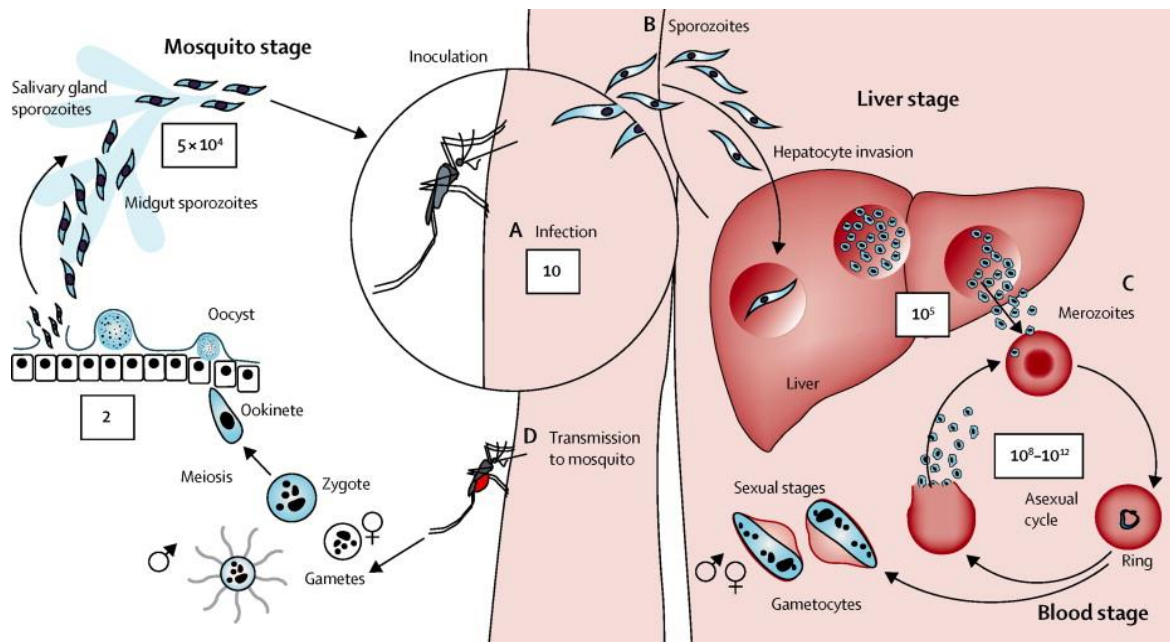


Figure 1.3 Asexual and Sexual life cycles of *Plasmodium falciparum* in mosquito and the human host. (A) Parasite life cycle begin when motile sporozoite injected into human skin during mosquito of anophelines blood meal. (B) sporozoites seek their way to the liver and each sporozoite infect hepatocyte, multiply and stay in the liver for one week with no obvious sign of disease. (C) Hepatocyte schizonts rupture and release thousands of merozoites into blood circulation, starting asexual life cycle (blood-stage life cycle), illness symptoms occur at blood-stage and develop later to severe disease if not been treated. Blood stage takes roughly 48 hrs to be completed, where parasite multiplies and develop into different forms (ring, trophozoite and schizont). (D) Some parasites develop into gametocyte (a sexual form of the parasite), taken by anopheline mosquito during blood-feeding, and replicate sexually to produce a zygote, then develop into, Ookinete and Oocyst. Oocyte rupture, releasing sporozoites which migrate to mosquito salivary gland, waiting for next mosquito blood-feeding to be inoculated into a new human host. The entire life cycle of *P.falciparum* takes approximately one month to be completed. (source: white et al., 2014).

A few hundred of sporozoite parasites will invade hepatic cells after their injection into blood circulation. But one study found that *P.falciparum* does not inject from a mosquito of *anopheles* directly into the blood circulation but into the dermis first (Hafalla, Silvie, & Matuschewski., 2011). Sporozoites usually take from between 15 minutes to a few hours before invading hepatocytes. Sporozoites travel to the liver through their continuous gliding movement from the skin to arrive in the blood circulation to penetrate and traverse many of the defensive hepatic

macrophages (Küpfers cells) (White et al., 2014). The mobility of parasites is powered by the actomyosin motor and mediated by a group of proteins TRAP (thrombospondin-related anonymous protein), that enable the parasite to invade both salivary glands of the mosquito and human host. Ultimately, the invasive sporozoites grow, feed and multiply in the new host's liver cells to form thousands of merozoites; roughly 10000 to 30000 merozoites will be produced within 5 to 7 days. Eventually the merozoites burst from the liver hepatocytes into bloodstream and invade erythrocytes (Greenwood et al., 2008).

On completion of up to 14 days of intrahepatic growth and multiplication, merozoites are released (Figure 1.4) from the hepatocytes through merosomes that bud off from infected hepatocytes (Graewe et al., 2011). Merozoites released within the blood circulation are available to infect an erythrocyte, which starts next step of infection termed the (intra)erythrocyte stage or blood-stage (Figure 1.5) which includes the commonly described ring, trophozoite and schizont morphological stages (Weatherall et al., 2002). The invasion of erythrocytes is a multi-step process that takes minutes only to invade the red blood cells by merozoite, without lysing them, due to the presence of specialised organelles that prevent lysis (White et al., 2014). Three membrane-bound granules that play a vital role in the attachment process of the parasite are rhoptries, micronemes and dense granules that help the parasite to attach on the surface of red blood cells.

During erythrocyte invasion, the merozoite reorients to bring the apical end into contact with the RBC cell membrane to form an irreversible close-junction between the parasite and blood cell. The merozoites release the contents of their membrane bound vesicles which include a range of adhesive proteins. After entry, the parasite starts a new life cycle consists of three stages: ring, trophozoite, and schizont. *P.falciparum* and like other *Plasmodium spp.* utilises haemoglobin as a source of amino acids for anabolism (Weatherall et al., 2002).

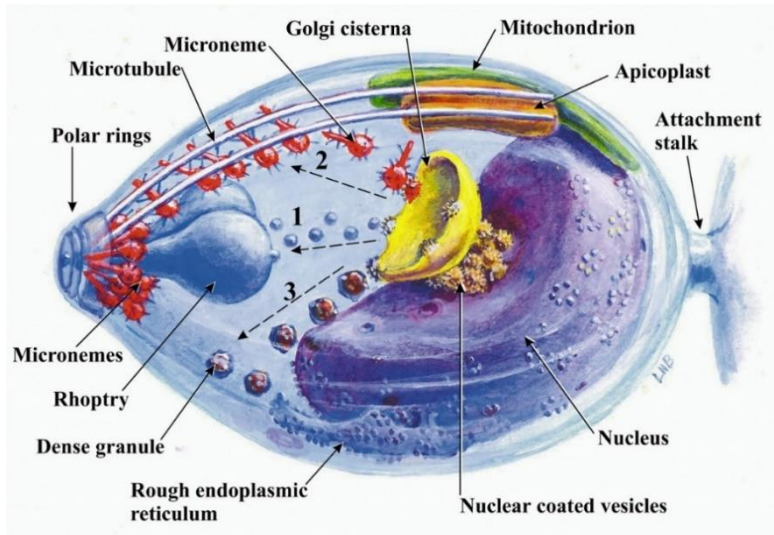


Figure 1.4 Illustration of a *P.falciparum* merozoite (Source: Bannister et al., 2003).

After 48 hours of the invasion, schizonts form and release up to 30 to 40 daughter merozoites to invade a new erythrocyte as apart of its blood life cycle. The merozoite invasion to erythrocyte is a multi-step process and it is crucial when merozoite distinguish between erythrocytes and other cell types and for parasite survival (Bannister & Sherman 2009). Merozoite invasion is very rapid, it takes 15 seconds to complete the invasion, and that because merozoite is the only extracellular form of parasite blood stage life cycle and become a target to immune cells (Boyle et al., 2013).

The early attachment of merozoite to erythrocyte is likely to be supported by MSPs (Merozoite Surface Proteins) which cover the merozoite surface. Moreover, the interaction of merozoite adhesive proteins such as reticulocyte-binding homologue (PfRh) and erythrocyte binding ligands (EBLs) also play important roles in parasite-host interaction (Satchwell., 2016). After attachment, the merozoite reorients so that the apical tip become in direct contact with the erythrocyte membrane. The merozoite then forms a tight junction between the parasite and erythrocyte (Cowman & Crabb., 2006). The parasitophorous vacuole is formed

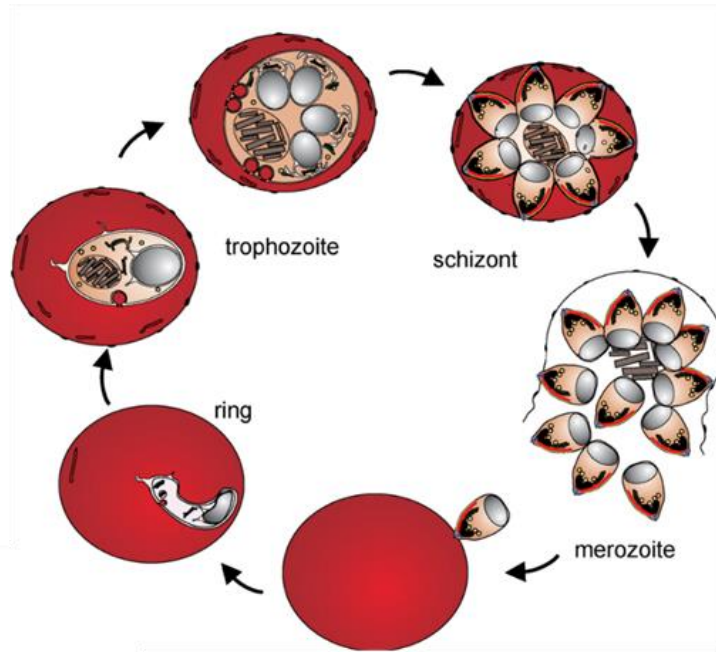


Figure 1.5 Schematic illustration of *P.falciparum* intraerythrocytic lifecycle. Merozoite invades erythrocyte and subsequently develop through three distinct stages, ring, trophozoite and schizont where parasite divided into roughly 30 merozoites then rupture to invade a fresh erythrocyte. Full blood stage life cycle takes approximately 48 hrs. (Source Tilley et al., 2011).

now and an actin-myosin motor drives the inward mobility of merozoite. Rhoptries and micronemes release proteins which are associated with and form a tight junction which moves around merozoite surface powered by this actin-myosin motor. Finally, the parasite seals parasitophorous vacuole, discharge dense granules and transform into a ring stage (Figure 1.6).

The growing parasite inside the erythrocyte catabolizes the haemoglobin, reduces the deformability of the host cell by changing the actin-spectrin skeleton that changes the morphology of red cells as well as increases the permeability to support import of nutrients and expel waste products (Arama & Troye-Blomberg, 2014).

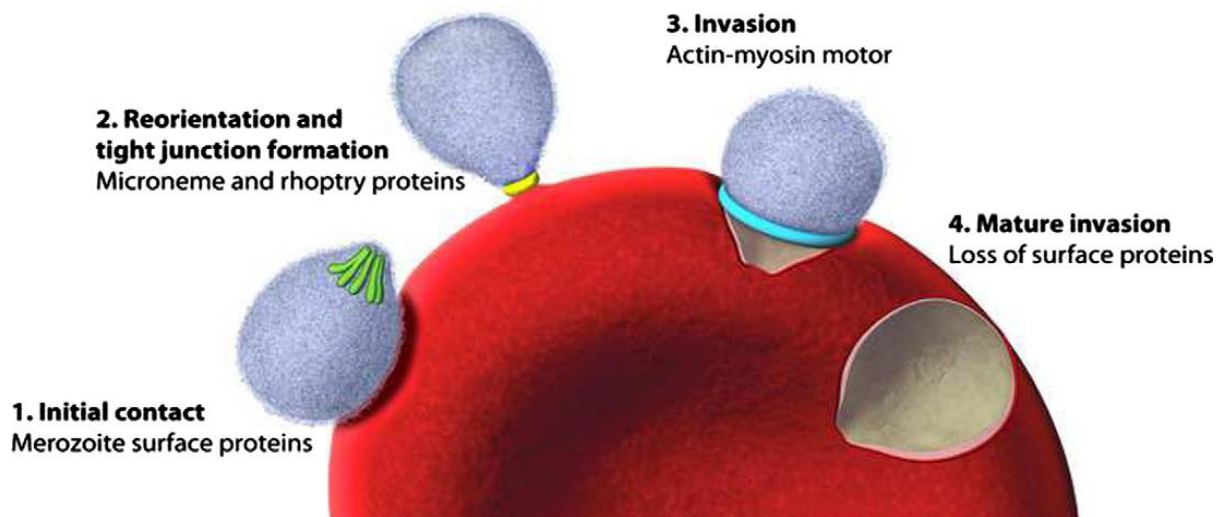


Figure 1.6: Schematic representing the invasion steps of the *P.falciparum* merozoite into an erythrocyte. (1) parasite establish attachment with erythrocyte surface, MSPs mediated the first contact followed by attachment proteins such as (PfRh) and (EBL). (2) Parasite re-orient and proteins released from micronemes and rhoptries which leading to form a tight junction. (3) Actin-myosin power-driven merozoite to invade erythrocytes. (4) invasion lead in loss of merozoite surface protein and develop intraerythrocytic development cycle (Boyle et al., 2013).

In a suspected adult infected person, the parasite population can reach more than 100 million in the blood circulation. The asexual blood-stage takes approximately 48 hours in *P.falciparum*, *P.vivax*, and *P. ovale*. While it takes 72 hours in *P.malariae* and 24 hours in *P.knowlesi* (Arama & Troye-Blomberg., 2014). The blood cycle is associated with all of the signs and symptoms of the disease, including a range of general features such as fever, fatigue, muscle and joint pain, vomiting and abdominal pain. Infection with *P.falciparum* shows further complications associated with unique aspects of pathological development based on its cytoadhesive properties, with cerebral malaria as a particular example of this (Cowman, Berry, & Baum., 2012).

After the blood-stage cycle, gametocytes are formed that can be transmitted to a mosquito vector during a blood meal event- within the midgut, these gametocytes undergo their final maturation. The male gametocyte divides into many flagellated microgametes which are then

available to fertilize female macrogametes. Fertilization forms a zygote and further development takes place to form an ookinete within 18 hours from a blood meal. The slowly motile ookinete penetrates the midgut wall to form an oocyst. Within this structure, meiosis occurs to generate large numbers of haploid sporozoites (Marreelli & Castelli., 1999). The sporozoites are released from oocysts and travel through the haemocoel to infect the mosquito salivary gland be available to reinitiate and infection in a new human host.

1.3 Clinical features of malaria

The clinical symptoms of malaria disease are associated with blood-stage infection, however, uncomplicated malaria is usually asymptomatic. Often, the common signs of malaria disease are unspecific and may be shared with other diseases, although a laboratory investigation with a suspected person in an endemic area will confirm whether malaria infections are present. The initial symptoms include fever, headache, fatigue, muscle weakness, nausea, vomiting and abdominal pain (Weatherall et al., 2002). Most patients with uncomplicated malaria infection show signs of anaemia and in children, the liver can become larger after several days of infection. Meanwhile, jaundice is very clear in adults infected with malaria (White et al., 2014).

The majority cases of uncomplicated malaria symptoms present with nonspecific signs and they are common among most *Plasmodium spp*, including fever, jaundice, nausea, diarrhoea, hyperventilation and vomiting. Signs occur in three stages (cold, hot and sweating), that will repeat every 36 or 48 hours. Uncomplicated malaria means that the patient circulating parasites with no symptoms (Bartoloni & Zammarchi., 2012). Most infected persons with uncomplicated malaria have few physical findings, mild anaemia and liver enlargement (after several days of incubation especially in children). Uncomplicated malaria infection may lead to severe malaria that threatens human life if the disease is not treated (White et al., 2014). Many factors influence

on the duration of malaria infection such as antimalarial drugs, immune status of the host, the way of transmission and the species of parasite (Bartoloni & Zammarchi., 2012). In uncomplicated malaria, the incubation period of *P.malaria* and *P.vivax* may take up to two weeks while a more variable incubation period for *P.falciparum* (between 9 to 30 days) may be expected (Bartoloni & Zammarchi., 2012).

Severe malaria is defined as a dysfunction of one or more multiple vital organs of the host due to infection with the malaria parasite (WHO, 2012). The majority of cases of severe malaria results from infection with *P.falciparum* and rarely with *P.vivax* or *P.ovale*. The features of severe malaria may include renal failure, pulmonary oedema, cerebral malaria, severe anaemia, and metabolic acidosis; these complications of severe malaria may lead to death if not treated as soon as possible (Gachot & Ringwald., 1998). Severe malaria could increase death cases due to two pathways: first, severe anaemia leading to hypoxia and cardiac failure and second cerebral malaria (Menendez, Fleming, & Alonso., 2000). Severe malaria is a consequence of complications from the progression of malaria infection. In severe malaria, the immune system of the host fails to keep the infection under control. The clinical manifestations of severe malaria depend on the age and the clinical status of the patient, severe anaemia and hypoglycaemia are common in children, meanwhile, kidney injury and jaundice are more common in adults (Gachot & Ringwald., 1998). Severe malaria leads to serious medical conditions which include many pathological changes:

(i) Pulmonary oedema: acute lung injuries can occur a few days after infection with severe *P.falciparum*, and they may develop after a short time of treatment. Acute respiratory distress syndrome is a feature complication in adults with severe malaria (White et al., 2014). The first sign of pulmonary oedema is an increase in respiratory rate, however, this indication is similar to many diseases making diagnosis difficult without appropriate facilities, moreover, acidosis and pulmonary oedema may occur together during the infection course with severe malaria

(Trampuz et al., 2003). The pathogenesis is not fully understood and parasite sequestration in pulmonary vascular is unclear but the endothelial damage which is inflammation-mediated might have a role in pathogenesis (White et al., 2014).

(ii) Renal dysfunction/kidney injury: severe malaria may cause kidney injury and can occur at any age, but it is common particularly in adults. Acute kidney injury is pathologically similar to tubular necrosis and is associated with dysfunction with other vital organs (Brabin et al., 2015). The majority of cases of malarial renal failure caused by *P.falciparum* and rarely *P. vivax* and affected usually children aged from four to eight years (Barsoum., 2000). In acute renal failure, due to infection with *P.falciparum*, the serum creatinine concentration can become higher than 265mM. The mortality rate of patients with renal dysfunction is higher compared with patients with no kidney failure (Gachot & Ringwald, 1998). Following kidney injury, 60-70% of severe malaria cases with an initial elevated concentration of serum creatinine return into normal within 17 days (Nguansangiam et al., 2007).

Haemodialysis should provide treatment that will improve the outcomes of patients. Renal syndromes associated with renal dysfunction due to infection with severe malaria can be categorised into two groups: chronic glomerulopathy that mainly occurs in African children and acute renal failure associated with *P.falciparum* in southeast Asia, India and Sub-Saharan Africa (Barsoum, 2000). Jaundice is the most common complication to occur with acute renal with more than 75% cases resulting from excessive haemolysis (Tangpukdee et al., 2006). Both thrombocytopenia and anaemia are found in 70% of cases associated with malarial acute renal failure.

(iii) Cerebral malaria; is considered one of the acute neurological disorder of severe malaria complication and may lead to coma (WHO., 2018). Rosette phenomenon and cytoadhesion are the main features of CM, where rosette is the adherence of IE to non-IE and cytoadhesion is the

IE binding to the endothelium and other cells in the brain microvasculature (Udomsangpetch et al., 1989). Both of cytoadhesion and rosette lead sequestration of IE and non-IE (Leitgeb et al., 2011) cause obstruction of blood flow in the microvasculature (MacKintosh, Beeson & Marsh, 2004). *P.falciparum* erythrocyte membrane Protein 1 (PfEMP1) is the main mediator of IE cytoadherence to endothelium cells, which are expressed on the surface of IE and bind to a range of host receptors such as ICAM1, CD36 and endothelial protein C receptor (EPCR) (Hviid & Jensen., 2015). The mortality of cerebral malaria ranges from 10% to 50% (Trampuz et al., 2003). Many pathological changes occur during brain infection for both adults and children including retinopathy with haemorrhage and rising of blood lactate–pyruvate level (White et al., 2014). Post-mortem studies of patients with cerebral malaria shows no clear evidence of cerebral oedema in adults while it is clear in African children (Potchen et al., 2012). Artemisinin and quinine are used to treat cerebral malaria with artemisinin usually acting on early and late stages of parasite development while quinine act only on the late stages of parasite infection (Newton & Krishna., 1998; Idro, Jenkins, & Newton, 2005).

(iv) Severe anaemia is considered the main feature of severe malaria in children and pregnant women. The prevalence of anaemia in endemic areas of Africa varies between 31% to 90% in children (Premji et al., 1995) and between 60% to 80% in pregnant women (Menendez et al., 2000). Thrombocytopenia also occurs and it is common even in uncomplicated malaria (White et al., 2014). In patients with uncomplicated severe *P.falciparum*, the Hb level is usually within the normal range in the first 24 hours, followed by fever, then followed by a significant decrease in the Hb (Wickramasinghe and Abdalla., 2000). Pathophysiology of severe anaemia disease act on two sides, that increase the destruction of erythrocytes and decrease the production of erythrocytes (Menendez et al., 2000). Blood transfusion could be very important to manage malaria severe anaemia and it is easy to administer and that can be life-saving, however, the

source of blood for transfusion is very important and variable in an endemic area with malaria that may carry HIV (Menendez et al., 2000).

(v) Malarial acidosis is a common complication of severe malaria, defined as the increased production lactic and keto acids (Allen, O'Donnell, Alexander, & Clegg., 1996). There are many factors that may be associated with severe malaria acidosis: fever, severe anaemia, hypervolemia (English, Muambi, Mithwani, & Marsh, 1997). Metabolic acidosis combined with cerebral malaria presents a strong signal for subsequent fatal outcomes. To manage acidosis sodium bicarbonate was used in past, but it failed to control the acidotic state. A N-acetylcysteine inhibitor of tumour necrosis factor has been used also as an alternative to control acidosis but has failed to decrease the mortality rates (Watt, Jongsakul, & Ruangvirayuth, 2002). Dichloroacetate is a cofactor used in the correction of glucose and lactate kinetics in children with severe acidosis malaria where it induces the activity of pyruvate dehydrogenase and accelerates the oxidative removal of lactate and consumption of glucose (Maitland & Newton, 2005).

(vi) Severe malaria in pregnancy can cause abortion or death of pregnant women and their foetus and is a major public health challenge in endemic areas (Dellicour et al., 2010) (Figure 1.7). There are many significant symptoms and complications of severe *P.falciparum* infection associated with malaria in pregnancy (such as high parasitaemia, severe anaemia hypoglycaemia, acute pulmonary oedema and premature labour. Infection with severe malaria relies on many factors such as immunity levels in the pregnant and the current trimester.

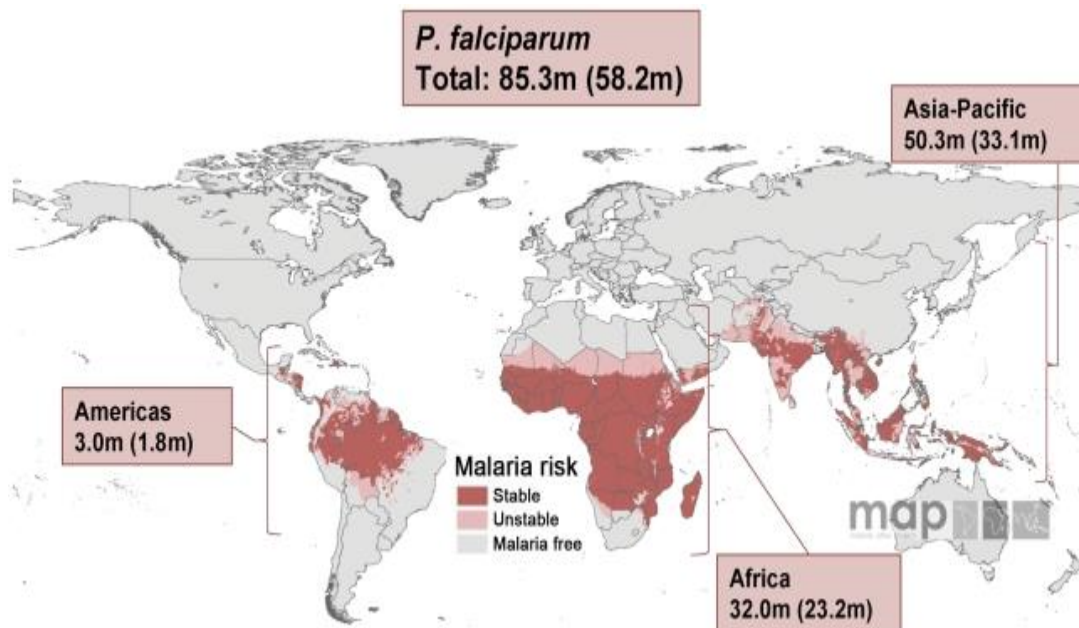


Figure 1.7: Malaria risk map for *P. falciparum* and corresponding number of pregnancies in each continent in 2007. The number of pregnancies in three affected continents (with those at risk of malaria indicated in parentheses) (Source: Dellicour et al., 2010)

One of the most significant pathophysiological disorders that may occur during pregnancy due to malaria infection is placental malaria which is an accumulation of infected red blood cells in intervillous space in the placenta. Congenital malaria occurs in approximately 5% of neonates but clears in 62% of cases (Falade et al., 2007). HIV-infected mothers are highly likely to infect with congenital malaria, that has affected negatively on birth weights of babies (Potchen et al., 2012). The mortality rate of pregnant women infected with *P.falciparum* may reach 50%. For severe malaria in pregnancy, the treatment recommended by the WHO is the use of artesunate or quinine. For uncomplicated malaria, artemisinin-based combination therapy is the best option to treat such cases because it has proven efficacy and safety. Certain drugs are no longer recommended to avoid complications that may threaten pregnant life. Clindamycin and clindamycin -based combination therapies are now avoided because they cause hypoglycaemia in pregnant women, in addition, they may increase infection resistance towards treatment (Schantz-Dunn & Nour., 2009; Orton & Omari, 2008).

1.4 Malaria treatment

For uncomplicated *P.falciparum* infection, artemisinin combination treatment (ACT) is recommended as the first line to treat uncomplicated *P.falciparum* malaria and other malaria species in regions with high multidrug resistance (Achan et al., 2011). The main challenge to supply ACT is the cost and its limited availability compared to quinine which is relatively cheap and widely available (Achan et al., 2011). For non-*P. falciparum* uncomplicated malaria, chloroquine is the first choice for treatment followed by primaquine to treat intrahepatic infections resulting from infection with *P.ovale* and *P.vivax* parasites (Walker, Nadjm, & Whitty, 2014). Quinine is an effective anti-malarial drug for non-*P. falciparum* malaria and has a rapid action against schizonts and gametocytes of *P.vivax* and *P.malaria* (Walker et al., 2014). Quinine is commonly prescribed intravenously at a dose of 10 mg/kg, three times a day, the recommended dose is given by slow infusion (Walker et al., 2014). In the case of treatment failure with quinine, WHO suggests a combination of quinine and doxycycline or tetracycline as the second-line therapy option for uncomplicated malaria infection and quinine plus clindamycin for pregnant women infected with malaria (Smith et al., 2008). The combination of quinine and azithromycin show high efficacy in multi-drug resistance malaria. The combination of quinine and doxycycline has proven effective in the treatment of chloroquine- and multi-drug resistant *P. falciparum* (Gaillard, Madamet, & Pradines, 2015).

Artemisinin is an antimalarial drug that is now used widely to treat severe *P.falciparum* and has pharmacodynamic properties that offer advantages over other antimalarial drugs, such as; fast onset action and the inhibition of multiple stages of the parasite life cycle. It can be administered orally or intravenously; it kills more rapidly and it is now one of the several anti-malarial drugs used to treat malaria in areas with chloroquine resistance (Krishna, Uhlemann, & Haynes, 2004). One of the best properties of artemisinin is that it attacks and kills parasites

throughout the blood cycle stage whether is ring or in schizont form (Woodrow., 2005) and the action of the drug may extend to target gametocyte development.

Anti-malarial drug resistance, especially in *P.falciparum*, is a significant problem facing the malaria eradication programme that may lead to an increase in malaria incidences (Achan et al., 2011). Most malaria-endemic areas, except Central America, have reported widespread resistance in *P.falciparum* to chloroquine. Moreover, mefloquine resistant *P.falciparum* has been reported in the western provinces of Cambodia and eastern provinces of Myanmar, although non-*P. falciparum* parasites are still sensitive to chloroquine. Resistance to artemisinin is rising in East Asia and can result in clinical failure to treat malaria patients (Walker et al., 2014) although, drug resistance phenomenon is currently concentrated in South East Asia. The development of *P. falciparum* drug resistance has been documented in many areas of the world and sulfadoxine/pyrimethamine was one of the drugs that *P.falciparum* has grown resistant in South Asia, Oceania, sub-Saharan Africa, South Asia and the Amazon basin. *P.vivax* chloroquine resistance was also reported in areas of Oceania, including Indonesia and Papua New Guinea.

Genetic analysis of chloroquine drug resistance in *P.falciparum* shows a mutated gene termed *pfcr* (*P. falciparum* chloroquine resistance transporter) is a key determinant, although other mutations may support the extent of the chloroquine resistance (Fidock et al., 2000). Resistance to amodiaquine appears to result from mutation of the *pfpg* (*P.falciparum* p-glycoprotein homologues-1) (Reed, Saliba, Caruana, Kirk, & Cowman., 2000).

The induction and then global spread of drug-resistance highlights the urgent need for new drugs with a new mechanism of action. Ideally, these drugs need to be effective against all species that infect human, be effective against current drug-resistant strains, ideally with

different components in a combination therapy targeting different targets of parasite life cycle to rapidly reduce parasitaemia and improve the clinical outcomes (Burrows et al., 2017).

1.5 Prevention

There is no effective vaccine that can fully protect against malaria and, until recently, there has been no licenced vaccine against *P.falciparum* (Hill., 2011). There are high demands for an effective vaccine that could save millions of lives and reduce malaria infection around the world especially in endemic areas (Drew & Beeson, 2015). The most recent candidate vaccine under development targets only one stage of the parasite life cycle, and that does not prevent or stop malaria infection completely. The multi-target vaccine is the required vaccine that involves more than one stage of the malaria life cycle and the pre-erythrocyte stage vaccine has been the most successful vaccine until now (Hill., 2011). Merozoite surface proteins (MSPs) are a potential target of vaccine designs because they are always under the attack of immune defence cell by the host. The essential purpose of vaccine is to stimulate the memory T-cell response and antibodies to a few antigens of malaria infection repeated, however, the main challenge that faces vaccine synthesis is the parasite life cycle itself, because the parasite changes morphologically during host life cycle and shows antigenic variation that enable parasite to escape from immune defensive cells (Arama & Troye-Blomberg., 2014). In addition, *P.falciparum* show significant genetic diversity, particularly of PfEMP1 (*Plasmodium falciparum* membrane protein) taken as an example as there are some 60 different *var* genes encoding for the production of this exported membrane-bound protein in a parasite genome (Gardner et al., 2002).

To obtain a successful vaccine, three major elements should be taken into consideration in vaccine development; first, the vaccine should contain multi immunogenicity that stimulates

multi-immune response; second, it should contain compounds that enhance the immune system to respond to malaria infection and work on many stages of infection including the liver stage and blood-stage; third, it should include multiple epitopes that are restricted to production by histocompatibility (MHC) complexes to defeat parasite genetic diversity and antigenic variation (Shi et al., 1999).

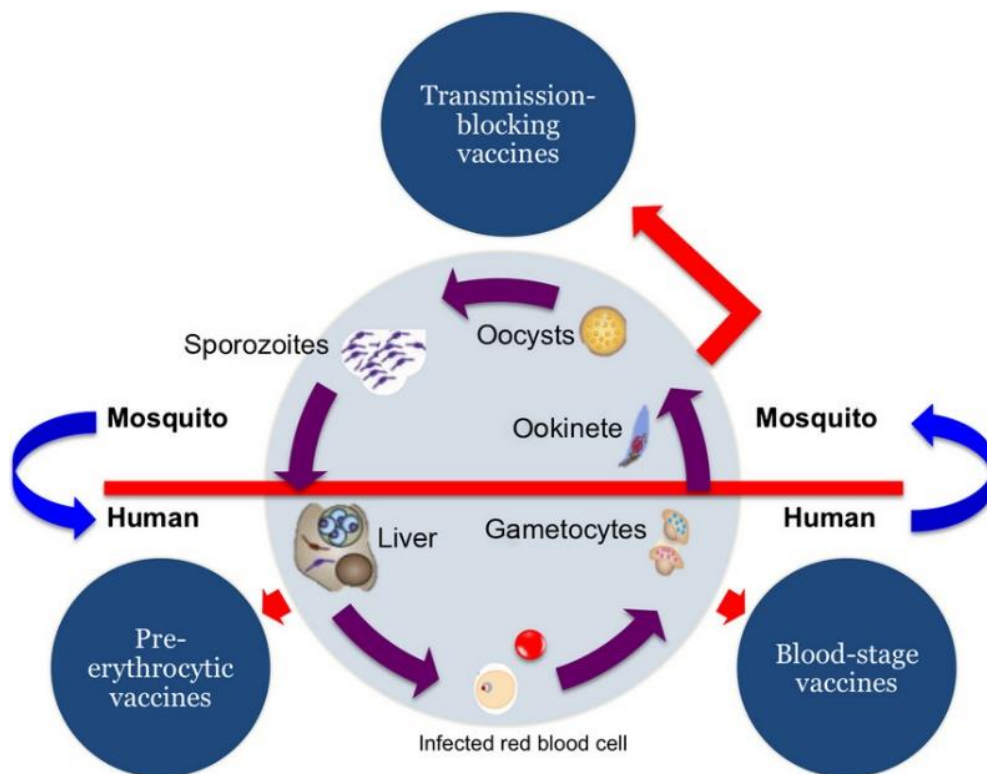


Figure 1.8 Illustrate the development of *P.falciparum* vaccine. Different stages of parasite life cycle could be a potential target for vaccine development. Vaccine block parasite transmission to the human host, vaccine inhibit blood-stage cycle by blocking merozoite invasion into erythrocyte and vaccine inhibit sporozoite invasion into hepatocytes. (source Arama & Troye-Blomberg, 2014).

The RTS,S vaccine (commercially called Mosquitrix) is one of the most advanced vaccines and acts against *P.falciparum* circumsporozoite protein (CSP) and provides immunity during the pre-erythrocyte stage. The vaccine acts specifically during the parasite journey from skin to liver or infected hepatocytes that stimulate antibodies of human acquired immunity to inhibit the invasion of sporozoites for hepatic cells and its replication during liver stage infection and clear the parasite before going to infect the red blood cells (Arama & Troye-Blomberg., 2014) (Figure 1.8). RTS, S vaccine is considered the only advanced vaccine to provide efficacy in semi immunised adults, children and infants in endemic areas (Halbroth & Draper., 2015). RTS,S was developed by GSK in collaboration with the Walter Reed Army Institute of Research. The RTS,S vaccine is a complex vaccine composed of several elements: T cells epitopes to CSP are fused with HBsAg, a hepatitis B virus antigen and together encoded in a recombinant hepatitis B virus vaccine developed by GSK (Halbroth & Draper., 2015) and assembled to Virus-Like Protein (VLP) with infused copies of HBsAg (Cohen, Nussenzweig, Vekemans, & Leach., 2010). The result of immunisation with RTS,S in infants aged 6 to 12 weeks, given as a monthly dose for three months, presented moderate action and excellent safety, 30% real immunisation against clinical malaria and 26% against severe malaria (Clinical trial study published by The RTS,S Clinical Trials Partnership 2014). While 55% immunisation against all sorts of *P.falciparum* appeared in older children their ages between 5 to 17 months and 35% protection towards severe malaria during 14 months. The result of RTS,S trial phase III shows protection against malaria in children aged between 5-17 months and efficacy of the vaccine against severe malaria in ages between 6 to 12 weeks (Moorthy & Okwo-Bele, 2015). RTS,S/AS01 vaccine has been recommended by WHO for a pilot immunization programme, from the beginning of 2019, the vaccine will deliver to three sub-Saharan countries and for selective areas to be provided to young children through immunisation routine (WHO, the malaria vaccine implementation programme (MVIP).

Chemoprophylaxis is an alternative option to protect or prevent individuals from catching malaria. Chemoprophylaxis is recommended for those who intend to travel or live in endemic areas. Atovaquone, doxycycline, proguanil, primaquine, and mefloquine are common prophylactic agents used in the prevention of malaria. In fact, there are no perfect reliable chemoprophylaxis agents and diagnosis should always present as a tool to detect malaria in any febrile patients who have come from infected areas (White et al., 2014). Chemoprophylaxis is recommended for pregnant women in endemic areas. A full course twice during pregnancy offers partial protection against malaria and sulfadoxine-pyrimethamine used for this purpose (2013). Mefloquine is the only safe chemoprophylaxis prescribed to travelling pregnant women because no harmful effects have been shown in the second and third trimester of pregnancy (Schlagenhauf et al., 2012). For children, who are the most affected by infection with malaria, approximately 80% of cases. WHO recommended using Amodiaquine and Sulfadoxine-pyrimethamine as prophylaxis for children aged between 3 to 29 months and to administer monthly not more than four doses in areas from the beginning of annual transmission season (WHO, 2012). Chloroquine is also an important prophylactic agent, in endemic areas where chloroquine resistance has not been reported, chloroquine should be recommended.

1.6 Inhibition of *P.falciparum* merozoite invasion/egress by glycosaminoglycans (GAGs) and other inhibitors

Most current antimalarial drugs have an intraerythrocytic effect by targeting different aspects of the blood-stage life cycle of *P.falciparum*. Examples include (i) chloroquine and artemisinin which target intercellular food vacuole (Fidock et al., 2000; Klonis et al., 2011), (ii) doxycycline, azithromycin and clindamycin that target apicoplast function and thus prevent schizonts to fully mature (Dahl and Rosenthal 2007; Goodman, Su and McFadden 2007), (iii) pyrimethamine that inhibits DNA replication (Cowman et al. 1988) and (iv) atovaquone and

proguanil that targeting mitochondrial bc₁ complex function (Fry and Pudney., 1992; Dick Dickerman et al., 2016). At the present, there is no licensed drug that targets the extracellular form of parasite merozoite, although azithromycin has shown merozoite invasion inhibition activity at very high concentrations (Wilson et al., 2015). However, the ease of bloodstream access to the extracellular merozoite and the multiplicity of targets available offers an attractive target for agents that inhibit merozoite reinvasion and thus reduce parasite proliferation and the associated disease burden.

Recently many inhibitors have been proposed specifically to target merozoites by inhibition merozoite egress or invasion (Figure 1.9). These include; quinolyldrazones that inhibit the subtilisin 1 serine protease which is required for merozoite egress (Gemma et al., 2012) and hydroxyethyl amine and aminohydantoinis that target plasmepsin IX and X which are both essential for merozoite egress (Pino et al., 2017; Nasamu et al., 2017).

Heparin, which is polysaccharides belonging to the glycosaminoglycans family, has been reported to inhibit parasite growth *in vitro* where the inhibition is reported to be through the blocking of the merozoite invasion process (Butcher, Parish and Cowden 1988; Boyle et al., 2017). Many GAGs have been identified to block *P.falciparum* merozoite invasion, with these mainly being sulphated GAGs from a range of different sources, including; dextran sulphate (Butcher et al., 1988), curdlan sulphate (Havlik, Rovelli and Kaneko., 1994; Evans et al., 1998), carrageenan from seaweed (Adams et al., 2005), fucosylated chondroitin sulphate (Bastos et al., 2014), sulphated cyclodextrins (Crandall et al., 2007), K5 polysaccharides (Boyle et al., 2010), inulin sulphate, xylan sulphate, tragacanth sulfate and scleroglucan sulphate (Boyle et al., 2017). In addition to inhibiting erythrocyte invasion by *P. falciparum*, GAGs have also been reported to inhibit non-human malaria parasite.

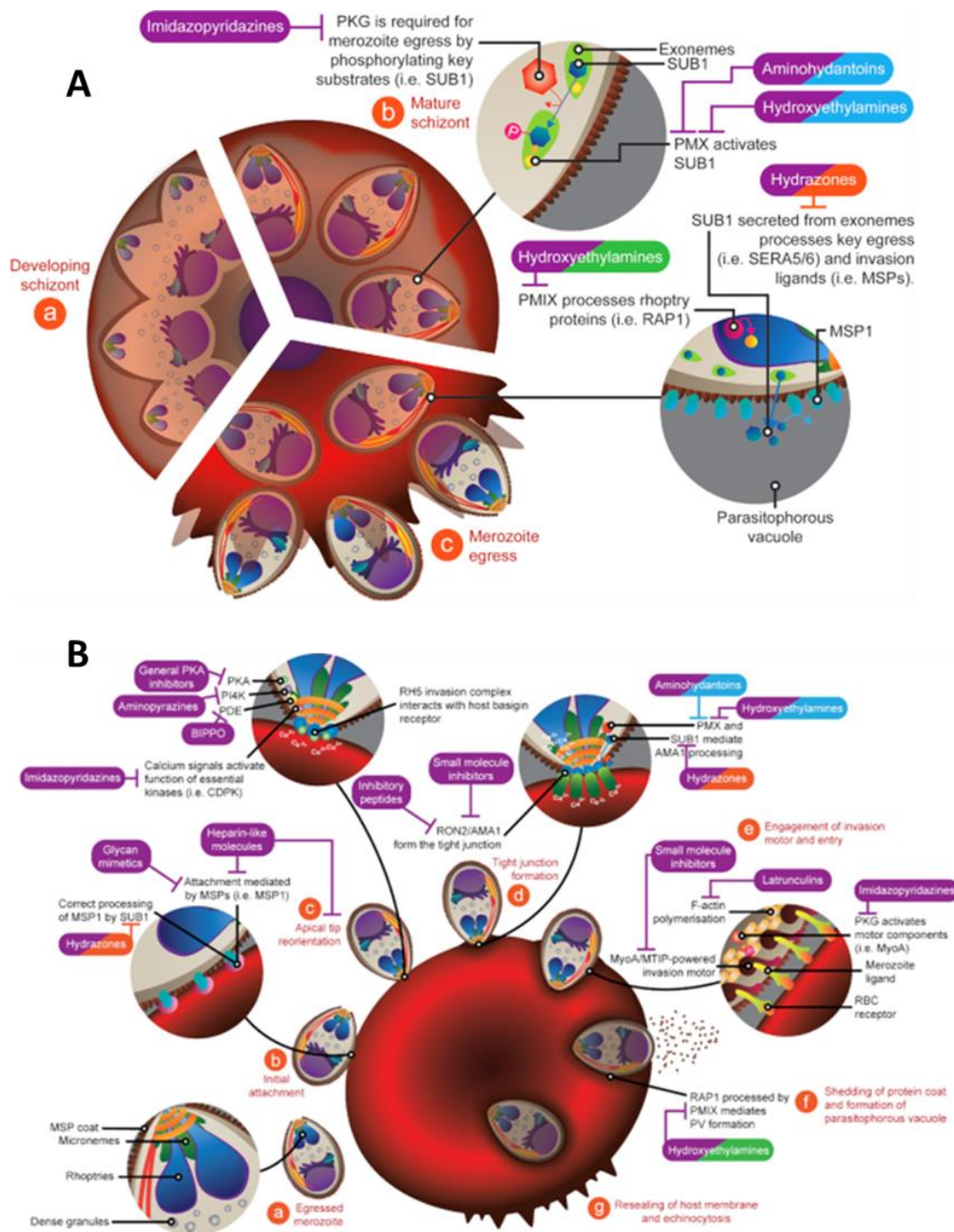


Figure 1.9 Schematic illustrating the targets of *P.falciparum* merozoite inhibitors. (A) during merozoite development and egress from an erythrocyte and (B) during binding and invasion of a new host erythrocyte. (Source: Burn et al., 2019)

Heparin has been shown to inhibit the zoonotic *P.knowlesi* (Lyth et al., 2018), with this observation leading to a proposal that the inhibition of pan-species is potentially possible with sulphated GAGs. Whilst the exact mechanism of sulphated GAGs inhibition is not well

understood, several targets of inhibition have been proposed. Heparin is reported to inhibit early essential steps of merozoite invasion to erythrocyte by targeting MSP1 (Boyle et al., 2010), and interacting with rhoptry microneme proteins involved in the merozoite reorientation (Baum et al., 2009; Kobayashi et al., 2010; Kobayashi et al., 2013). Much more recently, heparin has also been reported to inhibit merozoite egress and dispersal (Glushakova et al., 2017) - thus, heparin and other sulphated GAGs, seems to inhibit multiple merozoite invasive proteins. Therefore, it is unlikely that a parasite would develop resistance to these sulphated GAGs, in fact, the attempts to obtain a parasite-resistant to heparin was unsuccessful (Boyle et al., 2010). Sulphated GAGs have been evaluated *in vivo* in mice models and shown to block merozoite invasion as well as disrupting cytoadhesion (Xiao et al., 1996).

The inhibition effect of heparin and other sulphated GAGs have been reported not only in targeting merozoite invasion but extended to include prevent cytoadhesion and disrupt rosette formation. These studies include the sulphated GAGs dextran and fucoidan sulphate (Rowe et al., 1994; Barragan et al., 1999), carrageenan (Adams et al., 2005), curdlan sulphate (Havlik et al., 2005; Helen M. Kyriacou et al., 2007) and fucosylated chondroitin sulphate (Bastos et al., 2014).

Heparin has been evaluated clinically as an adjunct therapy for *P.falciparum* severe malaria (Smitskamp and Wolthuis., 1971; Munir et al., 1980; Rampengan., 1991), with curdlan sulphate also used to treat severe/cerebral malaria (Havlik et al., 2005). However, due to their anticoagulation properties, increasing the risk of haemorrhage, as well as the risk of heparin-induced thrombocytopenia, heparin was not recommended to be used as an adjunct therapy to treat malaria.

The idea of modified heparin or other heparin-like mimetics that exhibits low anticoagulation activity but may also affect either invasion or infected erythrocyte binding is attractive as a potential adjunct therapy. Various heparins have been employed in other clinical areas, for

example; a non-anticoagulant low molecular weight heparin (LMWH) was used as antiangiogenic in an animal model (Pisano et al., 2005) and similarly, reduced anticoagulant heparin show anti-cancer growth inhibition (Yu et al., 2010). In *P.falciparum*, LMWH and low anticoagulant sulphated GAGs have been reported in several studies, showing both anti-cytoadhesion, rosette disruption and invasion blocking activity – and several with low anticoagulation activity. Curdlan sulphate has a ten-fold reduction in anticoagulation activity when tested in a clinical trial with severe *P.falciparum* (Havlik et al., 2005), Low anticoagulant heparin disrupt rosettes *in vitro* (Carlson et al., 1992), and the low anticoagulant glycan inhibit merozoite invasion and disrupt rosettes (Vogt et al., 2006). A chemically modified LMWH derivative with low anticoagulation disrupts rosettes (Skidmore et al., 2008; Boyle et al., 2017), a semi-synthetic GAGs with low anti aPTT and PT (Skidmore et al., 2017) and a low anticoagulant, sulphated GAGs inhibit merozoite invasion *in vitro* (Boyle et al., 2017). Recently a low anticoagulant, LMWH sevuparin which is a negatively charged depolymerized heparin with MW ~8000 Daltons and very low anticoagulation activity, has been evaluated in phase I/IIa clinical trial as an adjunct therapy to treat uncomplicated *P.falciparum* malaria (Leitgeb et al., 2017). This trial showed sevuparin inhibits merozoite invasion with no anticoagulation effect at concentrations lower than 6 mg/kg. The phase I work showed the sevuparin was well-tolerated and safe, however, the potency of sevuparin was relatively low as the effect of sevuparin and drug was very close to the control of using the drug alone. Chemical modification of heparin and other sulphated GAGs, however, may provide a start for the development a future adjunct therapy for malaria treatment, and offer an additional option to meet the challenge of treating patients with drug-resistant malaria.

1.7 Glycosaminoglycans

Glycosaminoglycans (GAGs) are unbranched, linear polysaccharides, consisting of repeated disaccharides units linked by glycosidic bonds (α or β) between amino sugar and a uronic acid in the disaccharide unit to form a complex structure (Köwitsch et al., 2017). GAGs are present on the surface of most cells types as a key constituent of the extracellular matrix. Sulphated GAGs, except hyaluronan (HA), are synthesised enzymatically in the cell's Golgi apparatus and then exported to the plasma membrane surface. Sulphated GAGs are typically present in cells as proteoglycans, where side chains are attached to a protein (Gabius., 2009). There are six key groups of GAGs: heparin, heparin sulphate, chondroitin sulphate (CS), dermatan sulphate (DS), keratan sulphate (KS) and hyaluronic acid (HA) (Figure 1.10).

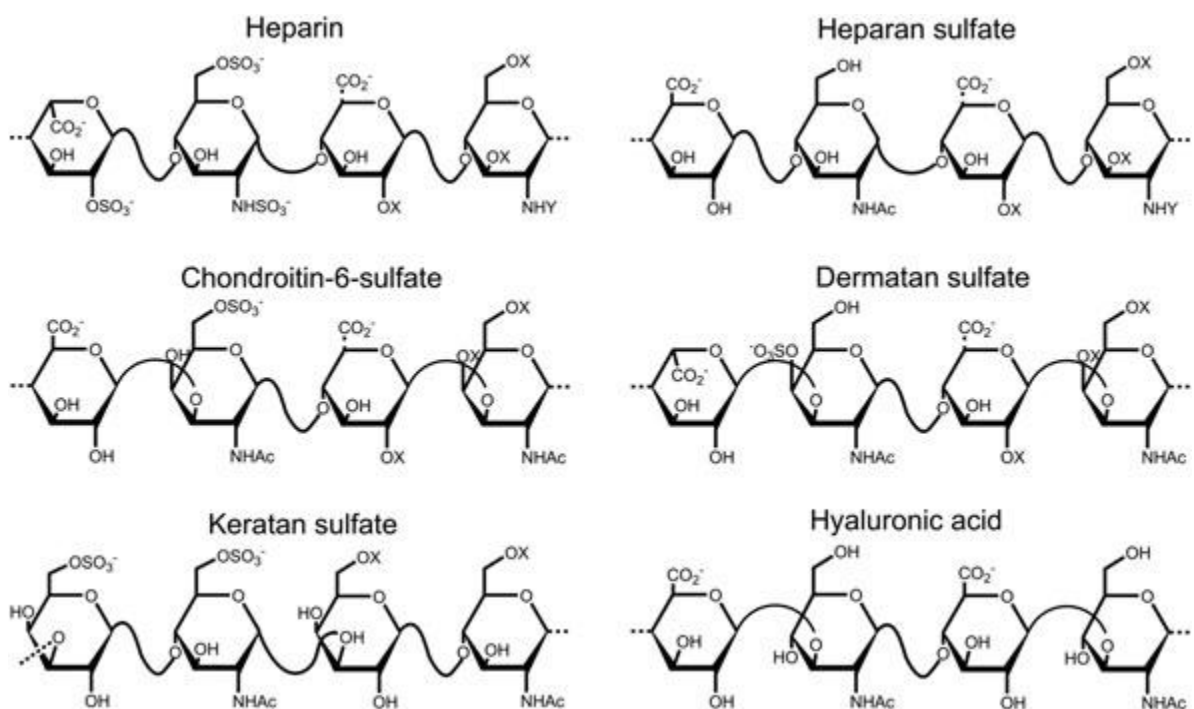


Figure 1.10 Illustrates the major repeated disaccharides in six major glycosaminoglycans (source: Köwitsch et al., 2018)

1.7.1 Heparan and heparin sulphate

Heparan sulphate (HS) and heparin are like all GAGs, linear polysaccharides made of repeated disaccharides subunits. They mainly consist of uronic acid (1-4) glucosamine, with different patterns of substitution of the disaccharides subunits, the substitution is N-sulphate, O-sulphate and N-acetyl groups, making both GAGs, structurally, the most complex polysaccharides when compared with other polysaccharides in the GAG family (Rabenstein, D. L., 2002). Heparin and HS are built from the identical monosaccharide structure blocks, the uronic acid of the uronic acid-(1 4)-D-glucosamine repeating disaccharides may be either α -L-iduronic (IdoA) or β -D-glucuronic acid (GlcA), mutually of which may be 2-O-sulfated (Ido(2S) and GlcA(2S)). The β -D-glucosamine (GlcN) may be either N-sulphated (GlcNS) or N-acetylated (GlcNAc), both of which may be 6-O-sulfated (GlcNS(6S) and GlcNAc(6S)) and the GlcNS and GlcNS(6S) may also be 3-O-sulphated (GlcNS(3S) and GlcNS(3,6S)) (Rabenstein., 2002). Heparin disaccharides are built of iduronic acid of which IdoA2-S and glucosamine N-S and additionally GlcA. By contrast, HS disaccharides predominantly consist of glucuronic acid and N-acetylated glucosamine (Köwitsch et al., 2017). Notably, heparin is highest negatively charged of all known biomolecules and the degree of sulphation in heparin is higher than that of HS (Nelson et al., 2008), and the distribution of sulphation over heparin is more equal than that in HS where there are alternating high sulphation and lower or non-sulphated sections (Powell et al., 2004). Both heparin and HS are produced as proteoglycans, Heparin is synthesised in connective tissues type mast cells and basophils, while HS is synthesised by all mammalian cells (Rabenstein., 2002; Varki., 1999).

HS and heparin have distinct biological functions. Heparin inhibits a wide range of biological activities including complement activation, angiogenesis, tumour growth factor and viral entry. Heparin is a well-known anticoagulant and has been used for decades to treat different serious clinical conditions such as thromboembolism. The anticoagulation activity is the result of

heparin interaction with thrombin, a serine protease inhibitor that mediates the anticoagulant activity of heparin (Jin et al., 1997). Heparin inhibits antithrombin (AT) by binding AT with a specific and unique sequence of heparin polysaccharides where only one-third of heparin chains have this anticoagulation property (Rabenstein., 2002). HS instead plays a key role in biological functions where HS mediate the biological function by binding to proteins such as; inhibition of blood clotting (Marcum et al.,1986), cell adhesion (Lindahl et al.,1994), regulation of cell growth and proliferation (Perrimon et al., 2000), vital role in angiogenesis (Iozzo et al., 2001), tumor metastasis (Hulett et al., 1999) and in viral invasion by acting as receptors to for the virus invasive ligands (Shukla et al., 1999).

I.7.2 Dermatan sulphate / Chondroitin sulphate

Chondroitin sulphate (CS) is a linear polysaccharide, consist of repeated disaccharides units of N-acetyl galactosamine (GalNAc) or glucuronic acid (GlcA) linked by β 1-4 or 1-3 linkage with sulphation group present C-4 GalNAc(Janet M et al., 2002). Dermatan sulphate (DS) is also known as chondroitin sulphate (CSB) where iduronic acid is present in DS which distinguishes it from CS. DS and CS vary in their MW and length, 5-70 kDs (Linhardt et al., 2006; Volpi., 2007). Both DS and CS found to have different vital roles in many biological processes where found as proteoglycans as DSPG and CSPG, for instance in the regulation of fibrillogenesis (Dunkman et al., 2014), they also interact with neuron and neural cell adhesion molecules (Mauler et al., 1994), interact with growth factor of fibroblasts (Trowbridge and Gallo, 2002), act as regulator during inflammation, tumour development and wound healing by effect on the signalling course in the cell (Volpi., 2011).

1.7.3 Keratan sulphate (KS)

Keratan sulphate is a polysaccharide consist of repeated disaccharides of which GlcNAc and galactose linked by β 1-4 and 1-3 linkage, both may which sulphated at C6. The MW of KS diverges and array 5-25 kDa , dependent on the source of KS (Hopwood and Robinson., 1973) KS found naturally, highly concentrated in the cornea. KS classified into three classes, depending on KS O or N connecting to amino acid core proteins: KS-I KS is N-linked via GlcNAc to asparagine, KS-II where O- linked through GalNAc to serine, KS-III is O-connected through mannose to serine (Uchimura at al., 2015). KS-I is distinguished from KS-II by its lower sulphation degree, and longer chain length, where KS-II is highly sulphated and shorter, also, KS-II found in cartilages meanwhile KS-I found mainly in the cornea which is responsible for corneal transparency and tissue dehydration (Köwitsch et al., 2018). KS-III is found in proteoglycans of nervous tissue and brain (Uchimura., 2015).

1.7.4 Hyaluronan (Hyaluronic acid)

Hyaluronic acid (HA), unlike other GAGs, is not sulphated and non-linked to protein cores, synthesis by integral membrane protein and release to the extracellular space (Weigel and DeAngelis., 2007). HA structurally is unbranched polysaccharides, consist of repeated disaccharides of GlcA linked via β (1-4) to β (1-3) GlcNAc glycosidic linkage. HA is found in difference placed in human tissues, such as; synovial fluids, skin, umbilical cord and cartilage where found to be at high concentrations in these human tissues (Fraser et al., 1997). The MW of HA is varying and decrease with age (drop from 2000 kDa to 500kDa) (Holmes et al., 1988) which have a negative impact on its biological functionality. HMW HA has an immunosuppressive and anti-inflammatory, while the LMW HA has a reverse action, it exhibits angiogenic, immunostimulatory properties (Stern et al., 2006).

1.8 A role for GAGs in mediating *P.falciparum* pathogenicity

Rosette formation and cytoadhesion both lead to serious consequences which may include; obstruction of microvasculature, tissue hypoxia and organ failure (for review see Von Itzstein et al., 2008). Glycosaminoglycans such CSA and HS are recognised to have a role in *P.falciparum* cytoadhesion and merozoite invasion by facilitating host cell- IE interactions. For example, CSA which is expressed in many cell surfaces, erythrocyte and placenta during the pregnancy mediates parasite cytoadherence within the placenta. IE is concentrated within the intervillous blood space where CSA expressed on the syncytiotrophoblasts of the placenta act as a receptor for PfEMP1 on the surface of IE (Gill et al., 2009). Heparan sulphate was observed to have high affinity and more frequent binding to IE in isolates from children with severe malaria compared with those with mild malaria, suggesting that HS could be one of the sequestration receptors that contribute to malaria severity (Heddini et al., 2001). In addition to the roles of CSA and HS in rosetting and cytoadhesion, both were found to play a role in the regulation of placental inflammation a consequence of parasite adhesion. Heparin is also suggested to act as a receptor for merozoite invasive ligands during erythrocyte invasion, with heparin showing an ability to bind MSP1-41 and MSP1-33, suggesting that heparin or heparin-like molecules are receptors for the merozoite invasion process (Boyle et al., 210).

1.9 Objectives of this study

As outlined above, heparin and a range of GAGs used as heparin-mimetics have been evaluated in some *P. falciparum* strains for their ability to reverse cytoadhesion or disrupt resetting. There is less information on their effect on blocking the erythrocyte reinvasion pathway, few exploring the cross-strain activity and the use of either direct microscopic examination or a flow cytometry assay limits the scalability of these assays.

These limitations were explored here through objective 1: the development and validation of a novel bioluminescent plate-based assay – utilising a neuraminidase sensitive strain NF54 to complement a neuraminidase insensitive Dd2 transgenic strain already available. Panels of heparin medicines, low molecular weight heparins, and chemically modified heparins, sulphated complex carbohydrates from a range of sources as well as naturally sulphated GAGs from marine sources were tested in this novel assay. This material provided for objective 2: the screening and confirmation of hits from these libraries as concentration-dependent inhibitors of *in vitro* growth in two *P. falciparum* strains.

Hits were taken forward for objective 3: To determine the relative anticoagulation activity of these hits and define the inhibitory action to merozoite egress and/or erythrocyte invasion. The results of these studies are discussed in the wider context as their potential for development as an adjunct therapy for severe malaria.

Chapter two: Materials and Methods

2.1 Materials

Plasticware were sourced, unless otherwise indicated, from Greiner Bio-one or Starlabs. All chemicals were provided by Sigma or VWR. Human blood that used for *P.falciparum* culture was provided to Paul Horrocks as an approved user by The National Blood and Transplant Service (account H064) and stored and disposed of under the HTA License 12349. All work in the Category III cell culture facility was done as described in the Health and Safety Executive approved Code of Practice for this facility. All glycosaminoglycans (GAGs) were kindly provided by the Skidmore Laboratory, School of Life Science, Keele University. All GAGs were diluted in water and final stock concentration of was 10mg/ml.

2.2 Material stock (reagents)

50X Malaria Sybr Green I fluorescence (MSF) lysis buffer

20 mM Tris-HCl,(Ph 7.4) 5 mM EDTA, 0.008% saponin and 0.08% and 0.8% Triton X

Cytomix buffer composition

120 mM KCl; 0.15 mM CaCl₂; 10mM K₂HPO₄/KH₂PO₄, pH 7.6; 25 mM Hepes, pH 7.6; 2 mM MEGTA, pH 7.6; 5mM MgCl₂; pH adjusted with KOH)

20X SSC (3.0M NaCl, 0.3M sodium citrate)

175.3g NaCl and 88.2g sodium citrate were added to 800ml sdH₂O, the pH of the solution adjusted to 7.0 by adding HCl and made up to 1 L with sdH₂O. The solution was then autoclaved and stored at room temperature.

50X Tris-Acetate-EDTA (TAE) buffer

242g of Tris-base, 57.1 ml of 100 % glacial acetic acid and 100 ml of 0.5 M EDTA (pH 8.0) were added to a total volume of 1 L of sdH₂O. The solution autoclaved and stored at room temperature.

Ethylene Diamine Tetra Acetic Acid (EDTA) 0.5M, pH8.0

93.05g of disodium EDTA.2H₂O was added to 400ml sterile distilled water (sdH₂O) and sited on a magnetic stirrer. 10g of NaOH pellets were added, the pH adjusted to 8.0 by adding (10N NaOH) and then made up to 500ml with sdH₂O. The solution was then autoclaved to sterilise.

Glucose solution (45%w/v)

90 g of D-glucose was added to 200 ml of sdH₂O and the solution mixed on a magnetic stirrer, filter sterilised and then stored at 4°C.

Glycerolyte freezing solution

Freezing solution is composed of Glycerol 57 g; Potassium Chloride 30 mg; Sodium Lactate 1.6 g; Sodium Phosphate Dibasic 124.2 mg; Sodium Phosphate Monobasic 51.7 mg per 100 ml dH₂O; pH 6.8 adjusted with phosphoric acid. The solution was then stored at 4°C.

Hypoxanthine solution (X1000)

340 mg of hypoxanthine was added to 25 ml of 1N NaOH to achieve a 1000X stock concentration. This solution was stored at -20°C in 0.5mL aliquots.

LB agar

LB agar was purchased from Merck. 37.0 g of agar was suspended in 1 L of sdH₂O and mixed on a magnetic stirrer. The agar then autoclaved and either used immediately or stored at 4°C.

LB broth

LB broth purchased from Merck. 25.0 g was suspended in 1 L of sdH₂O, mixed on a magnetic stirrer and then stored at 4°C until used.

SOC medium

To 950ml sdH₂O, 5 g of yeast extract, 20 g tryptone and 0.5 g of NaCl were added and homogenised on a magnetic stirrer. 10 ml of 250 mM of KCl was added to the solution and pH 7.0 was achieved with 5 N NaOH and 5 ml of filter-sterilized 2M MgCl₂ was. The final volume of a solution made up to 1L with sdH₂O, autoclaved and stored at -20°C.

WR99210 stock

0.05 g of WR99210 (a gift from Jacobus Pharmaceuticals, Princeton, NJ) was added to 1 ml of DMSO to prepare a 25 mM stock for long-term storage at -20°C. For short-term use, a 25 µM stock was prepared by diluting 1µl of the 25 mM stock to 1 ml of complete medium (1/1000 dilution). 100 µl of the 25µM short-term stock was added to 500 ml of *P. falciparum* culture medium to provide a final 5nM concentration required for drug pressure.

2.3 List of equipments

1. GloMax®-Multi+ Microplate Multimode Reader with Instinct® (Promega, UK).
2. Incubator 37 °C (Nuair).
3. Microbiology Safety Cabinet (ICN Flow).
4. Centrifuge- U-320R (Boeco, Germany).
5. CX21FS1 Microscope (Olympus).
6. JB Aqua 5 Water Bath (Grant.)
7. Shaker incubator (Certomate HK).
8. Fluorescent microscope (Evos cell imaging system, Life technologies).
9. Electroporator (Bio-Rad genpulsar XCELL).
10. Benchtop centrifuge (Sigma).
11. Bacterial culture incubator (Scientific Laboratory Supplies).
12. Gel document system (Syngene).
13. Electrophoresis unit (Jencons).
14. Autoclave (Tuhnauer).
15. Real-time PCR (Applied Biosystems, Step One Plus).
16. Conventional PCR (Eppendorf® Mastercycler).
17. Thrombostat 1 (Behnk Elektronik GmH &co. KG)
18. Flow Cytometer (Guava® EasyCyte, Merck)
19. Hybridization incubator (Techne, HB-1D hybridizer).
20. Light microscope with camera (Dialux 20EB, infinity camera)

2.4 Cell culture materials

2.4.1 Preparation of complete and incomplete *P. falciparum* cell culture medium

Incomplete cell culture medium comprised 500 ml of RPMI (Roswell Park Memorial Institute)-1640 medium (Sigma) with the following components added; 2.5 ml of 1N NaOH, 2 ml of 45% (w/v) glucose solution, 18.75 ml of 1M HEPES buffer solution (Sigma), 5ml of 200 mM glutamine solution (Sigma), 0.5 ml 1000x Hypoxanthine solution, 1.25 ml of 10 mg Gentamicin Sulphate (Sigma). To prepare complete cell culture medium, the following components were also added; 20 ml of human serum and 20 ml of 5% albumax -II.

2.4.2 Preparation of human serum and erythrocytes

Human fresh blood O Rh+ was supplied by National Blood and Transfusion Science (UK Bristol). All work was carried out in a Health and Safety Executive approved CAT-III facility according to standard operating procedures. On delivery, human blood was stored in labelled 50 ml tubes and kept at 4°C for up to four weeks. To prepare a 50% of haematocrit stock for *P.falciparum* cell culture, the upper serum phase was removed and the red blood cells suspended with an equal volume of incomplete cell culture medium and then collected by centrifugation (8 min, room temperature, 4000 rpm). The upper phase was removed, and the red blood cells resuspended with an equal volume of incomplete medium, mixed and centrifuged (3500 rpm, 5min, at room temp). The washed red blood cells were suspended finally in an equal volume of incomplete medium, mixed and then stored at 4°C. Human serum was provided as a discrete product or was collected from blood deliveries. Serum was complement inactivated by heating to 57°C for 30 min, then stored at -20°C in 40 ml aliquots.

2.5 *P.falciparum* cell culture methods

2.5.1 *In vitro* intraerythrocytic continuous culture of *P.falciparum*

Parasite stocks were typically continuously cultured at a 2% haematocrit (HCT) and between a 0.5 to 3% parasitaemia as originally described by (Trager and Jensen, 1976) and modified later by Freese *et al*, 1988. Cultures were maintained under 1% oxygen, 3% carbon dioxide and 96% nitrogen (BOC, special gases) and at 37°C. The growth of the parasite culture was controlled by diluting the culture with fresh complete media and replacement of infected red blood cells with fresh uninfected stock. The parasitaemia of the culture was regularly assessed by light microscopy of a 10% Giemsa-stained thin smear. A thin blood smear was dried and fixed with absolute methanol and dried again, the slide covered with 10% Giemsa stain and left to stain for 5 minutes. The stain was washed off with water and left to air dry. Parasitaemia and parasite life cycle staging was assessed by using a 100x oil immersion objective lens.

Dd2^{Luc} strain was developed by Wong *et al.*, (2011) to temporally express luciferase in trophozoite stages under the control of a *Pfpcna* flanking sequence. This strain requires 5nM WR99210 of drug selection. The NF54 strain was provided by the Merrick laboratory and requires no selective drug pressure. In this study, a NF54^{Luc} was developed, and like the Dd2 strain above, temporally expresses luciferase and requires 5nM WR99210 of drug selection.

2.5.2 Sorbitol-synchronisation of *P. falciparum* culture

To obtain a homogenous single-stage population, parasites were synchronised with sorbitol as originally described by Lambros and Vanderberg (1979). Predominantly ring-stage parasite culture was collected by centrifugation at 3000rpm for 5 minutes (room temperature). The supernatant was removed and 5 pellet volumes of 37°C pre-warmed 5% sorbitol was added to the red blood cell pellet and incubated at 37°C for 10 minutes. The synchronised culture was collected by centrifugation (1800 rpm, room temperature, 5 mins). The supernatant was

removed, and the red blood cell pellet added to a culture flask with an appropriate volume of fresh blood and complete cell culture medium.

2.5.3 Storage of *P. falciparum* culture

Highly synchronized ring stage (~10% parasitaemia) parasite cultures are stored at -80°C for future use. The red blood cells in a predominantly ring stage culture were collected by centrifugation for 5 minutes at room temperature at 1800rpm. The supernatant was removed, and the red cell pellet volume estimated. The final process requires addition of five volumes of glycerolyte freezing solution to the prepared three volumes of red blood cells. The first volume of glycerolyte freezing solution is added drop by drop and mixed continuously. After leaving this for five minutes the remaining four volumes of glycerolyte freezing solution are added gradually, again with continual mixing. 0.8 ml of samples were aliquoted into sterile freezing vials (NUNC) and stored at -80°C until required.

To thaw a frozen sample, the vial of frozen *P.falciparum* was taken from -80 °C and moved to the water bath at 37°C for one minute and then transferred into a 50 ml centrifuge. A 1/5th volume of 12% NaCl was added slowly to the sample and left for 5 minutes. Ten pellet volumes of 1.8% NaCl were then carefully added, one volume at a time with continual mixing. Finally, 10 volumes of 0.9% NaCl in 0.2% glucose were added in the same way. After this, the sample was centrifuged (1800rpm, 5 min, room temperature) and the final pellet resuspended in complete culture medium, gassed and placed at 37°C.

2.6 Transfection and monitoring of luciferase expression

Transfection carried out by using Gene Pulser Xcell™ Electroporation System (Biorad, UK) as described by Hasenkamp et al., (2013). In a 2mm cuvette (Bio-Rad), 180 µl of 1x cytomix, 20-40 µl of plasmid DNA (delivering between 20-40µg of plasmid(s) and 200 µl of cytomix-washed uninfected erythrocytes were all mixed gently and subjected to a standard electroporation condition [310V, 960µF and ∞Ω resistance]. The DNA-loaded erythrocytes were immediately transferred into a small flask containing 20ml of complete medium and 200µl of NF54 trophozoite-infected erythrocytes (at about 3-5% parasitaemia), gassed (1% O₂, 3% CO₂, and 96%N₂) and placed in a 37°C incubator. Drug selection pressure was applied two days post-transfection using 2.5nm WR99120 which added to the parasite culture to maintain plasmid DNA episomally within the parasite.

Two days post-transfection, Parasite growth and luciferase expression was monitored to confirm the transfection of the episomes with the luciferase reporter gene. A blood smear was made and examined under a light microscope to establish erythrocyte reinvasion. Luciferase expression was monitored using a standard luciferase assay. In a 96 multi-well tissue culture plate (Sarstedt, UK) 40 µl of resuspended transfected parasite culture was added to 10µl of 5x lysis buffer (Promega, UK) and 50 µl of luciferase buffer. The luciferase bioluminescence signal is reported in relative light units (RLU) using a Glomax Multi Detection System (Promega, UK). Data were transferred into an excel spreadsheet using the Instinct™ software (Promega).

2.7 Isolation of DNA from *P.falciparum*

Total DNA, including any episomal plasmid materials, were isolated from transfected parasites using one of two methods. The first described is a standard phenol-chloroform extraction protocol, the second protocol was done using a QIAamp® DNA isolation kit from the blood.

2.7.1 Phenol-chloroform DNA extraction method

The erythrocyte pellet from at least 100ml of 2% HCT culture with a high (>5% trophozoite and schizont staging) was collected by centrifugation (1800rpm, 5 min, room temperature) and washed twice with 25ml of chilled 1xPBS. The pellet was then resuspended in 25ml of 1xPBS/0.1% saponin. After two minutes, the released parasites were collected by centrifugation (4000rpm, 10 min, room temperature). The parasite pellet was resuspended in 1840 µl of DNA extraction buffer (1200µl sdH₂O, 200µl TN9 [500mM Tris HCl pH9, 2M NaCl], 400µl 0.5M EDTA and 40µl 50mg/ml-1 Proteinase K) and gently mixed by pipetting several times. After this 200µl of 100% SDS was added and mixed gently in a sealed tube in rotating incubator at 50C⁰ overnight. The following morning, 1ml of phenol/chloroform/isoamyl alcohol (25:24:1, Sigma) was added to the tubes and then taped to a microcentrifuge tube rotator for 60 min at room temperature. After this, the aqueous and phenol phases were separated by centrifugation (4000rpm, 10 min, room temperature). The upper aqueous phase was transferred to a clean microcentrifuge tube and the phenol/chloroform extraction repeated for 20 mins. After collecting the aqueous phase again, this had a 1/30th volume of 3M sodium acetate pH5.5 added and mixed by inversion before 0.6 volume of isopropanol (Sigma) was added to the aqueous phase and mixed by inversion. DNA that precipitates after mixing in the isopropanol was collected by spooling the end of a bacterial streaking loop. This DNA was then suspended in a small volume (between 100-200µl) of T₁₀E₁

buffer (10mM Tris HCl, 1mM EDTA, pH8.0) to achieve a 1-2 μ g/ μ l concentration, then DNA pellet was stored at 4 $^{\circ}$ C.

2.7.2 QIAamp® DNA extraction method

The total genetic material from parasite-infected erythrocytes was isolated and purified using the standard protocol provided by the manufacturer of the QIAamp® DNA Blood Kit (Qiagen). Briefly, 200 μ l of iRBC (>5% trophozoite and schizont staging) was collected by centrifugation and an equal volume of ice-cold 1x PBS/0.3% saponin was added, mixed well and placed on ice for 5 min. The released parasites were then collected by centrifugation at 14000 rpm, 4 $^{\circ}$ C for 1 min. The supernatant was removed and the parasite pellet washed with an equal volume of ice-cold 1xPBS ensuring the pellet was completely resuspended. The parasites were again collected by centrifugation before being resuspended in 200 μ l of 1x PBS. 20 μ l of the Qiagen-supplied protease buffer was added and mixed well with the sample before 200 μ l of buffer A1 was added to the sample, mixed using a vortex for 15s and incubated at 56 $^{\circ}$ C for 10 min. The sample was then centrifuged briefly to collect the sample before 200 μ l of absolute ethanol was added to the sample and mixed again using a vortex for 15 seconds. This solution was applied to a QIAamp Mini spin column (in 2 ml collection tube), centrifuged at 6000g for 1min and the filtrate discarded and the column (with the bound DNA) placed in a new 2 ml collection tube. 500 μ l of buffer AW1 was added to the Mini spin column, centrifuged at 6000g for 1min and the filtrate discarded. Next, 500 μ l of buffer AW2 was added to the column and centrifuged (14000 rpm room temp for 3 min at room temperature) and the filtrate discarded. The mini spin column then placed in a fresh 1.5 ml microcentrifuge tube and 30 μ l of elution (AE) buffer added then sample kept at room temp for 10 min, centrifuged at 8000 rpm for 1 min. The concentration of DNA in the eluted sample was determined using a Nanodrop before storage at 4 $^{\circ}$ C.

2.8 Assays of growth inhibition in intraerythrocytic *P. falciparum*

Typically, growth inhibition assays were done using synchronized trophozoite stage parasites exposed to the compound/drug being evaluated for one cycle of intraerythrocytic growth (48 hrs). Assessment of the growth inhibition, normalised to controls for 100% growth (no compound/drug) or 0% growth (typically a 10 μ M super lethal dose of chloroquine), was made using either plate-based assays or by flow cytometry.

2.8.1 Multiwell plate-based assays of growth inhibition in *P. falciparum*.

These growth inhibition assays were done using a 96-multiwell tissue culture plate (Sarsted, UK). 100 μ l of complete medium was added to all test wells except for the first column where an appropriate volume of complete growth medium was added depending upon the dilution factor (typically this was 200 μ l for a two-fold dilution series). This first column of the plate was supplied with an appropriate volume of the molecule of interest (Glycosaminoglycans GAGs or drugs) and mixed by repeated pipetting. Serial transfers of an appropriate volume (typically 100 μ l in a two-fold dilution series) from each column provided for a serial dilution of the molecule of interest. After this GAG/drug dilution, 100 μ l of a master mix of *P. falciparum* culture which consists of 2% synchronous trophozoite stage parasites at a 4% hematocrit in complete medium was added. This then provided for 200 μ l assays at a 2% parasitaemia and 2% haematocrit.

Whilst the starting parasitaemia would be varied depending on the growth inhibition assay, the haematocrit and total volume were constant. Positive controls for a 100% growth were provided by no drug control. The 0% growth was established with a 10 μ M super lethal concentration of chloroquine. After the dilution was complete, 200 μ l of incomplete growth medium was added to outermost wells on each plate to minimize edge effect evaporation. The plate was moved to a humidified box and gazed with keep incubation condition of 1% O₂, 3% CO₂ and 96% N₂ at

37°C. For most experiments, a two-fold dilution series was used, with three technical repeats on each plate (a plate, therefore, being used to test two molecules of interest). Typically, three biological repeats were done for each molecule of interest. Data were extracted into an Excel sheet via Instinct™ software (Promega). Growth inhibition data from were normalised against the 100% and 0% controls. Here, normalised growth in the test well is defined as [signal in test well – mean signal at 0% growth]/ [mean signal at 100% growth – mean signal at 0% growth] X100. The mean and standard deviation of typically n=9 repeats, being plotted on a log concentration normalised response curve in GraphPad Prism v5.0 (GraphPad Software, Inc., San Diego, CA) to establish the 50% Effective concentration (EC₅₀) and their 95% confidence intervals (95%CI). Assessment of parasite growth was made on a plate-based assay of Dd2^{luc} and NF54^{luc} using either a luciferase assay or a Malaria Sybr Green I fluorescence assay.

2.8.2 Luciferase Assay

The luciferase assay used is adapted and modified from that reported by Hasenkamp et al., (2012) and used here to explore the growth inhibition and invasion blocking effects of glycosaminoglycans on Dd2^{luc} or NF54^{luc} strains. The 96-microwell plates were incubated at 37°C for either 6, 48 or 96 hours depending on the nature of the experiment. In 96-multiwell white plate (Greiner, UK), 40 µl of Dd2^{luc} or NF54^{luc} wells were transferred and 10 µl of 5X Passive Lysis Buffer (Promega, UK) was added and carefully mixed. 50 µl of the standard luciferase substrate (Promega, UK) was added. The plate was shaken gently and the bioluminescence signal, in relative light units (RLU), immediately measured on a Glomax Multi Detection System (Promega, UK). Bioluminescence provides variation in raw data, influenced by parasitaemia, culture health and staging as well as substrate used, time for assay etc. However, like any robust assay system, normalization controls for these and has been demonstrated for our bioluminescent parasites in Hasenkamp et al., (2012).

2.8.3 Malaria Sybr Green I fluorescence (MSF) Assay

This Protocol was described previously by Smilkstein et al. (2004). Sybr Green I (Invitrogen, UK supplied as a 5000X stock) was added to 1x MSF lysis buffer in 1:5000 ratio. This was then mixed and placed in the dark until use. For the assay, 100 µl of MSF/Sybr Green I buffer was added to a black 96-multiwell plate (Greiner, UK) and an equal volume of parasite culture from the growth inhibition assay was added and the plate shaken gently to homogenise the well contents. This plate was placed at room temperature in the dark place for 30-60 minutes. The fluorescent signal, in RLU, was then measured through the blue fluorescent module (excitation 490nm: emission 510–570nm) of a Glomax Multi Detection System (Promega, UK).

2.8.4 Flow cytometry-based assays of growth inhibition in *P. falciparum*.

A flow cytometry approach to monitor the growth inhibition of different GAGs has been adapted here from the original report of Boyle et al. (2010). Synchronized Dd2^{luc} or NF54^{luc} trophozoites were cultured in the presence of the GAG of interest according to the standard 96-well plate protocol described above (section 2.8.1) The experiment was performed as at least three independent biological repeats (n=3) and the growth inhibition measured by flow cytometry after 48 and 96 hours of incubation. Parasite cultures were mixed to resuspend the monolayer and washed twice with 1x PBS (Sigma). The washed red blood cell pellet was collected by microcentrifugation (13000rpm, 30 sec, room temperature) and 5 µl of the red blood cell pellet suspended in 90 µl of complete medium (4% haematocrit) was mixed with the same volume of 10% ethanol/1X PBS containing a 10X concentration of SYBR Green I dye (provided as a 10,000X stock, Invitrogen) and incubated for 20 minutes in the dark.

The collected data was analysed and plotted using Guava EasyCyte™ HT System and GuavaSoft 3.1.1 software (Millipore, USA).

To determine the parasitaemia in the culture, the population of red blood cells were determined by plotting the forward scatter (FSC) and side scatter (SSC) of each event (Figure 2.1A). This population was gated (Figure 2.1B) and for this population, the side scatter plotted against the fluorescence signal using the Yellow -Blue (YEL-B) filter as indicated for the use of the SYBR Green I dye (Figure 2.1C). 20,000 cells were analysed for each sample. To monitor the growth inhibitory effect of each GAGs at the concentration tested, the normalised growth was determined against an untreated control. In the example shown here, the untreated control is represented in panel C of figure 2.1 (3.63%), with the experiment represented in panel D. Here, the normalised growth in the experiment would be $(0.46/3.63 \times 100)$ 12.7% of the untreated control. The mean and standard deviation of n=3 biological repeats were plotted using GraphPad Prism v5.0 (GraphPad Software, Inc., San Diego, CA).

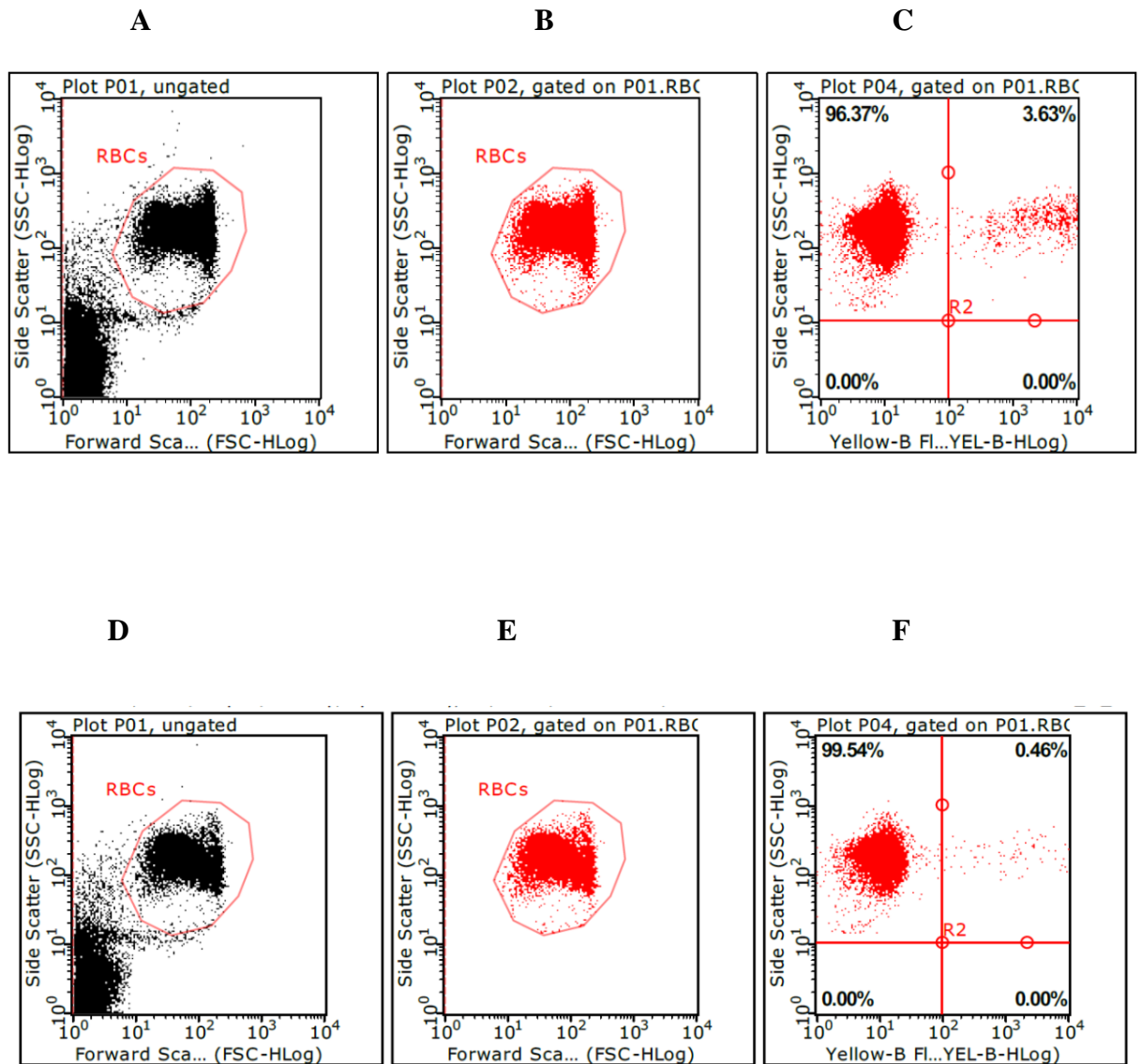


Figure 2.1 Shows flow cytometry dot plot growth inhibition assay using SYBR Green I DNA stain method after 48 hours incubation.

C, F represent parasitaemia of untreated sample (iRBC only), treated parasite with 100 $\mu\text{g/ml}$ of Tinzaparin (LMWH) or with unfractionated heparin respectively. Infected and uninfected (20,000 cells) were gated and labelled as RBC (A, D) meanwhile unlabelled are components of dead parasite or debris. B, E represents gated RBC only.

2.9 Monitoring the time course of *P.falciparum* intraerythrocytic development in the presence of GAGs

The experiment was carried out using the standard 96-microwell microplate condition (section 2.8.1). Highly synchronized Dd2^{luc} or NF54^{luc} schizonts (34-40 hours post-infection) were treated with a fixed 100µg/ml concentration of GAG of interest and incubated at 37°C for 48hrs to complete one intraerythrocytic cycle. At 18, 24, 48 hours after the start of the experiment, the contents of the well were resuspended and 10 µl used to prepare a thin smear that was fixed and stained with 10% Giemsa. The slides were examined under a 100x oil immersion lens using a light microscope. For each experiment, and three biological repeats were done, 100 infected red blood cells were identified, and the morphological parasite stage recorded. Photographs were captured using the Dialux 20 EB microscope connected with a camera (InfinityX) and processed using the DPXview pro software.

To more closely explore the phenomenon of merozoite clusters formed with some GAGs at high concentrations, synchronized Dd2^{luc} and NF54^{luc} schizonts (34-40 hours post-infection) were incubated for 48 hours with different concentration of GAGs. As described above, thin smears of the treated and untreated parasite cultures were examined by light microscopy and a count of different morphological forms done. The experiment was carried out using the standard 96 microplate conditions and for three biological repeats (n=3).

Where fluorescent imaging of infected erythrocytes were required, a method adapted from MacKenzie & Ruxton (2015) was used after some modifications. After 48 hours of incubation, GAG treated, and untreated parasite were resuspended, and a thin smear slide was prepared. These slides were stained with SYBR Green I (Invitrogen) diluted 1:1000 in 10% ethanol in the dark at room temperature for 20 minutes. After washing generously with water, slides were examined and photos taking using the EVOS cell imaging system (Life Technologies) under 100x oil emersion magnification using the GFP filter (emission 510nm)

2.10 Molecular Methods

2.10.1 Plasmid DNA transformation of *Escherichia coli*

Plasmid DNA was transformed into chemically competent *E. coli* (Bioline) according to the manufacturer's instructions. Briefly, Up to 4 µl of a 10 ng plasmid DNA stock, or up to 10 µl of a ligation reaction, was added to the chemically-competent *E. coli* and kept on ice for 30 min and followed by heat shock (42°C, 30 sec). These cells were then placed on ice for 2 min. Then 250 µl of SOC medium was added to the cells and these then placed in a shaking incubator at 37°C for 45 min at 225 rpm. Three volumes of 10, 30, 100 µl of the transformed *E. coli* were spread over three pre-prepared Ampicillin selective plates (90mm LB agar plates supplemented with 100µg/ml ampicillin). These plates were inverted and kept at 37°C overnight. The next day, single colonies were picked and inoculated into 5 ml of LB medium containing 100µg/ml ampicillin and placed on a shaker incubator at 37°C at 225 rpm to grow overnight.

2.10.2 Plasmid DNA minipreparation from *E. coli*

Plasmid DNA was isolated and purified from *E. coli* according to manufacturer instructions of the GeneJET system (Thermo Scientific). A 1ml culture of overnight growth of *E. coli* was transferred to 1.5 ml Eppendorf tube and collected by centrifugation at 8000 rpm, room temperature for 2 min. The supernatant was discarded and the bacterial pellet resuspended in 250 µl of the supplied resuspension solution. Cells were suspended completely through vortexing until clumps became homogenised and 250µl of the supplied lysis solution was added and mixed by inverting the tube 6-8 times. After this, 250 µl of neutralization buffer was added that precipitates the protein/lipid content on inversion. The lysate was cleared by centrifugation for 5 min at 12000g at room temperature and transferred to a Gene JET column and centrifuged for 1 min at 12000g at room temperature. The flow through was discarded and 500 µl of

supplied wash solution was added and centrifuged for 1 min at 12000g at room temperature. The flow through was discarded and the spin column placed in a sterile 1.5 ml Eppendorf tube. 30 µl of supplied elution buffer was added to the centre of the column and kept for 10 min at room temperature before the eluting the DNA by centrifugation for 1 min at 12000g at room temperature. The quality and concentration of the purified plasmid DNA were checked using a Nanodrop device before the plasmid was stored at -20°C.

2.10.3 Maxi plasmid DNA preparations from *E. coli*

To prepare plasmid material for transfection of *P. falciparum*, a maxipreparation using a Qiagen Maxi Plasmid DNA preparation kit was used according to the manufacturer's instructions. Bacterial culture (between 200 to 300ml in LB supplemented with 100µg/ml ampicillin) was grown whilst shaking overnight. The bacteria were harvested by centrifugation 6000g for 15 min at 4°C and then fully resuspended in 10 ml of buffer P1 (50mM Tris-HCl pH8.0, 10mM EDTA, 100µg/ml RNase). Then 10ml of buffer P2 (200mM NaOH, 1% SDS) was added and mixed thoroughly by inverting 6-8 times to obtain a viscous appearance and kept 5 min at room temperature. Then 10ml of ice-chilled P3 buffer was added (3.0M sodium acetate pH5.5) and immediately mixed by inverting 6-8 times and incubated on ice for 20 minutes. At this time, a Qiagen Tip500 was equilibrated by adding 10ml of the supplied QBT buffer and allowed to empty by gravity flow. During the equilibration, the bacterial lysate was cleared by centrifugation at 20000g for 30 minutes at 4°C. The cleared lysate was added to the Tip500 and allowed to empty by gravity flow. The Tip500 with the now bound plasmid DNA was washed twice with 2 x 30ml of the supplied QC wash buffer. The plasmid DNA was finally eluted by adding 15 ml of the supplied QF buffer which was then mixed in a 50ml tube with 10.5 ml of room temperature isopropanol to precipitate the plasmid DNA. The DNA was collected by high-speed centrifugation at 15000g for 30 min at 4°C. The DNA pellet was washed with 5ml

of 70% ethanol and then centrifuged at 15000g for 10 min at 4°C. The supernatant was carefully discarded and DNA pellet air-dried for 10 min. The DNA pellet was redissolved in a suitable volume of water (200-300 µl) to provide an approximately 2µg/µl concentration as determined using a Nanodrop.

2.10.4 Restriction digests

All restriction endonucleases were sourced from Promega. Plasmid DNA or gDNA was restricted according to the manufacturer's instructions. Typically for a plasmid restriction, 0.5µl of the restriction enzymes was used to restrict between 0.5 to 2µg of DNA in a 20µl volume of the appropriate 1x fast green buffer (diluted in sdH₂O from a 10x stock). The restriction digest was incubated at 37°C in a heated block for 1 hour. The restricted DNA was size-fractionated on an agarose gel and the DNA stained with ethidium bromide visualized using a UV gel documentation system (Syngene).

2.10.5 Agarose gel electrophoresis and imaging

Agarose gel electrophoresis for DNA size fractionation was used routinely to assess restrictions of plasmid DNA or genomic DNA fragments. The concentration of agarose gel ranged between 0.8% to 2% with larger fragments separated on lower concentration gels. To prepare a 1% agarose gel, 1g of agarose powder (Invitrogen) is added to 100 ml of 1XTAE buffer (made from dilution from a 50XTAE stock). The mix was then heated in an 800W microwave oven for 1-2 minutes, with regular checking and mixing, to dissolve the agarose and then cooled to approximately 45°C. To this cooled agarose solution, 3 µl of a 10 mg/ml EtBr solution was added before the liquid poured to set in a cast. Typically a 50-100ml gel would require at least 30 mins to become solid for use – at this time it was immersed in 1XTAE buffer in a gel tank and the comb for the wells removed at this time. For most gels, 5 µl of a standard DNA ladder

(Invitrogen) was added to the first well. Restriction digests or PCR reactions etc were then loaded, in 1X loading dye to the remaining wells. Electrophoresis was typically done between 80-100V (8-10V/cm) for 45 minutes. The DNA in the gel was then visualized using the UV gel documentation system.

2.10.6 Purification of DNA fragments from agarose gel

Restricted DNA fragments were isolated and purified using the S.N.A.P. gel purification kit as supplied by the manufacturer (Invitrogen). DNA was size-fractionated in a maximum of a 1% agarose gel that was stained with ethidium bromide. Under a short exposure to low-intensity long-wave UV light, the desired DNA fragments were isolated and then transferred to clean 1.5 ml Eppendorf tube containing the supplied binding solution (10ul per 10mg of gel slice). The sample was mixed by vortexing and incubated at 60°C for 10 minutes until the gel slices dissolved completely. The gel mixture was transferred to a minicolumn assembly and incubated for 1 minute at room temp. The mixture then centrifuged at 14000rpm for 1 min at room temperature and washed twice using 700µl and then 500µl of the supplied wash buffer, each time using centrifugation at 14000rpm for 1 minute at room temperature. The column was finally transferred to clean 1.5ml microcentrifuge tube contain and 35µl of nuclease-free water added to the column, left for one minute and then eluted at 14000rpm for 1 min at room temperature. As well as using the Nanodrop to confirm the concentration of eluted DNA, typically 5 µl of the eluted DNA sample was size-fractionated and visualized on an agarose gel.

2.10.7 DNA ligations

Both vector and insert DNA fragments used in this study provided complementary overlapping ends. As such as standard T4 ligase (Invitrogen) reaction were done using the materials provided by the manufacturer in 10 µl reaction volumes. Ligations were prepared with between 10-30 ng of vector sequence with different ligations using a 1:1 and a 1:3 vector: insert ratio. Reactions were incubated at room temperature for at least 5 hrs, and normally overnight. Ligations were then transformed into chemically competent *E.coli* cells as described above in section 2.10.1

2.10.8 Polymerase chain reaction (PCR)

PCR was performed using MyTaq™ Red Mix kit (Bioline) using the manufacturer's instructions. The normal PCR reaction volume was 50 µl. This included; 2µl of DNA template (typically 10ng of plasmid or 100ng of genomic DNA), 1µl each of forward and reverse primers (20ng/µl), 25µl My Taq Red Mix and 22 µl of distilled water. PCR cycling conditions (using an Eppendorf Master cycler Personal thermocycler) were typically;

- (i) 95°C for 4 min,
- (ii) 95°C for 1 min (melting step)
- (iii) 53°C for 1min (hybridization step- adjusted based on the oligo annealing temperatures)
- (iv) 68°C for 1 min (extension step – adjusted for 1000bp product/min)
- (v) Repeat steps (ii) to (iv) for 30 cycles
- (vi) 68°C for 10 min (final extension) and hold at 18°C

PCR genotyping was deployed to distinguish between the transfected NF54^{Luc} and laboratory strain Dd2^{Luc}. *MSP1*, *MSP2* and *GLURP* were the three loci selected for comparison of the PCR length polymorphisms (Ridzuan et al., 2016) between these two strains. See (Table 2.1)

Table 2.1 shows primers used for PCR genotyping

Gene/family	Primer	Sequence
MSP-1	MI-OF	5' CTAGAAGCTTTAGAAGATGCAGTATTG 3'
	MI-OR	5' CTAAATAGTATTCTAATTCAAGTGGATCA 3'
GLURP	G-OF	5' TGAATT GAAGATGTTCACTGAAC 3'
	G-OR	5' GTGGAATTGCTTTTTCTTCAACTAA 3'
MSP2	M2-OF	5' ATGAAGGTAATTAACATTTGTCTATTATA 3'
	M2-OR	5' CTTTGTACCATCGGTACATTCTT 3'

2.10.9 Quantitative real-time PCR (qRT-PCR)

Total genomic DNA was isolated following DNA extraction method described previously (see 2.7.2). SYBR Green master mix (Applied Biosystems) was used for all qPCR in this study and performed on a StepOnePlus real-time PCR system (Applied Biosystems). Primers were designed to amplify a fragment of the luciferase gene, approximately (350bp); forward primer 5'-AATCCGGAAGCGACCAACGC-3', and reverse primer 5'-CGCGTCGAAGATGTTGGGGT-3'. The PCR mix was prepared according to the manufacturer's instructions, briefly, 1µl of gDNA (concentrations ranged between 30 to 83 ng/µl for template used), 10 µl of SYBR Green buffer, 2µl each of the primers (20ng/µl) and 6µl of H₂O to provide a final total of 20µl. qPCR conditions were 95°C for 10 mins, followed by 40 cycles of 95°C for 15 s and 60°C for 60 s. Using the 2^{-ΔΔCt} method for relative quantitation of copy number, the copy number of the luciferase gene in NF54^{Luc} (compared

against Dd2^{luc} defined here as 1 in the ratio analysis), and compared to standards using chromosomally-located control (housekeeping) genes, seryl-tRNA synthetase (s-tRNA syn) , aldolase and Actin (β -actin1) (Table 2.2). Each relative quantification experiment was performed in triplicate and three independent biological repeats were done. Data were analysed using Step-One (V2.3) software and plotted using GraphPad Prism v5.0 (GraphPad Software, Inc., San Diego, CA).

Table 2.2 (housekeeping) genes primers used in q-PCR assay

Gene	Primer	Sequence	Reference
seryl-tRNA	F R	5'-AAGTAGCAGGTCATCGTGGTT-3' 5'-TTCGGCAC-ATTCTTCCATAA-3'	(Salanti et al., 2003)
Aldolase	F R	5'-TGCACTGAATATATGAATGCC-3' 5'-GACATATTTCTTTTCATATCCTG-3'	(Lee et al., 2006)
Actin (β -actin1)	F R	5'-AGCAGCAGGAATCCACACA-3' 5'-TGATGGTGCAAGGGTTGTAA-3'	(Salanti et al, 2003)

2.10.10 Probe preparation for southern blotting

A 350bp PCR of the luciferase gene was used to prepare a probe for Southern blots analysis. The oligonucleotide primers used were Forward- 5' GGCCCGGCGCCATTCTATCCGC 3' and Reverse-5'GCCCATACTGTTGAGCAATTCAC3'. After the PCR was size-fractionated, the product was gel purified as described previously (See2.10.6).This product was used as a template in a PCR DIG Probe Synthesis Kit (Roche) protocol that incorporates DIG-dUTP into the PCR product Briefly, 2.5 μ l (~26 ng) of DNA template added to 10 μ l each of forward and reverse primers (20ng/ μ l), 5 μ l 10xPCR DIG probe synthesis mix, 5 μ l dNTP (40 μ M), and 0.75 μ l enzyme mix and distilled water up to 50 μ l. The PCR amplification conditions were the same

as used in the example above. The amplified labelled probe was then used for hybridization to the Southern blot.

2.10.11 Southern blotting

Genomic DNA (10µg/lane) were restricted in 30µl volumes overnight and size-fractionated on a 15-20cm long 0.8% agarose gel in 1x TAE buffer. The control molecular weight marker was DIG-DNA molecular weight marker II (0.12-23.1kbp) (Roche) [5µg(500µl stock concentration)], 10 µl mixed with 2 µl of 5X loading dye .The DNA was size-fractionated slowly (maximum of 80V) for 4-6 hrs. After UV gel documentation, the agarose gel was soaked in 500 ml of depuration solution (0.2 N HCl) for 15 minutes with gentle agitation. This was replaced with 500 ml of denaturation solution (0.5 M NaOH, 1.5 M NaCl) for 45 minutes with gentle agitation. Finally, the gel was washed twice in 500 ml neutralising solution (0.5 M Tris-HCl pH7.5, 1.5 M NaCl) for 20 minutes with gentle agitation with a final brief was in distilled water. Hybond N+ (GE Healthcare products) was pre-soaked in 2x SSC and placed on top of the gel, followed by a paper towel stack (see Figure 2.2) in a DNA transfer apparatus.

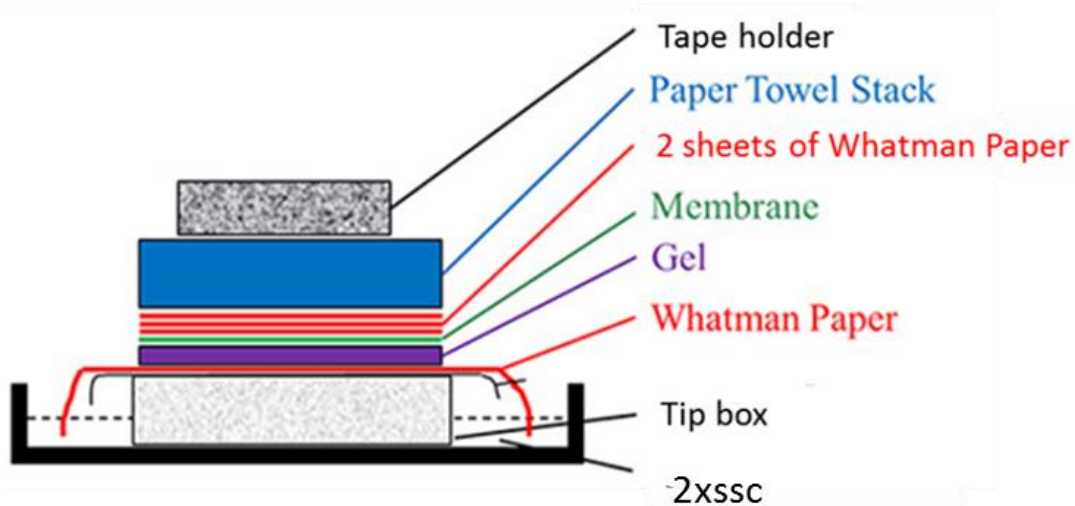


Figure 2.2. Illustration of a southern blotting apparatus. The schematic shows the relative order of the Whatman 3M wick underneath the gel, with the Hybond N+ membrane on top of the gel and the 2XSSC drawn through the gel by capillary action to transfer the DNA from the gel onto the Hybond N+ membrane.

After an overnight transfer, the Hybond N+ membrane was rinsed 2xSSC and exposed for three minutes to 302 nm UV (DNA side down). This membrane was pre-hybridized by incubating with 25 mL of pre-heated Easy-Hyb solution (GE Healthcare) for 4 hours whilst rotating in a 42°C hybridisation oven. The DIG-labelled PCR probe (c 500ng to achieve 20 ng/ml) was heat-denatured for 5 minutes at 95°C and snap cooled immediately on ice and added to the membrane in 25ml of pre-heated Easy-Hyb solution. The DIG labelled probe was incubated overnight at 42°C in the rotating hybridisation oven. After this, the membrane was washed twice with 2x SSC, 0.1% SDS (100 ml/wash) for 15 minutes at room temperature. The wash was repeated twice using 0.5x SSC, 0.1% SDS (50 ml/wash) for 15 minutes at 68°C in the hybridisation oven. The membrane was removed and rinsed for 5 minutes in 50 ml of 1x DIG washing buffer (Roche) and blocked with 50 ml 1x blocking solution for 30 minutes. The membrane then incubated with a diluted anti DIG in 1X blocking solution for 30 minutes at room temperature. The membrane was washed twice with 50 ml of 1x DIG washing buffer in a small tray and equilibrated for 5 minutes in 5 ml 1x detection solution and placed (DNA side up) on a plastic

film. 20 drops (~0.5 ml) of CDP-Star ready-to-use solution (chemiluminescent substrate for alkaline phosphatase) was added to the membrane and then sealed with saran wrap and incubated in the dark for 5 minutes at room temperature. The wrap was removed to remove excess solution, resealed with saran wrap and placed (DNA side up) in a FluorChem M imaging system to document the fluorescent signal.

2.11 Prothrombin time (PT) assay

This assay was utilized to evaluate the anticoagulation activity of GAGs for the extrinsic and common pathway. 50 μ l ml of human plasma or (plasma control) was added in cuvette contain ball bearing followed by adding 50 μ l of HPLC grade water (for control) or with two-fold dilution series (100 μ g/ml) heparin and incubated for 1 minute at 37⁰C in. After 1 minute exactly, 50 μ l of pre-warmed thromborel S reagent was added. Coagulation time measured by using Thrombostat 1(Behnk Elektronik GmH &co. KG).

2.12 Activated thromboplastin time (aPTT) assay

To evaluate GAGs anticoagulation activity for the intrinsic and common pathway. In a cuvette containing a ball bearing, 50 μ l of normal human or control plasma was added to 25 μ l ml of HPLC grade water for control or with two-fold dilution series (100 μ g/ml) heparin followed by adding 50 μ l of pathromtin SL reagent and incubated for 2 minutes at 37⁰C. 25 μ l of pre-warmed CaCl (50 mM) was added to the solution immediately after 2 minutes of incubation. Clotting time was measured by using Thrombostat 1(Behnk Elektronik GmH &co. KG).

Chapter three: Generation and validation of NF54^{luc} transgenic parasite strain expressing a trophozoite stage-specific luciferase reporter

3.1 Introduction

Transgenic *Plasmodium* parasite strains provide valuable tools in the study of these parasites, supporting studies as diverse as investigating cell-host interaction to exploration and evaluation of new parasite inhibitors and vaccines (Othman et al., 2017). Genetic modification of *Plasmodium falciparum* is currently limited to manipulation of the intraerythrocytic stages, maintained by continuous *in vitro* culture systems (Trager and Jensen, 1976), with this process made more challenging as delivery of exogenous DNA to the parasite needs to cross four membrane barriers: (i) erythrocyte plasma membrane, (ii) parasitophorous vacuole membrane (iii) parasite plasma membrane and (iv) the nuclear membrane barrier (for review see Horrocks & Lanzer., 1998). In addition, the extreme bias in parasite DNA AT content – particularly in non-coding regions, makes subcloning these sequences within *E.coli* more challenging (Wu et al., 1995; Horrocks & Lanzer., 1998). However, these challenges have been overcome, with the first *Plasmodium* species manipulation achieved by Goodewardene et al., (1993), who described the transient expression of a luciferase reporter gene into the avian malaria parasite *Plasmodium gallinaceum*. This work was shortly followed by the successful transfection of *P. falciparum* by Wu et al., (1995).

Generation of a *P. falciparum* transgenic parasite, using electroporation to introduce exogenous DNA into parasite cell, requires the use of plasmid DNA carrying different DNA elements which are all required for the transfection to succeed. Selection markers (often drug resistance genes) with an appropriate promoter and terminator sequences play an important role in plasmid DNA maintenance (replication and segregation) for both episomal maintenance or integration into the parasite genomic DNA (Goonewardene et al., 1993; van Dijk et al., 1997). Common

bacterial selectable markers include; neomycin phosphotransferase, blasticidin S deaminase (Botstein et al., 1999) , puromycin-N-acetyltransferase conferring resistance to blasticidin S, geneticin (G418) and puromycin, respectively (De Koning-Ward et al. 2001) or the use of human/parasite dihydrofolate reductase (DHFR) conferring resistance to the antifolates pyrimethamine or WR9921(McElwain et al., 2002). The plasmid construct also often has a fluorescent or luminescent reporter based on the proposed application of this marker gene (Marin-Mogollon et al., 2019). The first description of a bioluminescent based assay of parasite growth was by Cui et al., (2008). This assay was later further evaluated for antimalarial drug discovery (Wong et al., 2011; Hasenkamp et al., 2013) where a Dd2 strain containing a luciferase reporter gene ($Dd2^{luc}$) flanked by the 5` and 3` regulatory regions of the proliferating cell nuclear antigen (PCNA) gene providing a strong stage-specific expression of luciferase in trophozoites. This same GM parasite has demonstrated a range of uses in the investigation of epigenetic gene regulation, exploring transfection methods and their efficiencies as well as a new assay studying the pharmacodynamics of drug action (Wong et al., 2011; Hasenkamp et al., 2013; Ullah et al., 2017).

We plan here to use the same reporter system (Wong et al., 2011) but instead introducing it into a different parasite strain - NF54. $Dd2^{luc}$ was developed using *Bxb1* integrase system which mediates the integration of a sequence bearing an *attP* site into the genomic DNA at a previously integrated *attB* site (Adjalley et al., 2010; Nkrumah et al., 2006). With NF54^{attB} strain being available this was the intended approach here. In other work described here, we achieve a stable transfection in the NF54 parasite using a plasmid construct bearing Rep20 sequences. Rep20 is a unique repeated, 21 bp sequence found in all subtelomeric of the 14 *P. falciparum* chromosomes and is not found in other eukaryotes (McElwain et al., 2002). It has previously been shown that plasmids bearing a rep20 sequence lead to an episomal maintained plasmid by

promoting plasmid segregation between daughter merozoites and by mediating plasmid tethering to the chromosomes (O'Donnell et al., 2002).

We used these approaches to transfect NF54 parasite phenotype with the same luciferase construct we already have available in the Dd2^{luc} strain. The new genetically modified NF54^{luc} parasite is required for our planned investigations of the invasion inhibition effect of heparin and other sulphated GAGs. Heparin and related sulphated GAGs have been reported in several previous studies to inhibit parasite growth, mainly by blocking merozoite invasion into the uninfected erythrocyte (Leitgeb et al., 2017; Boyle et al., 2017; Clark et al., 1997; Xiao et al. 1996) and this inhibition is likely mediated by targeting key merozoite invasive proteins and inhibiting parasite–erythrocyte ligand interactions (Boyle et al., 2010). In addition to blocking processing of merozoite surface proteins (MSP), heparin has been found to mask the apical surface of merozoite by binding with various merozoite apical proteins, such as the erythrocyte-binding antigen-175 (EBA-175) (Kobayashi et al., 2013). These ligands of merozoite-erythrocyte interaction bind with a range of erythrocyte receptors (Sim et al., 1994; Cowman et al., 2017). There are three principle erythrocyte receptors localized on the erythrocyte cell surface important for merozoite invasion; glycophorin (gp) A or B and an unidentified trypsin sensitive molecule termed X. (Mitchell et al., 1986; Hadley et al., 1987; S.A. Dolan et al., 1994). For example, the merozoite ligand EBA-175 binds to sialic acid residues on gpA (sialic acid-dependent) (Orlandi et al., 1992). Cloned parasite isolates have been shown to employ a range of alternative pathways to invade erythrocyte (Dolan et al., 1990; Dolan et al., 1994). Importantly, Dd2 has a neuraminidase-sensitive invasion phenotype, where merozoite invasion is dependent on sialic acid which is cleaved off by neuraminidase treatment (Binks & Conway, 1999). However, the NF54 strain acts the same as its progeny 3D7 strain and has an alternative invasion pathway in that it is neuraminidase-resistant, i.e merozoite invasion of the erythrocyte is non-sialic acid dependant (Theron et al., 2010).

Here I describe the generation and then validation a NF54^{luc} transgenic parasite strain that bears the same luciferase reporter system as the existing Dd2^{luc} strain available in the laboratory. This line will then be available to use alongside Dd2^{luc} in GAGs inhibition studies as a second independent strain, with an alternative invasion phenotype, to explore the potential for strain-dependent invasion inhibition effects.

3.2 Results

3.2.1 Comparison of plate-based fluorescence versus bioluminescence assays of intraerythrocytic growth inhibition using glycosaminoglycans

Assays of inhibition of intraerythrocytic growth using microplate assays usually use the Malaria Sybr Green I Fluorescence (MSF) assay. This assay was originally developed by Smilkstein et al., (2004) and is based on the emitted fluorescence signal of Sybr Green I when intercalated into DNA – with the DNA content of the *in vitro* assay dependent on the growth and multiplication of a parasite culture over 48 hours. However, initial experiments using a plate-based Sybr Green I assay to monitor the inhibitory effect of heparin over 48 hours on a starting 2% trophozoite Dd2^{luc} culture (Figure 3.1) showed that increasing concentrations of heparin did not lead to a decrease in fluorescence signal as the growth inhibitory effect increased, but rather led to an increase in fluorescence. Microscopic examining (data not shown) of cultures exposed to high concentrations of heparin did not show an increase in parasite numbers, with the opposite true when no parasites were observed. We concluded that there was a heparin-Sybr Green I affect that leads to an increase in fluorescence. This is also true for low molecular weight heparins and glycosaminoglycans isolated from marine sources (Figure3.1), these compounds reflecting materials assessed in Chapters 4 and 5 of this thesis.

The Dd2^{luc} strain used is a transgenic strain that expresses high levels of luciferase in the late trophozoite stage – with the expression linked to the S-phase of parasite growth (Wong et al., 2011). This strain has also been evaluated to measure the growth inhibitory effects of compounds and determine their EC₅₀ (Hasenkamp et al., 2013). Using a plate-based luciferase assay, concentration-dependent inhibition of parasite growth was observed for all the glycosaminoglycan compounds previously tested in the MSF assay (Figure 3.1). Based on this

data, it was determined that plate-based assays to determine growth inhibitory effects of glycosaminoglycans should use a luciferase assay.

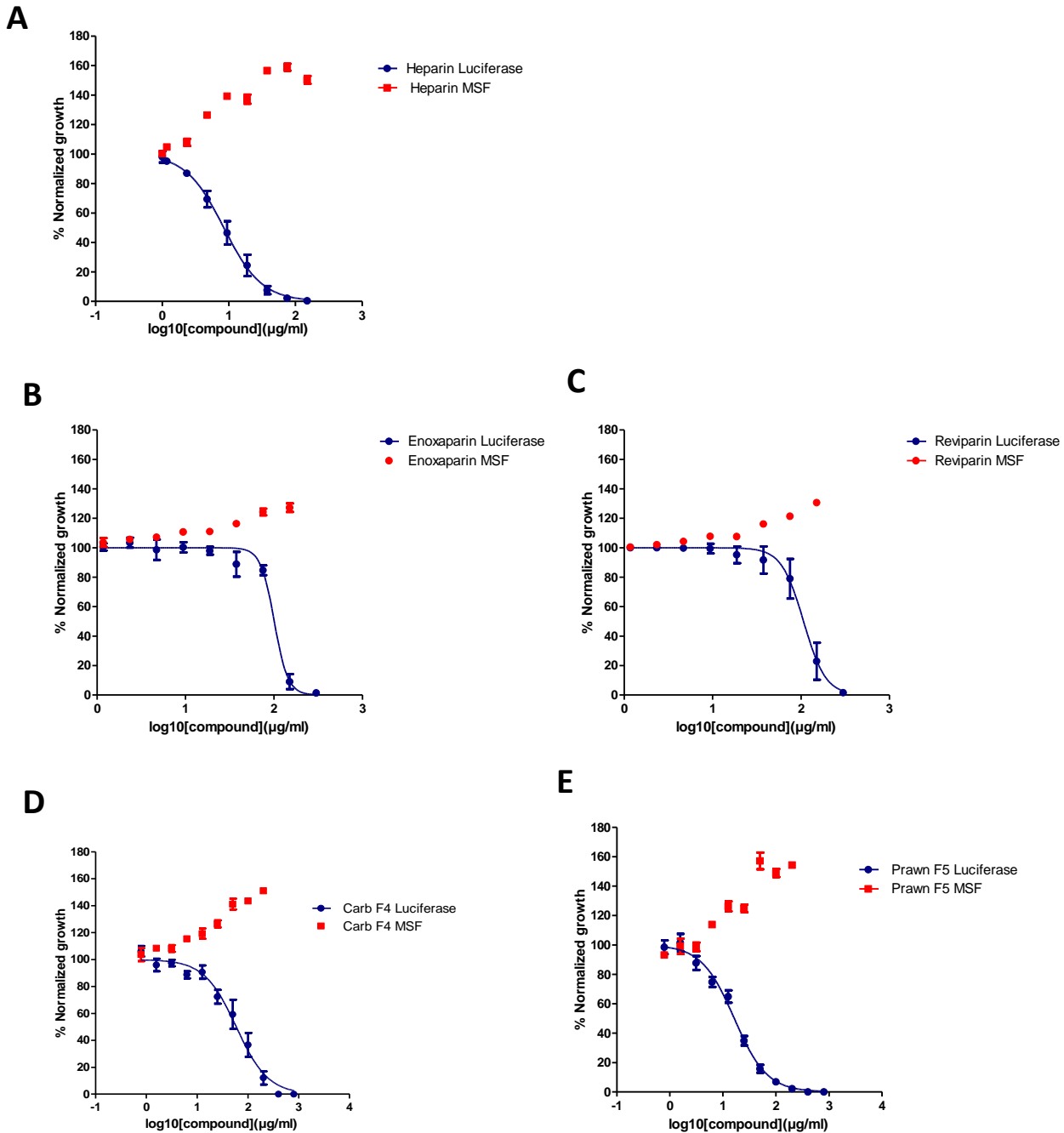


Figure 3.1 Comparison of plate-based MSF vs. luciferase assays. The growth inhibition **A** of heparin, two low molecular weight heparins **B**, **C** (enoxaparin and reviparin) and two marine-derived glycosaminoglycan fractions **D**, **E** (Crab fraction 4 and Prawn fraction 5) in a MSF fluorescence (red) and luciferase (blue) assay. The mean \pm stdev of $n=6$ (technical triplicate with two biological repeats) are shown for each assay.

3.2.2 Generation the NF54^{luc} transgenic parasite

The development of the Dd2^{luc} strain tested here is described in Wong et al. (2011). Here co-transfection of a Dd2^{attB} (developed by Nkrumah et al., 2006) with (i) a PΔ1 plasmid with an *AttP* site that also had a luciferase expression cassette and blasticidin C drug selection cassette (Blasticidin-S deaminase gene) and (ii) pINT plasmid (Nkrumah et al., 2006) that bears a neomycin drug selection cassette and the mycobacteriophage Bxb1 integrase that mediates chromosomal integration of PΔ1 by catalysing recombination between incoming *attP* and the chromosomal *attB* (chromosome 7).

Also available from Professor Fidock (Columbia University, New York, USA) was a NF54^{attB} strain. As well as NF54 having distinct drug resistance phenotypes to Dd2 (see Hasenkamp et al., 2013), it also has a distinct erythrocyte invasion phenotype as well. Dd2 is significantly dependant on sialic acid on glycoporphins – and its invasion of erythrocytes is therefore neuraminidase-sensitive, unlike NF54 (Theron et al., 2010). Whilst erythrocyte invasion is trypsin sensitive in both strains, Dd2 invasion is not affected by chymotrypsin (Theron et al., 2010). The NF54 strain offered a second, independent strain to use in assays to monitor invasion of erythrocytes by glycosaminoglycans.

Using the pINT and PΔ1 plasmids, a co-transfection to produce DNA-loaded erythrocytes (Hasenkamp et al., 2013) to genetically modify NF54^{attB} was done in duplicate. After three attempts, each with duplicate experiments, no recovery of parasites post-drug selection or any luciferase signal above background was seen. Also available in the laboratory was a standard NF54 strain. It was decided to generate a stable episome parasite NF54 strain by transfection using PΔ1 and blasticidin C drug selection alone. Again, using the same DNA preloading into erythrocytes transfection protocol, this was done three times, each experiment being done in duplicate. The same monitoring of Giemsa-stained thin blood smears and luciferase expression was done for at least 30 days in all experiments, but no genetic modification was shown.

A revised approach was decided on. It was decided to source the pDC2-CAM-GFP-NC-hDHFR-rep20 plasmid from Professor Fidock. In this plasmid, there is (i) a green fluorescent protein (GFP) expression cassette, (ii) a WR99210 antifolate drug selection cassette (based on the human dihydrofolate reductase gene, hDHFR) and (iii) *P. falciparum* subtelomeric *Rep20* repeats. It has previously been shown that *Rep20* play an important role in plasmid segregation between two daughters cells and in the maintenance of the episomal plasmid (O'Donnell et al. 2002). The stage-specific luciferase cassette (*pcna* 5'UTR-luciferase- *pcna* 3'UTR) from PΔ1 can be removed as a *ApaI-PstI* fragment and used to replace the GFP expression cassette in pDC2-CAM-GFP-NC-hDHFR-rep20 see (Figure 3.2). After the subcloning was completed, a plasmid (MH3) was identified in a restriction screen as containing the luciferase expression cassette in the new pC2 plasmid backbone (Figure 3.3).

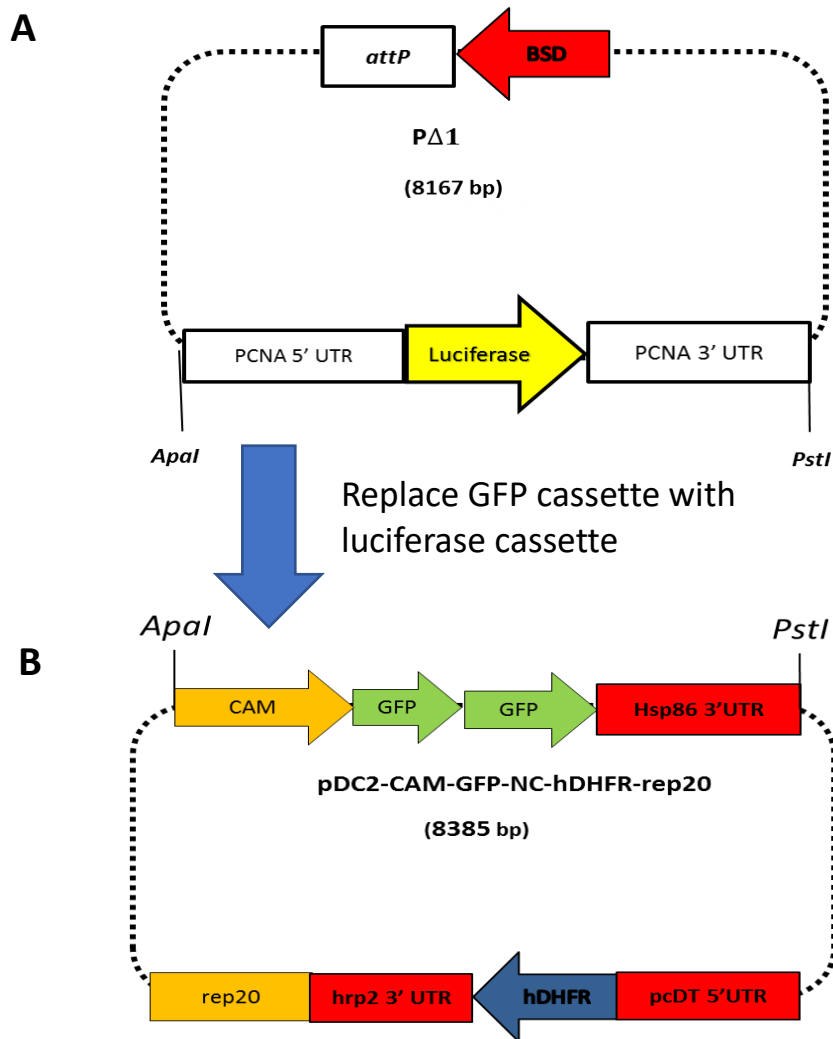


Figure 3.2 Scheme describing the luciferase cassette subcloning strategy. The stage-specific luciferase expression cassette from (A) P Δ 1 was removed as a *Apa*I-*Pst*I fragment and used to replace the GFP cassette in (B) pDC2-CAM-GFP-NC-hDHFR-rep20 using the same restriction sites. BSD, blasticidin S deaminase; attP/attB are BxbI integrase sites; PCNA, proliferating cell nuclear antigen, a DNA replication protein; UTR, untranslated region; CAM, calmodulin 5'UTR; HSP86, heat shock protein 86; hrp2, histidine-rich protein; hDHFR, human dihydrofolate; rep20, *P. falciparum* subtelomeric repeat 20.

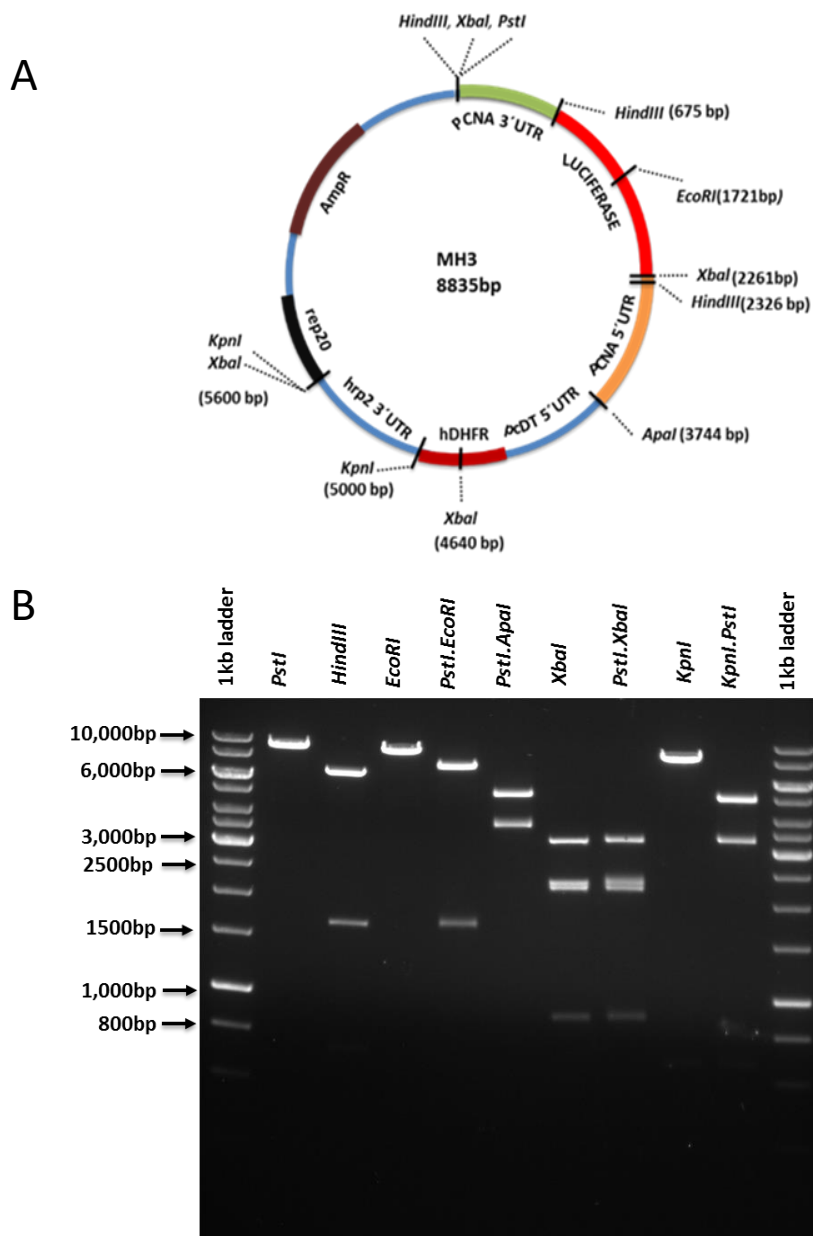


Figure 3.3 Restriction analysis of MH3. (A) Map of the MH3 plasmid illustrating the relative orientation and sizes of the components of this plasmid (PCNA, proliferating cell nuclear antigen; UTR, untranslated region; hrp2, histidine-rich protein; hDHFR, human dihydrofolate; PcDT, *Plasmodium chabaudi* DHFR-TS; rep20, *P. falciparum* subtelomeric repeat 20; AmpR, ampicillin resistance) (B) Size fractionated restrictions (see above) of MH3 plasmid to confirm the correct structure of the plasmid. The 1kb ladder was sourced from BioLines.

Transfection of NF54 with MH3 plasmid was done using the same plasmid-preloading of erythrocytes. This was done in duplicate, with a biological repeat of the duplicate approximately a week later. After two days, 2.5nM WR99210 selection was applied and monitoring of Giemsa-stained thin blood smears and luciferase expression started.

A thin smear was taken every two days from the four transfections, monitoring for rings to show a new reinvasion event and measuring luciferase luminescence. In all four cultures (NF54^{luc1}, NF54^{luc2}, NF54^{luc3}, NF54^{luc4}) an increase in luciferase signal above background (typically above 200 counts with a background of 50 counts) was found after 23 days post-transfection (Figure 3.4). Ring stage parasites were seen at the 24th, 25th-day post-transfection for NF54^{luc1} and NF54^{luc2} respectively. Meanwhile, NF54^{luc3} and NF54^{luc4} in the second biological repeat had ring-stage parasites observed on the 26th and 29th-day post-transfection, respectively (Figure 3.4). At this stage, NF54^{luc2} and NF54^{luc4} were stored in liquid nitrogen and not investigated any further. NF54^{luc1} and NF54^{luc3} were expanded, aliquots stored and taken forward to validate the transfectants.

3.2.3 Validation of the NF54^{luc} transgenic parasite

A series of experiments were carried out to validate the production on a NF54^{luc} transgenic line that expresses luciferase from an episomal MH3 plasmid. The first determination was that the same trophozoite stage-specific expression was produced from the MH3 plasmid.

The *Pfpcna* gene from which the 5' and 3' UTR flanking sequences are used in MH3 is expressed strongly at the onset of DNA replication, corresponding to mature trophozoites and early schizonts (between 26-36 hours post-invasion) (Hasenkamp et al., 2012). There are low levels of luciferase expression in rings, early trophozoites and in late schizonts.

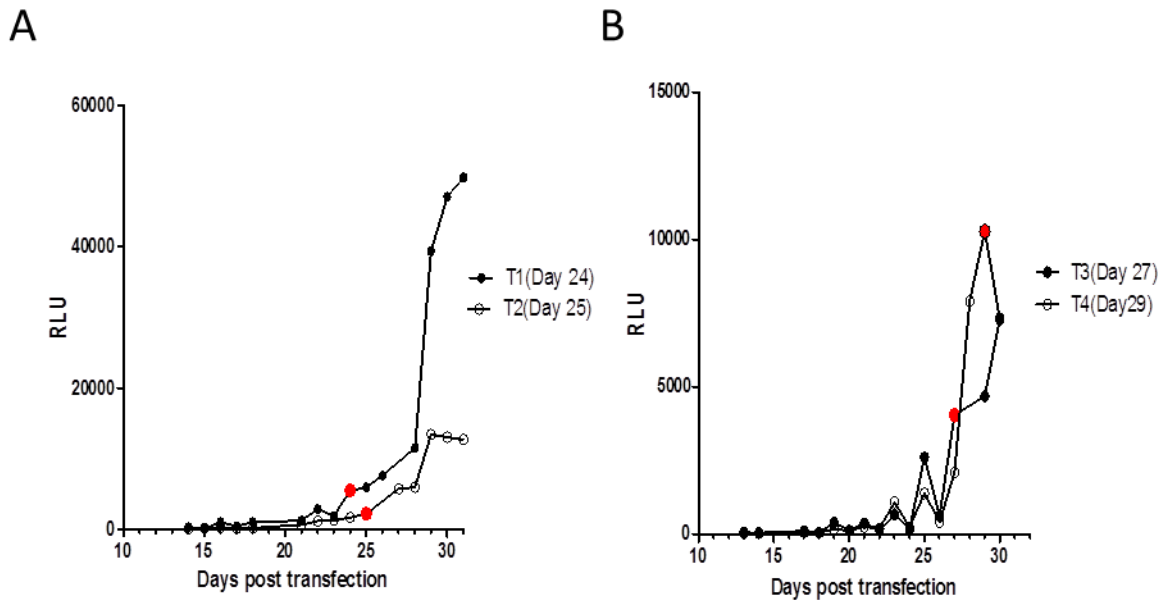


Figure 3.4. Monitoring of transfections. The luciferase expression level in the transfections in the two biological repeats (here A and B) post-transfection are shown. A positive result was considered above 200 counts. These all occurred before the first observation of ring stages (red symbol) on Giemsa-stained thin smears.

To confirm the same stage-specific expression, $NF54^{luc1}$, $NF54^{luc3}$ and $Dd2^{luc}$ were tightly synchronized using sorbitol lysis. Starting with a ring stage culture (approximately 6-10 hours post-infection), samples of 2% haematocrit and 2% parasitaemia cultures were maintained at 37°C with harvests done at early trophozoites (18-24 hours post-infection), mature trophozoites/early schizonts (26-36 hours post-infection) and in mature schizonts (after 36 hours post-infection). Samples for luciferase assays (40µl of 10 ml cultures, done in technical triplicate) and Giemsa-stained thin smears (to confirm staging, see Figure 3.5A) were done. The experiment was repeated three times for $NF54^{luc1}$ and $NF54^{luc3}$ with $Dd2^{luc}$ only done the once as this has previously been published (Wong et al., 2011).

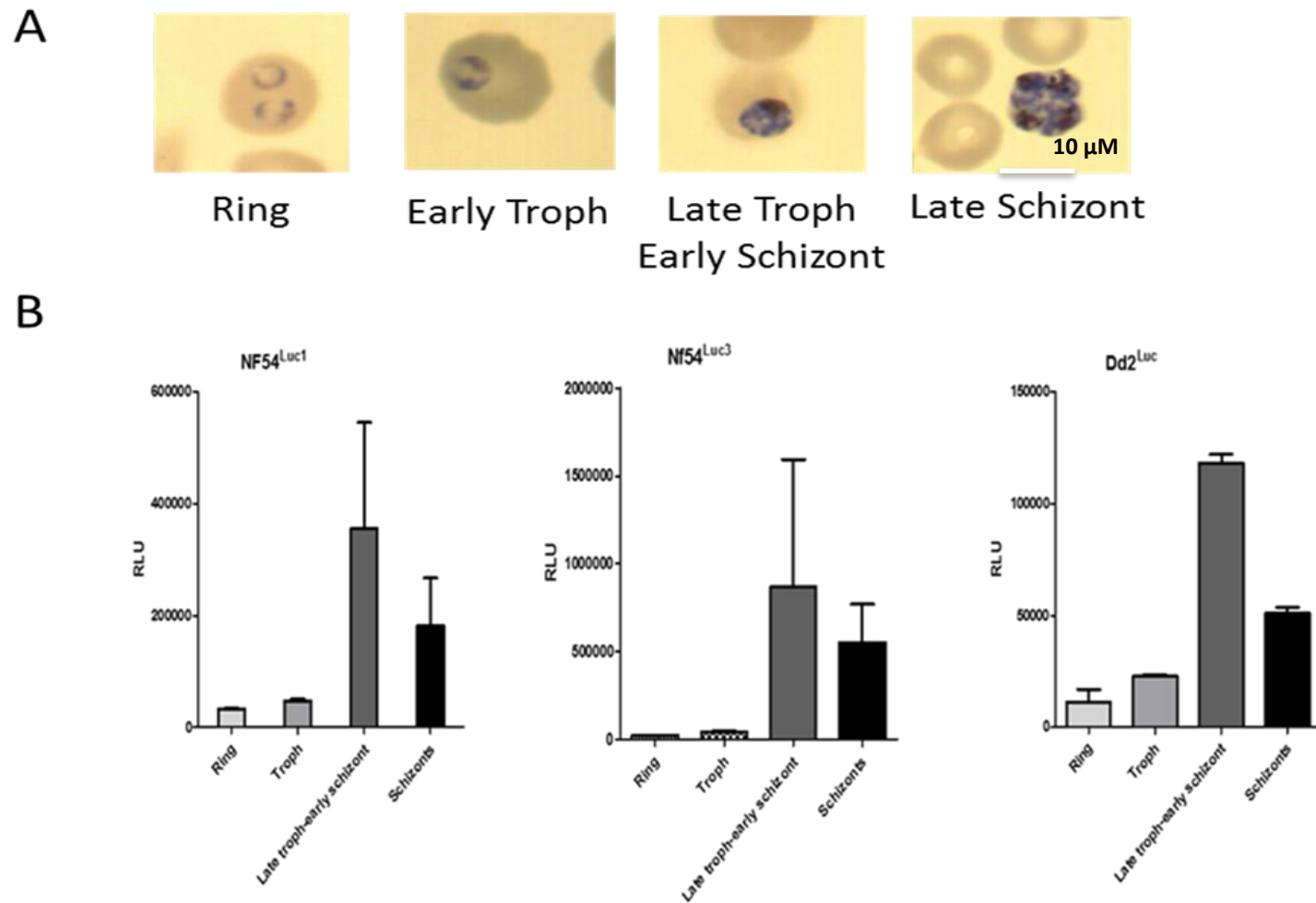


Figure 3.5 Monitoring stage-specific luciferase expression. The intraerythrocytic developmentally-linked expression of luciferase was done on synchronised parasites (**A**) for Giemsa-stained images of named parasite stage and the relative light units (RLU) plotted in (**B**). The bars represent the mean signal with whiskers showing the stdev of n=9 measurements in NF54 and n=3 in Dd^{luc}

The stage-specific luciferase signal in NF54^{luc1} and NF54^{luc3} is directly comparable to that with Dd2^{luc} (Figure 3.5B). The luciferase levels peak in mature-trophozoites/early schizonts at the time when DNA replication commences and is linked to the upregulation of the proliferating cell nuclear antigen (Horrocks et al., 1996). Using the same luciferase gene expression cassette in NF54 has created the same luciferase expression profile. Interestingly, the stage-specific pattern is the same, but the level of expression of luciferase appears different, with the luciferase expression from the episomal plasmid(s) in NF54^{luc1} and NF54^{luc3} higher than that of the integrated copy in Dd2^{luc}.

Both NF54^{luc1} and NF54^{luc3} were transfected with MH3 plasmid that contains an hDHFR drug resistance marker, a gene that confers resistance to the antifolate WR99210. Here we validated the transfection by determining *in vitro* resistance to WR99210 in NF54^{luc1} and NF54^{luc3} strains. The effect of WR99210 on these two transgenic parasites was determined *in vitro* using a 48 hours MSF assay. Corresponding estimates of EC₅₀ data were developed in both transfected NF54 parasite strains, in the untransfected NF54 and Dd2^{luc} (which also maintains a copy of hDHFR on chromosome 7 (Nkrumah et al., 2006; Wong et al., 2011)). The assay was carried out using two-fold dilution series in triplicate and as two independent biological repeats (Figure 3.6) and the EC₅₀ obtained from these log concentration-response curves reported in Table 3.1.

As expected of the now WR99210 resistant strains, the EC₅₀ in the transgenic NF54^{luc1} and NF54^{luc3} is higher than untransfected NF54 parasite (Table 3.1). The mean EC₅₀ of untransfected NF54 is 0.056 nM meanwhile NF54^{luc1} is 49 nM and NF54^{luc3} 15nM and certainly similar to that of the WR99210 resistant Dd2^{luc} (35.7nM). Unsurprisingly, the WR99210 resistance Index (EC₅₀ in transgenic strain/untransfected strain) is high (Table 3.1).

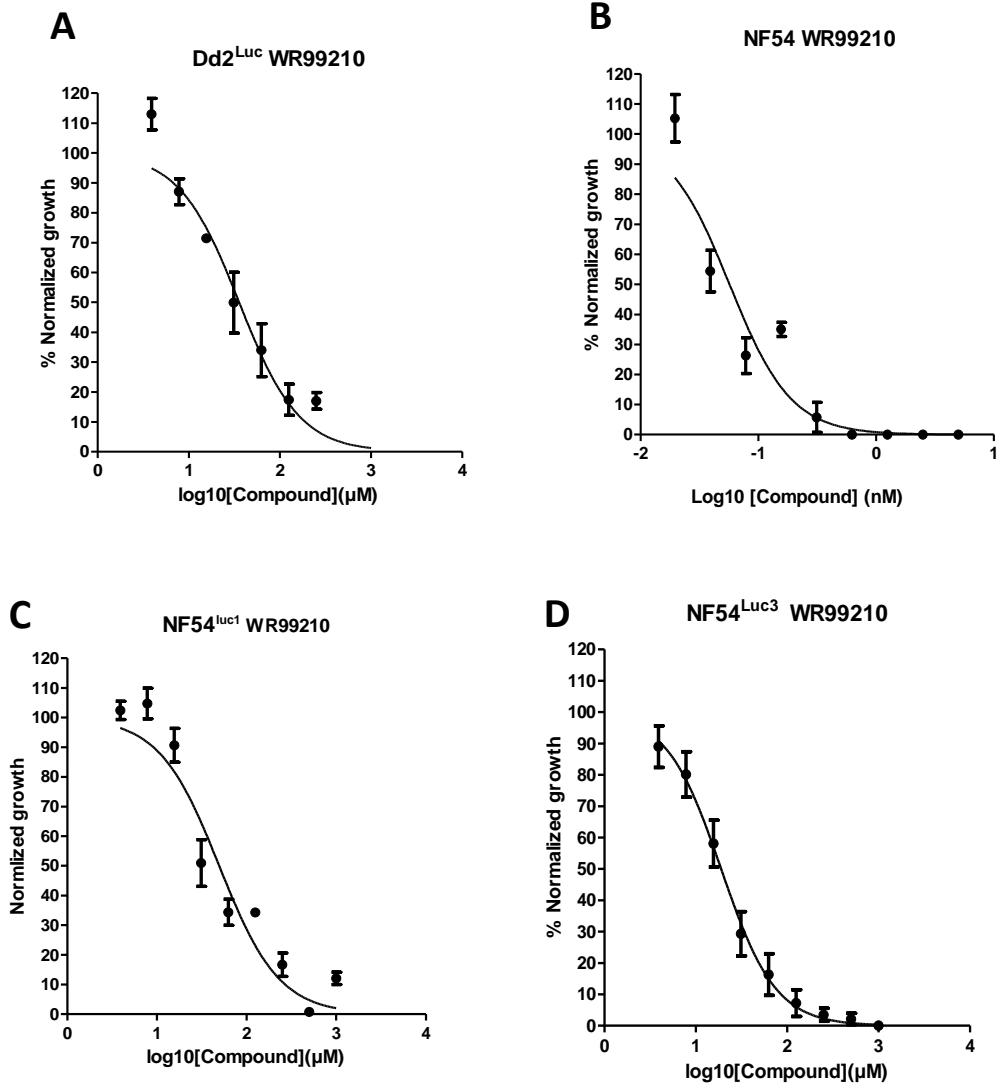


Figure 3.6 NF54 transfected with MH3 are more resistant to the antifolate WR99210. Log₁₀ concentration-normalised response curves for WR99210 in the indicated parasite lines **A**, **B** (Dd2^{luc}, NF54), **C**, **D** (NF54^{luc1}, NF54^{luc3}). Each data point represents the mean with standard deviation (n=6).

Table 3.1: Showing mean EC₅₀ of WR99210 in nM and resistance index (obtained by dividing value EC₅₀ of NF54^{luc} on non-transgenic NF54 parasite).

Strain	Mean EC ₅₀ (nM)	95 % CI	Resistance index ^a
Dd2 ^{luc}	35.7	24.7-51.5	ND
NF54	0.056	0.03-0.08	ND
NF54 ^{luc1}	49.5	31-78.1	875
NF54 ^{luc3}	18.9	17.5-20.4	321

NF54^{luc1} and NF54^{luc3} both show trophozoite stage-specific luciferase expression and are resistant to WR99210 – as is Dd2^{luc}. There is risk of contamination of newly transgenic strains with Dd2^{luc}, that could result from the regular use of Dd2^{luc} in most experiments, was tested by molecular genotyping over the polymorphic regions of *MSP1* (Merozoite surface protein 1) block2, *MSP2* (Merozoite Surface Protein 2) block 3 and *GLURP* (Glutamate-Rich Protein) RII repeat region, based on their common use of genetic polymorphisms in malarial epidemiological studies (Ridzuan et al. 2016). Total gDNA from NF54 (untransfected strain), NF54^{luc1}, NF54^{luc3} and Dd2^{luc} were isolated using a blood Mini (QIAGEN) kit. Genomic DNA from an unrelated strain, HB3, was available in the laboratory. The isolated DNA was analysed by genotyping *MSP1* block2, *MSP2* block 3 and *GLURP* RII repeated regions using oligonucleotide primers (Ridzuan et al. 2016). Approximately 50 ng of DNA used in all PCR reactions and the sizes of the PCR products compared by performing gel electrophoresis and visualized of Ethidium Bromide stained gels (Figure 3.7).

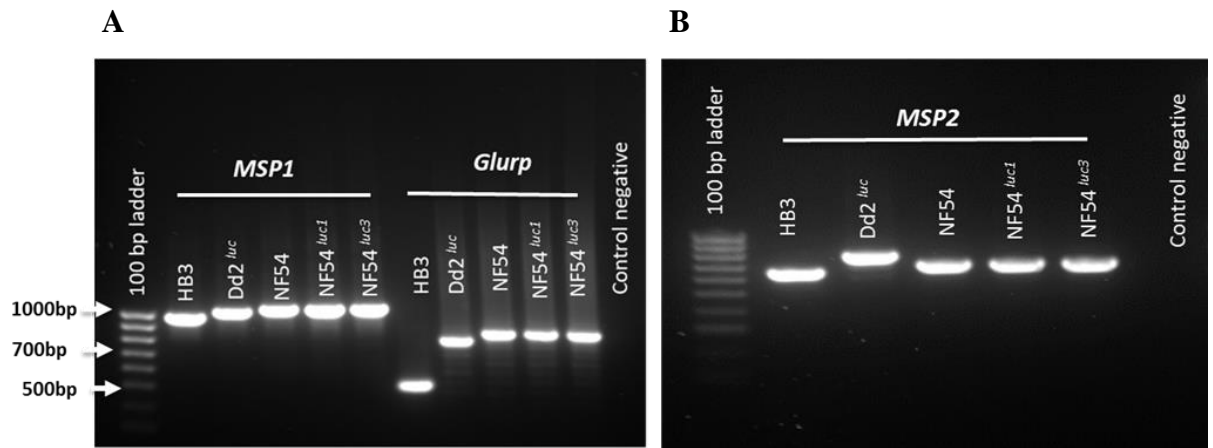


Figure 3.7 Genotyping of HB3, Dd2^{luc}, NF54, NF54^{luc1} and NF54^{luc3} Size fractionated PCR products following amplification over polymorphic regions in (A) *MSP1* and *Glurp* genes and (B) *MSP2* gene.

For all three polymorphic genes, the size of the amplified product was the same for NF54 and the derived transfected strains. Whilst there were only small differences in the size of the PCR products for NF54 and Dd2 (*MSP1*) and NF54 and HB3 (*MSP2*), comparison across all strains across all genes shows that Dd2, HB3 and the three NF54 parasite genotypes can be predicted from each other. This confirms that the NF54^{luc1} and NF54^{luc3} are genetically distinct from Dd2^{luc}, but also that they are genetically the same as each other and NF54 at these three gene positions.

3.2.4 NF54^{luc} transgenic parasites do not appear to lose the reporter plasmid following a period of drug-selection removal

To select for potential homologous integration events, episomally transfected parasites are usually exposed to the loss of drug-selection (during which the episomal plasmid can become lost in the absence of selection) for three weeks and then drug selection reapplied (O'Donnell

et al., 2002). With the luciferase reporter being simple to assay, the loss of the luciferase signal as the plasmid is lost on the removal of WR99210 can be monitored. Sequences that may act as sites of homologous recombination between MH3 and the nuclear genome are Rep20, PCNA 5' and 3' flanking sequences and hrp2 3' flanking sequence (see Figure 3.3).

WR99210 selection was removed from NF54^{luc1} and NF54^{luc3} and Dd2^{luc} (this is control as the hDHFR gene is already integrated and should not be lost). Over a period of 50 days in the absence of WR99210, the parasite cultures were synchronised and adjusted to 2% trophozoite parasitaemia at 2% HCT and a luciferase assay done (Figure 3.8).

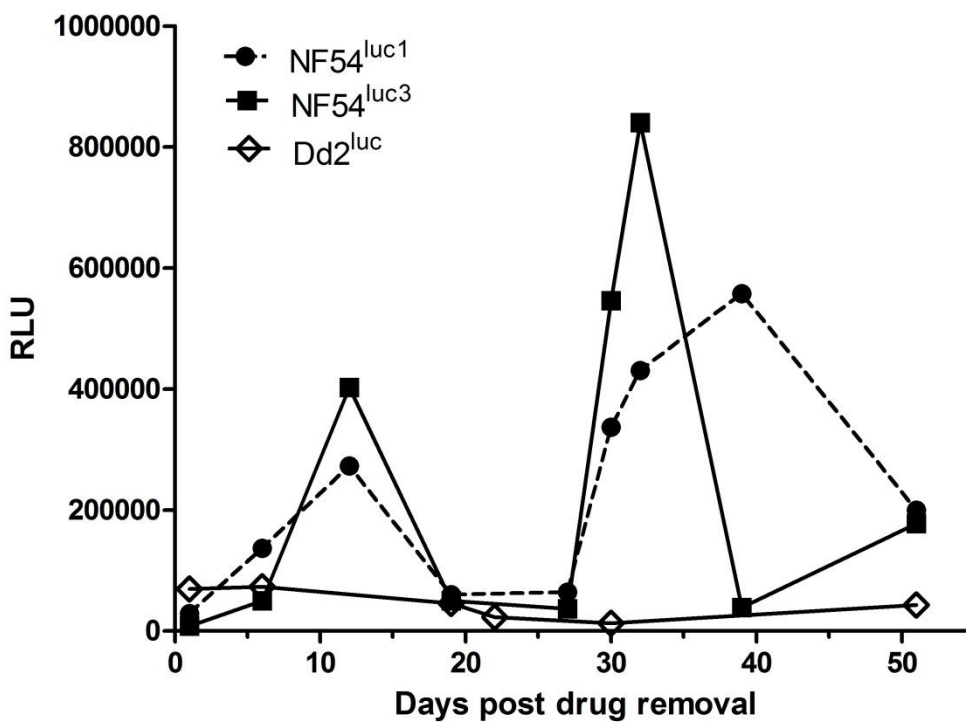


Figure 3.8: Time-course of luciferase expression following removal of WR99210. Luciferase signals in trophozoites of NF54^{luc1}, NF54^{luc3} and Dd2^{luc} over 50 days.

It was expected that in NF54^{luc1} and NF54^{luc3} that the luciferase signal would decrease as the episomal MH3 plasmid was lost – with the luciferase signal in Dd2^{luc} being relatively constant. The data shows that the Dd2^{luc} signal is reasonably constant over the 50 days monitored (Figure 3.8). The signal for NF54^{luc1} and NF54^{luc3} varies dramatically, with this variation probably resulting from changes in parasitaemia and the exact life stage selected for the luciferase assay – but it does not show the expected loss of luciferase signal over time as the plasmid is lost. An EC₅₀ assay was repeated for WR99210 after 50 days of drug selection removal for both NF54^{luc1} and NF54^{luc3} to monitor WR99210 resistance in these two strains. This concentration-response curves (Figure 3.9) and EC₅₀ values determined (Table 3.2) show that both NF54^{luc1} and NF54^{luc3} are still WR99210 resistant even after a long period of growth in the absence of drug selection pressure.

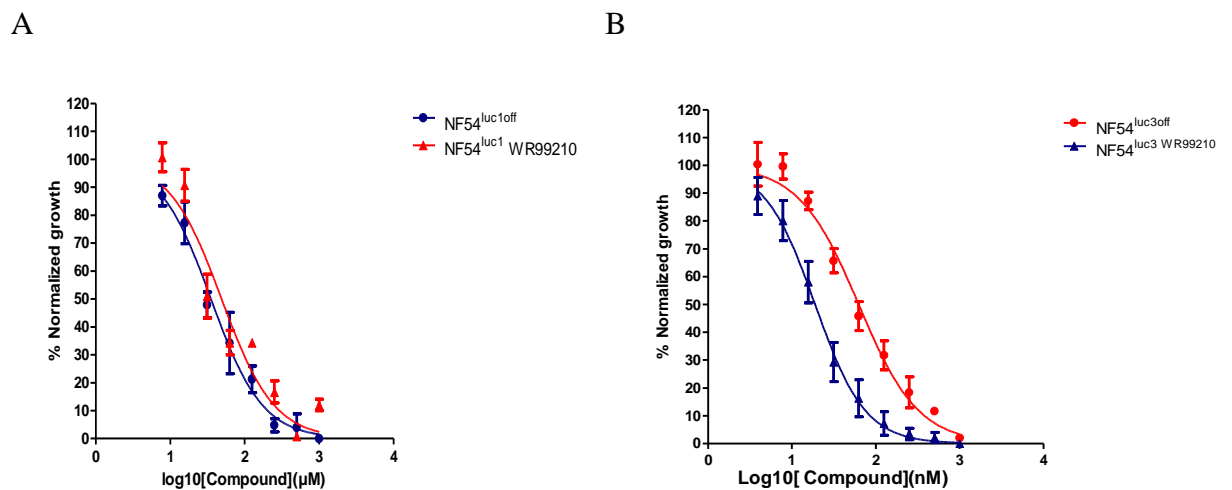


Figure 3.9 NF54^{luc1} and NF54^{luc3} are resistant to WR99210 after 50 days in the absence of selection. Log concentration normalised response curves for NF54^{luc1} (A) and NF54^{luc3} (B) maintained on WR99210 (red) or after 50 days removal from WR99210 (blue). Mean ± stdev (n=6) are shown.

Table 3.2: Showing mean and 95% confidence intervals of the EC₅₀ to WR99210 in nM and resistance index (obtained by dividing value EC₅₀ determined in these transgenic lines compared to non-transgenic NF54 parasite in Table 3.1) ^b Data from Table 3.1

Strain	Mean EC ₅₀ (nM)	95% CI	Resistance Index ^a
NF54 ^{luc1 b}	49	31-78.1	875
NF54 ^{luc1off}	35	29.8-41.5	625
NF54 ^{luc3 b}	18	17.5-20.4	321
NF54 ^{luc3off}	62	51.5-77.9	<1000

Interestingly, there is a very slight reduction in resistance in NF54^{luc1} (but with overlapping 95% CI) and a larger reduction in NF54^{luc3}, the latter EC₅₀ reduced by three-fold (although still 321 times more resistant than the untransfected NF54) and the 95% CI do not overlap. The original stage-specific luciferase expression in NF54^{luc3} was approximately twice that of NF54^{luc1} (Figure 3.5), suggesting that perhaps there were more episomal copies of MH3 present. And, in this period of no drug selection, some, but not all, of the episomal plasmid, was lost.

3.2.5 NF54^{luc} transgenic parasites appear likely to maintain episomal plasmid after removal of drug selection pressure

There may be two explanations here – and they are not necessarily exclusive of each other. The first is that whilst the original report that plasmids bearing a *Rep20* sequence are lost during culture in the absence of drug selection (O'Donnell et al., 2002), this has only been shown in this study and may not be true of all plasmids/parasite clones it is placed within. Or, the rate of losing the episomal plasmid with a *Rep20* sequence is different in different plasmids/parasite

strains. The alternative is that there has been a very rapid and efficient homologous integration of MH3 into any of Rep20, PCNA 5' and 3' flanking sequences or hrp2 3' flanking sequences in the parasite genome.

To explore whether there was episomal plasmid present in NF54^{luc} parasites after 50 days of drug selection, total genomic DNA was isolated and 100ng of material from NF54^{luc1} and NF54^{luc3} after 50 days drug selection free were transformed into chemically competent *E.coli* and then plated onto ampicillin selection agar plates. In the first attempt, no bacterial colonies were observed for either DNA sample. A repeat of the experiment, using the same conditions provided only one colony-forming unit using the NF54^{luc1} parasite DNA. Plasmid DNA was prepared from this colony and a restriction of the isolated plasmid done compared to that of the original MH3 plasmid prepared for the genetic modification of the parasites (Figure 3.10).

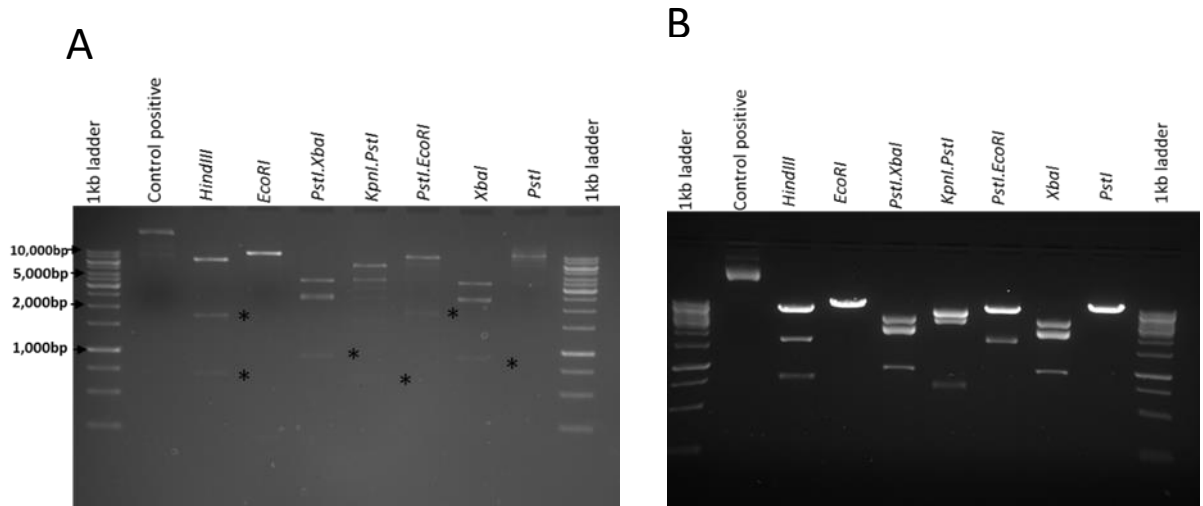


Figure 3.10 Comparative restriction mapping analysis. Gel electrophoresis of restricted (see enzyme over respective lane) plasmid isolated from (A) NF54^{luc1} off WR99210 selection and (B) the original MH3 plasmid. Faint bands in (A) are picked out with stars to aid comparison with (B).

From this restriction digest analysis, it is clear that the rescued MH3 plasmid from NF54^{luc1} off WR99210 is essentially the same as the MH3 plasmid before transfection. This suggests that the rescued plasmid is either (i) present episomally in the parasite after removal of the drug selection and/or (ii) contamination of the transformation with exogenous MH3 plasmid on surfaces in the laboratory. The latter conclusion resulting from the recovery of only one CFU after two attempts of *E. coli* transformation.

In order to explore further whether NF54^{luc} parasites have integrated MH3 into gDNA, q-PCR was exploited to determine the relative quantification of luciferase gene copies present before and after the loss of WR99210 selection pressure using the $2^{-\Delta\Delta C_t}$ method. Genomic DNA was isolated from NF54^{luc1}, NF54^{luc3}, NF54^{luc1 off}, NF54^{luc3 off} and Dd2^{luc}. The relative quantification of a *luciferase* gene copy number was determined using a Sybr Green I Taqman assay (StepOnePlus, Applied Biosystems) using internal standards of *P. falciparum* β -*actin1*, *aldolase* and *seryl-tRNA synthetase* genes. A no DNA template was included in the experiment as a negative control. The relative quantification (RQ) of *luciferase* using the known integrated luciferase reporter in Dd2^{luc} was established as 1, with *luciferase* RQ values in the NF54^{luc1}, NF54^{luc3}, NF54^{luc1 off}, NF54^{luc3 off} samples (mean and stdev of n=3 biological repeats) reported in Figure 3.11.

The Relative Quantification of luciferase expression from the different strains was analysed by ANOVA (Bonferroni's Multiple Comparison post-test). Here, comparing NF54^{luc} luciferase copy number before and after the removal of drug selection showed a loss of luciferase copy number as WR99210 was removed. However, the reduction in copy number in NF54^{luc1} is small and not significant. The reduction in copy number is greater in NF54^{luc3} and is also significant. Interestingly, both NF54^{luc} strains after WR99210 removal have a copy number that is close to half that of Dd2^{luc}. In the original report for Dd2^{luc} (Wong et al., 2011) the Southern blot analysis did suggest that at least two copies of the p Δ 1 plasmid had integrated – suggesting that at least

one copy of MH3 is present after removal of drug selection, but that this is the minimal required to survive drug pressure.

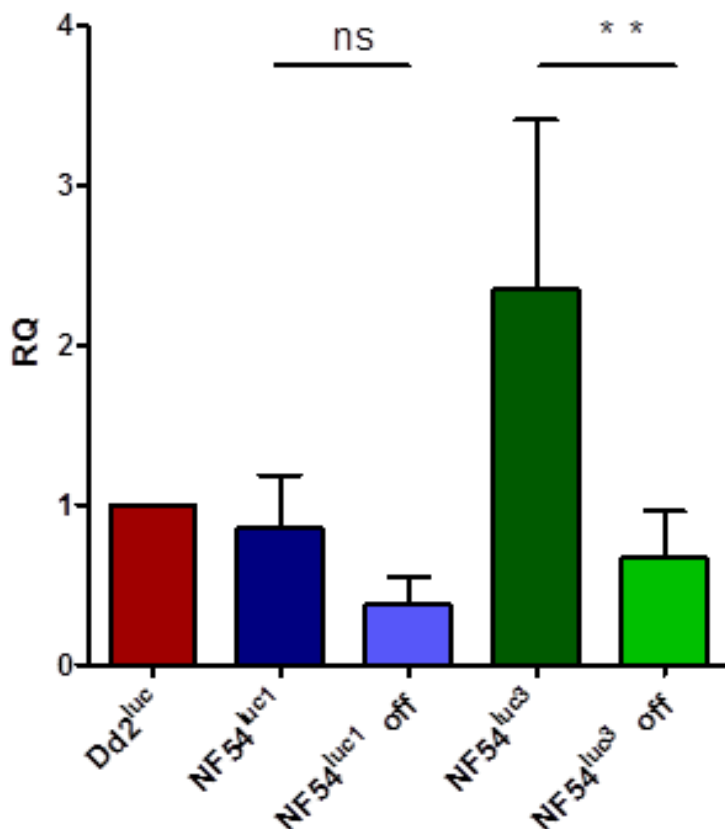


Figure 3.11 Quantitative analysis of luciferase copies before and after WR99210 removal in NF54^{luc} parasites. Relative quantification (RQ) of *luciferase* gene expression in the parasite lines indicated. The data is the mean (\pm stdev) from three biological repeats, each of three technical repeats. Ns, not significant; ** $p < 0.001$ (Bonferroni's Multiple Comparison post-test)

To explore if MH3 plasmid has integrated into NF54^{luc}, a Southern blot of restricted genomic DNA isolated from NF54^{luc1} before and after the removal of WR99210, and NF54^{luc1}. As any integration site is unknown and MH3 plasmid might be episomal, the restriction enzymes were

chosen to frequently cut parasite gDNA (biased in AT content) and had at least one site in MH3 plasmid (Figure 3.4). gDNA was restricted with *ApaI*, *KpnI*, *PstI* and *EcoRI* and the DNA size-fractionated and southern blotted. PCR, using the biotin-dUTP incorporation method was used to prepare a probe to the *luciferase* gene for hybridization. The assumption was that the restriction enzymes *ApaI*, *PstI* and *EcoRI* but not *KpnI* will hybridise to 8835bp episomal plasmid band – with variations from this suggesting the MH3 had integrated. Southern blot analysis (Figure 3.12) indicate that *ApaI*, *PstI* and *KpnI* give bands of the expected size (*ApaI* and *PstI* of 8.8Kbp and *KpnI* at 8Kbp) for episomes in NF54^{luc1} before and after the removal of drug selection. The larger bands in *PstI* and *KpnI* are probably uncut plasmid. The signal from *EcoRI* is not expected. There is a single *EcoRI* restriction site in MH3 (Figure 3.4) that was confirmed again after this result (data not shown). The presence of a weak luciferase signal at about 2Kbp could suggest that (i) there has been an integration event but this is not observable using the other three restriction enzymes or (ii) that the MH3 plasmid in the parasite does contain a new *EcoRI* site introduced early after transfection.

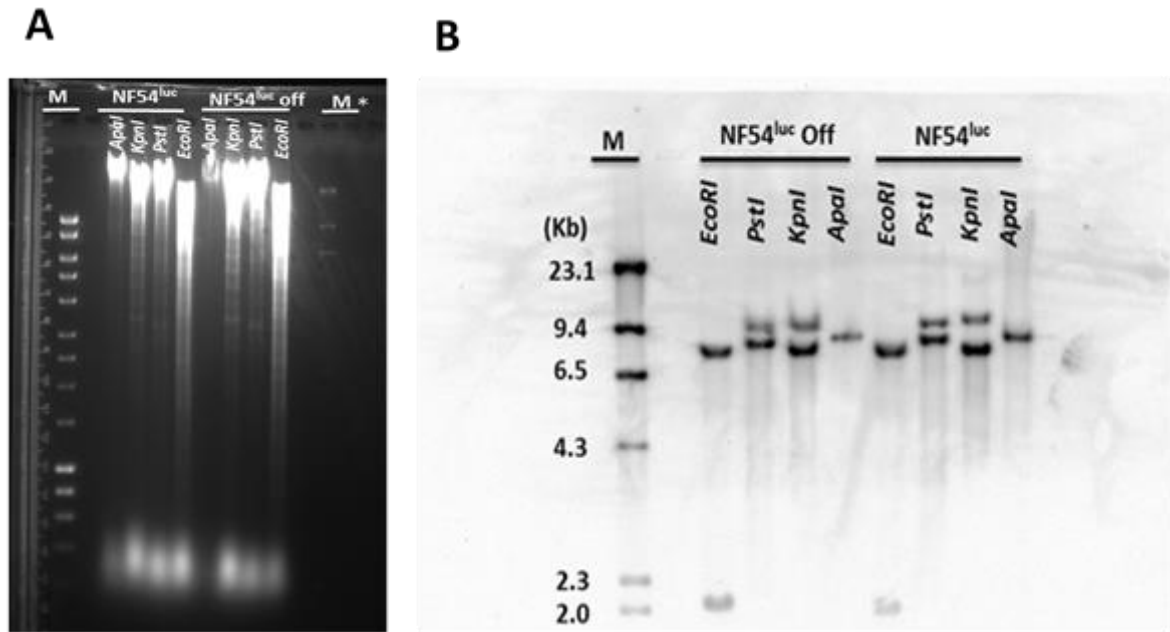


Figure 3.12 Southern blot analysis of NF54^{luc1}. (A) Ethidium bromide stained gel electrophoresis of restricted gDNA, M is DNA marker (B) Southern blot using a biotinylated probe to *luciferase* gene. DNA fragment sizes are indicated in kilobase pairs.

3.2.6 Stage-specific inhibition of *in vitro* growth in NF54^{luc} using heparin

Previously, we demonstrated that the MSF assay can't be used to investigate the growth inhibition activity of different glycosaminoglycans against the blood stages of *P.falciparum*. We showed that the luciferase activity in Dd2 could report concentration-dependent growth inhibition, and we next tested whether the same was true in the new NF54^{luc} strain generated here (from this point on, NF54^{luc} is stated – this is NF54^{luc3}). Highly synchronized, 2% trophozoite stage of NF54^{luc} and Dd2^{luc} strains, were incubated with three concentration of heparin (100, 33 and 11 $\mu\text{g/ml}$), with technical triplicate and three biological repeats (n=9). Growth inhibition was determined over 6 and 48 hours of incubation using the standard luciferase-based assay. The luciferase data were normalized against untreated control and a mean \pm SD of n=9 of normalized growth (%) plotted (Figure 3.13). As expected, there was no

cytotoxic effect of heparin in the 6 hours of incubation of trophozoites in both strains – heparin does not affect maturing trophozoites. But after 48 hours of incubation, and the completion of one parasite life cycle, we can see a concentration-dependant effect of heparin, that suggests that heparin is acting at the schizont to ring-stage transition into a new host erythrocyte. Importantly, there appears to be no difference between the stage-specific and concentration-specific responses between $Dd2^{luc}$ and $NF54^{luc}$, indicating we have a luciferase-based reporter of glycosaminoglycan inhibitory activity in two distinct genetic backgrounds.

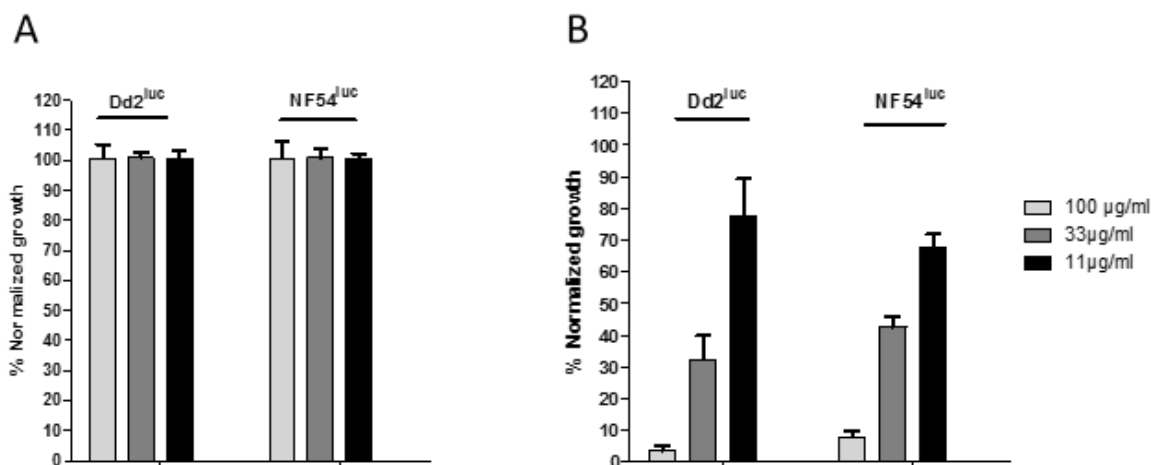


Figure 3.13 Stage and concentration-dependant inhibition of parasite growth by heparin in $Dd2^{luc}$ and $NF54^{luc}$. The proportion of normalised growth (compared to untreated control) from a luciferase assay using the strains and heparin concentration as shown after (A) six hours of incubation in trophozoites and (B) after 48hrs of incubation of trophozoites. Bars show the mean \pm stdev of n=9 data

3.3 Discussion

Discovery for future drugs requires reliable, robust and simple methods that can be readily adapted for high-throughput screening (Burrows et al., 2014). Antimalarial action *in vitro* was for a long time determined by uptake by the parasite of the radioactive substrates, such as [³H] hypoxanthine, to measure parasite viability following drug treatment (Elabbadi et al., 1991). Whilst these radioisotope-based assays are reliable and accurate, they rely on expensive materials, expensive detection devices and generate radioactive waste. Other alternative growth inhibition assays have been developed using (inexpensive) fluorescent-based dyes that intercalate into parasite DNA such as Hoechst 33258 (Smeijsters et al., 1996), 4,6-diamidino-2-phenylindole (DAPI) (Baniecki et al., 2007) and SYBR Green I (Smilkstein et al., 2004; Johnson et al., 2007). The latest innovation in assays of parasite growth used genetic engineering of the parasite to enable them to express a bioluminescent, usually luciferase, reporter and then exploit the sensitivity of this assay is simple but robust assays (Cui et al., 2008; Sandra Hasenkamp et al., 2013). Fluorescent-based assays have been used to explore growth inhibition and invasion blocking activity of heparin and related sulphated GAGs against *P.falciparum*. These assays, however, rely on flow cytometry to count the fluorescently-labelled infected erythrocytes – a process that requires wash steps, flow on a potentially expensive machine. Our initial steps in exploring the production of a plate-based assay with heparin, Enoxaparin, Reviparin and refined GAG fractions from Crab (F4) and Prawns (F5) revealed issues with GAG-fluorescent dye interactions irrespective of the presence of the parasite DNA. The key objective here was to establish whether a simple plate-based assay for heparin and other sulphated GAGs could be used based on a luciferase assay – and develop a new parasite strain genetically modified to share the same reporter characteristics as the available Dd2^{luc} strain, although in a different genetic background with a known distinct invasion phenotype i.e produce NF54^{luc}.

I report the generation of a transgenic *P.falciparum* NF54^{luc} strain that expresses a luciferase reporter using the same stage-specific patterning as in Dd2^{luc}. This assay was then validated to show that the effect of the heparin on inhibition of parasite growth was both concentration-dependent and linked to the parasite reinvasion phase at the end of intraerythrocytic development. Interestingly, luciferase-based assays have not been previously exploited to explore GAGs growth inhibition activity with most studies using microscopic or flow cytometry-based assays as methods to measure growth inhibition activity of GAGs (Rieckmann et al., 1978; Boyle, et al., 2010; Boyle et al., 2017; Marques et al., 2016). This chapter, therefore, reports the first use of luciferase-expressing transgenic lines as well as the preparation and validation of a new NF54^{luc} strain for this purpose.

The first two approaches used to transfect *P.falciparum* were unsuccessful. The first approach used the pINT and PΔ1 plasmids in a co-transfection using DNA-loaded erythrocytes to transfect the NF54^{attb} strain provided by David Fidock's laboratory. This approach was first described by Nkrumah et al., (2006) with the NF54^{attb} strain reported first in Adjalley et al., (2010). Use of the bxb1 integrase system to prepare Dd2^{luc} from Dd2^{attp} was described by Wong et al., (2011). Despite four repeat transfections (in pairs) no transfectants were recovered. The pINT and PΔ1 plasmids were from the same source as the previous study. One potential issue considered was that the NF54^{attb} strain had been accidentally mixed with NF54. The Dd2^{attp} strain is easy to differ from Dd2 as it is WR99210 resistant due to the hDHFR resistant marker cotransfected with the attB site. In the NF54^{attb} strain, the hDHFR selection marker was removed after insertion of the attB site and so remains WR99201 sensitive – just like NF54 (Adjalley et al., 2010). The second approach was to transfect NF54 (obtained from American Type Culture Collection ATCC) episomally with the PΔ1 plasmid alone – this plasmid having the luciferase gene reporter and BSD selection marker. Again, despite repeated attempts, this

approach was unsuccessful too, and no transfectant parasites were recovered even after six weeks of post-transfection follow up. This failure led to the revised subcloning of the *pcna*-luciferase expression cassette into the new host plasmid strain with the more amenable hDHFR drug selection marker and the potential for the Rep20 repeats to support efficient plasmid segregation into daughter cells on parasite replication (O'Donnell et al., 2002). Plasmid MH3 was introduced using DNA-loaded erythrocytes in four separate transfections, and all were successful.

In the new transgenic NF54^{luc} parasite, luciferase stage-specific expression was evaluated to be equivalent to that of Dd2^{luc}, where the luciferase signal developed from early trophozoite stage and peaked at the trophozoite-schizont stages consistent with expression linked to a DNA replication protein (Hasenkamp et al., 2012). As a precursor to selecting potentially DNA-integrated parasite populations for clonal selection, the NF54^{luc1} and NF54^{luc3} transgenic lines had the WR99210 drug selection removed. The luciferase signal was monitored over the next 50 days to monitor the reduction in luciferase signal as episomal plasmid is lost in the absence of the WR99201 drug pressure. The evidence suggested no real loss in luciferase signal over this time and parasites recover at the end of the drug off period were both bioluminescent and resistant to WR99201 - NF54^{luc1off} and NF54^{luc3off} still resistance to WR99210 with EC₅₀ of 35 and 62 nM, respectively. Interestingly, in the only other report of plasmid curing with Rep20 parasites by O'Donnell et al., (2002), they report a significant loss of episomal plasmid after only 20 days. The two Rep20 plasmid constructs are different and this may account for the difference in behaviour, although only two reports exist of this behaviour. Follow up with Professor Fidock by my supervisor did not help as the Fidock team do not use this plasmid construct much or have done plasmid curing experiments. However, to try to understand whether the MH3 plasmid DNA was either integrated (and had done so at very high efficiency)

or was still episomal, we attempted to recover MH3 plasmid DNA from NF54^{luc^{off}} into *E.coli* by the transformation of a DNA preparation from the parasite. Two attempts were made, with only the second experiment providing a single colony, transformation of *E.coli* with DNA isolated from other episomally transfected parasite would provide an appropriate positive control to understand how many CFU would grow under these conditions (although this positive control was not available at the time of the experiment). Although this was of apparently unchanged MH3 plasmid. That only one colony was recovered was not considered as evidence of there being episomal plasmid DNA in the parasite as this could also have been the result of environmental contamination following the megaprep of MH3 required to give enough DNA for the transfection experiments. Quantitative PCR between parasites before and after plasmid curing show no significant loss of luciferase copy number in NF54^{luc^{1off}} compared to NF54^{luc¹}, meanwhile, NF54^{luc^{3off}} plasmid loss compared to NF54^{luc³} was significant, although it may be that NF54^{luc³} started with high levels of plasmid DNA. Interestingly, both NF54^{luc} strains after WR99210 removal have a copy number that is close to half that of Dd2^{luc} where Dd2^{luc} has been reported likely by Wong et al. (2011) to have two copies of luciferase integrated into chromosome 7. This suggests that at least one copy of MH3 is perhaps present after removal of drug selection in both NF54^{luc^{1off}} and NF54^{luc^{3off}}, with this the minimal required to survive any following drug pressure. The expectation was that a Southern blot analysis would resolve this issue. Analysis of luciferase in NF54^{luc¹} and NF54^{luc^{1off}} strongly suggests MH3 is episomal, with restriction enzymes analysis giving either the expected giving plasmid size 8835bp or another other slower migrating signal that may due to uncut plasmid. With some frustration, the presence of a weak luciferase signal at about 2Kbp using *EcoRI* could also suggest that (i) there has been an integration event but this is not observable using the other three restriction enzymes or (ii) that the MH3 plasmid after transfection contains a new *EcoRI* site introduced by a mutation event early after transfection.

At this point, we acknowledged that we had generated a NF54^{luc} transgenic parasite resistant to WR99210, with the correct stage-specific expression of luciferase and that the NF54^{luc} parasite, when used in luciferase assay to test the growth inhibition activity of heparin, showed similar concentration-dependent activity to that in Dd2^{luc}. We had therefore delivered on the key aim of the research to have a genetically modified strain of NF54 equivalent to Dd2 for our screening assays. Further efforts to determine exactly what had happened to MH3 required cloning of the strain and likely whole-genome sequencing, with Rep20, pcna and other *P. falciparum* sequences in MH3, there are multiple potential sites for homologous recombination for integration and this was not the objective of the study.

The NF54^{luc} transgenic parasite has, however, been taken further in other research in our laboratory. This strain is also chloroquine-sensitive, where Dd2^{luc} is chloroquine-resistant (Ullah et al., 2017). Mrs Mufuliat Famodimu is using both NF54^{luc} and Dd2^{luc} in studies of the rate of kill of the MMV Malaria Box and TCAMs drug discovery libraries. In addition, the potential to re-engineer the MH3 plasmid, particularly as it has been shown to be effective in transfection success, to put new stage-specific control sequence around the luciferase reporter gene to explore kill action at other developmental stages is interesting. Or, alternatively to use MH3 to put the sensitive luciferase viability reporter into new genetic background, eg in artemisinin-resistant parasites.

Chapter Four: Investigating the erythrocyte invasion-blocking potential of Low Molecular Weight Heparins (LMWH)

4.1 Introduction

Low molecular weight heparins (LMWHs) are widely used anticoagulants and comprise of heparin fractionated by depolymerizing heparin chemically or enzymatically. LMWHs have different clinical applications as anticoagulants and are commonly used as prophylactics for the management of venous thrombosis risk that may lead to deep venous thromboembolism during a range of surgical procedures (Hirsh et al., 2001). Depolymerisation results in shorter heparin fragments with a lower molecular weight (MW), with mean MW, ranged approximately between 4000-7000 daltons (Hirsh, Levine MN., 1992), some one-third of the size of heparin. Similar to heparin, LMWHs are heterogeneous regarding molecular weight and their anticoagulation activity (Gray et al., 2008). Various chemical and acid depolymerization methods lead to different LMWHs products, by virtue of where they introduce the break in the polysaccharide chain, including leading commercial products such as Tinzaparin, Enoxaparin, Reviparin and Dalteparin. Whilst these LMWHs are distinct from one another and heparin, their anticoagulant mechanism of action is similar to heparin. Heparin works as an anticoagulant through binding to anti-thrombin (ATIII) using a distinct pentasaccharides motif. This binding increases ATIII affinity for Factor Xa and thrombin, sequestering them from the coagulation cascade. Whilst there is no dependence of the polysaccharide unit length for Factor Xa binding (Figure 4.1), the sequestration of thrombin is dependent on a minimal unit length of 18 saccharides (Pavao., 2002). For heparin, most of the polysaccharides are at least 18 saccharide units or more and are typically 30-50 saccharide units (Köwitsch et al., 2018). LMWHs, however, are typically shorter than this 18-saccharide length, which means that whilst a LMWH

polysaccharide may contain the pentasaccharide that binds to ATIII, it will only sequester Factor Xa and not thrombin (Hirsh, Levine MN., 1992) (Figure 4.1). This results in a medicine that is favoured as an anticoagulant in terms of the route of administration and better-regulated kinetics of anticoagulation that does not need as regular a monitoring schedule as is used with unfractionated heparin (Warkentin et al.,1995). In addition, the shorter chain lengths of LMWH result in a lower affinity of interaction with Platelet Factor 4 (PF4). The formation of a PF4 tetramer, stabilised by heparin, can lead to the development of autoantibodies to the PF4 complex that leads to heparin-induced thrombocytopenia (HIT). Therefore, the decreased incidence of HIT offers another benefit in the use of LMWH (Walenga et al., 2004).

Due to differences in how LMWHs are produced, there are differences in their inhibition of blood coagulation, that reflects differences in how they affect the binding capacity to factor Xa. For example, LMWHs with higher MW tend to inhibit factor IIa (thrombin formation) over Factor Xa with LMWHs with lower MW showing a more specific inhibition of Factor Xa binding (Thomas et al., 2015). These pharmacokinetic differences are described in the FXa/FIIa ratio and are shown here in Table 4.1 (Gerotziafas et al., 2007)

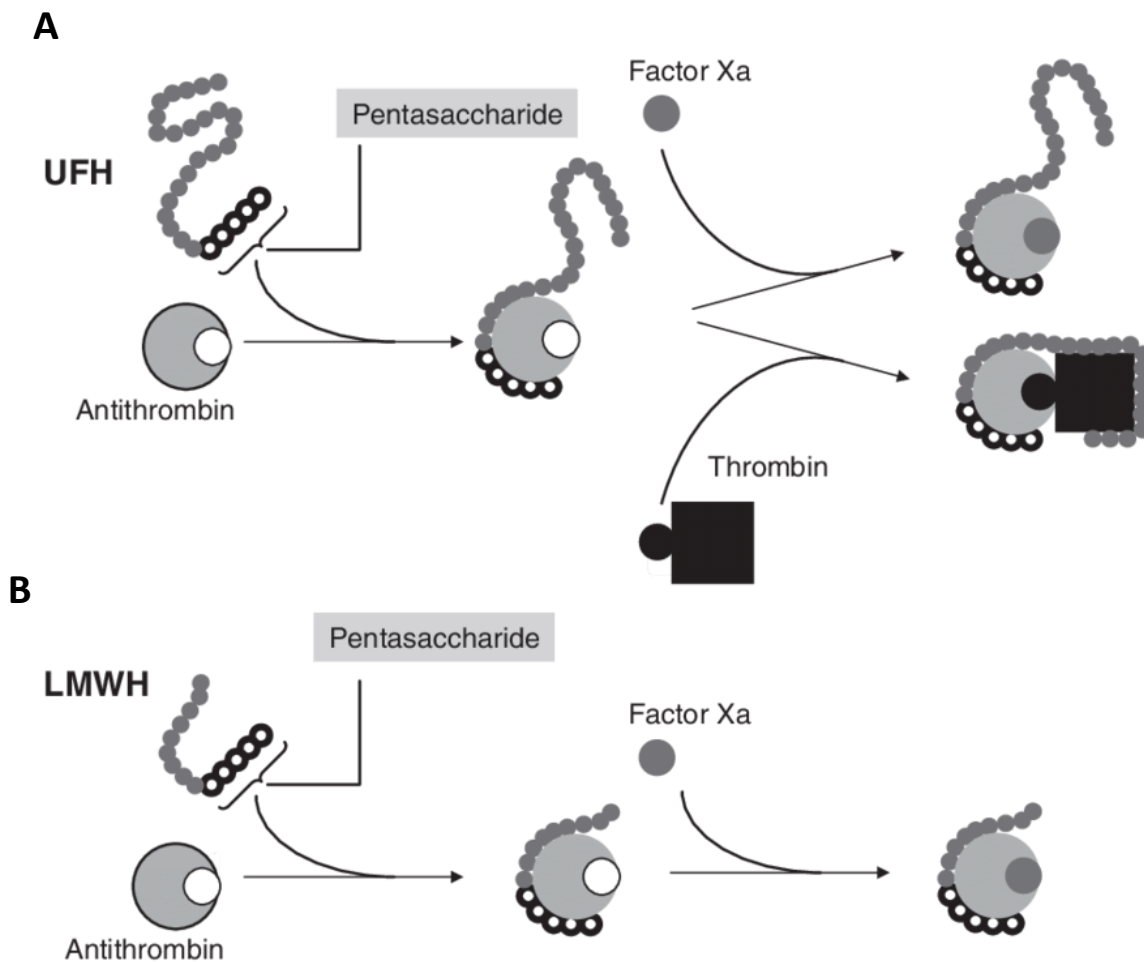


Figure 4.1 The difference between (A) heparin and (B) LMWHs mechanism of action and their binding ability to coagulation factors (Gerd R. Hetzel & Christoph Sucker, 2005)

Table 4.1 Common LMWH anticoagulant, molecular weight and their anti FXa/FIIa, anti FXa/FIIa ration (This table reproduced from Thomas, Lybeck et al., 2015).

LMWH	Trade name	Mean MW (kDa)	Anti FXa/FIIa(anti-Fxa IU/mg)	Anti FXa/FIIa ratio
Unfractionated heparin	Heparin	15	193/193	1
Tinzaparin	innohep	6.8	90/45	2.0
Dalteparin	Fragmin	6.0	130/52	2.5
Enoxaparin	Clexane	4.2	100/25	3.9

Several methods are used to depolymerise unfractionated heparin to LMWH (Gray et al., 2008). These include; (i) nitrous acid and organic nitrite are used to break the heparin chain at N-sulphated glucosamine residues, leaving a characteristic anhydromannose reducing-end residue which is usually reduced to anhydromannitol, (ii) chemical or enzymatic beta-elimination method that leaves an unsaturated uronic acid residue at the non-reducing terminus or (iii) oxidative depolymerisation, which produces the least specific structure in the resulting product (for examples see Table 4.2).

Table 4.2 LMWHs preparation methods (This table reproduce from (Hirsh et al., 2001)

LMWH	Method of preparation
Tinzaparin (innohep)	Enzymatic depolymerisation with heparinase
Dalteparin (fragmin)	Nitrous acid depolymerisation
Enoxaparin (Clexane , lovenox)	Benzylation followed by alkaline depolymerisation
Reviparin (Clivarine)	Nitrous acid depolymerisation, chromatographic purification

An example of how differences in production methods that lead to differences in the chemical structure of LMWHs and thus their activity is shown between dalteparin (Fragmin®) and tinzaparin (innohep®). Dalteparin is produced by controlled nitrous depolymerization of sodium heparin sourced from porcine intestinal mucosa, and yields molecules composed of acidic sulphated polysaccharides chains. These polysaccharide chains contain 2,5-anhydro-D-mannitol residues as end groups. Tinzaparin produced enzymatically by the controlled

depolymerization of heparin using heparinase from a bacterial source (*Flavobacterium heparinum*), results in molecules with predominantly 2-O-sulpho-4-ene-pyranosuronic acid structure at the non-reducing end and a 2-N,6-O-disulpho-D-glucosamine structure at the reducing end of the chain. These differences in the manufacturing process result in the differences in the pharmacokinetic anticoagulation profiles described for these products in Table 4.1.

In addition to heparin being used as an anticoagulant, heparin has shown activity by inhibiting *P.falciparum* intraerythrocytic growth *in vitro* as well as other sulphated glycosaminoglycans such as dextran sulphate, which inhibit parasite growth *in vitro* and *in vivo* in a mammalian mouse model (Boyle et al., 2010). This inhibition is described as being mediated through blocking merozoite access to the erythrocyte (Kulane, A. et al., 1992). Further, heparin has also been shown *in vitro* to provide anti-cytoadhesion, rosette disrupting and merozoite invasion blocking activity; (Rowe et al., 1994; Clark, Su, & Davidson, 1997; Barragan et al., 1999). Furthermore, heparin have been shown growth and merozoite invasion inhibition activity in zoonotic malaria parasite *P. Knowlesi* (Lyth et al., 2018) and *P. berghei* (L Xiao et al., 1996).

Heparin possesses not only blood-stage inhibitory activities but also, that heparin and other sulphated GAGs have inhibited sporozoite invasion of hepatocytes (Samuel j et al., 1992). It is apparent that heparin, as well as other sulphated GAGs, offer an opportunity to inhibit more than one point in the life cycle of more than one *Plasmodium spp.* These mechanism(s) of heparin action are not well understood. *P.falciparum* growth inhibition by heparin has been described (Boyle et al., 2010), where heparin seems to inhibit parasite growth by blocking the invasion of erythrocytes by merozoite by inhibiting the first essential step of erythrocyte invasion through the merozoite surface protein 1 (MSP1). Thus, in contrast to most other

antimalarial drugs, heparin apparently inhibits the extracellular stages of *P.falciparum* development (Danny W. Wilson et al., 2013). Additional research suggests that heparin target several merozoite proteins, including the erythrocyte binding protein 140 (EBA-140) (Kobayashi et al., 2013) as well as rhoptry and microneme proteins involved in reorientation and signalling steps of invasion (Baum et al., 2009). If it is expected that heparin and other GAGs inhibit parasite invasion by targeting multiple invasive proteins, this multi-site targeting may reduce the possibility of the parasite developing effective resistance to many processes simultaneously. This seems to be likely as efforts to generate parasite resistant to heparin *in vitro* were unsuccessful (Boyle et al., 2010).

Heparin has previously been used as an adjunct therapy to treat patients with severe malaria (Smitskamp & Wolthuis 1971; Munir et al., 1980; Rampengan 1991) these trials, however, were halted due to the high anticoagulation activity of heparin that led to bleeding. Recently, a low-anticoagulant LMWH has been developed, sevuparin, which has anti-plasmodial growth inhibition activity but lacked anticoagulation activity. Sevuparin is a negatively charged polysaccharide derived from heparin with eliminated antithrombin binding (Anna M Leitgeb et al., 2017). Sevuparin, like heparin and LMWHs, has an array of chain lengths, with 6-16 units of repeated disaccharides of 2-N-sulfo-6-O-sulfo-glucosamine and iduronic-2-O-sulfate acid (Figure 4.3) with an average of molecular weight of around 8000 daltons (Telen et al., 2016). Unlike heparin and LMWHs, Suviparin has no anticoagulation properties, as the specific saccharides sequences required to bind to ATIII have been removed from sevuparin, resulting in low levels of binding to anti-IIa and factor Xa (Telen et al., 2016).

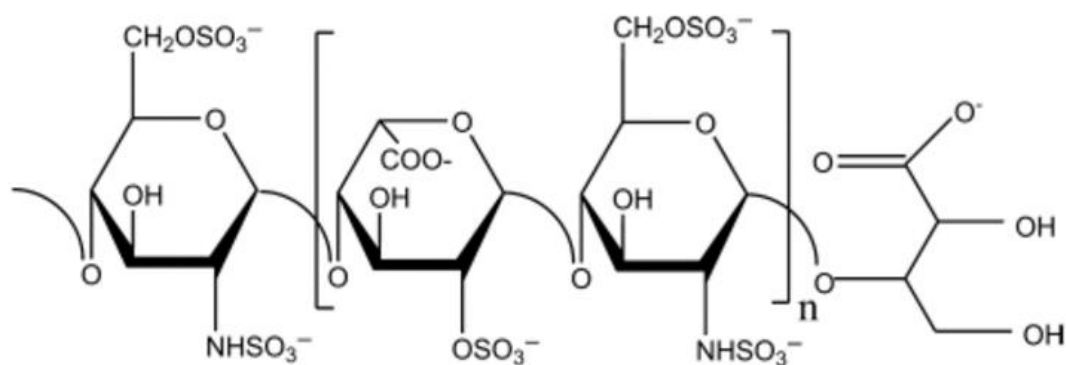


Figure 4.2 The chemical structure of LMW sevuparin. The polysaccharide consists of repeated units of the 2-N-sulfo-6-O-sulfo-glucosamine and iduronic-2-O-sulfate acid disaccharide. (Sourced from Telen et al., 2016).

Sevuparin's properties have been exploited in multiples disorders and disease. In non-infectious disease, sevuparin has shown the ability to bind to multiple adhesive legends which are responsible for vascular occlusion in sickle cell disease (Telen et al., 2016). This binding leads to a reduced adhesion and occlusion of capillary blood flow from cytoadhesive sickle cells (White et al., 2019). Whilst the same anti-cytoadhesion efficacy is found using heparin (White et al., 2019) and the LMWH Tinzaparin (Telen et al., 2016), sevuparin is a leading clinical trial Phase II drug candidate to treat vaso-occlusion crises (VOC) in sickle cell. Interestingly, sevuparin also disrupts rosetting formation and cytoadherence of *P.falciparum*, *in vivo* studies in rats (Saiwaew et al., 2017). In humans, sevuparin has been evaluated in patients with uncomplicated malaria, where sevuparin showed a dose-dependent anti-rosetting and anti-cytoadhesion activity (Saiwaew et al., 2017) and been evaluated recently as an adjunct therapy in clinical trial phase I/II (Anna M Leitgeb et al., 2017).

Whilst the intraerythrocytic growth-inhibition activity of heparin and enoxaparin have been evaluated, a systematic exploration of this activity across a range of different LMWH has not. In this chapter, a systematic side-by-side comparison of the *in vitro* the growth inhibition and erythrocyte invasion-blocking effects of the commercial LMWHs tinzaparin, dalteparin,

enoxaparin and reviparin are explored. In addition, using the NF54^{luc} transgenic parasite described in the previous chapter, these activities are explored in more than one genetic background of *P. falciparum*.

4.2 Results

4.2.1 Low molecular weight heparins (LMWHs) inhibit intraerythrocytic parasite growth *in vitro*

Whilst the invasion-blocking potential of heparin has been previously demonstrated (Boyle et al., 2010), a systematic and comparative demonstration of the same activity for LMWH has not. Four LWMH were commercially sourced; Tinzaparin, Enoxaparin, Deltaparin and Reviparin. Their potential in blocking intraerythrocytic growth over one 48hr cycle was determined and compared against unfractionated heparin and the structurally unrelated dextran sulphate. Their effect on blocking intraerythrocytic growth was each done at three concentrations (100, 33.3 and 11.1 $\mu\text{g/ml}$) with their effect normalised against an untreated control (100% growth). The experiments were done as technical triplicates in three biological repeats (n=9) using both Dd2^{luc} and NF54^{luc}. Using the luciferase assay, normalized growth was determined and the mean \pm StDev of n=9 of normalized growth (%) plotted (Figure 4.3).

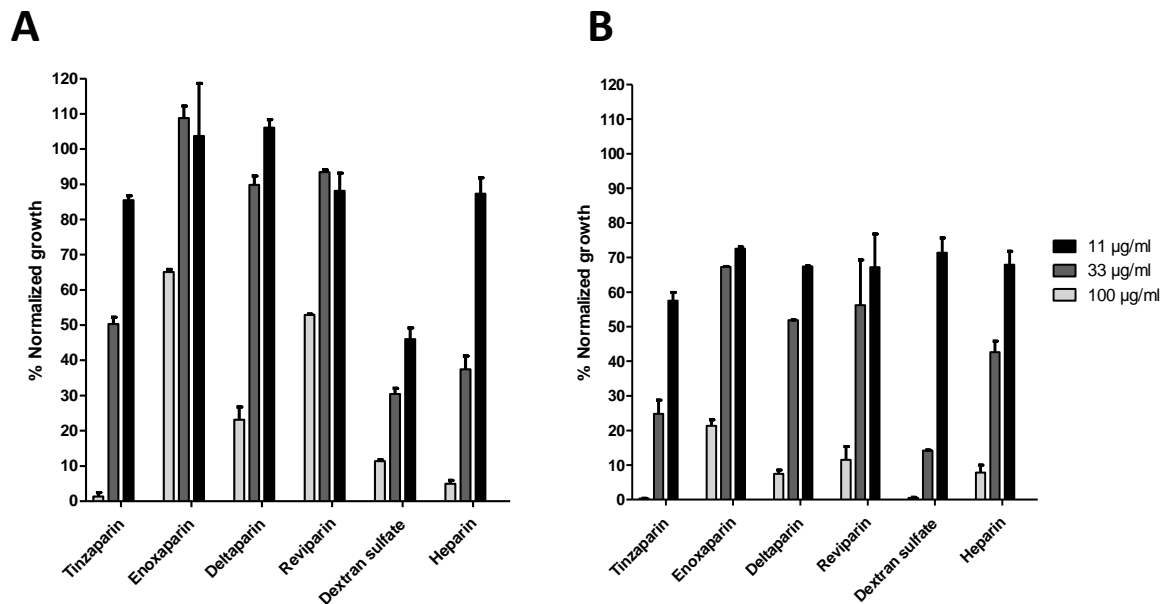


Figure 4.3 Growth inhibition activity of LMWH, dextran sulphate and heparin. The % normalized growth (compared to untreated control) of the indicated compound/concentration (see key) against (A) Dd2^{luc} and (B) NF54^{luc} after 48 hours incubation is shown. Bars represent mean \pm StDev from n=9 experiments.

As expected, there is a concentration-dependent response in growth inhibition for heparin. The same is also true for the LMWH and dextran sulphate. Comparison of the data for different compounds in Figure 4.3 indicates that dextran sulphate and heparin appear the most potent inhibitors of intraerythrocytic growth, followed by the LMWH tinzaparin and dalteparin with the least potent inhibition provided by enoxaparin and reviparin. This relative order appears to be present in both Dd2^{luc} and NF54^{luc}, suggesting that there is no readily strain-dependent difference. To analyse this further, the % normalised growth for each compound at each concentration were compared between Dd2^{luc} and NF54^{luc} in a scatterplot and a linear regression of the data done (Figure 4.4).

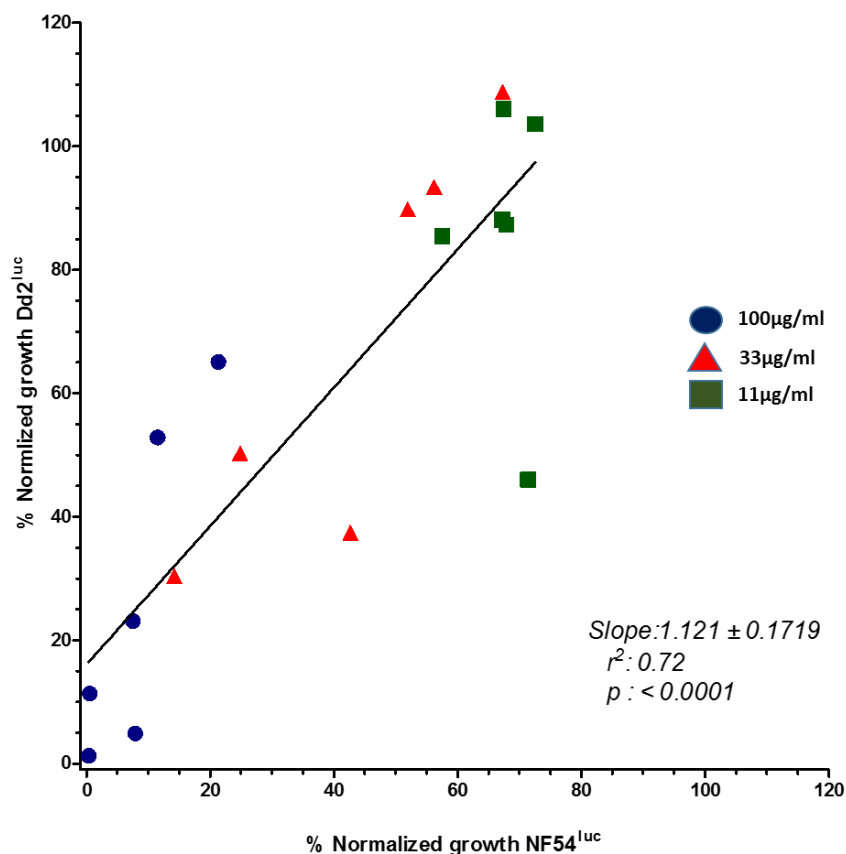


Figure 4.4 Scatterplot correlation of inhibitory effects of LMWH in Dd2^{luc} and NF54^{luc}
 The mean % normalised growth for each compound/concentration in Dd2^{luc} and NF54^{luc} have been plotted (see key for concentration data) and a linear regression performed.

The linear regression provides a slope of 1.2 ± 0.17 that suggested that there is a direct linear relationship between the effect of each concentration of each compound on the two distinct strains. The slight bias to Dd2^{luc} is apparent in Figure 4.4 where the NF54^{luc} normalised growth appears to reach a 75% growth irrespective of the concentration used. We consider this is unlikely to be a systematic error as we see the effect in three biological repeats, each performed using cultures produced on different days. The correlation ($r^2=0.72$) and significance ($p<0.0001$) suggests that these compounds do not apparently show strain-dependent differences in their effect. Of note is that whilst the 100 and 11.1µg/ml data cluster to the left and right of

the chart, respectively, that for 33.3 $\mu\text{g/ml}$ shows greater variation. Here, the three most potent activities in both strains are recorded for dextran sulphate, heparin and tinzaparin.

To provide more specific information using the provisional relative ranking of LMWH growth inhibition data, serial dilutions (two-fold) were used to do log concentration versus normalised growth plots to allow an EC_{50} of this growth inhibition to be measured. NF54^{luc} and Dd2^{luc} at trophozoite stage (2% parasitaemia, 4% HCT) were collected and incubated with two-fold of serial dilution of either LMWHs, heparin or dextran sulphate for 48hr. using the screening data, initial concentrations of 300 $\mu\text{g/ml}$ were used for the LMWH and 100 $\mu\text{g/ml}$ for heparin and dextran sulphate. The experiment was carried out as technical triplicates with three biological repeats. Parasite growth was normalized against untreated control and mean \pm SD of n=9 of normalized growth (%) plotted (Figure 4.5). Using a non-linear regression tool, these graphs were used to estimate the EC_{50} values in both strains along with their 95% confidence intervals (Table 4.3).

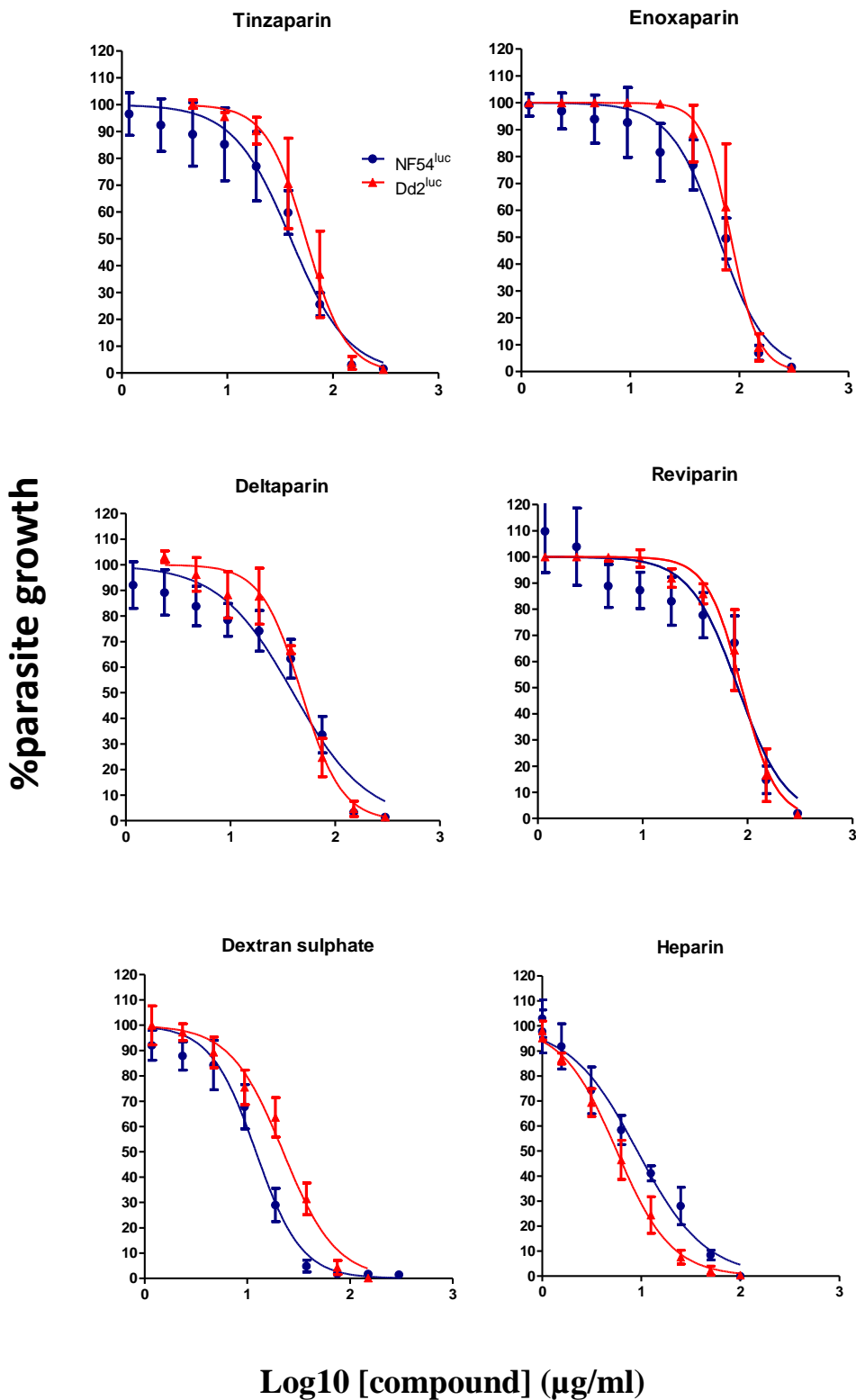


Figure 4.5 Log concentration *versus* normalised growth plots to determine EC₅₀. Log concentration normalized response curves for the indicated LMWH, heparin and dextran sulphate in Dd2^{luc} (red) and NF54^{luc} (blue) are shown. Each point represents the mean and StDev of n=9 data.

Table 4.3 EC₅₀ values of growth inhibition effect of LMWHs in Dd2^{luc} and NF54^{luc}

Compound	Dd2 ^{luc}		NF54 ^{luc}	
	Mean EC ₅₀ (µg/ml)	95% CI	Mean EC ₅₀ (µg/ml)	95% CI
Heparin	5.6	5.2- 6.1	9.1	7.31- 11.4
Dextran	22.3	18.3-27.1	12.3	10.1-14.4
Dalteparin	47.5	40.7-55.5	39.5	26.4-59.1
Tinzaparin	55.5	49.4-62.2	39.8	31.4-50.5
Enoxaparin	83.3	78.2-88.7	64.1	50.8-80.9
Reviparin	87.5	78.6 -97.5	80.9	55.8-117.3

To correlate the EC₅₀ values for each compound between the two strains, a linear regression analysis was performed between the NF54^{luc} and Dd2^{luc} data (Figure 4.6). The slope of 1.13 ± 0.12 indicates a near 1:1 correlation between the EC₅₀ values in NF54^{luc} and Dd2^{luc}. The correlation is strong (r^2 0.95, $p=0.0008$) and with the EC₅₀ data agreeing with the screening data, this establishes a relative order of growth inhibition of heparin > dextran sulphate > dalteparin and tinzaparin > enoxaparin and reviparin in both NF54^{luc} and Dd2^{luc}.

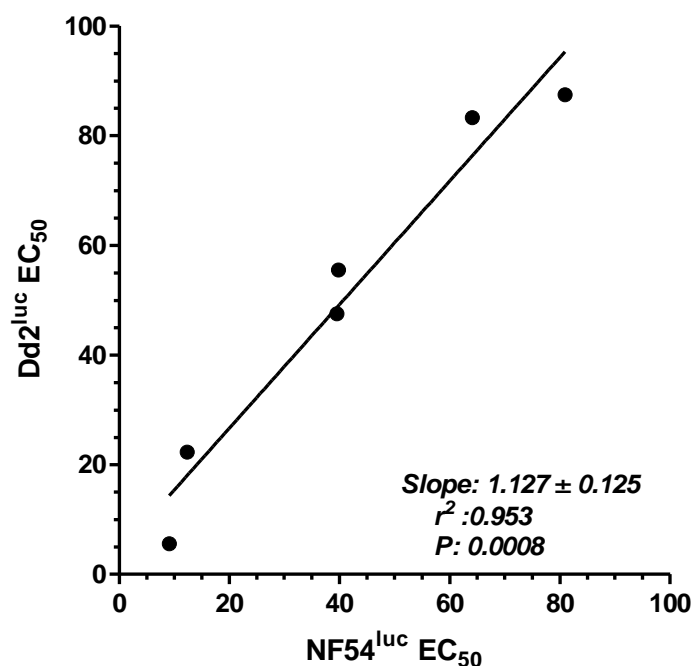


Figure 4.6 Scatterplot correlation of LMWH, heparin and dextran sulphate EC₅₀ in Dd2^{luc} and NF54^{luc}. The EC₅₀ for each compound in Dd2^{luc} and NF54^{luc} have been plotted and a linear regression performed.

4.2.2 Correlating the Luciferase growth assay date with flow cytometry Growth Inhibition Assays (GIA)

In chapter 3 it was shown that a plate-based fluorescence assay of the inhibition of parasite growth using heparin or other GAGs did not provide a useful assay. The growth inhibition effect of heparin and GAGs has, however, been demonstrated using a flow cytometry assay using fluorescent DNA intercalating dyes such as Sybr Green I (Bei et al., 2010 Jin Woo Jang et al., 2014; Boyle et al., 2017) The limitations of this flow cytometry assay are; (i) the protocol requires that samples are collected and washed before and after staining with the dye and is, therefore, a more time-consuming process and (ii) this method requires access to a flow cytometer and appropriate data analysis software. This equipment demand is balanced in the luciferase assay with a need to access to a luminometer, but also a limitation of the luciferase

assay is that the assay can only be done using genetically modified strains. However, in moving forward with a luciferase-based assay system, I decided to test whether the 48 hr luciferase assay data developed for Figure 4.3 for the NF54^{luc} strain correlates with normalised growth inhibition data developed using the same compounds and concentrations – but measured on a flow cytometer. Here the cultures were set up and exposed in the same way as for the luciferase experiment, with three biological repeats done. The starting parasitaemia was reduced to 0.5% as the experiment was allowed to proceed over two cycles of parasite growth, with samples harvested at both 48hr and 96hr to compare against the 48hr data from the luciferase assay. This modification was added as flow cytometry approaches use either 1 or 2 cycles of growth and we wanted to evaluate both timepoints here.

Using the forward scatter versus yellow fluorescence signal of the intact erythrocyte gated population, the proportion of Sybr Green I stained (i.e infected) erythrocytes can be measured. For each treated culture, this parasitaemia estimate was normalised against the parasitaemia of the untreated sample in that biological control series. Three repeats provided for a mean and StDev of these three repeats (Figure 4.7) for the 48hr and 96hr flow cytometry assays.

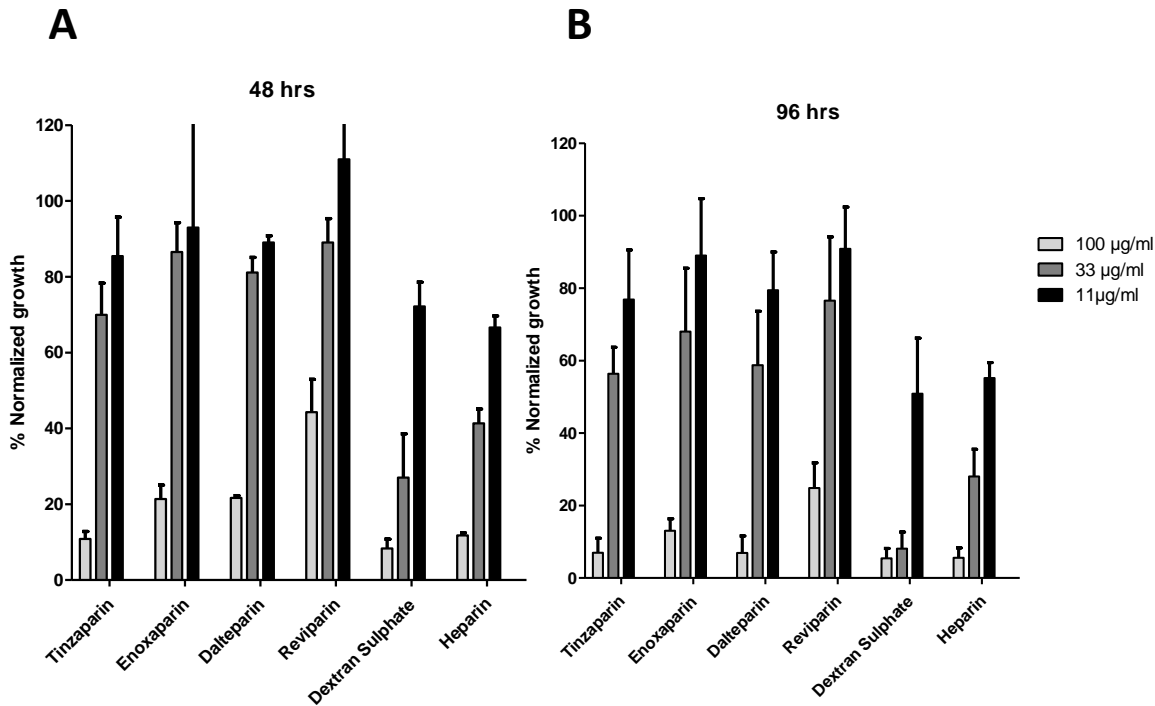


Figure 4.7 Growth inhibition activity of LMWH, dextran sulphate and heparin assessed by flow cytometry. The % normalized growth (compared to untreated control) of the indicated compound/concentration (see key) at (A) 48hrs and (B) 96 hrs in NF54^{luc} when exposed to the indicated concentration of the compound. Bars represent mean \pm StDev from n=3 biological repeats.

To compare these data against the corresponding 48hr luciferase data, regression analyses comparing each set of normalised growth inhibition assay (GIA) data for the different compounds/concentrations were done (Figure 4.8). This regression analysis shows no real difference between the 48hr luciferase GIA data and both of the 48 hr and 96 hr flow cytometry GIA data with the slopes and regression constants essentially the same. These data suggest a good, but not exact correlation between the growth inhibition data developed using these two methods. Correlation between datasets developed using the same approach was proven when the 48hr and 96hr flow cytometry GIA data were compared against each other (Figure 4.6C). Here the regression provides a tight and significant correlation between the two data sets (slope

of 0.97, r^2 of 0.93 and $p < 0.0001$). This is not a 1:1 ratio as the regression line is offset, reflecting that after 96hr the degree of growth inhibition provided by these compounds is greater than at 48hr.

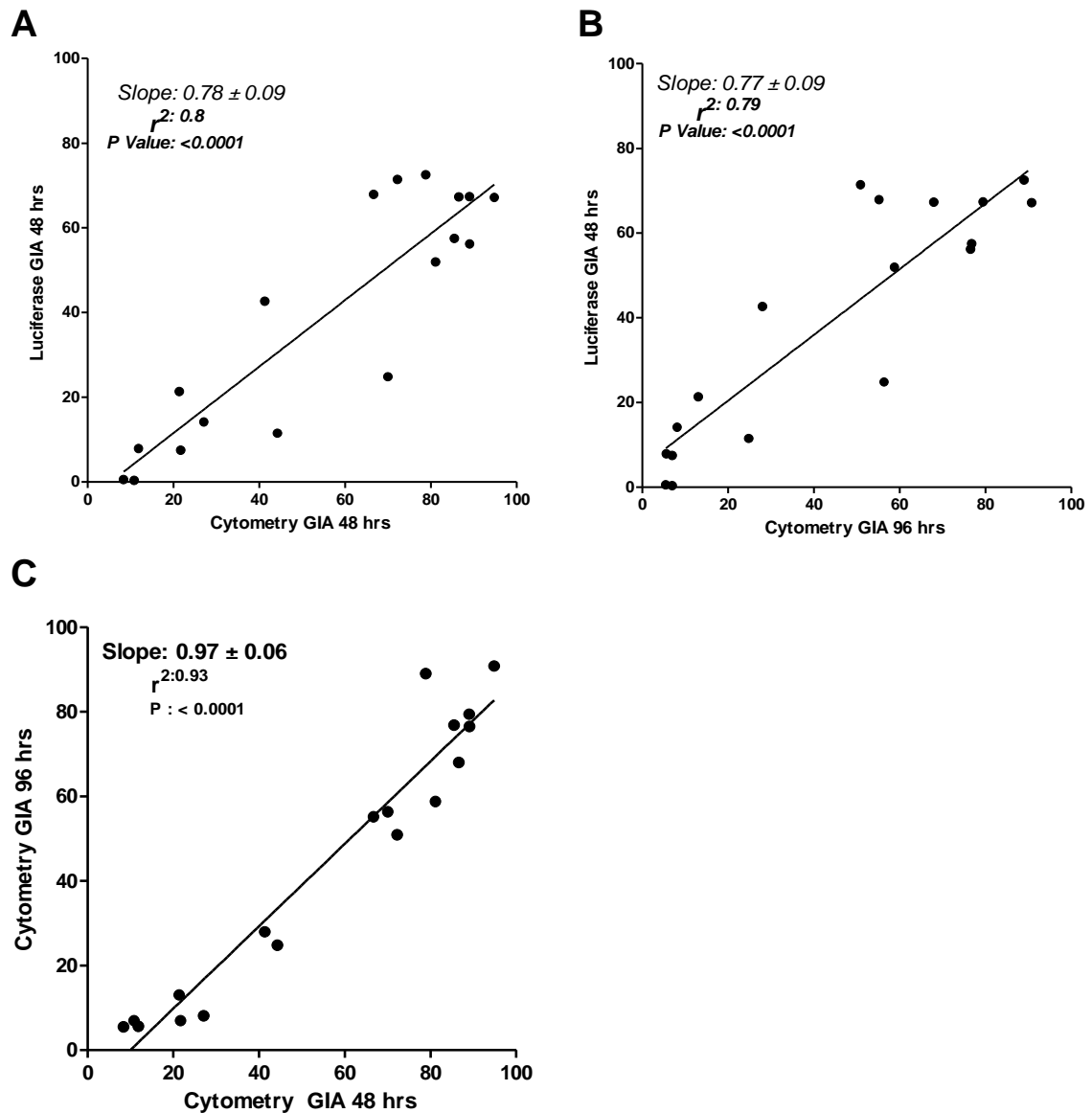


Figure 4.8 Exploring the correlation between luciferase and flow cytometry growth inhibition assays. Scatterplots correlating the mean normalised growth inhibition of (A) luciferase 48 hr *versus* flow cytometry 48hr, (B) luciferase 48 hr *versus* flow cytometry 96hr and (C) flow cytometry 48 hr *versus* flow cytometry 96 hr. The parameter reported is indicated on each axis and the results of the linear regression indicated. These data were developed only using the NF54^{luc} strain.

4.2.3 LMWHs inhibit parasite growth by blocking erythrocyte invasion

Heparin has been shown to inhibit *P. falciparum* growth by blocking merozoite invasion of a new host erythrocyte (Wahlin et al., 1992; Boyle et al., 2010; Recuenco et al., 2014). Following the demonstration that LMWH inhibits intraerythrocytic growth in two different strains of the parasite with a concentration-dependent effect similar to heparin and dextran sulphate (although with higher EC₅₀), the next step was to establish that the inhibition effect of LMWH was mediated at the level of erythrocyte rupture and reinvasion. Erythrocyte rupture and invasion is typically assessed by exposing a synchronised schizont stage culture to the blocking agent and culturing for 18 hrs. The rupture/reinvasion inhibition effect is determined by a microscopic examination of a Giemsa stained thin smear to observe newly established ring stage infections. A normalized invasion inhibition is then expressed as follows;

$$\text{Normalised invasion inhibition (\%)} = 100 - \left(\frac{A}{B} * 100 \right)$$

Where A is the mean ring stage count from three biological repeats after exposure to the blocking agent and B is the mean from three matched controls with no blocking agent. Dd2^{luc} and NF54^{luc} schizont stage cultures were exposed to 300, 100 and 33.3µg/ml of LMWH, heparin or dextran sulphate, with three independent biological repeats. The higher starting concentrations used in this screen was based on the high EC₅₀ of the LMWH. The mean and StDev of the normalised invasion inhibition from three biological repeats (n=3) for each concentration of each compound were plotted (Figure 4.9).

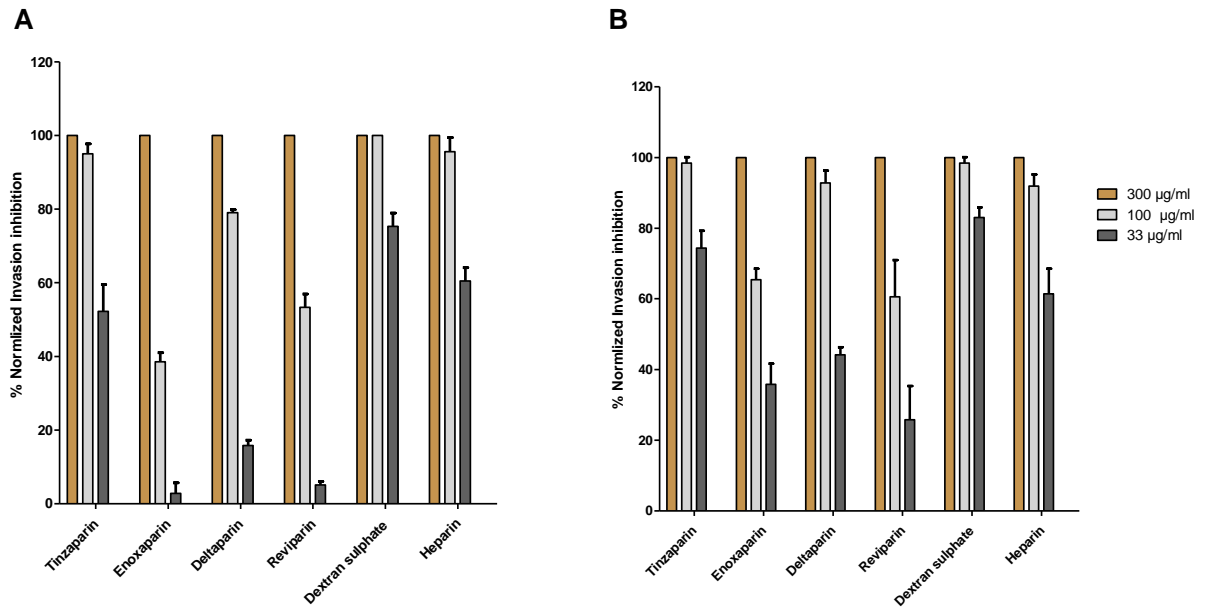


Figure 4.9 Invasion inhibition assessment of LMWH by microscopy. The mean \pm StDev (n=3) of the normalized invasion inhibition (compared to untreated control) for the indicated concentration (see key)/compound in (A) Dd2^{luc} and (B) NF54^{luc}.

From this figure, there appears to be a similar concentration-dependent invasion blocking effect in the two parasite strains. To confirm this a regression analysis of the normalised invasion inhibition data for each concentration/compound in both NF54^{luc} and Dd2^{luc} were plotted and a linear regression done (Figure 4.10). A strong linear correlation was found ($r^2=0.95$ and $p < 0.0001$) with a slope of 1.38 ± 0.07 . That the slope did not reveal a direct 1:1 comparison is likely based on two facts. First, that fixed concentrations of the compounds were tested in the two strains, rather than different fold concentrations based on the EC₅₀ data determined, and there is a trend (all compounds except heparin) where these compounds have a slightly stronger inhibitory effect in NF54^{luc}. Also, secondly, these data are based on manual counting observations – requiring a significant amount of time and subject to human error.

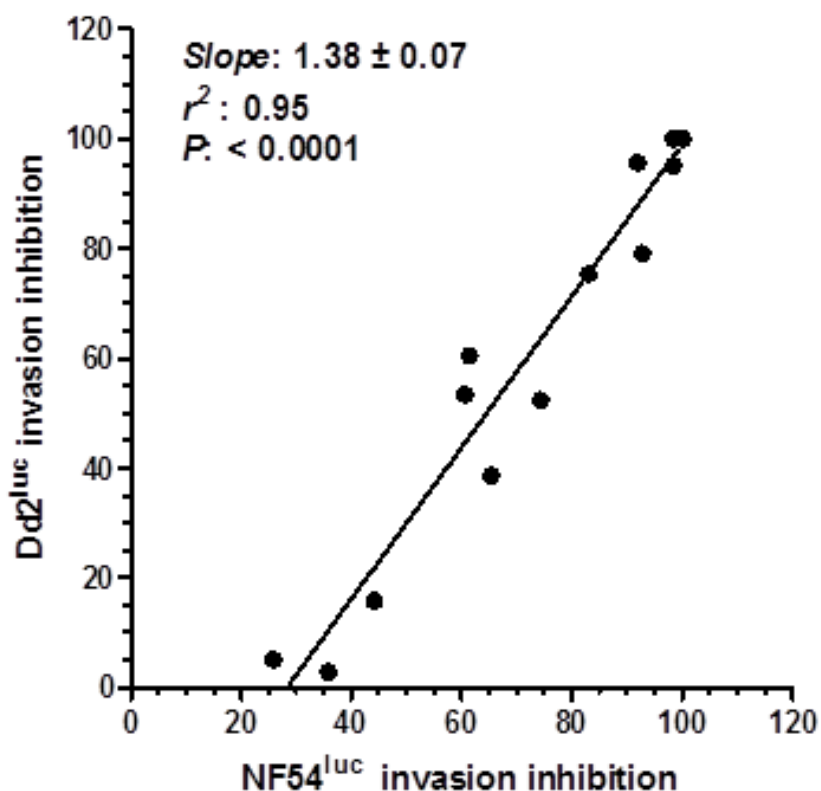


Figure 4.10: Linear regression analysis of invasion inhibition between NF54^{luc} and Dd2^{luc} strain. Each point represents the mean of (n=3).

Visual confirmation that the process of invasion was blocked using the LMWH compounds was done by taking samples of culture prior to the preparation of thin smears for light microscopy, staining the samples with the fluorescent Sybr Green I dye (primarily stains nucleic acid) and observing wet mounts of the culture using a fluorescent microscope. This was done only using samples from tinzaparin, dalteparin and heparin at 300 or 100 µg/ml – these compounds and concentrations showing the highest invasion blocking activity described in Figure 4.9. Interestingly, whilst it would be expected that merozoites would not be readily visible in experiments where no ring-stage parasites are observed, it was difficult to observe merozoites. In Figure 4.11 images of merozoites adjacent to erythrocytes, and potentially blocked during the invasion of erythrocytes, are shown. Given the very low numbers of events observed, and

that these fluorescent images could not definitely be indicated as evidence of invasion blocking (the merozoite may be laying against the erythrocyte) a more systematic counting was not done.

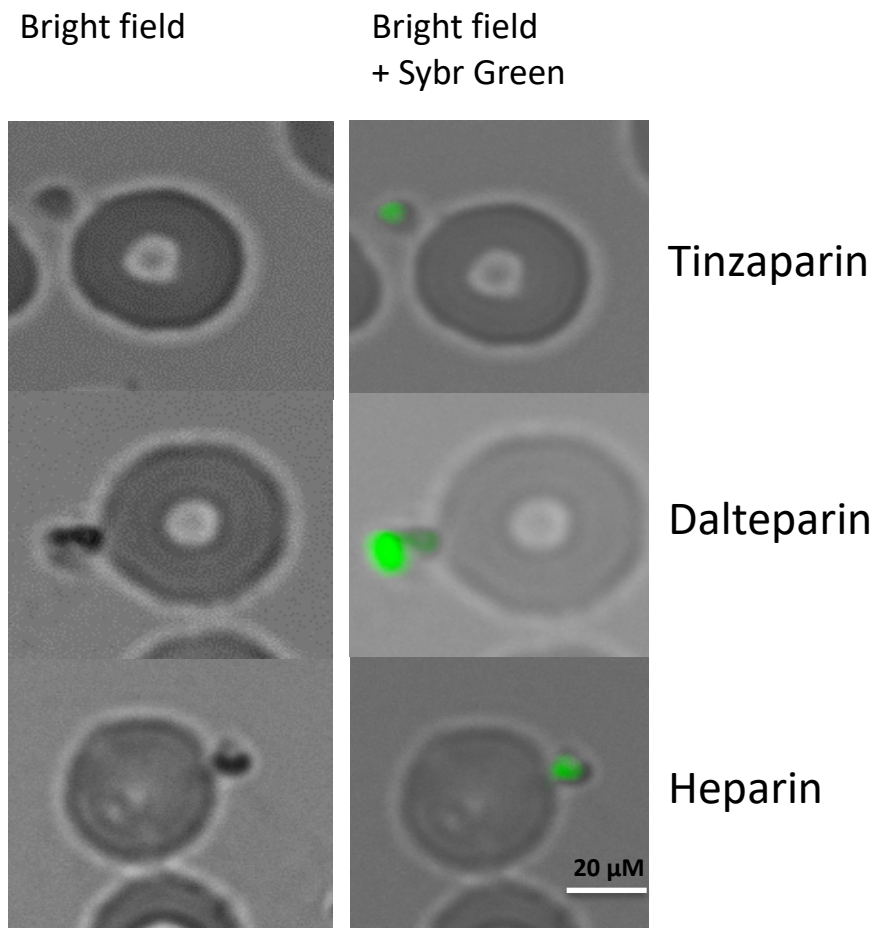


Figure 4.11 Bright field and fluorescent imaging of merozoites following heparin or LMWH treatment. Dd2^{luc} parasites exposed to 300 μg/ml of the indicated compound and stained with Sybr Green I fluorescent dye.

4.2.4 Exploring the inhibition of erythrocytic rupture and merozoite release by LMWH and heparin

Recent work by Glushakova et al. (2017) reported during this study identified a second *in vitro* effect of heparin on the inhibition of parasite growth. Their work specifically explored the action of heparin in the inhibition of the rupture of the infected erythrocyte membrane and/or release and dispersion of merozoites. Either one or both of these effects will prevent the invasion of new erythrocytes and establishing a new ring stage infection as shown above. To explore this effect, a time course morphological study was started. This time course recognised that by only looking at heparin or LMWH treated cultures shortly after the invasion (i.e the 18 hrs used above) may not allow morphological differences between unruptured, but otherwise normal, schizont and a cluster of merozoites trapped inside an erythrocyte to be discriminated between.

As assay strategy was decided that looked at exposing the treated schizont culture for 48hrs, with a morphological examination of Giemsa-stained thin smears by light microscopy (Figure 4.12A). Samples were harvested from a 2% schizont (4% haematocrit) culture treated with 100µg/ml of each LMWH, heparin or dextran sulphate with an untreated control for comparison. At 18hrs, 24 hrs and 48hrs, samples were removed and the proportion of each major intraerythrocytic stage (ring, trophozoite and schizont) as well as what are described here as “clustered merozoites” determined from counts of 100 infected erythrocytes (see Figure 4.12B for examples). The merozoite cluster was defined as an erythrocyte sized stained parasite material, which does not appear retained in an erythrocyte membrane, which is still associated with a darkly stained vesicle (the parasite food vacuole presumably trapped with the clustered merozoite). This observation is consistent with the activity of heparin in both inhibiting infected erythrocyte rupture as well as the dispersal of merozoites (Glushakova et al., 2017). The

experiment was conducted for three independent biological repeats, with the mean and StDev of the proportion of these four morphological stages plotted (Figure 4.13).

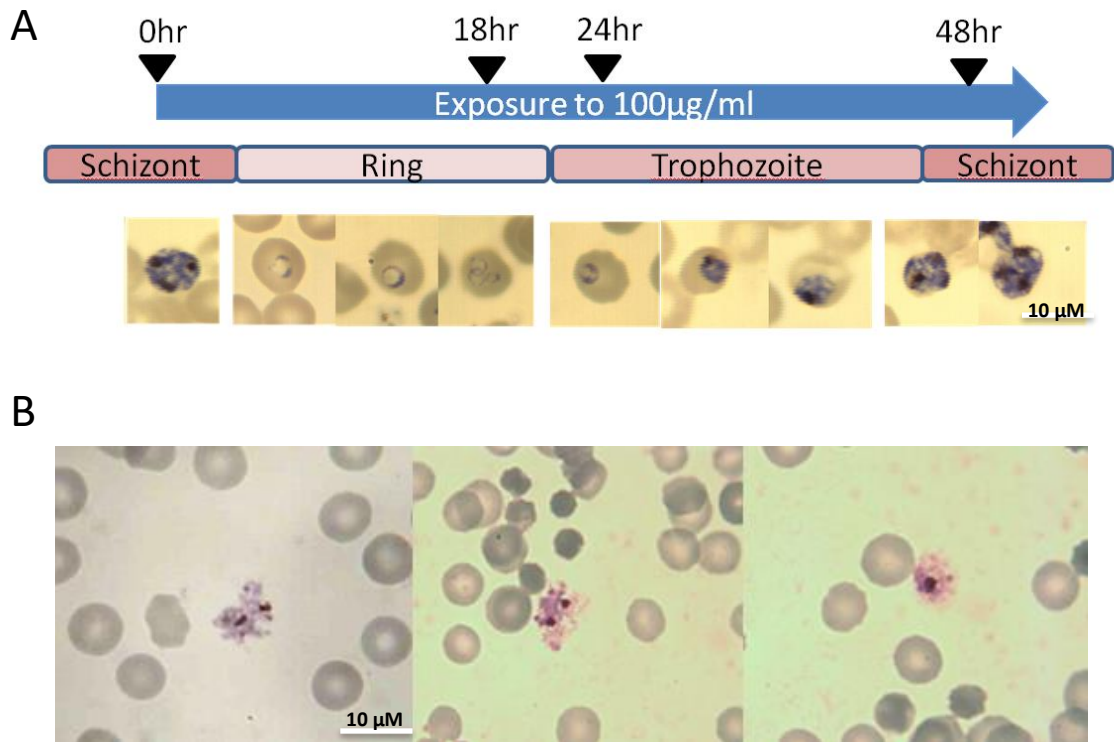


Figure 4.12 (A) Schematic representing the time course assay. Synchronised schizonts were exposed (or left untreated in a control) to 100µg/ml of the compound. The culture was examined at 18, 24 and 48hrs. The expected main morphological stage of an untreated culture is shown below the time course. Representative Giemsa-stained thin smears for each main morphological stage is shown below. **(B)** Example images representing a clustered merozoite – showing their size compared to an erythrocyte, that there is no clear erythrocyte membrane and that they all appear with pigmented centre.

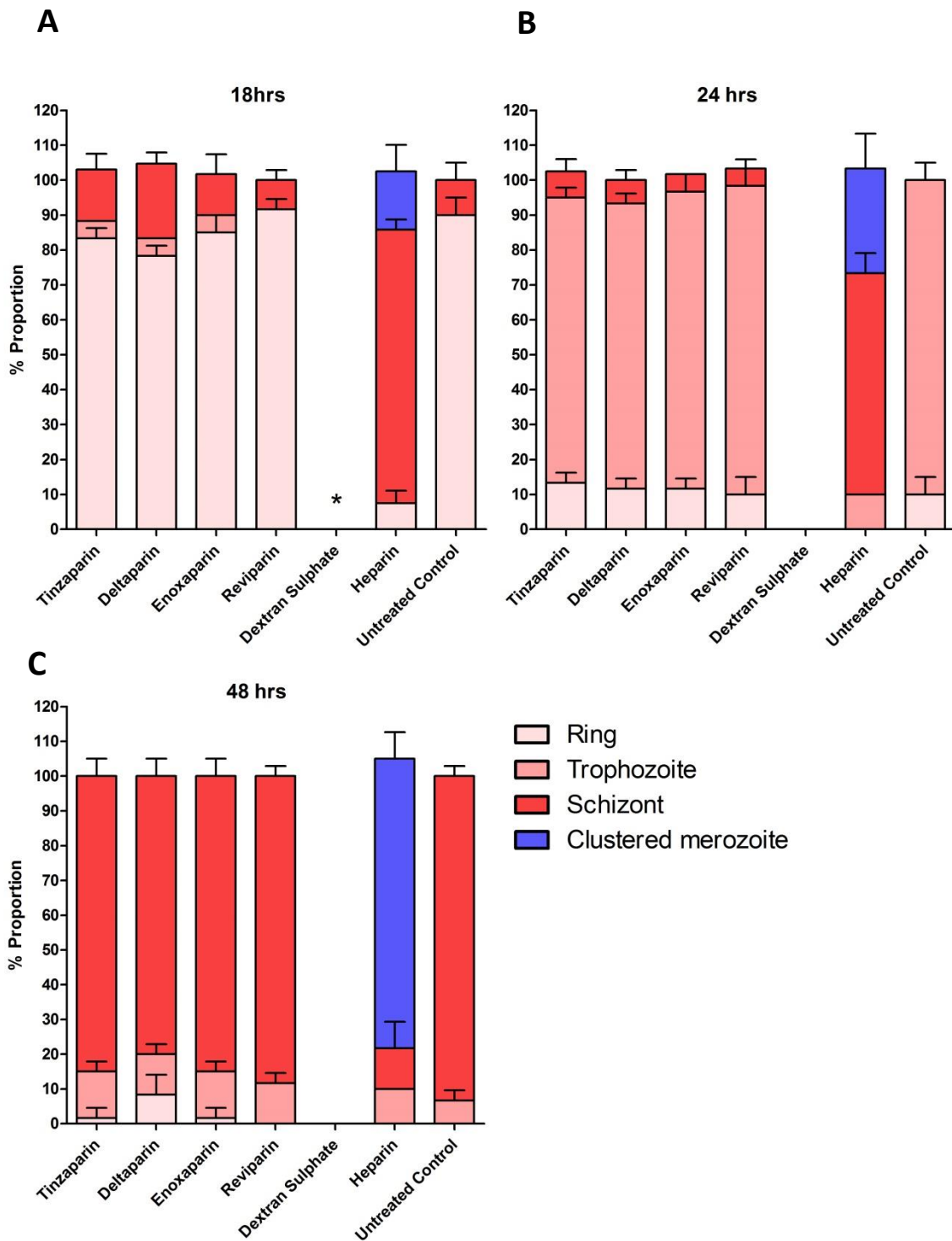


Figure 4.13 Staging of morphological stages following treatment with LMWH, dextran sulphate and heparin. The mean proportion \pm StDev of each of the main intraerythrocytic stage or clustered merozoite is represented (see key). These proportions are based on the counts of 100 NF54^{luc} infected erythrocytes/clustered merozoites over (A) 18 HRS, (B) 24hrs, (C) 48 hrs from three independent experiments. No data (*) is available for dextran sulphate as at 100 μ g/ml no reinfection occurred nor were clustered merozoites observed.

This experiment provided data distinct to that of the ring stage count. The latter provides an indication of the relative inhibition of reinfection – and allowed a ranking of heparin against the LMWH to be determined. This time course experiments counts up to 100 infected erythrocytes, irrespective of the total number. In fact, for dextran sulphate, at 100µg/ml no reinfection occurred in any of the three repeat experiments nor were clustered merozoites observed at any time. The control, untreated, cultures show the expected progression from predominantly rings at 18hrs to predominantly trophozoites at 24 hrs and predominantly schizonts at 48hr.

As previously reported by Glushakova et al., (2017) who also used NF54 and a concentration of 100µg/ml of heparin, they see evidence of the inhibition of erythrocyte rupture and lack of merozoite dispersal, creating clustered merozoites. The same observation is observed here. At 18 hrs, schizonts are most predominant as opposed to rings. This is probably, heparin has delay schizont rupture . As you move forward 6 hours, the proportion of merozoite clusters increases to a point where about 80% of the observed parasites appear to be merozoite clusters at 48 hrs. The same effect does not, however, seem to be evident from the four LMWH. Here, despite our observation that at 100µg/ml there is between 40% (Enoxaparin) to 95% (Dalteparin) inhibition of reinvasion – compared to 95% inhibition by heparin – there was not readily observed merozoite clusters in any treatment using a LMWH.

4.3 Discussion

Most severe malaria deaths in hospitalized children happen within the first 24 hours (A. M. Dondorp et al., 2008). In order to provide time for antimalarial therapies to work, research has explored the potential for adjunct therapies (eg. steroids, anticonvulsants, monoclonal antibodies, volume support, acidosis correction and iron chelation) to support the immediate first 24 hours, although these show little or no benefit (Maitland., 2015). The effect of heparin in inhibiting *P.falciparum* growth by blocking merozoite invasion and the reversal of cytoadherence and rosetting as an adjunct therapy have also been explored (Smitskamp & Wolthuis 1971; Munir et al., 1980; Rampengan., 1991), although these studies were not progressed due to the risk of heparin-induced thrombocytopenia. Given that LMWH retain their anticoagulation activity, although with a far less reduced risk of thrombocytopenia, we have explored here the growth inhibitory effect of four common LMWH here, recognising that whilst we know LMWH do inhibit intraerythrocytic growth (Boyle et al., 2017), these growth inhibition activities have not been systematically characterised, and not beyond one *P. falciparum* strain.

The LMWHs used in this study showed a concentration-dependent reduction in parasite growth in two strains (NF54^{luc} and Dd2^{luc}) in the novel luciferase growth inhibition assay. The correlation of inhibitory effects between the two strains tested was good ($r^2 = 0.72$). Importantly, whilst this study also provided an estimation of the EC₅₀ for all LMWH in the two strains as well as a relative ranking of Dalteparin/Tinzaparin > Enoxiparin/Reviparin, and these data are in broad agreement with the provisional evaluation reported by Boyle et al (2017) that these are all weakly acting growth inhibitors (EC₅₀ predicted to fall between 20-100 µg/ml). Taking the EC₅₀ data, adding that of Sevuparin (mean EC₅₀ of 5.2 µg/ml and mean size of 8kDa from (Leitgeb et al., 2017), we note that there appears to be a correlation between the size of the low molecular weight heparins and their growth inhibitory activity (Table 4.4).

Table 4.4. Exploring the relationship between growth inhibition and MW of LMWH, heparin and dextran sulphate

Compound	Mean EC ₅₀ (µg/ml)	Mean MW kDs
Heparin	5.6-9.1	<15
Dextran sulphate	12.3-22.3	<15
Sevuparin	5.2	8
Tinzaparin	39.8-55.5	6.8
Dalteparin	39.5-47.5	6
Enoxaparin	64.1-83.3	4.2
Reviparin	80.9-87.5	3.9

Whilst there appears a pattern of relationship growth inhibition and MW in the compounds reported in this table, Sevuparin sits less well in this rank order - with its growth inhibition effect EC₅₀ of 5.2 µg/ml (Leitgeb et al., 2017) more similar to that of an unfractionated heparin and being slightly larger (mean size of 8KDa (Telen et al., 2016) from than the LMWH Tinzaparin. However, that a growth inhibition effect correlates with the size of a fractionated heparin does correlate with data on heparin and other sulphated GAGs length, in rosette disturbing (Rogerson et al.,1994;Barragan et al., 1999) ,cytoadhesion (L Xiao et al.,1996) and blood-stage parasite growth inhibition (Clark, Su, & Davidson, 1997; L Xiao et al., 1996).

The capacity of LMWH growth inhibition is not only determined by length but also by sulphation degree, where most of LMWH in this study are highly sulphated. Unsurprisingly, the correlation between the length of LMWHs and the growth inhibition is agreed with their main function as anticoagulants, LMWHs with higher MW are more potent to inhibit Anti-Xa factor (Hirsh et al., 2001) (see table 4.5).

Table 4.5 relationship between MW and anticoagulation activity of heparin fractions *

Heparin oligosaccharides	Molecular weight (Dalton)	Anti-Xa	Anti-IIa
8	2400	1.3	Nil
12	3600	2.58	Nil
16	4800	1.60	Nil
18	5400	0.95	0.51
24	7200	1.30	1.21

*Table was adapted from (Hirsh et al., 2001)

Using the ring stage counting assay the stage specificity of the LMWH inhibition was explored. As for heparin, the LMWH inhibits growth by interfering with the reinvasion of a new host erythrocyte. Our data (Figure 4.9) shows that all the LMWH, including the least potent reviparin and enoxaparin, completely block the formation of newly invaded rings at a 300 µg/ml concentration. The most potent effect using a 100 µg/ml concentration was that of tinzaparin, the largest of the LMWH tested. The correlation between these ring invasion inhibition studies in the two strains was high ($r^2=0.95$) suggesting that invasion blocking via these LMWH is not a strain-dependant phenomenon. Although an important qualification of this statement is that whilst the two strains tested here do have differences in their erythrocyte invasion phenotype,

they are still only two strains and the third strain with a different invasion phenotype would support this observation.

The ring invasion inhibition rank order data correlates well with the luciferase growth inhibition rank order assay. That is – heparin > dextran sulphate > tinzaparin/dalteparin > enoxaparin/reviparin. This same rank order of effect was observed when we tested the invasion blocking data using the flow cytometry assay approach in the NF54^{luc} strain. Importantly, when using either the luciferase or flow cytometry assays, the growth inhibition data correlates well ($r^2=0.8$) irrespective of whether the one cycle luciferase data is compared against the one or two-cycle flow cytometry data. A comparison between luciferase or flow cytometry growth inhibition assay with the ring invasion counting assay done using microscopy shows that each method provides relative benefits and issues in the monitoring of the growth inhibition effect (see also Table 4.6).

The luciferase assay, introduced in this thesis, offers advantages in terms of the rapid, robust and reliable development of data in a high throughput plate-based assay. The same reliable and robust data can be obtained by flow cytometry, but the latter method requires sample processing steps and without an automatic loader for the flow device, this is a time-consuming series of manual steps. Both methods, however, require specialist equipment, although the luminometer is cheaper than most flow cytometers. The most significant issue with the luciferase assay is that we can only study strains genetically modified to express the luciferase reporter protein.

Table 4.6 Comparison of the growth inhibition assays used in the LMWH study

Method	Pros	Cons
Luciferase	<ul style="list-style-type: none"> • Rapid rate based assay • Robust data (high signal to noise) 	<ul style="list-style-type: none"> • Need GM • Need luminometer plate reader
Flowcytometry	<ul style="list-style-type: none"> • Medium assay rate • Robust data as count > 10.000events • Doesn't need genetically modified parasite(GM) 	<ul style="list-style-type: none"> • Required Flow cytometer • Manual machines (read one single sample) are laborious
Microscopic counting	<ul style="list-style-type: none"> • Simple protocol • Only need light microscope • Doesn't need GM 	<ul style="list-style-type: none"> ▪ Bias in counting ▪ Laborious assay

In this study we report that LMWHs have no apparent effect on intraerythrocytic development – i.e. they are not cytotoxic to trophozoites such as drugs like artemisinin and chloroquine (Ullah et al., 2017). The growth-inhibitory effects are apparent after 48 hrs of parasite incubation with the LMWHs (Figure 4.3) and more specifically after 18 hrs of incubating schizont stage parasite with LMWHs (Figure 4.9). However, most studies related to *P.falciparum* growth inhibition by heparin and/or GAGs have reported that inhibition of parasite growth through the blocking the extracellular form of parasite (merozoite) binding to the host erythrocyte surface (Boyle et al, 2010; Boyle et al., 2017; Burns et al., 2019; Glushakova et al., 2017; Recuenco et al., 2014). During this study, we did observe some free merozoites attached to the surface of erythrocytes, but also observed a role for heparin in the blocking of parasite egress. Heparin delay schizont rupture, but not LMWHs nor dextran sulphate (Figure 4.13) and induced the formation of aberrant, irregular shaped schizonts (termed in this study as clustered merozoites) (Figure 4.12.B). These clustered merozoites have no clearly defined erythrocyte membrane and appear as parasite-derived material collected

around a food vacuole (based on black pigment). This phenomenon was readily observed after 48 hrs of heparin incubation, suggesting the delayed schizonts were converted into clustered merozoites and failed to establish the re-invasion process. Our observation of delay in schizonts rupture consistent with several reports (Boyle et al., 2010; Evans et al., 1998; Butcher et al. 1988). Evans et al., (1998) describes that curdlan sulphate has no effect on intraerythrocytic development but does effect schizonts by delaying rupture that the merozoites released failed to invade erythrocytes. Whilst these studies describe that heparin blocks merozoite invasion and schizonts rupture delay, they do not describe any morphological changes in heparin treated parasites. Moreover, many studies exploring the inhibitory effect of heparins release merozoites through a mechanical shear and therefore have not explored the action of heparin or other GAGs on schizont rupture. Our data suggest that heparin may not only inhibit parasite growth by targeting merozoite invasion of erythrocytes but also by blocking schizont rupture and/or merozoite egress and separation.

Notably, this schizont rupture/egress effect was not observed in parasites treated with dextran sulphate which showed potent growth inhibition. No aberrant schizonts were seen and suggest that the large MW dextran sulphate has no effect in inducing clustered merozoites but is perhaps solely inhibiting population growth through inhibition of merozoites invading erythrocytes. This suggests that there may be some difference in the mode of inhibition between heparin and dextran sulphate and, perhaps, that we need to study different classes of GAGs to explore whether there are differences in the growth invasion phenotype at schizont rupture and merozoite invasion.

LMWH did not show the same schizont rupture effect as heparin. LMWH treated parasites developed normally, with no delay in schizont rupture observed, and as the growth inhibitory effect occurred between the schizont and ring stage, this suggests LMWHs inhibited parasite growth solely blocking merozoite invasion of erythrocytes only. This potential difference

between LMWHs and heparin may arise a consequence of the reduced chain length in the LMWH limiting their capacity to cross-link between merozoites or between merozoites and another structure such as the food vacuole or disrupted host erythrocyte surface. Although given that LMWH is less potent in inhibiting growth, their effect on blocking schizont rupture may only be seen when an appropriate high fold-concentration is achieved. The experiments used a fixed concentration of 100 $\mu\text{g/ml}$ over 48 hrs. For heparin, this is 22x EC_{50} , whilst for the LMWH this is only 1.2-1.5x EC_{50} . At 300 $\mu\text{g/ml}$, a 3.6 to 4.4x EC_{50} all LMWHs showed complete invasion inhibition with no ring stages observed, however no merozoite cluster was seen in all three biological repeats tested. So, whilst it may be that the differences between the growth inhibition of heparin and LMWH are affected at different stages of egress and merozoite invasion, it is clear that the concentration-dependant inhibitory effects of heparin and LMWH at these stages are different. A model for this proposal is provided in Figure 4.14.

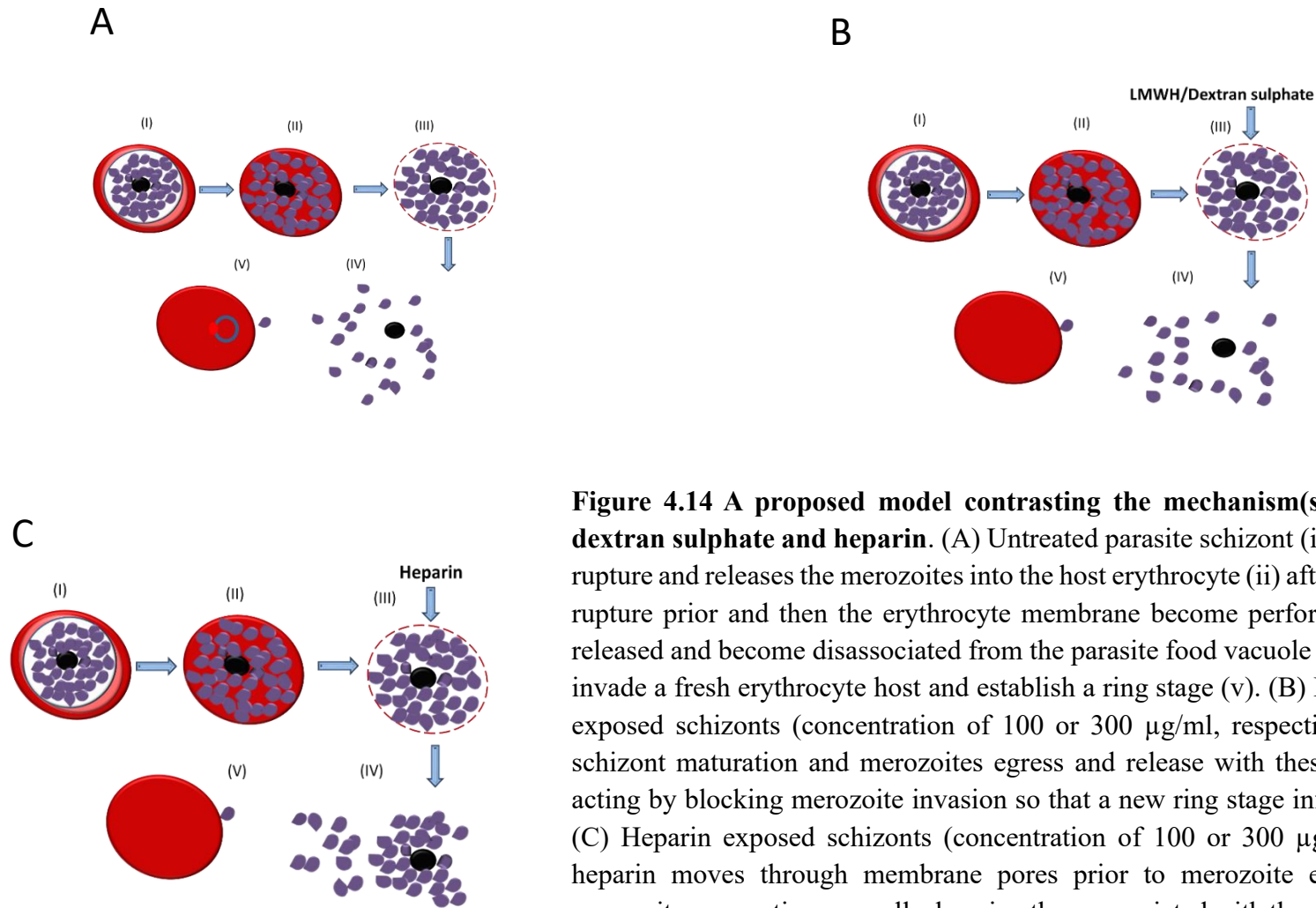


Figure 4.14 A proposed model contrasting the mechanism(s) of action of LMWH, dextran sulphate and heparin. (A) Untreated parasite schizont (i), Parasitophorous vacuole rupture and releases the merozoites into the host erythrocyte (ii) after parasitophorous vacuole rupture prior and then the erythrocyte membrane become perforated (iii), merozoites are released and become disassociated from the parasite food vacuole (iv) merozoites are free to invade a fresh erythrocyte host and establish a ring stage (v). (B) LMWH/Dextran sulphate exposed schizonts (concentration of 100 or 300 $\mu\text{g/ml}$, respectively) show no effect on schizont maturation and merozoites egress and release with these compounds apparently acting by blocking merozoite invasion so that a new ring stage infection is not established. (C) Heparin exposed schizonts (concentration of 100 or 300 $\mu\text{g/ml}$) delay schizont and heparin moves through membrane pores prior to merozoite egress. Heparin prevents merozoites separating normally, keeping them associated with the parasite food vacuole with a second target of heparin action by blocking merozoite invasion of the new host.

The observation described here of heparin blocking schizonts rupture may explained by study published recently by Glushakova et al., (2017) (It needs more methods such as live imaging microscopy to confirm it). Here they similarly describe the use of a 100 µg/ml concentration of heparin effectively blocking merozoite release and their clustering in three different parasite strains. The report describes how heparin enters an infected erythrocyte when the host erythrocyte plasma membrane perforates (after the rupture of the parasitophorous vacuole which is not affected) to block the complete erythrocyte membrane rupture and the trapping merozoites within the erythrocyte to prevent their dissemination and finally the formation of a clustered merozoites (morphologically-changed infected cell where most merozoite clustered within erythrocyte). The mechanism of egress blocking is likely due to heparin-binding with the inner aspect of erythrocyte membranes as well as targeting merozoite surface proteins organised onto the apical end of the merozoite. Interestingly, our Giemsa-stained heparin-treated clustered merozoites morphologically appear to be the last stage of the merozoite cluster formation, after the complete rupture of the erythrocyte membrane, with the merozoite material associated with the remnants of the food vacuole (Glushakova et al., 2017).

Das et al., (2017) demonstrated that *P. falciparum* actin-I (PfACTI) is essential and required for merozoite segregation during parasite egress. The absence of PfACTI, using a conditional knock out system, leads to the failure of merozoite separation and a defect in erythrocyte invasion. Interestingly, their Giesma stained images of rapamycin-treated parasites (Figure 4.15) shows clustered merozoites attached to food vacuole and are seems similar to the heparin-treated clustered merozoite in this study. Therefore, if we assume that heparin may have blocked the function of PfACTI, resulting in a delayed and/or complete loss of merozoite release, it would be interesting to explore if heparin interacts or inhibit ACTI protein.

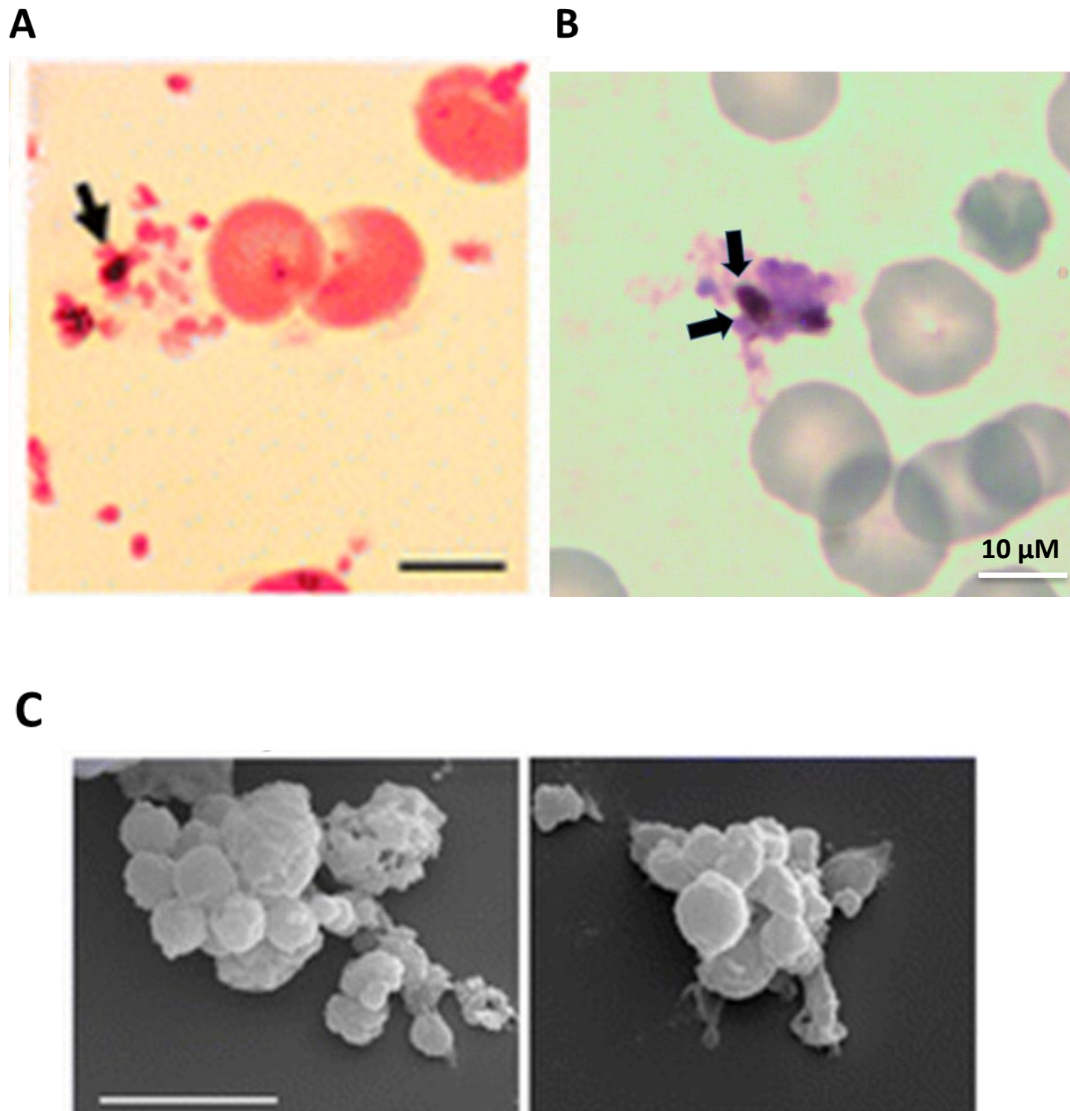


Figure 4.15. The similarity in Giemsa-stained images of merozoite clusters in PfACT knockout and heparin-treated schizonts (A) PfActI deficiency induced by rapamycin-treated parasite with the black arrow indicating the merozoites attached to the food vacuole. (B) NF54^{luc} parasite treated with 100 μg/ml of heparin for 48 hrs with the arrows indicate the merozoites attached to the food vacuole (image was taken using light microscopy under 100X oil emersion magnification). (C) Scanning electron microscopy of rapamycin-treated parasite, showing conjugated merozoite. Both A and C Source: (Das at el., 2017)

In considering the potential of LMWH as an adjunct therapy based on what we now know on their potency, some information on how LMWH is currently used clinically (and therefore considered likely to be a safe concentration to use) has been explored here to estimate the concentration of LMWHs and compared them to EC₅₀ values from this study. LMWH is used, for example, in the treatment and prophylaxis of thromboembolic disease, a specific example is the use of enoxaparin in infants and children (Albisett et al., 2001) (See Table 4.7A). Using the information about the dose and weight to determine the mass of heparin delivered, and an estimating of the total blood volume from an online calculator (<https://reference.medscape.com/calculator/estimated-blood-volume>) an approximate serum concentration of heparin (assuming 100% of the LMWH is available to inhibit parasite growth) for a series of weights correlating to young children (3000ml) to adults (6000ml) (See Table 4.7.B). From these simple predictions, it would suggest that safety guidelines for the use of LMWH would deliver between 5 to 20µg/ml of LMWH at best conditions. This contrasts with the estimated EC₅₀ for the inhibition of parasite growth of between 39.5 to 87.5 µg/ml. Therefore, it would appear that we could deliver 0.06-0.5 times the 50% effective concentration – much less than an amount that would be expected to support a reduction in parasitaemia in a culture that expands logarithmically every 48 hours. Therefore, there appears to be no support provided here for the use of LMWH as an adjunct therapy in reducing parasite growth by blocking the merozoite release and reinvasion process. Whilst there is a reduced risk of heparin-induced thrombocytopenia associated with LMWH, these compounds would need to have an increase in anti-plasmodial growth by some 10 to 84-fold (to achieve a potential delivery of a 5xEC₅₀ dose).

Table 4.7 Exploring the potential therapeutic use of LMWH as an anti-plasmodial agent. (A) Treatment and prophylactic doses of enoxaparin used for the treatment of thromboembolic disease in infants (3.5 to 5 kg (Albisetti et al., 2001). Estimates of blood volume were obtained from <https://reference.medscape.com/calculator/estimated-blood-volume>. (B) The treatment dose of enoxaparin based on weight for child (3000ml) to an adult (6375ml) and using a NHS summary prescription guide (2018). The two final columns in both tables provide the best estimate of the concentration of LMWH achieved compared to the EC₅₀ of their anti-plasmodial action in the last column.

A

Indication	Age group	Weight (Kg)	Dose (mg/Kg)	Total dose (mg)	Approximate Blood volume (ml)	Concentration (µg/ml)	Anti malaria range EC ₅₀ (µg/ml)
Thromboembolism	< 2 months	3.5	1.5 (therapeutic dose)	5.2	297	17.6	39.5-87.5
Thromboembolism	> 2months	5	1.0 (therapeutic dose)	5	425	11.7	39.5-87.5
Thromboembolism	< 2 months	3.5	0.75 (prophylactic dose)	2.6	2.97	8.8	39.5-87.5
Thromboembolism	> 2months	5	0.5 (prophylactic dose)	2.5	425	5.8	39.5-87.5

B

Dose (mg/Kg)	Total dose (mg)	Approximate blood volume (ml)	Concentration (µg/ml)	Anti malaria range EC ₅₀ (µg/ml)
1.5	60	3000	20	39.5-87.5
1.5	90	4500	20	39.5-87.5
1.5	127.5	6375	20	39.5-87.5

Chapter five: Investigation *in vitro* the growth inhibitory and invasion blocking effects of heparin mimetics in *P.falciparum*

5.1 Introduction

Resistance in *P.falciparum* to artemisinin-based combination therapies continue to be reported in Southeast Asia (Hati, Das, Roy, & Saha, 2018; Tun et al., 2015), raising concerns that the present antimalarial therapies will be soon ineffectual (Amaratunga, et al., 2016). There is a necessity to continue to discover a new class of drugs or compounds with different mechanisms of action, which are effective against all drug-resistant strains, can clear parasitaemia quickly and improve clinical outcomes (Burrows et al., 2017). In addition to these characteristics, any new class of compounds should target multiple lifecycle stages that could improve the efficiency of the drug and decrease the possibility of the parasite to develop resistance.

Severe malaria disease symptoms from *P.falciparum* malaria occur throughout the blood-stage infection, where the extracellular form of the parasite (merozoites) invade and then multiply inside erythrocytes. The small window of time during which schizonts rupture and release merozoites offer a novel target through invasion-blocking inhibitors (Danny W Wilson et al., 2015). This novelty arises as all current antimalarial drugs work by targeting the parasite within erythrocytes (Danny W. Wilson, Christine Langer, Christopher D. Goodman, Geoffrey I. McFadden, & James G. Beeson., 2013). The use of a compound that can block merozoite invasion, most likely in combination with current or future antimalarial drugs that target the intraerythrocytic stage, maybe valuable with this combination maximizing the efficacy of the drug, having cidal effects both intra and extracellular.

During *P.falciparum* infection, merozoite invades erythrocyte through a multi-step complex process, where receptor-ligand interaction involved to mediate the invasion event. Briefly: (i) the merozoite makes initial contact of the erythrocyte in a process mediated by merozoites

surface proteins (MSPs); (ii) the parasite deform the erythrocyte plasma membrane as it starts to move into the new host; (iii) during which the parasite forms a tight junction with erythrocyte; (iv) with the parasite forming a parasitophorous vacuole bringing in erythrocyte membrane through the action of an actin-myosin motor; (v) with the invasive pore then bonding after the parasite invades and enter the erythrocyte (Weiss et al., 2015) . Heparin is known to inhibit parasite merozoite invasion (as reviewed in chapter 4) by blocking one of these invasion steps. In addition, other sulphated GAGs with invasion inhibitory activities have been identified, including sulphated GAGs such as dextran sulphate (Butcher et al., 1988), curdlan sulphate, carrageenans, fucosylated chondroitin sulphate, K5 polysaccharides, suramin, polyvinyl sulfonate sodium salt, sulphated cyclodextrins, inulin sulphate, xylan sulphate, tragacanth sulphate and scleroglucan sulphate (Table 5.1).

Using heparin as an adjunct therapy is challenging due to its anticoagulation and heparin-induced thrombocytopenia (HIT) activity. Work here on LMWH (chapter 4) has shown some LMWH inhibit parasite growth *in vitro* at high concentration (100µg/ml). This low plasmodial growth inhibition activity requires higher concentrations to meet a useful clinical therapeutic dose. Sevuparin, by contrast, is a low-anticoagulation LMWH that has shown moderately potent *in vitro* invasion blocking activity and has been tested in a clinical trial (Leitgeb et al., 2017), although the efficacy of the inhibitors seems less potent *in vivo* than was perhaps hoped. Previous work has also explored the idea that heparin can be chemically modified to increase the anti-plasmodial effect and reduce its anticoagulation activity (Boyle et al., 2017). These chemical modifications work by modifying the degree of sulphation, or the position of sulphate groups, in the heparin L-iduronic acid-D glucosamine dimers and has been shown to impact on parasite growth inhibition activity and reduce anticoagulation activity (Boyle et al., 2017).

Table 5.1 Diversity of sulphated carbohydrates and heparin mimetics that inhibit parasite growth by blocking merozoite invasion into erythrocyte and/or inhibit parasite cytoadhesion

Compound	Activity	reference
Curdlan sulphate	block merozoite invasion	(Havlik et al., 1994, Evans et al., 1998)
Curdlan sulphate	malaria treatment (Clinical study)	(Havlik et al., 2005)
Carrageenans	inhibit parasite cytoadhesion	(Adams et al., 2005)
Fucosylated chondroitin sulphate	inhibit parasite cytoadhesion and block merozoite invasion	(Bastos et al., 2014)
K5 polysaccharides	block merozoite invasion	(Boyle et al., 2010)
Suramin	inhibit merozoite invasion	Fleck et al., 2003)
Polyvinyl sulfonate sodium salt	inhibit merozoite entry to the erythrocyte	(Kisilevsky et al., 2002)
Inulin sulphate, xylan sulphate, tragacanth sulphate and scleroglucan sulphate	block merozoite invasion	(Boyle et al., 2017)
Sulphated cyclodextrins	inhibit merozoite entry into the erythrocyte	(Crandall et al., 2007)
Sevuparin (LMWH)	Block merozoite invasion, anitcytoadhesion and disturb rosette forming	(Anna M Leitgeb et al., 2017, Saiwaew et al., 2017)

Heparin and other sulphated GAGs have also been identified in several studies to disturb rosettes and inhibit parasite cytoadherence, including; carrageenans (Adams et al., 2005), curdlan sulphate (Havlik et al., 2005; Helen M. Kyriacou et al., 2007), fucosylated chondroitin sulphate (Bastos et al., 2014), a synthetic heparin mimetic PI-88 (Yvonne Adams et al., 2006) as well as the LMWH sevuparin (Saiwaew et al., 2017). The low anticoagulant heparin DFX232 also shows rosette disrupting activity in infected erythrocytes isolated from clinical samples (Leitgeb et al., 2011). Modified heparin, or their mimetics, offer an opportunity to improve chemical inhibition of invasion of erythrocytes – with this anti-plasmodial activity being carefully balanced against any anticoagulant or HIT activity. Modifications of heparin and sulphated GAGs have been reported to inhibit HIV1 and HIV2 virus invasion (Yoshida et al.,

1995) and parallels with this antiviral activity and erythrocyte invasion activity has been recently reviewed (Burns et al, 2019). Chemically modified heparins and depolymerized LMWH derivatives have also been identified to disrupt *P.falciparum* rosette formation as well as having a reduced anti-coagulation activity (Skidmore et al., 2008). The potential for chemically modified heparins is of particular interest as they are already known to inhibit and reverse cytoadhesion to endothelial cells *in vitro* and they have reduced anticoagulation activity as determined in aPTT and PT assays (Mark A Skidmore et al., 2017). Similarly, chemical modification of heparin (although different to those used in the Skidmore et al., 2017 study reported above) as well as a panel of sulphated GAGs were also recently shown to inhibit merozoite invasion into erythrocyte as well as show a reduced anticoagulant activity compared to unfractionated heparin (Boyle et al., 2017).

Due to its anticoagulation/HIT risk, as well as concerns of contamination of this animal (porcine and bovine) material with prions or viruses, heparin has not been taken further in testing for their use as an adjunct therapy. Moreover, contamination of heparin with other sulphated GAGs (chondroitin sulphate) and the resulting adverse clinical effects (hypotension, swelling of the larynx) have been reported and have been identified as a further limitation of the use of heparin (Kishimoto et al., 2008, Viswanathan et al., 2008). An interesting alternative for chemically modified heparin is naturally sulphated GAGs isolated from marine sources (termed here as marine GAGs) these are often isolated from aquatic invertebrate species and provide a unique source of unexploited compounds. Marine GAGs have previously been assessed for their anti-plasmodial and other medicinal activities. For example, fucosylated chondroitin sulphate, isolated from the sea cucumber *Acaudina molpadioides* has anti-inflammatory effects (Hu et al., 2015), a shrimp heparin-like compound isolated from *Litopenaeus vannamei* also has demonstrated anti-inflammatory properties (Brito et al., 2008). Depolymerized fucosylated chondroitin also has a virus invasion blocking effect (Huang et al., 2013), as well as a *P.*

falciparum erythrocyte invasion blocking effect, with similar effects noted for GAGs isolated from other sea cucumber species *Ludwigothurea grisea* and *Isostichopus badionotus*, from the red algae *Botryocladia occidentalis* and from the marine sponge *Desmapsamma anchorata* (Marques et al., 2016; Bastos et al., 2014). The different sulphation levels in carrageenan isolated from seaweeds showed different growth inhibition activities against *P.falciparum*. They consist of three major types kappa (k), lambda (l), and iota (i). These carrageenans inhibit merozoite invasion as well as cytoadhesion of *P.falciparum in vitro* (Adams, Smith, Schwartz-Albiez, & Andrews, 2005), and reduced parasitaemia in mice infected with *Plasmodium berghei in vivo*, although the treatment with carrageenans did not result in the recovery and survival of infected mice (James & Alger., 1981).

Whilst a range of sulphated GAGs from non-mammalian sources have been identified to inhibit parasite growth (see Table 5.1 for examples), a systematic evaluation – particularly when compared to other chemically modified or low molecular weight heparin sources has not. One related study by Boyle et al., (2017), primarily looking at sulphated GAGs (the materials also available for this study) did carry out an evaluation of their effects on growth inhibition, although no differentiation between a merozoite clustering or merozoite invasion phenotype was assessed in that study. Here we take a range of potential heparin mimetics – chemically modified GAGs (including a novel over-sulphated heparin), GAGs from a variety of sources that have been sulphated (sulphated GAG) as well as several naturally sulphated GAGs (and their fractions) isolated from six marine species. This study sets out to provide a systematic evaluation of a range of activities (growth inhibition, anticoagulation, merozoite clustering/invasion) in two distinct parasites NF54^{luc} and Dd2^{luc} strains. The objective being a recommendation of compounds that would warrant further consideration based on their high anti-plasmodial action and low potential anticoagulation risk. Moreover, given that the

merozoite clustering phenotype has only been established for heparin, identification of other GAGs that elicit this phenotype is another objective of this research.

5.2 Results

5.2.1 Sulphated polysaccharides and chemically modified heparin inhibit *P.falciparum* growth *in vitro*

A panel of sulphated glycosaminoglycans, as well as chemically modified heparins, were made available by Dr Mark Skidmore of Keele University. The sulphated glycosaminoglycans available have been provisionally characterised for their *P. falciparum in vitro* growth inhibition effects (Boyle et al., 2017). In this study here the method for analysis (bioluminescence v original flow cytometry), concentrations evaluated (multiple concentrations tested here) and different parasites strains were tested. The same Boyle et al. (2017) study also explored the *P. falciparum in vitro* growth inhibition effects for a range of chemically modified and size-fractionated heparins – here we report a systemic characterisation of sulphation patterns on heparin as well as the inclusion of a novel “over sulphated” chemically modified heparin (CMH9). Therefore, a library of sulphated polysaccharides and chemically modified heparins have been tested for their growth inhibitory against two parasite strains (Dd2^{luc} and NF54^{luc}) over one cycle (48hrs) of growth. Heparin and dextran sulphate were included in each experiment for comparison with compounds as both are potent *in vitro* inhibitors of *P. falciparum* growth. Their effect on growth inhibition was each done at three concentrations (100, 33.3 and 11.1 µg/ml) with their effect normalised against an untreated control (100% growth). The experiments were done as technical triplicates in three biological repeats (n=9). The growth inhibition was determined using a luciferase assay, normalized growth was determined and the mean ± StDev of n=9 of normalized growth (%) plotted (Figure 5.1 and 5.2).

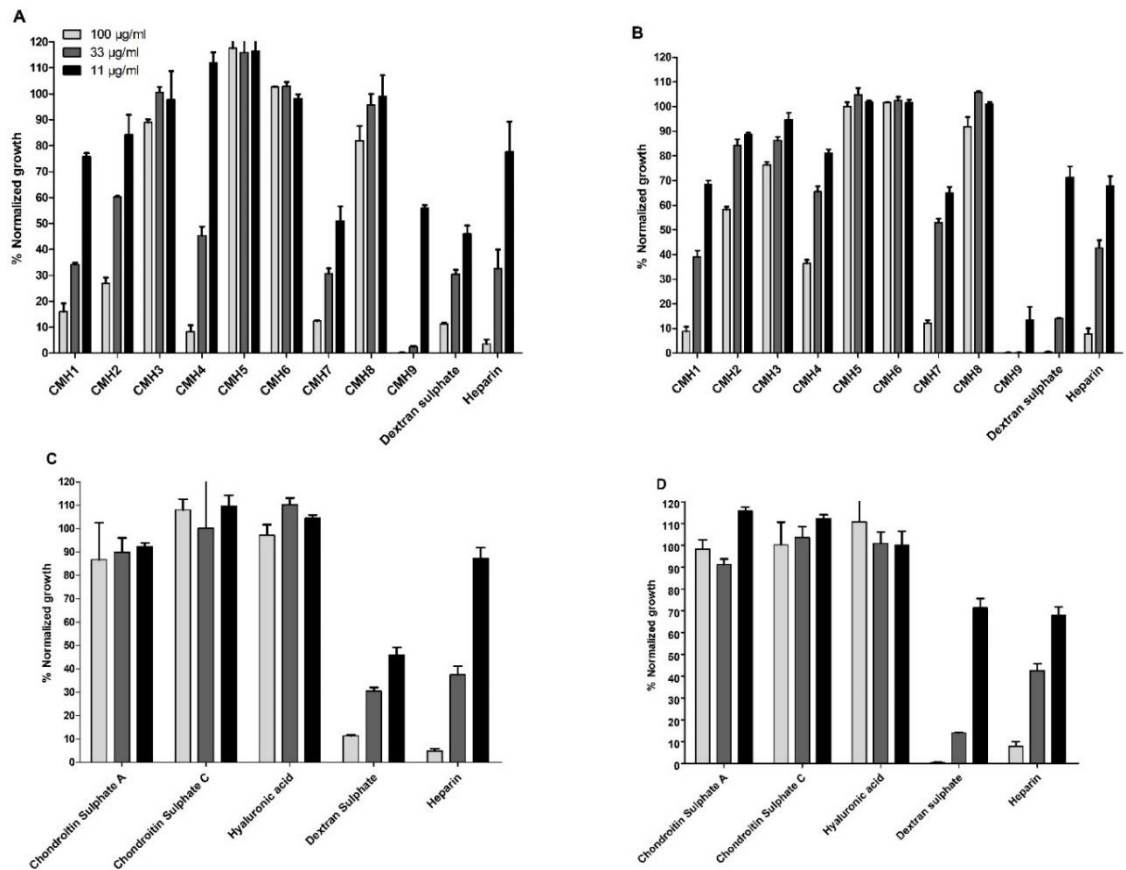


Figure 5.1 Growth inhibition activity of chemically modified heparins and other GAGs. The % normalized growth (compared to untreated control) of the indicated compound/concentration against (see key). (A, C) were done using Dd2^{luc} and (B, D) with NF54^{luc} for a 48 hours incubation. Bars represent mean \pm StDev from n=9 experiments. chemically modified heparin with the following modification: CMH1. Porcine mucosal heparin, CMH2. NAc heparin, CMH3. 2-de-O-S heparin, CMH4. 6-de-O-S heparin, CMH5. 2-de-O-sulfated and N-acetylated, CMH6. 6-de-O-sulfated and N-acetylated, CMH7. 2 and 6 de-O-sulphated and N-sulphated, CMH8. 2 and 6 de-O-sulphated and N-acetylated, CMH9 over sulphated heparin (also I-3 and A-3 sulphated as well as the usual I2S, A6S, NS)

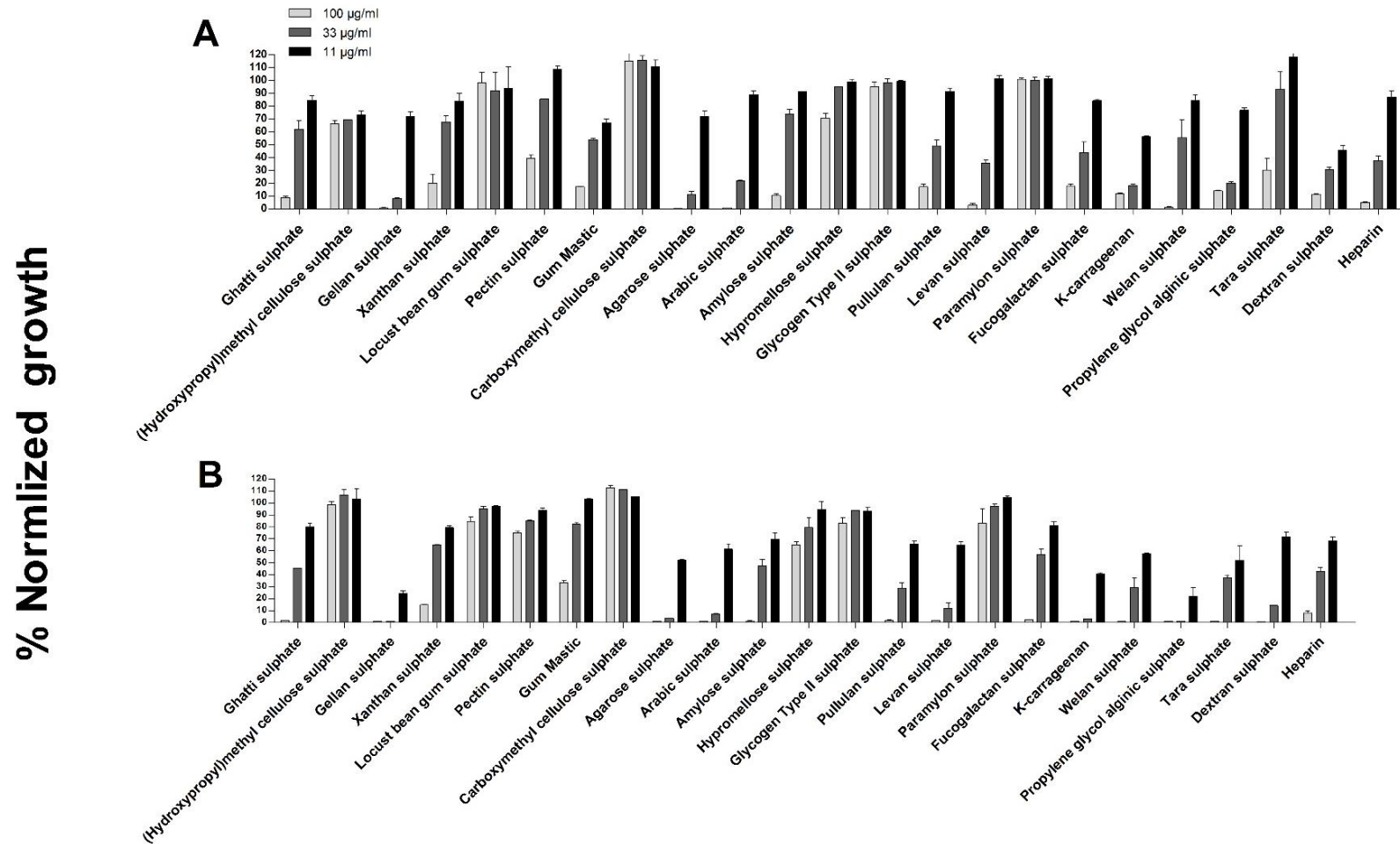


Figure 5.2 Growth inhibition activity of different glycosaminoglycans. The % normalized growth (compared to untreated control) of the indicated compound/concentration against (see key). (A) using Dd2^{luc} and (B) with NF54^{luc} for a 48 hours incubation. Bars represent mean \pm StDev from n=9 experiments.

Some GAGs clearly show a concentration-dependant inhibition in both Dd2^{luc} and NF54^{luc} strains; for example, CMH9, as well as sulphated agarose and gellan sulphate, appear to demonstrate strong inhibition of *in vitro* growth. Comparing the different concentration-effect for these compounds in Dd2^{luc} and NF54^{luc} provides evidence of similarity of action in both strains but also there is a rank order of action for the 37 different compounds tested. In order to compare the action of the same compounds in the two strains as well as construct a rank order of effect, the growth inhibition effect for all compounds at all concentrations in both strains was projected (Figure 5.3) and a Singular Value Decomposition used to provide a principle components analysis of this data. Data for the growth inhibitory effect of LMWHs from the previous chapter were also included in this analysis to compare their activity. This Singular Value Decomposition analysis was performed in Matlab by Professor Peter Andras of Keele University. In this analysis, the first principle component (PC1) accounts for 88.8% of all variation in the data (PC2 accounts for 8.5% of the data and PC3 the final 2.7% of variance) and is taken here as a single value (high values inhibit the strongest) of the concentration-dependant inhibition of growth to provide for a ranking process for the effect of the compounds in the two different strains (Table 5.2) (full table appendix I). Taking the PC1 data for each compound in the two strains tested allows for a linear correlation to be explored to test whether they show an equivalent effect in the two different strains (Figure 5.4). This correlation shows a significant correlation ($r^2=0.78$ and $p<0.001$) with a slope that suggests a 1:1 correlation between the PC1 data for the different compounds in the two strains (slope= 1.03 ± 0.09) suggesting that their activity in inhibiting growth is not strain-specific.

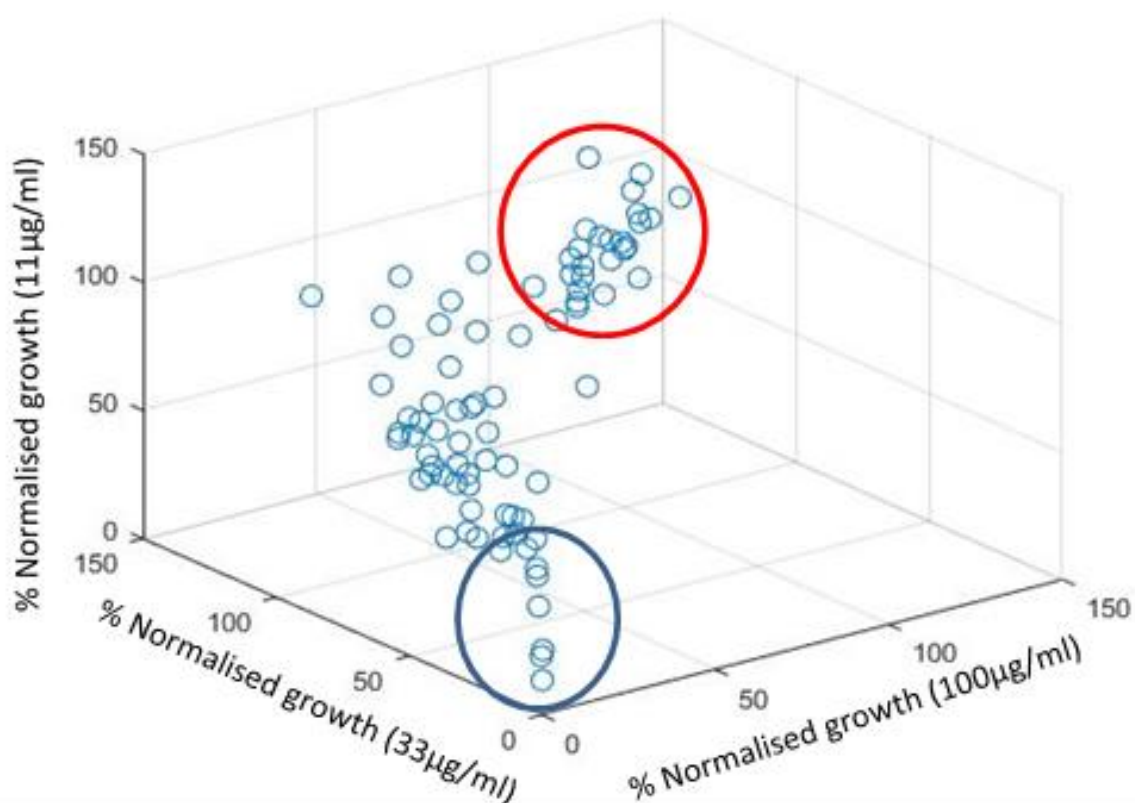


Figure 5.3 Three-dimensional projection of the growth inhibition data for modified heparins and sulphated GAGs. Projection show % normalized growth inhibition for each concentration of compound used. Blue circled compounds/concentrations are inhibition most effectively, whilst those in red are inhibiting less effectively.

Table 5.2 Ranking inhibition activity of compounds according to their PC1 values in Dd2^{Luc} and NF54^{Luc}.

Rank	Strain	Compound	PC1	Strain	Compound	PC1
1	Dd2 ^{Luc}	CMH9	73.2	NF54 ^{Luc}	CMH9	88.9
2	Dd2 ^{Luc}	Gellan sulphate	63.9	NF54 ^{Luc}	Propylene glycol alginic sulphate	84.9
3	Dd2 ^{Luc}	Agarose sulphate	62.3	NF54 ^{Luc}	Gellan sulphate	83.9
4	Dd2 ^{Luc}	K-carrageenan sulphate	55.3	NF54 ^{Luc}	K-carrageenan sulphate	77.5
5	Dd2 ^{Luc}	Dextran sulphate	51.4	NF54 ^{Luc}	Agarose sulphate	73.2

6	Dd2 ^{Luc}	Arabic sulphate	49.8	NF54 ^{Luc}	Arabic sulphate	68.04
7	Dd2 ^{Luc}	CMH7	48.9	NF54 ^{Luc}	Levan sulphate	63.7
8	Dd2 ^{Luc}	Propylene glycol alginic sulphate	45.7	NF54 ^{Luc}	Dextran sulphate	60.6
9	Dd2 ^{Luc}	Heparin	45.07	NF54 ^{Luc}	Tinzaparin	58.9
10	Dd2 ^{Luc}	Levan sulphate	35.8	NF54 ^{Luc}	Welan sulphate	55.6
11	Dd2 ^{Luc}	CMH1	35.8	NF54 ^{Luc}	Pullulan sulphate	52.6
12	Dd2 ^{Luc}	Tinzaparin	33.1	NF54 ^{Luc}	Tara sulphate	52.5
13	Dd2 ^{Luc}	Welan sulphate	30.5	NF54 ^{Luc}	CMH1	40.3
14	Dd2 ^{Luc}	Fucogalactan sulphate	26.0	F54 ^{Luc}	Amylose sulphate	40.2
15	Dd2 ^{Luc}	Gum Mastic	25.9	NF54 ^{Luc}	Heparin	39.8
16	Dd2 ^{Luc}	CMH4	22.3	NF54 ^{Luc}	Ghatti sulphate	37.6
17	Dd2 ^{Luc}	Ghatti sulphate	21.06	NF54 ^{Luc}	Dalteparin	33.8
18	Dd2 ^{Luc}	Pullulan sulphate	20.7	NF54 ^{Luc}	CMH7	30.6
19	Dd2 ^{Luc}	Amylose sulphate	10.2	NF54 ^{Luc}	Fucogalactan sulphate	29.9
20	Dd2 ^{Luc}	Xanthan sulphate	9.8	NF54 ^{Luc}	Reviparin	28.3
21	Dd2 ^{Luc}	CMH2	9.1	NF54 ^{Luc}	Xanthan sulphate	16.6
22	Dd2 ^{Luc}	Dalteparin	-13.6	NF54 ^{Luc}	Enoxaparin	12.7
23	Dd2 ^{Luc}	(Hydroxypropyl)methyl cellulose sulphate	-20.5	NF54 ^{Luc}	CMH4	0.2
24	Dd2 ^{Luc}	Arixtra	-22.9	NF54 ^{Luc}	Arixtra	-10.5
25	Dd2 ^{Luc}	Pectin sulphate	-23.08	NF54 ^{Luc}	Gum Mastic	-15.1
26	Dd2 ^{Luc}	Tara sulphate	-24.4	NF54 ^{Luc}	CMH2	-29.4
27	Dd2 ^{Luc}	Reviparin	-31.05	NF54 ^{Luc}	Hypromellose sulphate	-33.1
28	Dd2 ^{Luc}	Hypromellose sulphate	-48.08	NF54 ^{Luc}	Pectin sulphate	-43.5
29	Dd2 ^{Luc}	Chondroitin Sulphate A	-54.4	NF54 ^{Luc}	CMH3	-45.6

30	Dd2 ^{Luc}	Enoxaparin	-54.4	NF54 ^{Luc}	Glycogen Type II sulphate	-54.6
31	Dd2 ^{Luc}	CMH8	-56.8	NF54 ^{Luc}	Locust Bean gum sulphate	-57.8
32	Dd2 ^{Luc}	Locust Bean gum sulphate	-64.4	NF54 ^{Luc}	Paramylon sulphate	-60.1
33	Dd2 ^{Luc}	CMH3	-64.4	NF54 ^{Luc}	CMH8	-70.8
34	Dd2 ^{Luc}	Glycogen Type II sulphate	-67.6	NF54 ^{Luc}	Chondroitin Sulphate A	-71.3
35	Dd2 ^{Luc}	Paramylon sulphate	-73.8	NF54 ^{Luc}	CMH6	-75.9
36	Dd2 ^{Luc}	CMH6	-75.7	NF54 ^{Luc}	CMH5	-76.2
37	Dd2 ^{Luc}	Hyaluronic acid	-78.5	NF54 ^{Luc}	(Hydroxypropyl)methyl cellulose sulphate	-76.7
38	Dd2 ^{Luc}	Chondroitin Sulphate C	-81.8	NF54 ^{Luc}	Carboxymethyl cellulose sulphate	-90.2
39	Dd2 ^{Luc}	Carboxymethyl cellulose sulphate	-96.7	NF54 ^{Luc}	Chondroitin Sulphate C	-92.8
40	Dd2 ^{Luc}	CMH5	-100.5	NF54 ^{Luc}	Hyaluronic acid	-103.7

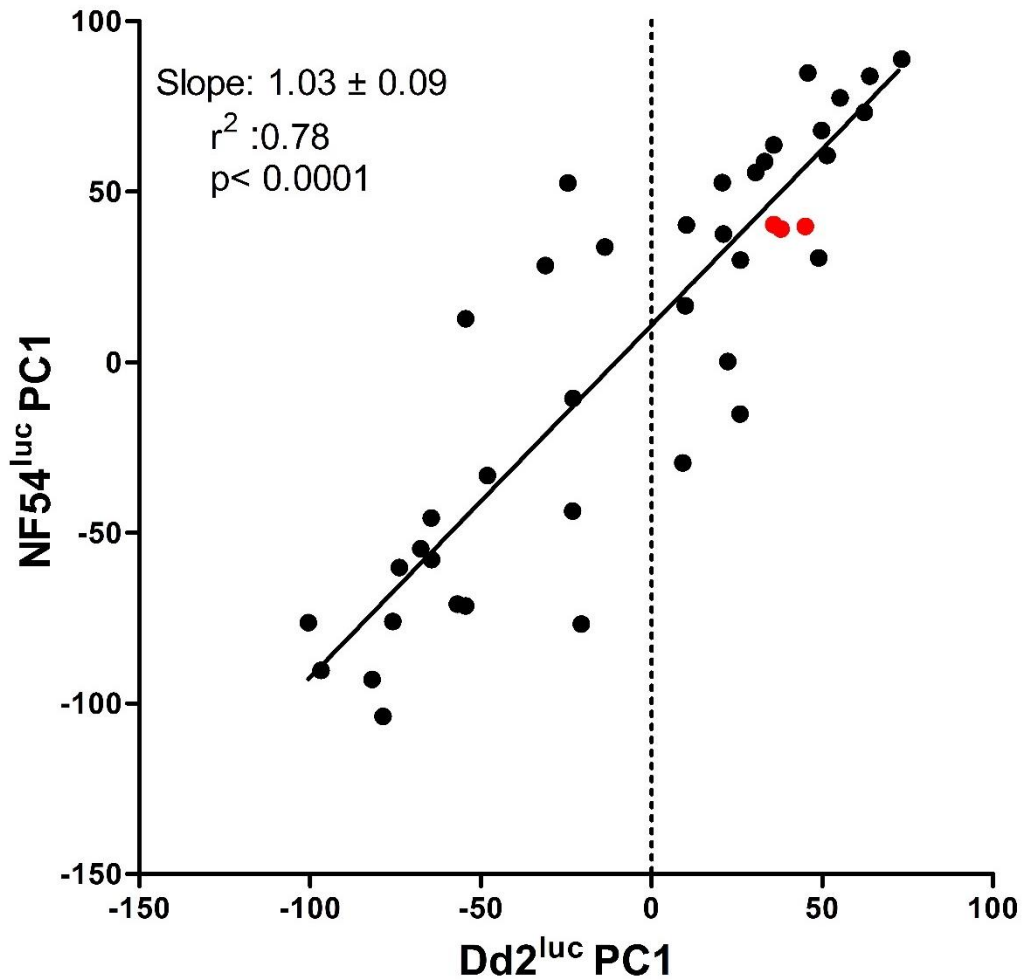


Figure 5.4 Correlation in growth inhibition in Dd2^{luc} and NF54^{luc}. PC1 values for all compounds listed in Table 5.2 are plotted for their effect on the two strains tested. A linear regression of these data is shown. The red symbols show the data for heparin in the different studies performed (heparin is control in all experiments used).

5.2.2 Determination of EC₅₀ for the most potent inhibitors of growth

Analysis of the initial screening data using principal component analysis provides for a ranking of the most potent inhibitory compounds, ie those with the highest PC1 value. Comparing the lists in NF54^{luc} and Dd2^{luc} identifies six compounds that fall in the top eight for both strains. These are the over sulphated heparin CMH9 as well as five sulphated GAGs; gellan sulphate, agarose sulphate, κ -carrageenan sulphate, Arabic sulphate and propylene glycol alginic sulphate. Using serial dilutions (two-fold), a log concentration versus normalised growth plots to allow an EC₅₀ of this growth inhibition were done. NF54^{luc} and Dd2^{luc} at trophozoite stage (2% parasitaemia, 4% HCT) were collected and treated with these six compounds for 48hr. The experiment was performed as technical triplicates with three biological repeats. Parasite growth was normalized against untreated control and mean \pm SD of n=9 of normalized growth (%) plotted (Figure 5.5). Using non-linear regression analyses, the EC₅₀ values in both parasite strains along with their 95% confidence intervals were determined (Table 5.3).

To explore the correlation between the EC₅₀ values for each inhibitor in the two strains, a linear regression analysis was applied between the NF54^{luc} and Dd2^{luc} EC₅₀ data (Figure 5.6). The slope of 0.76 ± 0.09 indicates a near 1:1 correlation between the EC₅₀ values in NF54^{luc} and Dd2^{luc}, again supporting that this inhibitory effect is not strain-dependent. The correlation is strong and significant ($r^2=0.94$, $p<0.0001$). The ranking of these EC₅₀ data agree broadly with the same ranking order determined from the screening data (Figures 5.1 and 5.2) and creates a relative order of growth inhibition of agarose sulphate and CMH9 > κ -carrageenan sulphate and propylene glycol alginic sulphate > gellan sulphate and Arabic sulphate in both NF54^{luc} and Dd2^{luc}.

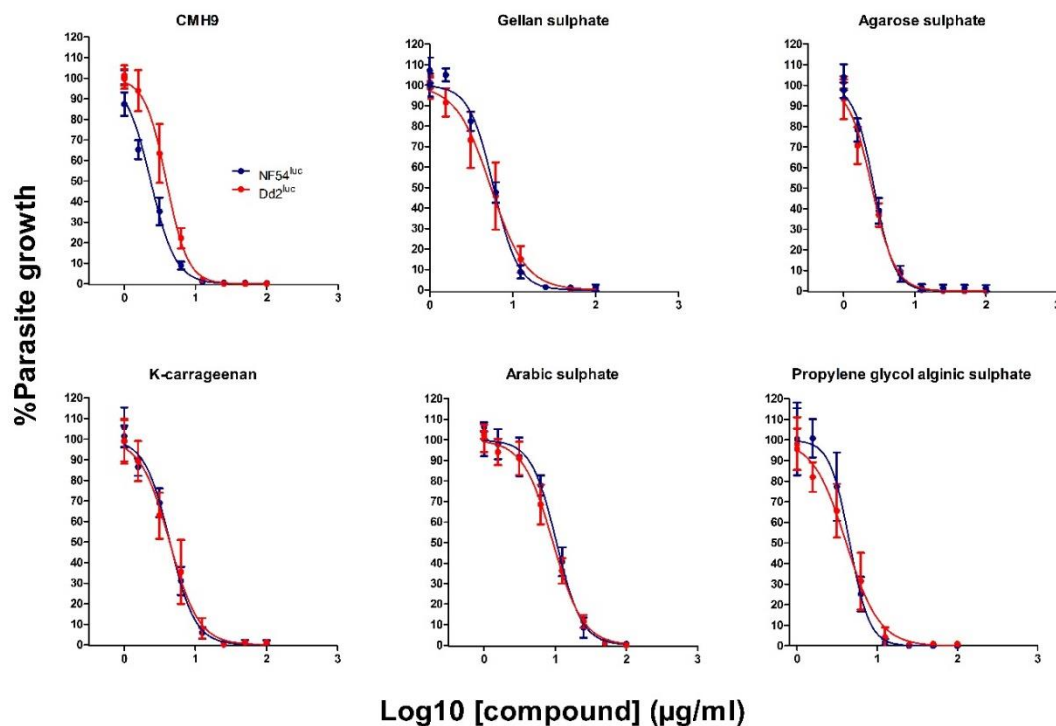


Figure 5.5 Log concentration *versus* normalised growth plots to determine EC₅₀. Log concentration normalized response curves for the chemically modified heparin (CMH9) and sulphated GAGs were determined in Dd2^{luc} (red) and NF54^{luc} (blue). Each point represents the mean and StDev of n=9 data

Table 5.3 EC₅₀ of the growth inhibition effect of CMH9 and the sulphated GAGs in Dd2^{luc} and NF54^{luc}

Compounds	Mean EC ₅₀ (µg/ml) Dd2 ^{luc}	95% CI	Mean EC ₅₀ (µg/ml) NF54 ^{luc}	95% CI
CMH9	3.8	3.6 - 4.0	2.3	2.0 - 2.7
Gellan sulphate	5.4	5.0 - 5.9	5.9	5.2-6.6
Agarose sulphate	2.5	2.1 - 2.8	2.6	2.3 - 2.9
K-carrageenan	4.3	3.9 - 4.7	4.3	3.8 - 5.0
Arabic sulphate	9.2	8.6 - 9.	10.4	9.5 -11.4
Propylene glycol alginate sulphate	4.0	3.6-4.5	4.5	4.3 - 4.6
Heparin (Chapter 4)	5.6	5.2-6.1	9.1	7.3-11.4
Dextran sulphate (Chapter 4)	22.3	18.3-27.1	12.3	10.1-14.4

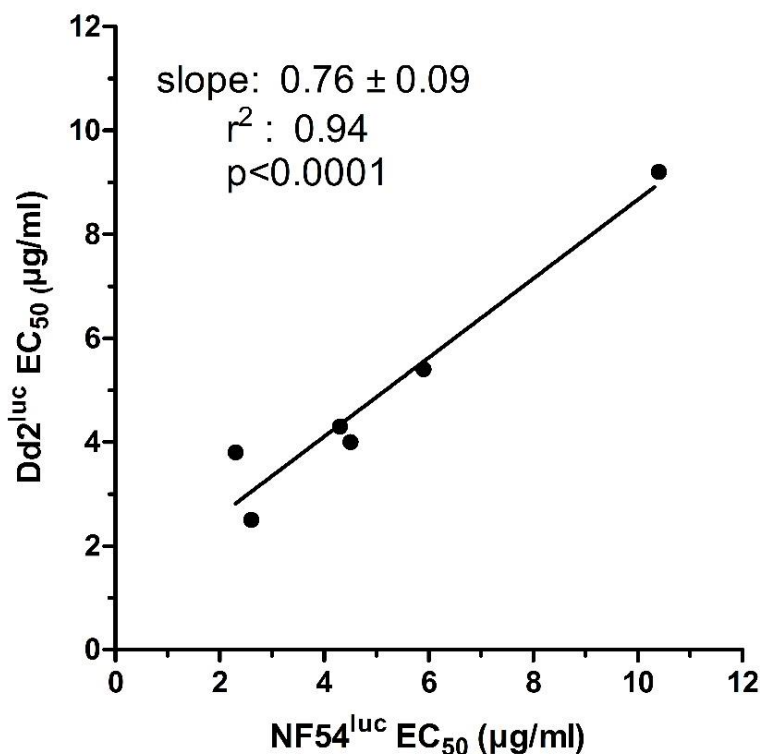


Figure 5.6 Scatterplot exploring the correlation between EC₅₀ of sulphated GAGs and CMH9 EC₅₀ in Dd2^{luc} and NF54^{luc}. The mean EC₅₀ for each compound in Dd2^{luc} and NF54^{luc} are plotted and a linear regression performed.

5.2.3 Exploring the stage-specificity of growth inhibition by CMH9 and sulphated GAGs

We have previously demonstrated in chapter 4 that growth inhibition by LMWH was mediated at the point of merozoite egress and erythrocyte invasion and, like unfractionated heparin, there is no apparent cytotoxic effect during the intraerythrocytic growth. The luciferase growth inhibition assay, done over 6 hours in trophozoites, offers the opportunity to assess cytotoxicity during parasite intraerythrocytic development (Ullah et al., 2017). To monitor this for the library of chemically modified heparins and sulphated GAGs, fourteen compounds were selected (see Figure 5.7) that reflected both highly potent and low potent effect during 48 hrs

of parasite growth and any concentration dependant cidality in the trophozoite stage tested. Compounds were incubated with trophozoite stage parasite (Dd2^{luc} or NF54^{luc}) in a three-fold series dilution of inhibitors (100, 33.3 and 11.1 μ g/ml) and incubated with the parasite for 6hr. Growth inhibition using luciferase-based assay was determined for three technical and biological repeats (n=9). The rapidly acting chloroquine was added at a super-lethal concentration (10 μ M) to demonstrate trophozoite cidality. Parasite growth was normalized against an untreated control and mean \pm SD of n=9 of normalized growth (%) plotted (Figure 5.7).

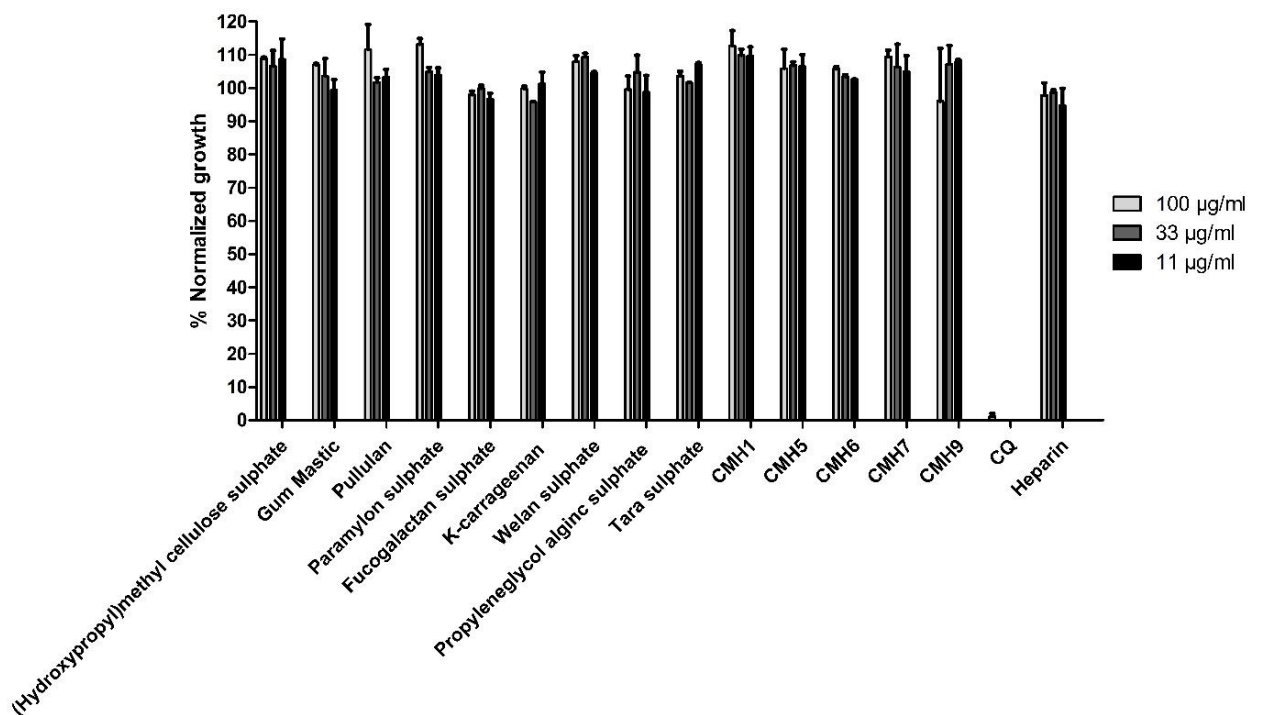


Figure 5.7 Demonstrating the apparent absence of a cytotoxic effect of chemically modified heparins and sulphated GAGs against the trophozoite intraerythrocytic stage. Bars represent mean \pm StDev from n=9 determinations of luciferase activity compared to untreated control. The key shows the three different concentrations used. CQ is chloroquine at 10 μ M concentration.

As expected, all the sulphated GAGs and chemically modified heparins, irrespective of whether they have potent or lack anti-plasmodial growth inhibition activity all show no apparent cytocidal activity against trophozoite stage parasites over 6 hrs. The next step was to establish whether the inhibitory effect is mediated at the level of erythrocyte rupture, merozoite release and reinvasion. Inhibition at this stage is typically assessed by exposing a synchronised schizont stage culture to the inhibitors and culturing for 18 hrs. The rupture/reinvasion inhibition effect is determined by a microscopic examination of a Giemsa stained thin smear to observe newly established ring stage infections. The same approach used in chapter 4 to assess the percentage of invasion inhibition was used here. Dd2^{luc} and NF54^{luc} schizont stage cultures were exposed to 100 or 11.1µg/ml of heparin (known control), CMH9, the sulphated GAGs as well as (hydroxypropyl) methylcellulose. The latter compound having been shown earlier to have no growth inhibitory effect at 100µg/ml (Figure 5.2). The mean and StDev of the normalised invasion inhibition from three biological repeats (n=3) for each concentration of each compound were plotted (Figure 5.8).

Comparison of the data from NF54^{luc} and Dd2^{luc} appears to show a similar concentration-dependent invasion blocking effect in these two parasite strains. As we expect, heparin shows an almost complete blocking of invasion at 100µg/ml, with high levels of inhibition still apparent at 11.1µg/ml – an observation that agrees with the same control when used in chapter 4. Similarly, we see no inhibitory effect from (hydroxypropyl) methyl cellulose with ring-stage cultures comparable to untreated controls. CMH9 and the sulphated GAGs all showed a complete 100% blocking effect at 100µg/ml with some variation in this effect apparent at 11.1µg/ml. These variations in effect suggest a rank order of invasion inhibition of agarose sulphate and CMH9 > propylene glycol alginate sulphate > κ-carrageenan sulphate > gellan sulphate and Arabic sulphate in both NF54^{luc} and Dd2^{luc} – a rank order almost identical to their 48hr growth inhibitory effect (Section 5.2.2).

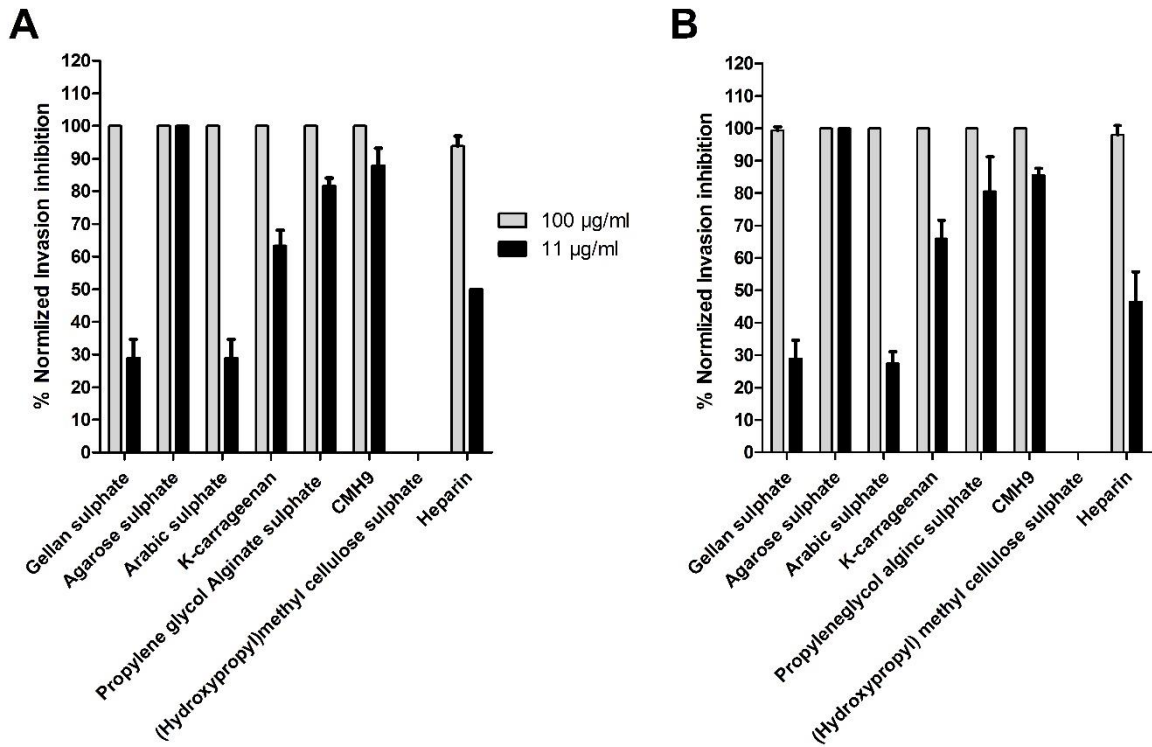


Figure 5.8 Assessing the effect of CMH9 and sulphated GAGs in blocking the reinvasion of erythrocytes. The mean \pm StDev (n=3) of the normalized invasion inhibition (compared to untreated control) for the indicated concentration (see key)/compound in (A) NF54^{luc} and (B) Dd2^{luc}.

To explore the similarity in compound activity in the two strains, a linear regression analysis of the normalised invasion inhibition data for 11.1µg/ml in both NF54^{luc} and Dd2^{luc} were plotted and a linear regression done (Figure 5.9). Only the 11.1µg/ml data was used as the data for 100µg/ml was typically 100% and showed little useful variance for this analysis. A strong linear correlation was found ($r^2=0.99$ and $p < 0.0001$) with a slope of 0.99 ± 0.02 , again indicating that the invasion blocking effect appears non-strain independent.

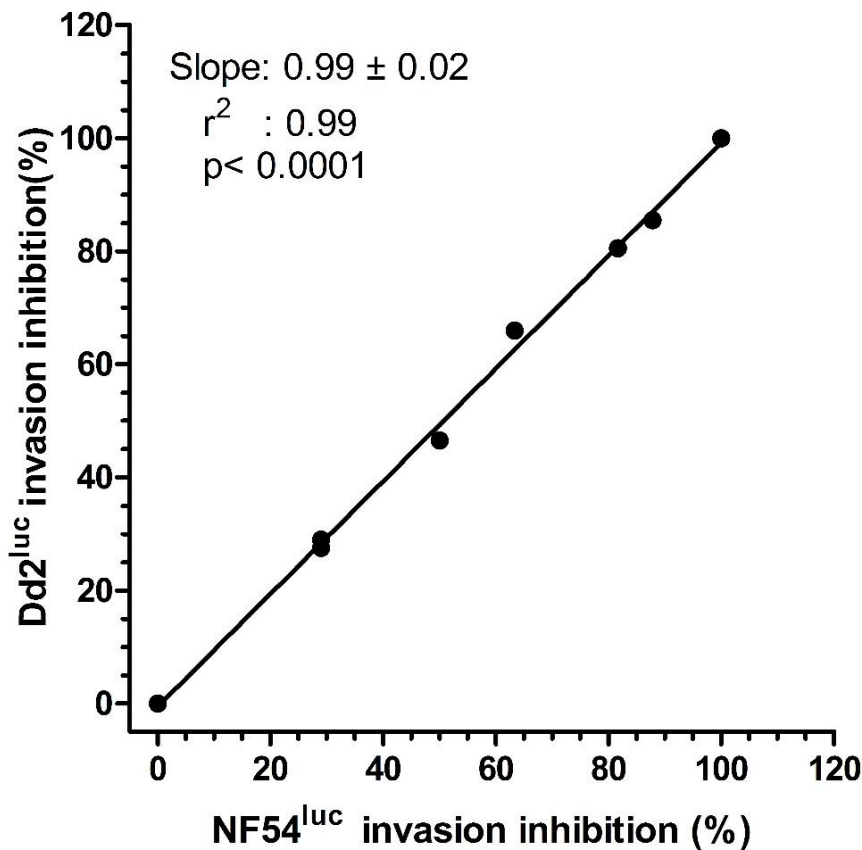


Figure 5.9 Scatterplot correlations of inhibition of erythrocyte reinvasion by CMH9 and sulphated GAGs in Dd2^{luc} and NF54^{luc}. The inhibition of erythrocyte reinvasion for each compound at 11.1µg/ml in Dd2^{luc} and NF54^{luc} have been plotted and a linear regression performed.

In chapter four, we investigated the effect of LMWH, dextran sulphate and heparin on schizont rupture – showing that only heparin has an effect on schizont rupture and described the formation of the clustered merozoite phenotype (Glushakova et al., 2017). Here we investigated if the highly potent inhibitors of 48hr growth and erythrocyte reinvasion (CMH9 and the 5 sulphated GAGs) were similarly capable of forming the clustered merozoites like heparin or if there was an absence of these clustered merozoites as seen with dextran sulphate. Agarose sulphate, gellan sulphate, propylene glycol alginic sulphate, κ-carrageenan, Arabic sulphate and

CMH9 were tested. In addition, two compounds that show no apparent growth inhibitory effect, CMH6 and chondroitin sulphate C (CSC) were tested here. As with the protocol described in chapter 4, the count of parasite phenotypes observed over three time points was done – and it is important to note that this data represents the proportion of the different stages (ring, trophozoites, schizonts and clustered merozoites) observed and not their absolute frequency (this being determined using the ring stage assay). Samples were harvested from a 2% schizont (4% haematocrit) culture treated with 100µg/ml of each inhibitor with an untreated control for comparison. At 18hrs, 24 hrs and 48hrs, samples were removed and the proportion of each major intraerythrocytic stage (ring, trophozoite and schizont) as well as what are described here as “clustered merozoites” determined from counts of 100 infected erythrocytes. As before, the merozoite cluster was defined as an erythrocyte sized stained parasite material, which does not appear retained within an erythrocyte membrane, which is still associated with a darkly stained vesicle (the parasite food vacuole presumably trapped with the clustered merozoite) (Figure 5.10 and 5.11). This observation is consistent with the activity of heparin and other strong GAGs inhibitors in both inhibiting infected erythrocyte rupture as well as the dispersal of merozoites. The experiment was conducted as three independent biological repeats, with the mean and StDev of the proportion of these four morphological stages plotted (Figure 5.12).

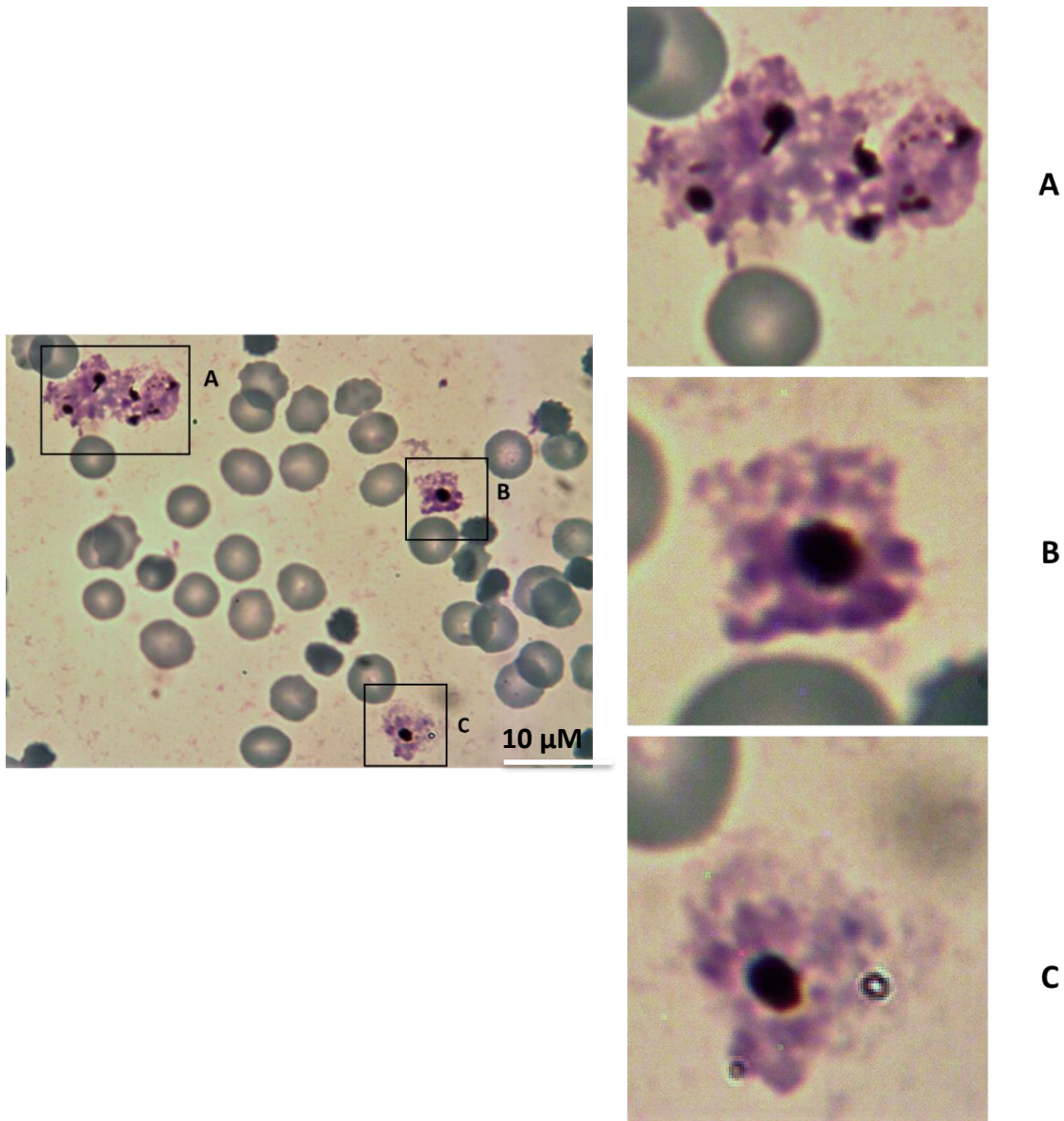
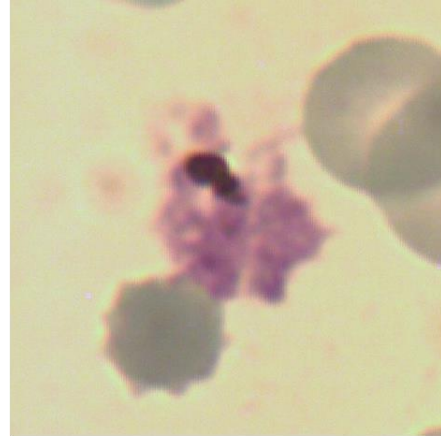
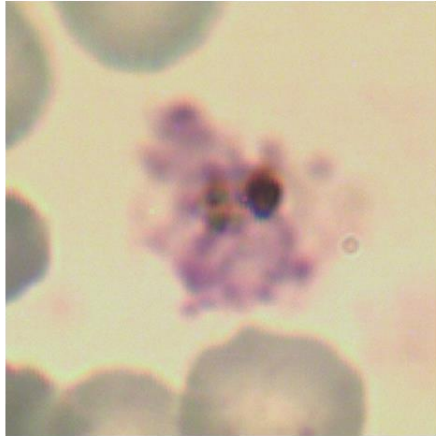


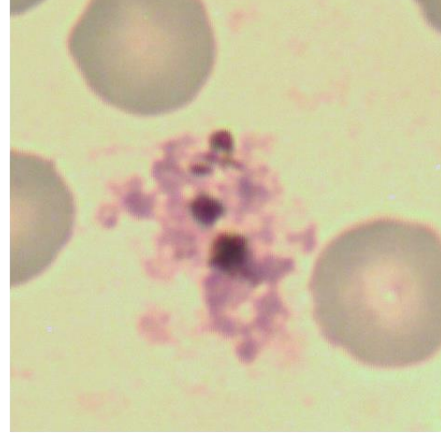
Figure 5.10. Example images representing the clustered merozoite phenotype. The photograph of a gellan sulphate (100 μ g/ml) treated NF54^{luc} culture as a Giemsa-stained thin smear observed by light microscopy under 100x magnification. **A B** and **C** represent close-up images of an erythrocyte sized stained parasite material, which does not appear retained within an erythrocyte membrane, which is still associated with a darkly stained vesicle – defined here as a merozoite cluster.

Figure 5.11 (next two pages) Representative examples of clustered merozoites from NF54^{luc} exposed to CMH9 and sulphated GAGs. Photographs of Giemsa-stained thin smears taken by light microscope under 100x magnification. **(A-H)** represent clustered merozoites observed on treatment with agarose sulphate, gellan sulphate, propylene glycol alginic sulphate, κ -carrageenan, Arabic sulphate, CMH9, unfractionated heparin and a mature schizont from untreated control.

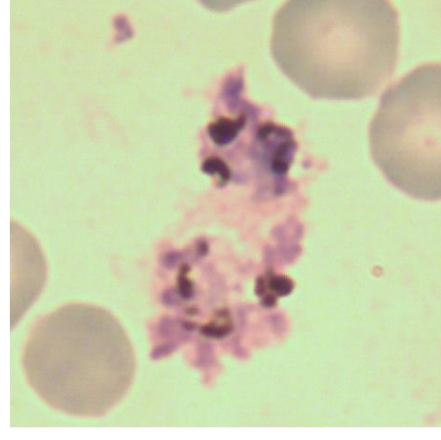
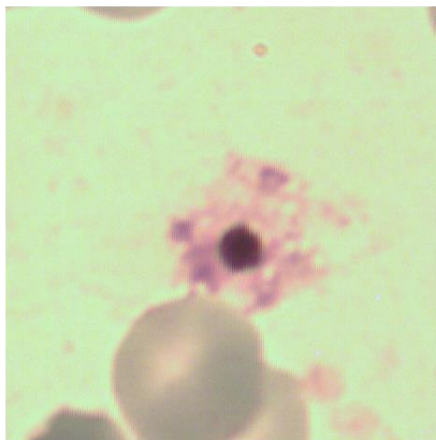
A



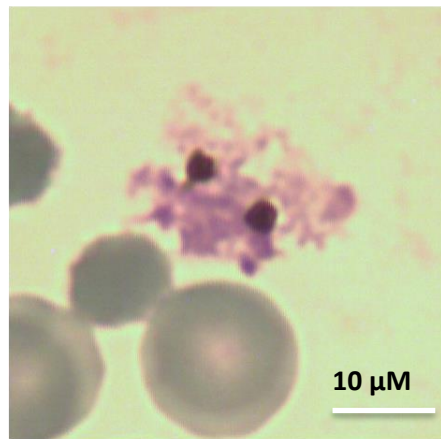
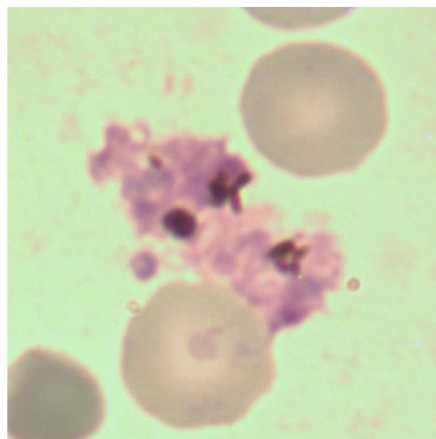
B



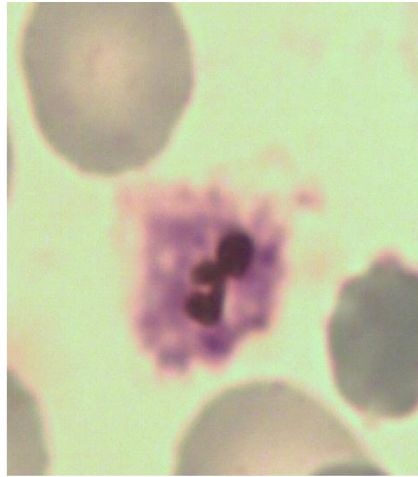
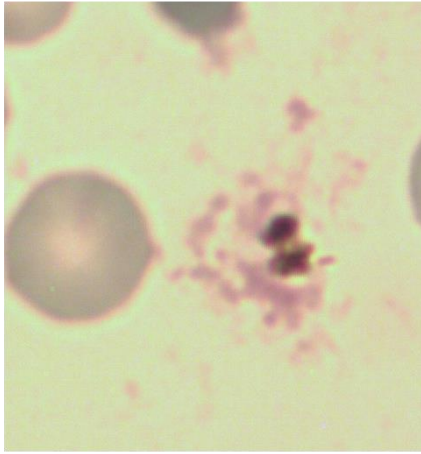
C



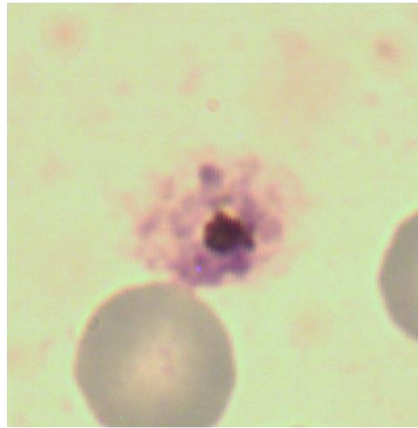
D



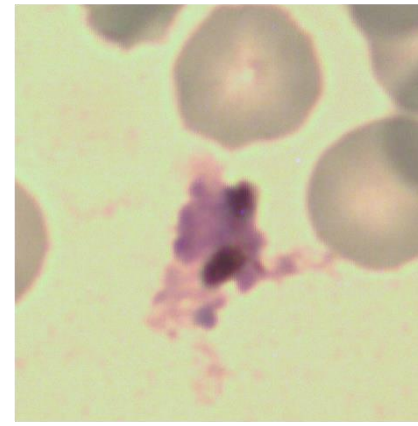
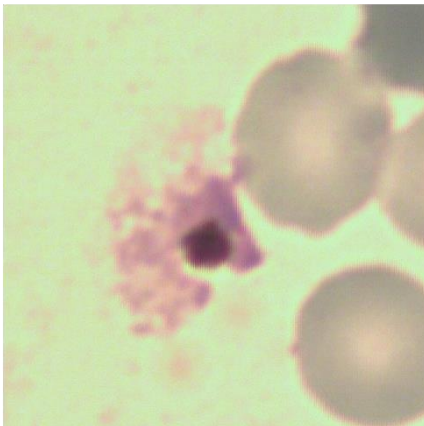
E



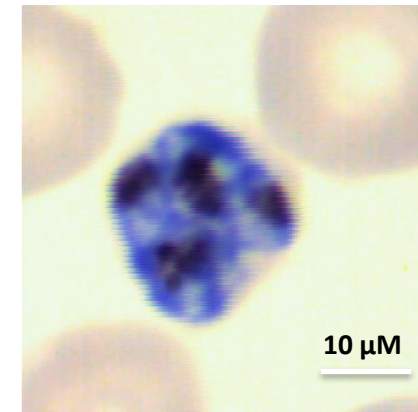
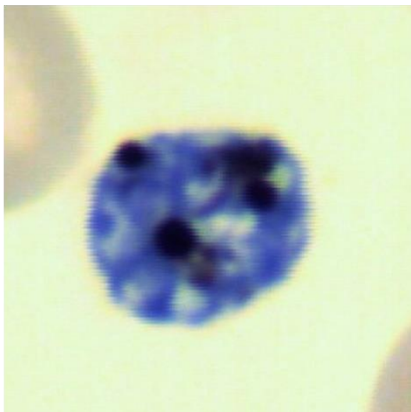
F



G



H



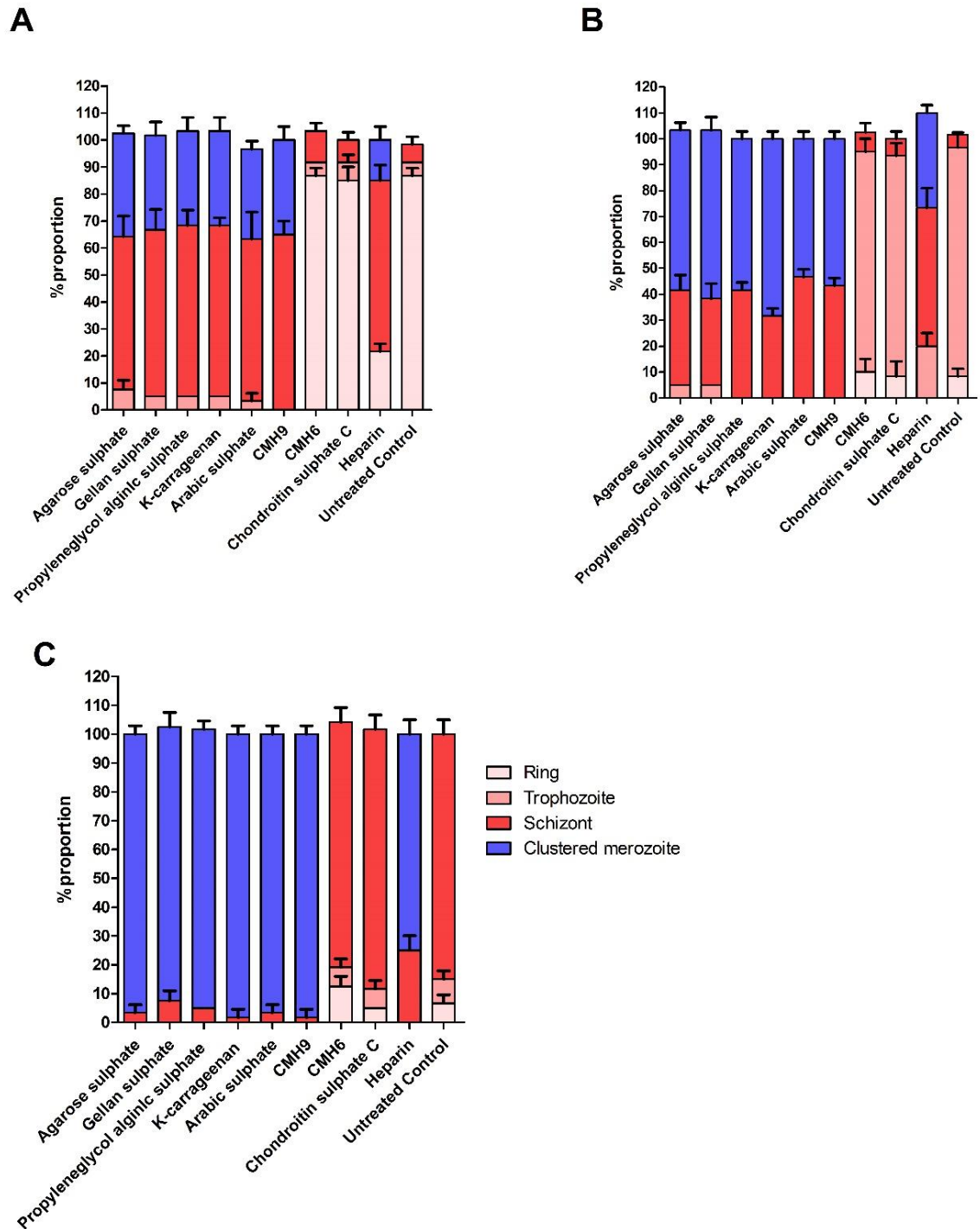


Figure 5.12 Morphological staging following treatment with CMH9 and sulphated GAGs. The mean proportion \pm StDev of each of the main intraerythrocytic stage or clustered merozoite is represented (see key). These proportions are based on the counts of 100 NF54^{luc} infected erythrocytes/clustered merozoites from three independent experiments. Morphological changes were monitored over (A) 18 hr, (B) 24 hr and (C) 48 hr.

All the potent inhibitors were taken forward show a time-dependent effect in the development of the clustered merozoite phenotype – suggesting that their growth inhibition and erythrocyte reinvasion blocking effect is most likely a result of the inhibition of the dispersal of free merozoites for reinvasion. This phenotype was described previously for heparin by Glushakova et al., (2017), and is now shown here for over sulphated heparin and five sulphated GAGs. In Figure 5.12, the effect of heparin, as previously reported in chapter 4, was repeated here. there is a delay in schizont rupture, with the relative frequency of observed merozoite clusters increasing over the next 30 hrs. The untreated control shows the expected progression in morphological staging over time, with compounds that show little effect in growth inhibition (CMH6 and CSC) showing no apparent effect on parasite morphology (ie appear the same as the untreated control). All six of the potent inhibitors taken show an inhibitory effect greater than that of heparin – more merozoite clusters are observed and they are observed at higher levels than earlier (Figure 5.12)

After showing that all six compounds apparently inhibit parasite growth by blocking merozoite release, we next set out to demonstrate if there is a concentration dependence to this effect. The same method described above was used to test the effect of these compound, highly synchronized NF54^{luc} and Dd2^{luc} parasites of schizont stage treated with three different concentrations (100, 50, and 25 µg/ml) of agarose sulphate, gellan sulphate, propylene glycol alginic sulphate, κ-carrageenan, Arabic sulphate and CMH9. The same unfractionated heparin, CMH6 and CSC controls were also tested. The effect of these inhibitors was monitored after 48 hr of incubation, a thin smear being Giemsa stained for treated and a count of the different morphological changes (clustered merozoites) and schizonts parasite stages for 100 infected cells done. An untreated parasite was also included, with the experiment done as three independent biological repeats (n=3), with the mean and StDev of the proportion of these four morphological stages plotted (Figure 5.13).

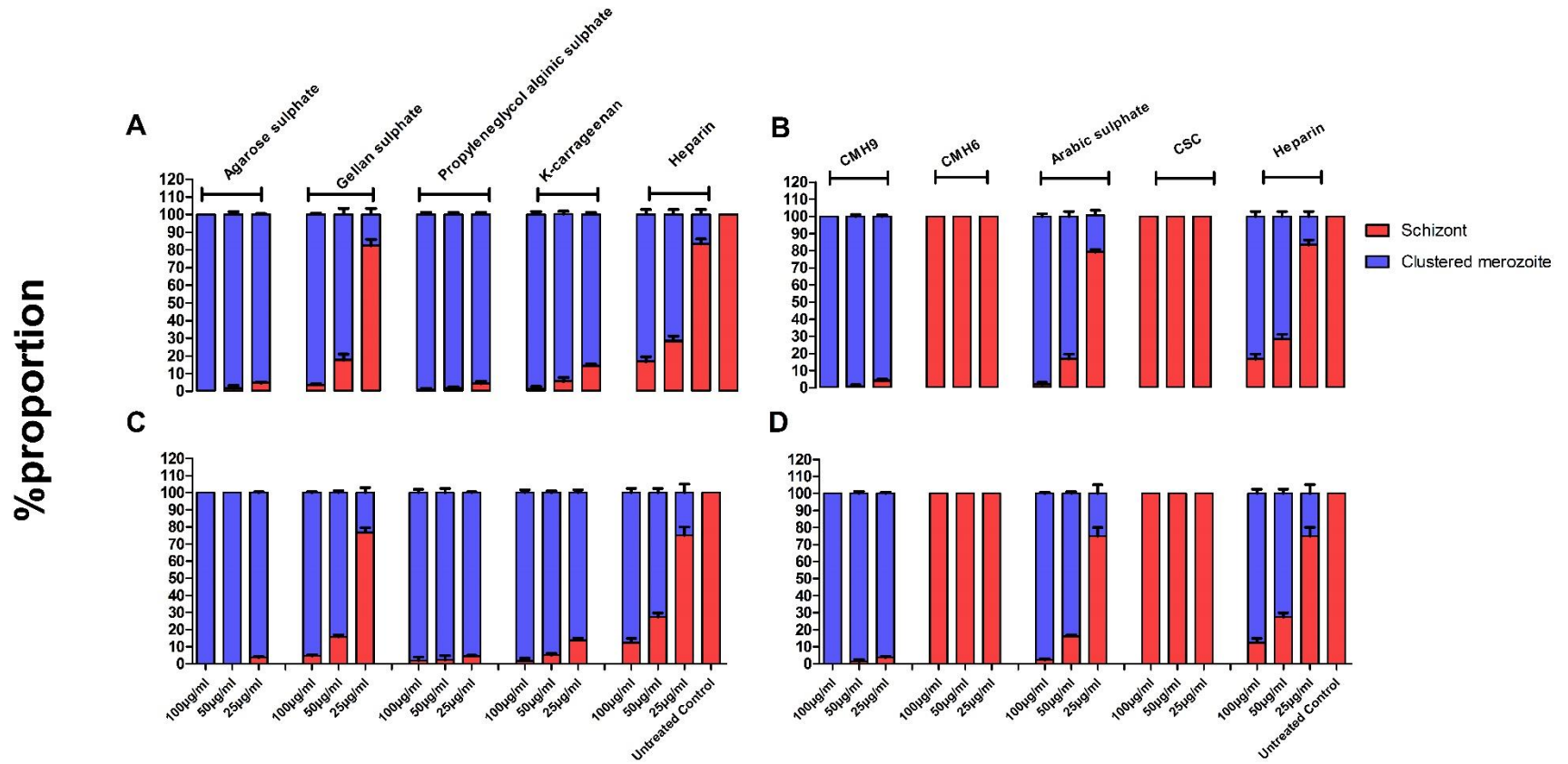


Figure 5.13 Concentration-dependent clustered merozoite formation by CMH9 and sulphated GAGs. The mean proportion \pm StDev of each of the main intraerythrocytic stage or clustered merozoite is represented (see key). These proportions are based on the counts of 100 of Dd2^{luc} (A-B) and NF4^{luc} (C-D) infected erythrocytes/clustered merozoites from three independent experiments. CSC, chondroitin sulphate C.

The control experiments worked as expected. Untreated samples consist entirely of schizont stages after 48hr of growth. CMH6 and CSC show no apparent effect on growth and share the same exclusive schizont morphology. Heparin shows a concentration-dependent effect, this had been suggested from the work in chapter 4 (100 and 300 $\mu\text{g/ml}$) but is clearly shown here in both NF54^{luc} and Dd2^{luc} parasite cultures. The relative proportion of clustered merozoites show that there is a similar concentration-dependent effect for agarose sulphate, gellan sulphate, propylene glycol alginic sulphate, κ -carrageenan, Arabic sulphate and CMH9 in both NF54^{luc} and Dd2^{luc} parasites. Interestingly, the relative proportions suggest the more potent inhibitors such as agarose sulphate, propylene glycol alginic sulphate, κ -carrageenan and CMH9 have a more potent concentration-dependent effect than do Arabic sulphate and gellan sulphate. These latter two compounds have a growth inhibitory EC_{50} similar to, or greater than, that of the unfractionated heparin, with all the other four compounds having a growth inhibitory EC_{50} less than heparin.

5.2.4 Assessing the anticoagulation activity of CMH9 and sulphated GAGs

Given the known issues associated with heparin's anticoagulant activity, an evaluation of the anticoagulant activity in these six leading candidates was determined. The clotting time of these compounds was measured using activated partial thromboplastin time (aPTT) and prothrombin time (PT). Briefly, PT is used to evaluate the effect the extrinsic clotting pathway, whereas the aPTT instead reports on the effect on the intrinsic clotting pathway. In these assays, human plasma was incubated at 37°C with two-fold dilution (starting with 100 $\mu\text{g/ml}$) of the compound being tested as well as the appropriate aPTT and PT assay substrate. All anticoagulation activity in both tests were compared to heparin (with a known anticoagulant activity) and dextran sulphate (no known anticoagulant activity). The experiment was conducted as three biological

repeats (n=3) with the mean \pm stdev of the clotting times being plotted against the concentration of the compound tested (Figure 5.14). Separate aPTT and PT data (appendix ii)

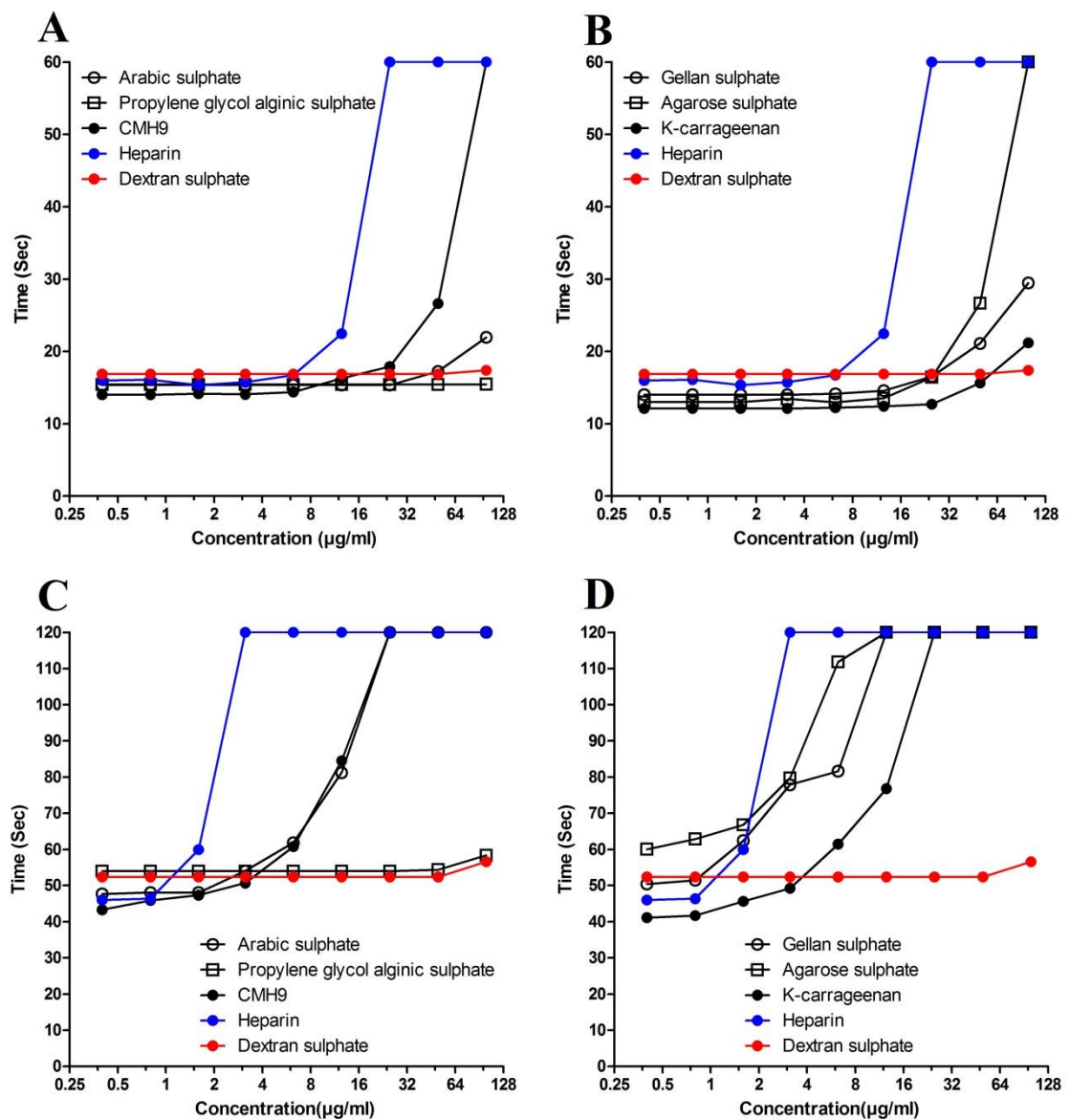


Figure 5.14 Assessing the anticoagulation activity of CMH9 and sulphated GAGs. Each data point represents mean (n=3) biological repeats. All anticoagulation activity of inhibitors (see key) was compared to heparin (blue) and dextran sulphate (red). (A and B) PT determined up to 60 seconds of incubation and (C and D) aPTT for up to 120 seconds.

The normal clotting time of untreated human plasma in a PT assay is 14-18 second and for an aPTT it is 40-60 seconds, depending on temperature, source of human serum/reagents. In the absence of an anticoagulant activity for an added compound, this clotting time for human serum remains unchanged. This is clearly seen for dextran sulphate which has no anticoagulant activity. The anticoagulant activity of heparin is evident in the PT assay at or about 25 μ g/ml as the sample does not clot within 60 sec. Similarly, for the aPTT assay, the anticoagulant activity at or about 3 μ g/ml prevents clotting within 120 sec. Analysis of the anticoagulation activity of all six inhibitors was reduced compared to heparin in both the PT and aPTT assays. The compounds with the highest anticoagulation activity were CMH9 (four-fold reduction compared to heparin in PT assay and 8-fold reduction in aPTT) and agarose sulphate (four-fold reduction compared to heparin in both aPTT and PT assays). With regards to the extrinsic pathway tested in the PT assay, all the remaining compounds showed at least an 8 fold reduction in anticoagulation activity compared to heparin, and in the case of Arabic sulphate, propylene glycol alginic sulphate and κ -carrageenan, these compounds are much more similar to dextran sulphate in the concentrations tested here. Similarly, for the aPTT assay of the intrinsic pathway, all the remaining compounds showed at least 8-16 fold reduction in activity compared to heparin. Of note, propylene glycol alginic sulphate was again more similar to dextran sulphate. What is of particular note here is that whilst for the majority of compounds tested here, they would show some anticoagulation activity within 2-4 fold of their EC₅₀ values, propylene glycol alginic sulphate would not with assays here showing that addition of 25 times their EC₅₀ concentration does not result in any appreciable detection of anticoagulation activity.

5.2.5 Initial evaluation of the anti-plasmodial activity of marine-derived glycosaminoglycans

Several opportunities to develop new sources of antimalarial drugs to tackle emerging *P.falciparum* antimalarial resistance are underway (Klein., 2013). Whilst this chapter has so far explored chemically modified heparins and sulphated GAGs, the following section explores the potential anti-plasmodial activity of GAGs isolated from a range of marine sources outlined in Table 5.4. These materials were isolated and provided for this work by a PhD student Courtney Mycroft-West from Dr Skidmore's team at Keele University. Their potential activity was tested here as (i) they represent a potentially valuable waste product from these easily available foodstuff marine species, (ii) are novel as whilst some marine GAGs have been tested previously for their anti-plasmodial activity (Marques et al., 2016), these have not and (iii) are already sulphated and do not need to be chemically modified prior to their testing in *P. falciparum*.

Table 5.4 Marine GAGs tested in this study

Polysaccharides common name	Species name
Crab	<i>Portunus pelagicus</i>
Scallop	<i>Placopecten magellanicus</i>
Squid	<i>Loligo opalescens</i>
Prawn	<i>Penaeus vannamei</i>
Salmon	<i>Oncorhynchus gorbuscha</i>
Pilchard	<i>Sardina pilchardus</i>

Crude (non-fractionated) GAGs from each of the six species were provided as an aqueous solution at a concentration of 10 mg/ml, incubated with NF43^{luc} parasite at three concentrations (100, 33.3 and 11.1 µg/ml) with unfractionated heparin at same concentration included as a known control for growth inhibition over 48hr. Growth inhibition was determined and normalised against an untreated control (100% growth). The experiments were done as technical triplicates in three biological repeats (n=9) with the mean ± StDev of n=9 of normalized growth (%) plotted (Figure 5.15).

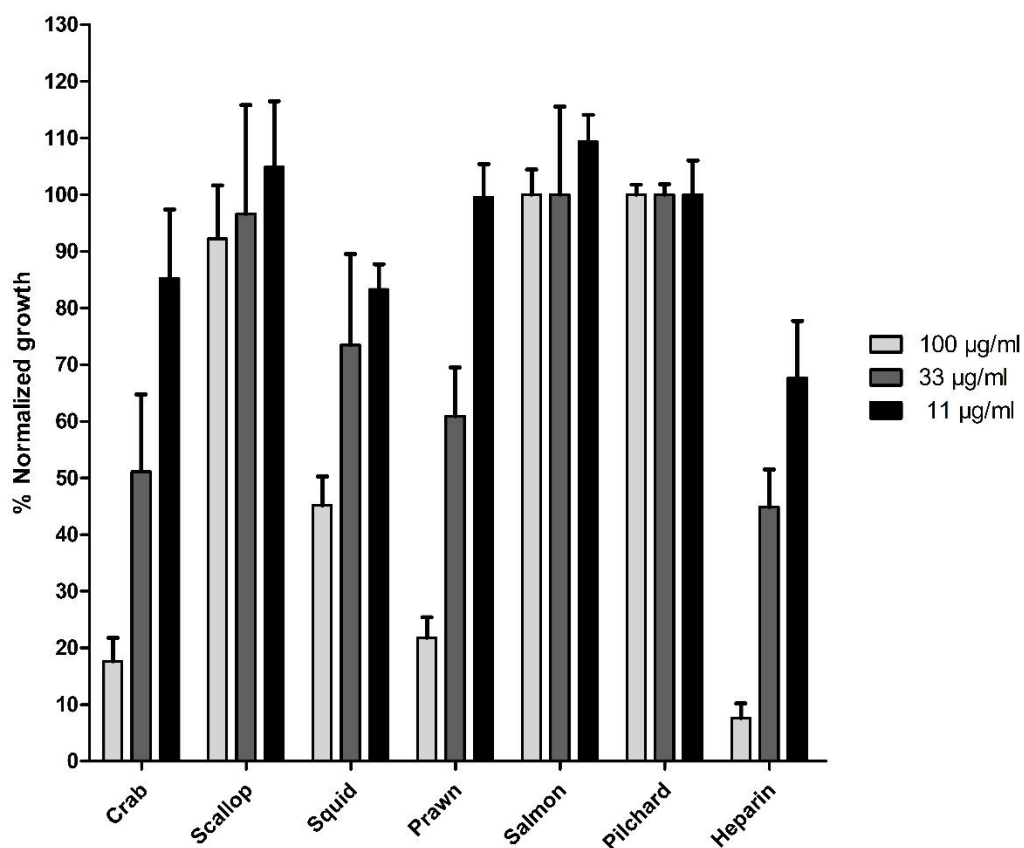


Figure 5.15 Growth inhibition of crude GAGs isolated from marine sources. The % normalized growth (compared to an untreated control) of the indicated compound/concentration (see key) against NF54^{luc} strain after 48 hours incubation is shown. Bars represent errors of mean ± StDev from n=9 experiments.

Whilst none of the marine GAG crude extracts were as active as heparin, three of them (Crab, Prawn and Squid) showed some concentration-dependent activity, with the remaining not showing any activity below 100µg/ml. The three crude marine GAGs samples were fractionated by a charge on an ion-exchange column by Courtney Mycroft-West and three to four fractions of each provided for the second round of anti-plasmodial action testing. These fractionated marine GAGs were tested for their growth inhibition following the same method used above, tested at three concentrations (100, 33.3 and 11.1 µg/ml), in NF54^{luc} parasite and for 48 hrs. Growth inhibition determined and normalised against an untreated control (100% growth). The experiments were conducted as technical triplicates in three biological repeats (n=9) with the mean ± StDev of n=9 of normalized growth (%) plotted (Figure 5.15).

Most of the fractions (F) showed no improvement in activity when compared to the crude samples (Figure 5.15). Only Prawn F5, Crab F3 and Crab F4 showed an apparent increase in anti-plasmodial activity compared to the original samples – and in all cases, there is >80% of growth inhibition at 100 µg/ml. To confirm this initial screening data, and provide an EC₅₀ concentration of this effect, these three fractions were taken forward for a full concentration-inhibition assay. NF54^{luc} strain parasites at trophozoite stage (2% parasitaemia, 4% HCT) were collected and incubated with two-fold of serial dilution of fractionated mGAGs of (prawn F5, crab F3 and crab F4) for 48hr. Based on the screening data, initial concentrations of 100µg/ml were used for the marine GAG fractions. The experiment was carried out as technical triplicates with three biological repeats. Parasite growth was normalized against untreated control and the mean ± SD of n=9 of normalized growth (%) plotted (Figure 5.17). Using a non-linear regression tool, these graphs were used to determine the EC₅₀ values along with their 95% confidence intervals (Table 5.5).

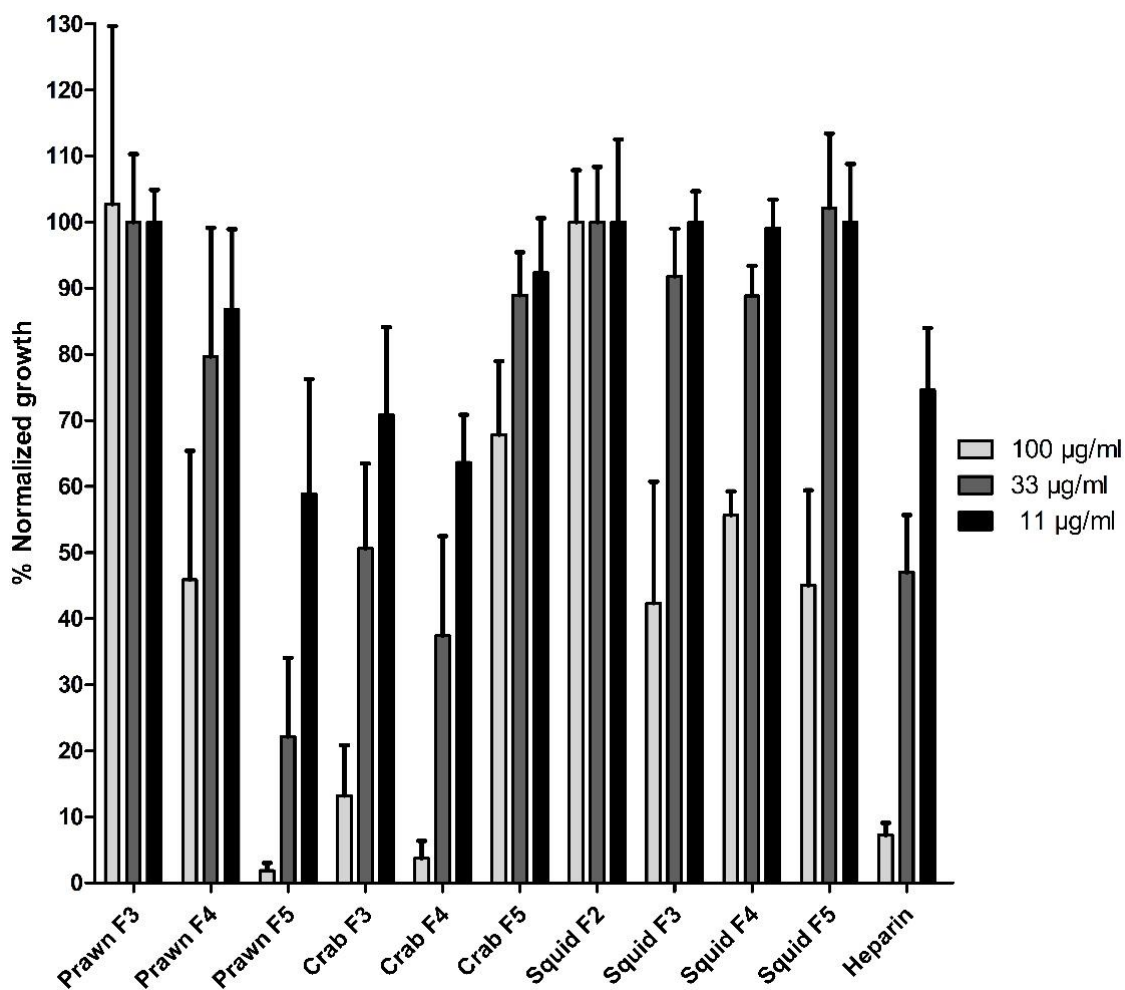


Figure 5.16 Growth inhibition activities of marine GAG fractions. The % normalized growth (compared to untreated control) of the indicated compound/concentration (see key) at 48hrs in NF54^{luc} when exposed to the indicated concentration of compound. Bars represent mean \pm StDev from n=3 biological repeats. F is referring to the fraction number

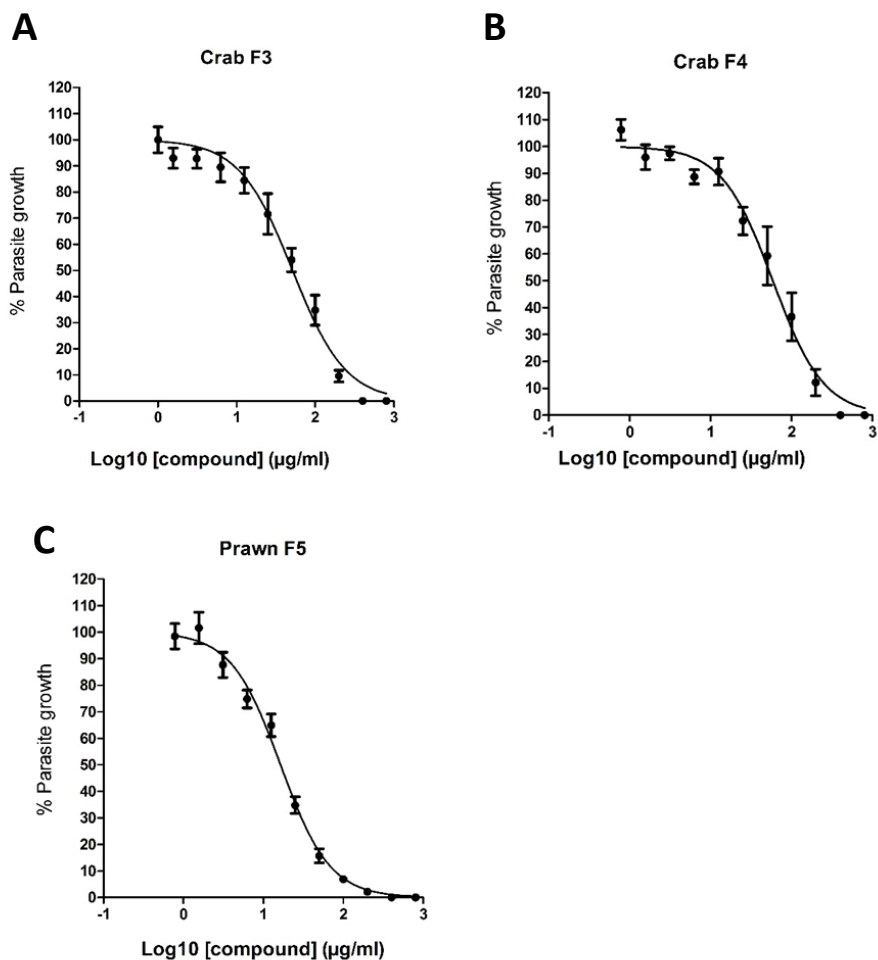


Figure 5.17 Log concentration *versus* normalised growth plots to determine EC₅₀ of most potent marine GAG fractions. Log concentration normalized response curves for the indicated marine GAG fractions from (C) prawn and (A, B) crab. Each point represents the mean and StDev of n=9 data.

Figure 5.5 EC₅₀ growth inhibition values of most potent marine GAG fractions.

Compound	Mean EC ₅₀ (µg/ml)	95% CI
PrawnF5	16.3	14.4 - 18.6
Crab F3	51.6	40.6 - 65.6
Crab F4	58.7	48.4 to 71.1
Heparin (Chapter 4)	9.1	7.3-11.4

To explore if these inhibitors inhibit parasite growth in the same way as heparin and other sulphated GAGs by blocking merozoite invasion or egress, changes in morphological progress on exposure to these fractions was monitored by light microscopy. NF54^{luc} was synchronized and collected at schizont stage and incubated in presence or absence (control) with 100 µg/ml of prawn F5, Crab F3 and Crab F4 (a concentration known to inhibit parasite growth by at least 80%) and incubated for 48 hrs. A thin smear of the treated parasite was then stained with Giemsa and examined by light microscopy. For all three compounds, and in at least two biological repeats, no clustered merozoites were observed. Wet mounts of the treated cultures were incubated with the fluorescent Sybr Green I dye and observing using a fluorescent microscope. For all three marine GAG fractions, free merozoites or merozoites adjacent to erythrocytes, and therefore potentially blocked during the invasion of erythrocytes, were observed (Figure 5.18). This would suggest that, at 100 µg/ml, the growth inhibition effect of these naturally sulphated marine GAGs is only mediated through merozoite invasion of erythrocytes.

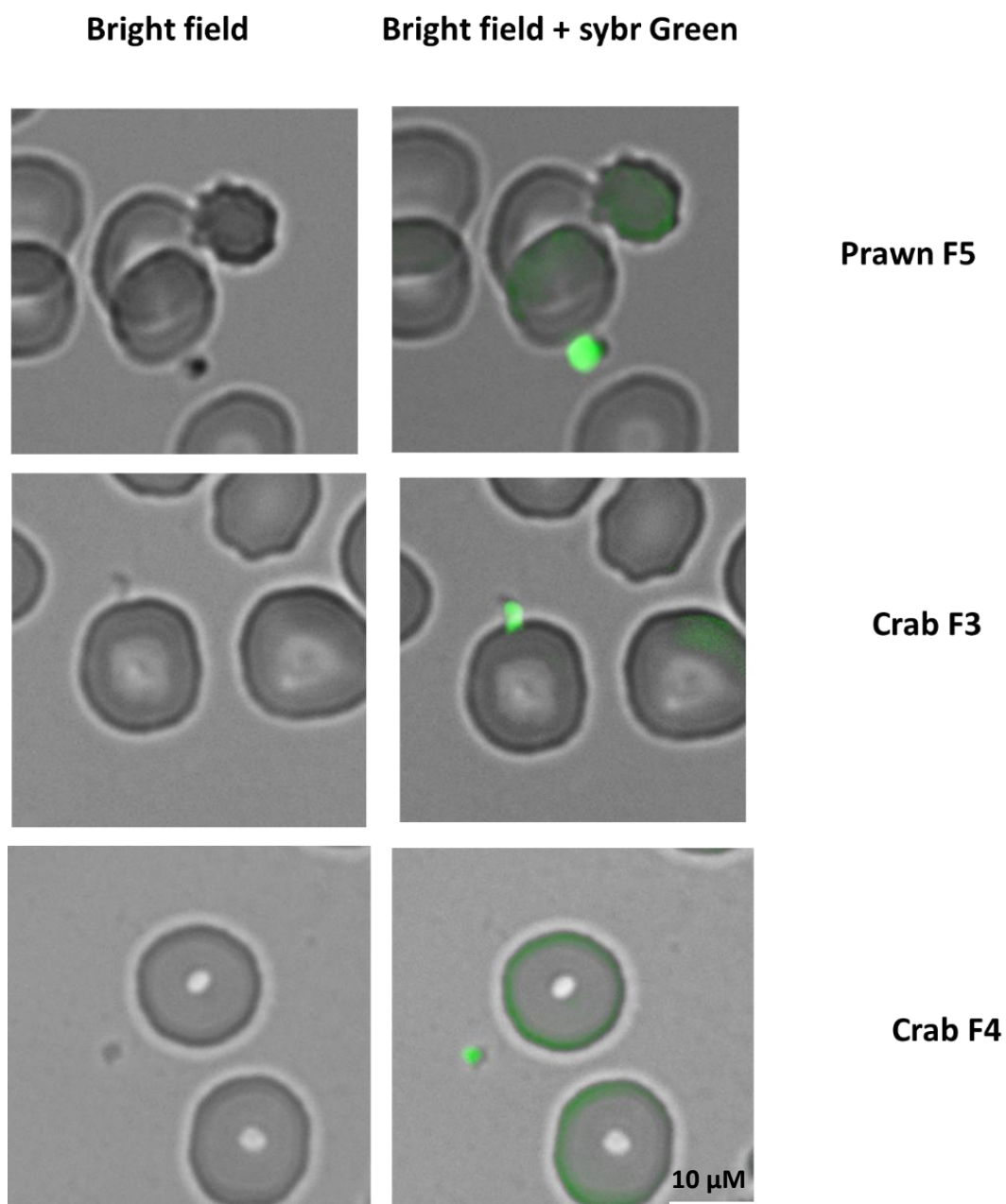


Figure 5.18 Bright field and fluorescent imaging of merozoites following Prawn F5, Crab F3 and Crab F4 treatment. NF54^{luc} parasite exposed to 100μg/ml of the indicated compounds and stained with Sybr Green I fluorescent dye. This example of treated parasite with Prawn F5 inhibitor and other inhibitors of Crab F3 and Crab F4 showing similar action of blocked merozoites.

5.3 Discussion

Blood stage *P.falciparum* infection is the symptomatic stage of a parasite infection that offers a series of advantages for targeting by drugs. The targets for these drugs are either free merozoite or merozoites within a permeable erythrocyte with easy access for drugs. The process of erythrocyte release and reinvasion of merozoites involves several coordinated processes that offer targets in protein-protein interactions, organelle relocation and release, protein phosphorylation or processing by protease cleavage as well as the action of an actin-myosin motor (Burns et al., 2019). These processes are all essential for continued replication and are unique to the parasite offering some potential drug selectivity when compared to the human host. Sulphated GAGs have been shown to have a merozoite invasion blocking activity (Boyle et al., 2017, Havlik et al., 1994, Bastos et al., 2014). This study extends and develops this research by;

- (i) reporting the novel over-sulphated CMH9 has potent anti-plasmodial activities
- (ii) reporting a systematic analysis of the activity of a large panel of chemically modified heparins and sulphated GAGs- particularly exploring their stage of activity in merozoite release and/or merozoite invasion
- (iii) validating the assay approach devised in chapter 4 using two different genetically modified parasite strains

The effect of chemically modified heparin on erythrocyte invasion has previously been reported (Clark et al., 1997; Boyle et al., 2017). This study here includes some of the same chemically modified heparins, but uniquely includes over-sulphated heparin where all O- and N- linked positions in the L-iduronic acid-D-glucosamine dimer have been sulphated. The data reported in this chapter (and summarised in Figure 5.19) indicates that sulphation of the nitrogen in the D-glucosamine appears important for the invasion blocking activity of the CMH. This position is sulphated in the potent blockers (>80% blocking at 100µg/ml) CMH4, CMH7 and CMH9 –

and is, by comparison, acetylated in the least potent blockers CMH3, CMH5, CMH6 and CMH8 (<20% activity at 100µg/ml). Interestingly, CMH2 lacks the N-sulphation but is O-sulphated at position 2 in L-iduronic acid and position 6 of D-glucosamine. All other CMH lacking the N-sulphation, also have one or both O-positions lacking sulphation. Together these data would suggest that, in the invasion assay system used here for Dd2 and NF54, that the degree of sulphation, as well as position of sulphate groups, is important in the invasion blocking antiplasmodial activity.

These data broadly agree with the observations of Clark et al., (1997) and Boyle et al., (2017) – with both reports using different sources of CMH to those used in this study. Clark et al. (1997) reports (i) that LMWH is less potent blockers of erythrocyte invasion and (ii) that de-sulphation at either N or O-linked (but particularly N-linked) positions reduce the invasion blocking activity. Similarly, Boyle et al. (2017) report that low N-sulphation or absent N-sulphation in several chemically modified heparins reduces their invasion blocking activity. This latter report also suggests that de-6-sulphation in D-glucosamine is perhaps the second most potent effect in blocking invasion. This would not agree with our data for CMH3 and CMH4 – both are N-sulphated, with the 2-sulphation on L-iduronic acid in CMH4 associated with more potent blocking activity than the 6-sulphation on Dglucosamine in CMH3. Also, of note is the range of strains used in these studies that report the similarity in action of these CMH; NF54 and Dd2 (in this study), FCR3 (Clark et al., 1997) and 3D7 and D10 (Boyle et al., 2017). This would agree with early reports of strain-independent blocking of erythrocyte invasion by unfractionated and heparin fractions (Kulane et al., 1992).

Invasion-blocking
(this study)

Rosette disruption
(Barragan et al., 1999) (Skidmore et al., 2008)

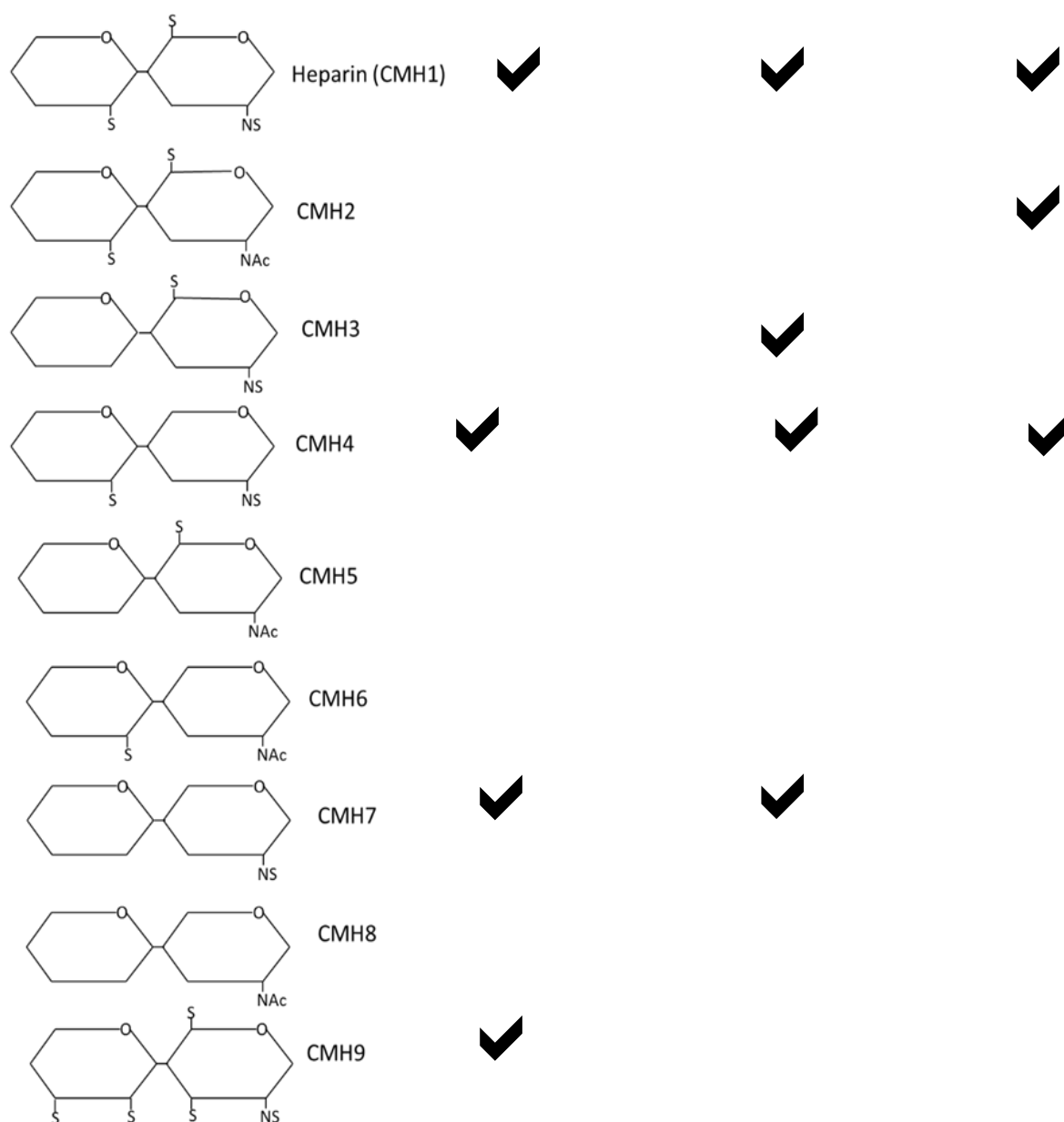


Figure 5.19 **Chemical modification of heparin and their effect on *P.falciparum* growth inhibition and disruption of rosetting.** Schematic representing a chemical modification of heparin, illustrating the position of sulphate groups on the L-iduronic acid 1-4 D-glucosamine dimer. CMH1 Porcine mucosal heparin, CMH2. NAc heparin, CMH3. 2-de-O-S heparin, CMH4. 6-de-O-S heparin, CMH5. 2-de-O-sulfated and N-acetylated, CMH6. 6-de-O-sulfated and N-acetylated, CMH7. 2 and 6 de-O-sulphated and N-sulphated, CMH8. 2 and 6 de-O-sulphated and N-acetylated, CMH9. Over sulphated heparin (also I-3 and A-3 sulphated as well as the usual I2S, A6S, NS). Invasion blocking here reported as >80% inhibition at 100µg/ml.

The Rosette disruption data are from Barragan et al. (1999) and represent >50% disruption at 100µg/ml and from Skidmore et al. (2008) and represent >50% disruption at 400µg/ml.

The same range of CMH has been tested for their effect on rosette disruption (Barragan et al., 1999; Skidmore et al., 2008). The Barragan study used FCR3S1 and Skidmore et al. used the R29 rosetting strain. Their rosette disrupting activity is plotted against the structures of the CMH dimers in Figure 5.19. Interestingly, the absolute requirement for the N-sulphation in D-glucosamine seen for erythrocyte adhesion is not seen for the rosette disrupting activity, with the Skidmore et al., (2008) study suggesting a role for 2-sulphation in L-iduronic acid. Further, there seems to be a limited agreement in the strain-dependent activity between these studies, with the Barragan et al., (1999) study suggesting that CMH rosette disrupting activity is not strain-dependant based on screening of 32 different isolates. This strain-dependency may result from the range of PfEMP1 on the IE surface in the different strains tested and the different uninfected RBC receptors being used for the rosette formation – distinct to the more restricted cell-cell interactions for erythrocyte invasion.

In this study, we identified a novel modification of over-sulphated CMH9 with modifications to I-3 and A-3 as well as the usual I2S, A6S, NS positions. CMH9 shows potent growth inhibition in both parasite strains with EC₅₀ in Dd2^{luc} of 3.8 µg/ml and in NF43^{luc} of 2.4 µg/ml, which is better comparing with unmodified heparin. This same over sulphated CMH9 also shows a significant potency in disrupting H1N1 virus entry (Skidmore et al., 2015), suggesting that an aspect of its activity must reside in the highly negatively charged polymeric structure. That being said, charge and size both seem to be important aspects of heparin's blocking activity, although the CMH series investigated here also does suggest that the position of the charge is important as well.

Because of the concern of heparin causing bleeding due to its high anticoagulation activity, some consideration of the anticoagulation activity must be made. This is considered in this study here where we show a reduction in CMH anticoagulation activity in both aPTT and PT

assays. Using the aPTT data from the Skidmore et al. (2015) study of H1N1 virus blocking activity, the PC1 invasion blocking activity for all chemically modified heparins including CMH9 in this study are plotted against a fold-change reduction in anticoagulation activity (Figure 5.20).

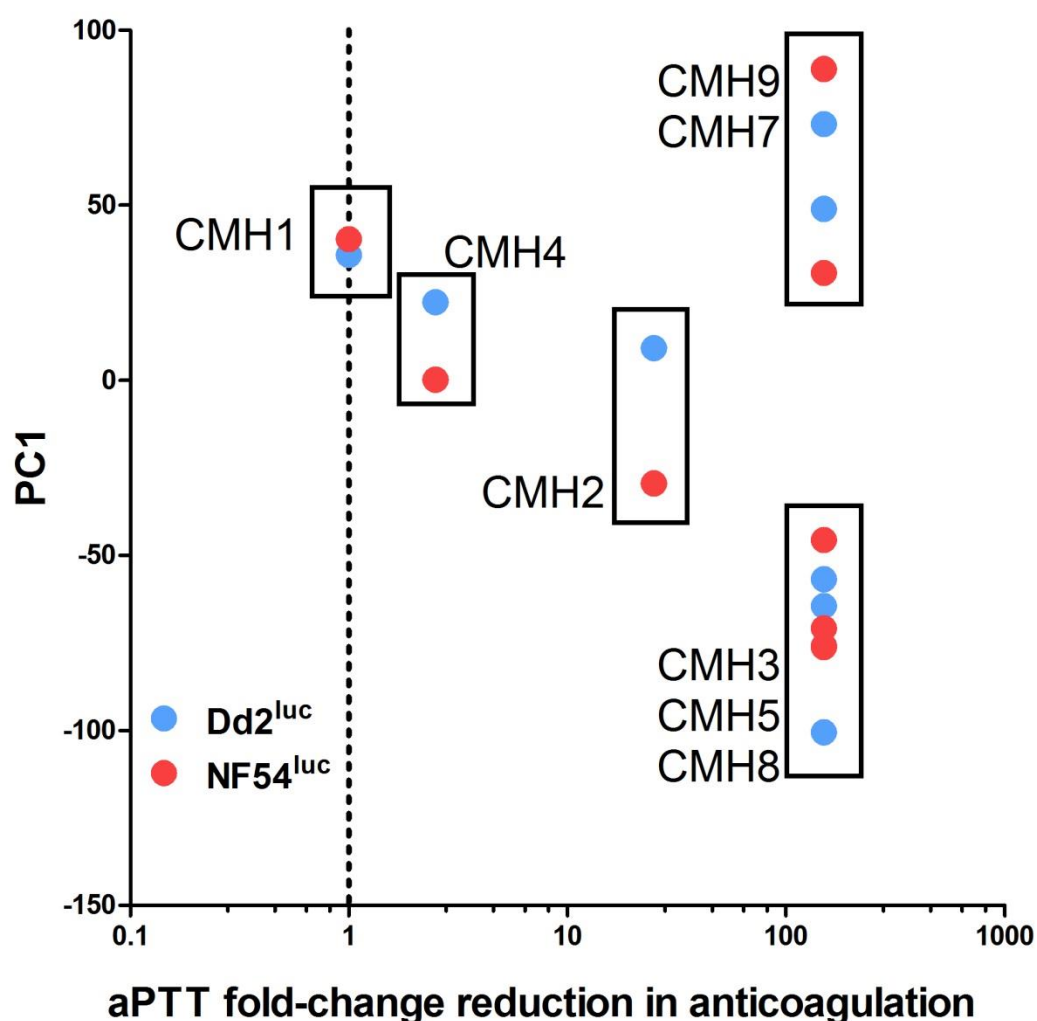


Figure 5.20 Reduced anticoagulation activity of CMH. The fold-change reduction in aPTT activity for the CMH (Skidmore et al., 2015) compared to porcine heparin (CMH1) is shown. The anti-plasmodial potency of CMH9 and CMH7 (high PC1 value) and reduced anticoagulation activity (>150 fold less anticoagulation activity).

An evaluation of the rosette disruption activity and reversal of endothelial adhesion by the over-sulphated CMH9 should be explored – with the opportunity to identify a compound with

reduced anticoagulation activity as well as a range of anti-plasmodial activities. Based on the identification that 2-sulphation of L-iduronic acid and 6-sulphation of D glucosamine both support rosette disruption and blocking of endothelial adhesion (both occur in unfractionated heparin), this would seem to be likely. In addition, however, consideration of activity in platelet factor 4 complex formation (ie the start of HIT activity) should be determined using synchrotron radiation circular dichroism (Skidmore et al., 2008) will be required to explore conformational changes with platelet factor 4.

In addition, this study determined the activity of a panel of sulphated GAGs from non-mammalian sources have been tested for their growth and invasion inhibition activity. We identified from 22 initial compounds, 5 additional compounds with high invasion-blocking activity; gellan sulphate, agarose sulphate, κ -carrageenan, Arabic sulphate and propylene glycol alginate sulphate. These chemically sulphated GAGs highlighted their growth inhibition performance and agree with previous observations where the sulphation is crucial for GAGs inhibition activity. Importantly, all the five tested GAGs were reduced in their anticoagulation activity (using the same aPTT data from Skidmore et al., 2015) when compared with unmodified heparin (Figure 5.21) – although by only 8 to 10-fold. Interestingly this portrayal of the anticoagulation and anti-plasmodial data revealed that there are no compounds in the optimal upper right quadrant (high blocking, low anticoagulation). Compounds such as carboxymethyl cellulose sulphate or locust bean gum sulphate display excellent reductions in anticoagulant activity – although display only minimal invasion blocking activity.

The inhibitory activity of these five sulphated GAGs was determined to be in the range of 2.5-10.4 $\mu\text{g/ml}$. Importantly, these same sulphated GAGs have been reported previously to have strong growth inhibition activity against *P.falciparum* (Boyle et al., 2017). This study, however, validated this observation in two additional strains and using a new invasion-blocking assay system – and extends the observation that GAGs, when used in invasion blocking assays, appear

to act in a strain independent manner. The same range of sulphated GAGs have been tested in HUVEC endothelial cell adhesion blocking studies against two IT strains (ItG and A4) and shown to have some differences in their blocking activities in both static and flow adhesion studies (Skidmore et al., 2017) – again where the cell to cell interactions require the parasite PfEMP1 ligand in the interaction.

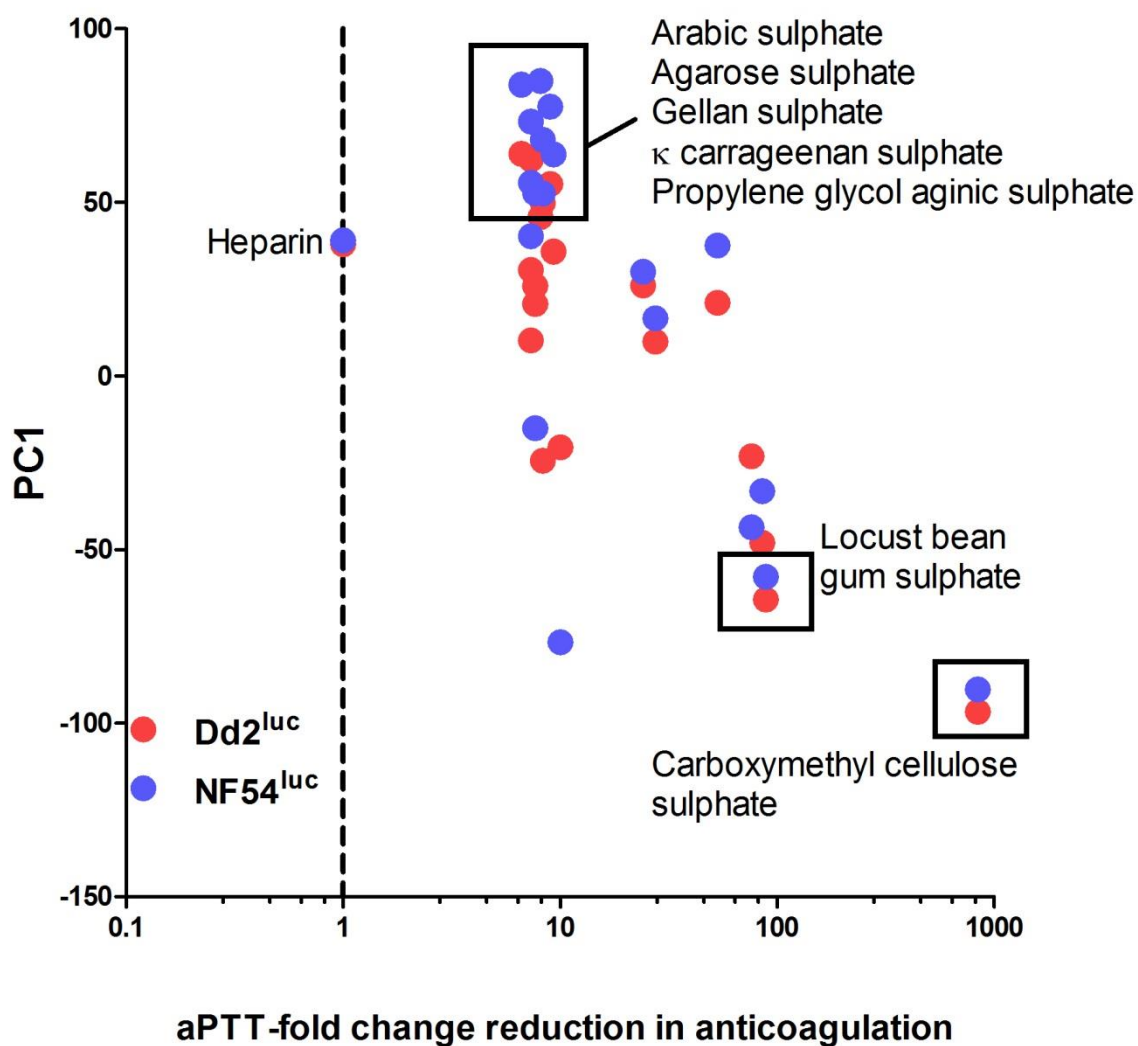


Figure 5.21 Reduction of the anticoagulation activity of sulphated GAGs compared to unmodified heparin (PMH). The fold-change reduction in aPTT activity for the CMH (Skidmore et al., 2015) compared to heparin (dotted line) is shown. The anti-plasmodial potency of the sulphated GAGs tested in this study are shown in Dd2^{luc} and NF54^{luc} (see key).

In addition to the reports in Boyle et al. (2017), gellan sulphate, κ -carrageenan, Arabic sulphate, and propylene glycol alginic sulphate have been tested elsewhere for their invasion blocking activity (Recuenco et al., 2014; Adams et al., 2005). Interestingly, the activity of these inhibitors varied in these studies. The sulphated κ -carrageenan in this study exhibited growth inhibition activity similar to that by Boyle et al., (2017), both studies used the same source, but previous work reported by Recuenco et al., (2014) describes that over-sulphated κ -carrageenan does not inhibit erythrocyte invasion and in another study by Adams et al. (2005), κ -carrageenan inhibits Dd2 invasion but not that of 3D7. It seems these variations may relate to the degree of sulphation of the GAG. However this is not as simple as increasing the overall sulphation level, the κ -carrageenan in Recuenco et al., (2014) was sulphated at 70% of all possible positions, meanwhile, gellan sulphate in the same study did block erythrocyte invasion and was sulphated at 37% of all positions by comparison. This seems to suggest that there may be different effects in different GAGs tested here that may correlate to optimal sulphation levels – rather than just high sulphation levels. It would, therefore, be of interest to further explore the effect of sulphation levels in the five GAGs tested here – particularly to see if this changes their anticoagulation activity – or, take the compounds like carboxymethylcellulose sulphate with low anticoagulation activity and explore whether the invasion blocking activity can be altered with different levels of sulphation.

Of note, given the earlier observations that some CMH act to disrupt rosettes, but do not block invasion, some of the sulphated GAGs tested in this study (Glycogen sulphate type II, Arabic sulphate, hydroxypropyl methylcellulose and paramylon sulphate) have been identified as blocking infected erythrocyte cytoadhesion to HUVEC endothelial have been shown here (except Arabic sulphate) to have weak (>20% inhibition at 100 μ g/ml) or no inhibitory activity against the two parasite strains tested here. This again raises the issue of whether a single sulphated GAGs may be suitable to block or reverse the invasion, rosetting and cytoadhesion

phenotypes of infected erythrocytes in any potential adjunct therapy, or whether mixes need to be considered.

Of note is variation in the structures (and sources) of the sulphated compounds tested in this study (Table 5.6). The variety of sources of the most active sulphated GAGs (seaweed, algae, bacteria and plant) reflect the full diversity of the sources for all the compounds selected in this study. Moreover, the structures of the most active compounds reflect simpler repeating disaccharide units (eg. propylene glycol alginate) to very complex branched and variably modified scaffolds (eg. gum Arabic) – reinforcing a developing message that how sulphate units are organised on these scaffolds is likely important in the activity of the sulphated GAGs over their non-sulphated starting material.

Table 5.6 Structural composition and sources of sulphated GAGs in this study

Compound	Structural composition	Source
κ -Carrageenan	(1-3)- β -D-galactose (G unit) - (1-4)- α -3,6-anhydroD-galactose (A unit)	Seaweed
Gellan sulphate	Glc residues, one glucuronic acid (GlcA), and one rhamnose (Rha) residue: [3- β -D-Glcp-(1-4)- β -D-GlcpA-(1-4)- β -D-Glcp-(1-4)- α -L-Rhap-(1-)]	Bacterial
Propylene glycol alginic sulphate	β -D-mannuronic acid and α -L-guluronic acid	Marine algae
Agarose	1,3-linked β -D-galactose and 1,4-linked 3,6-anhydro- α -L-galactose.	Chemical synthesis
Gum arabic	Gum arabic is a complex and variable mixture of arabinogalactan oligosaccharides, polysaccharides, and glycoproteins. They are mainly formed by chains of 3,6-linked β -D-Galactopyranose substituted in position 6 by side chains of 3-linked α -L-arabinofuranose	Plant

Dextran sulphate	α -1,6-D-glucose with two OSO_3Na moieties on each glucose ring	Bacterial
Pullulan	α -(1 \rightarrow 6)-linked (1 \rightarrow 4)- α -D-triglucosides	Fungal
Welan	A variably modified tetrasaccharide repeating unit of β -D-Glcp(1-4)- β -D-GlcA-(1-4)- β -D-Glcp-(1-4)- α -L-Rhap-(1)	Bacterial
Locust bean gum	(14)-linked β -D-mannopyranose backbone with branch points from their 6-positions linked to α -D-galactose (that is, 16-linked α -D-galactopyranose)	Plant

Gum ghatti	Complex and variably substituted structure that consists of L-arabinose, D-galactose, D-mannose, D-xylose, and D-glucuronic acid in a 48:29:10:5:10 molar ratio	Plant
Levan	Fructan polymer composed of β (2 \rightarrow 6)-linked fructose residues	Bacterial
Tara gum	Galactomannan polysaccharides, consisting of a linear main chain of (1-4)- β -D-mannopyranose units attached by (1-6) linkage with α -D-galactopyranose units	Plant
Amylose	Monosaccharide of D-glucose molecules joined together with a D-(1-4) or a D-(1-6) linkage	Plant
Hyaluronic acid	Repeating disaccharide structure [(1 \rightarrow 3)- β -dGlcNAc-(1 \rightarrow 4)- β -d-GlcA-]	Animal
Carboxymethyl cellulose	Carboxymethyl substituted β (1 \rightarrow 4)-linked glucopyranose residues	Chemical modified
Paramylon	β -1,3 polymer of glucose	Algal
Pectin	Complex polysaccharides that contain 1,4-linked α -Dgalactosyluronic residues	Plant

Xanthan gum	Variably modified β -(1-4)-D-glucopyranose glucan (as <u>cellulose</u>) backbone with side chains of -(31)- α -linked D-mannopyranose-(21)- β -D-glucuronic acid-(41)- β -D-mannopyranose on alternating residues.	Bacterial
-------------	--	-----------

We show here that all of the potent invasion inhibitors (CMH9, gellan sulphate, agarose sulphate, κ -carrageenan, Arabic sulphate, propylene glycol alginic sulphate) are not cytotoxic to intraerythrocytic stages of the life cycle – such as the effect of drugs like artemisinin and chloroquine to trophozoites (Ullah et al., 2017). The invasion blocking data indicated that the inhibition occurred within 18 hrs of incubation of trophozoites with inhibitors – with the blocking of invasion apparent with the decrease in new ring-stage parasites. Like for heparin (Glushakova et al., 2017), we report here the first description of other sulphated GAGs capable of producing the clustered merozoite phenotype indicating that at least some part of their action is in blocking the release of free merozoites. Here we define clustered merozoites as having no clearly defined erythrocyte membrane and appear as parasite-derived material collected around a food vacuole. The inhibition phenotype with these six compounds starts 18 hrs post-treatment, notably with a delay in schizonts rupture and is consistent with other descriptions of the inhibition using some of these compounds (Boyle et al., 2010; Evans et al., 1998; Butcher et al. 1988). Of note is that whilst these studies note the invasion inhibition (often defined as no reinvasion by merozoites), these and other studies (Recuenco et al., 2014; Adams et al., 2005; Boyle et al., 2017) do not describe merozoite clusters as defined here or by Glushakova et al., (2017). Our data based on the morphological similarity of the merozoite clusters produced by all these compounds is that they would work in the same way as heparin – that being primarily in blocking merozoite dispersal and then in blocking the invasion of merozoites into new

erythrocytes. Infected erythrocyte schizonts stage become leaky prior to egress (Lyon et al., 1997), presumably allowing the sulphated GAGs to penetrate through parasite-derived pores. When inside the erythrocyte, these compounds likely interact with the inner aspect of erythrocyte membrane and merozoite surface proteins resulting prevent merozoite dispersal. Glushakova et al.,(2017), reported that heparin has a high affinity to egress proteins such as MSP-1, where MSP-1 is suggested to interact with erythrocyte cytoskeleton component of spectrin in acting to disturb the cell membrane integrity and release from erythrocyte (Das et al., 2015). The clustered merozoites induced by the sulphated GAGs are also morphologically similar to those produced when antibodies that inhibit merozoite surface proteins and induce immune clusters merozoites (ICM) are added (Lyon et al., 1989, 1997). Corresponding with an evolving hypothesis of heparin acting to induce merozoite cluster formation (discussed in chapter 4 discussion) we may also assume that these sulphated GAGs may block the function of PfACT1, resulting in merozoite dispersal prevention.

The formation of the clustered merozoites is seen here using the most potent sulphated GAG and CMH9. It is also shown here for the first time that the formation of the clustered merozoite phenotype is concentration-dependant. What has yet to be worked out is whether these compounds are potent because they form merozoite clusters as part of their mechanism of action or whether all sulphated GAGs can form the merozoite cluster when enough of the compound is available. Looking for merozoite clusters across a wider range of the compounds tested in this study may help – we only did the morphological assessment of the most active compounds and a small number of low potency controls (CMH6 and chondroitin sulphate C). Of note, however, is that whilst dextran sulphate has reasonable anti-plasmodial potency, no merozoite clusters are observed. The potential for these compounds to explore the merozoite clustered phenotype is discussed further in chapter 6.

Naturally sulphated GAGs from marine sources have become increasingly popular for investigations of their anti-pathogenic activity and for their medical applications. For example, fucosylated chondroitin sulphate extracted from sea cucumber (Adams et al., 2005) has shown anti-plasmodial activity. That these compounds could be made available as a product of the food industry (high-value waste product) and that they are naturally sulphated and therefore no additional (and expensive) chemical modifications would be required to sulphate them, we initiated a pilot study to test these GAGs from animal marine source for their potential anti-plasmodial activity. Prawn F5, Crab F5 and Crab F4 fractions proved to have moderate to low anti-plasmodial activity, with EC₅₀ ranging between 16.3-58.7 µg/ml, all being less potent than heparin (9.5µg/ml). The anticoagulation activity of these mGAGs (Table 5.7) were made available by Courtney Mycroft-West of the Skidmore research group.

Table 5.7 aPTT EC₅₀ values for best marine GAG fractions (Data provided by Courtney Mycroft-West)

mGAG (fraction)	aPTT (EC₅₀/ µg/ml)
Prawn F5	30.44
Crab F5	38.92
Crab F4	49.94
Heparin	1.65

Whilst the marine GAG fractions have reduced (18.5-30 fold) anticoagulation activity compared to heparin in the aPTT assays – the absolute aPTT EC₅₀ values are in the same range as the anti-plasmodial activity – suggesting that some anticoagulation activity would be observed when the required anti-plasmodial concentrations of >60 µg/ml would be used in any

therapy approach. Whilst there are some opportunities from naturally sulphated GAGs, the data offered in this pilot study suggest that they are unlikely to be available from these materials.

Chapter Six: Overall discussion and perspectives

In this study, we have reported the screening and characterization of the *P.falciparum* erythrocytic stage invasion-blocking phenotype of a range of naturally occurring and synthetic sulphated GAGs. This work has identified six sulphated GAGs with greater antiplasmodial activity and reduced anticoagulation to unfractionated heparin. Further, with structural variations and changes to the sulphation patterns of CMH9 compared to heparin, all will unlikely cause heparin-induced thrombocytopenia. As discussed in chapters four and five though is that whilst these properties are promising, they do need to be improved. For example, sevuparin was shown in Phase I trials to be tolerated well by adult males and can be given as 360mg every 6 hours (Leitgeb et al., 2017). This is noted to be similar to similar doses using LMWH for adults, and would therefore necessarily be of the order of 40-80mg in young children (1.5mg/kg; see chapter 4). This would, for all the six compounds described, provide a maximum of a 2 to 8-fold EC₅₀ concentration assuming a 100% distribution. With evidence that sevuparin at 3mg/kg, and having an *in vitro* erythrocyte invasion inhibition effect in the same range at 5.2µg/ml, has only a minimal effect on the clinical trial – and little beyond that of the control arm of the study – this would suggest that none of these six compounds are likely useful hits to take to *in vivo* or clinical studies. Moreover, malaria infection induced thrombocytopenia in the face of high concentrations of inhibitors may increase the risk of haemorrhage.

These six compounds did, however, show an interesting invasion blocking phenotype. Glushakova et al., (2017) have recently described the effect of unfractionated heparin on merozoite egress using a range of imaging methodology. Heparin appears to gain access to the infected erythrocyte during a multistep egress process following parasitophorous vacuole

rupture but before rupture of the erythrocyte plasma membrane – likely through pores created as an early step in this process. The access of heparin at this point is likely at the final step of the 48hr life cycle. Fluorescently labelled heparin binds to targets on the inside of the infected erythrocytes and on the surface of merozoites (likely MSP1) (Glushakova et al., 2017) and this appears to delay the plasma membrane rupture. In addition, heparin also interferes with the release of free merozoites – resulting in the merozoite cluster (Figure 6.1) – preventing reinvasion by preventing free merozoites being available to bind to the surface of new uninfected erythrocytes.

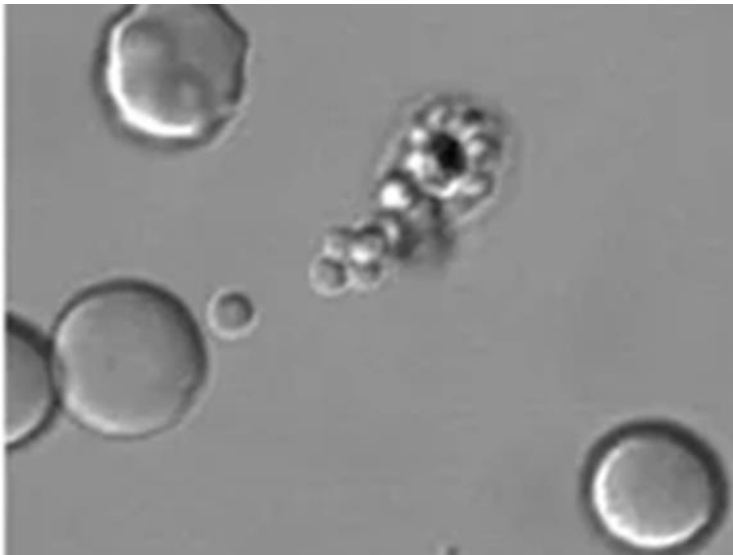


Figure 6.1 Confocal light microscopy of *P.falciparum* NF54 strain exposed to with heparin illustrating the merozoite cluster (Source: Glushakova et al.,2017)

Except for this study, no additional reports describing the merozoite cluster have been made. This study extensively describes this phenotype based on the multiple timepoint imaging studies and does so for a range of new compounds – all that have invasion blocking potency greater than heparin. The absence of previous descriptions may be due to most studies reporting the blocking effect after one time point (L Xiao et al.,1996; Clark, Su, & Davidsonl., 1997;

Boyle et al., 2010; Recuenco et al., 2014 Boyle et al., 2017) or that in studies of heparin blocking invasion they typically mechanically rupture the merozoites from mature schizonts (Holder et al., 1992; Blackman and Holder, 1992). These studies indicate that heparin or mimetics of heparin block the initial contact and apical reorientation of the merozoite (Boyle et al., 2010, reviewed in Burns et al., 2017) and therefore likely interact with several targets. These, along with the multiple intraerythrocytic targets for heparin described by Glushakova et al. (2017) is interesting as it suggests that resistance to heparin (or heparin mimetic) invasion-blocking effect would be less likely to develop resistance.

The six compounds identified here offer a range of chemical probes to further study the cell biology of merozoite egress. Much like imadazopyridazines (inhibitors of protein kinase G, PfPKG;(Dvorin et al., 2010, Baker et al., 2017) have shown the importance of release of the protease subtilisin in priming merozoite release, these compounds could be used in imaging studies (fluorescently labelled compounds, real-time imaging studies etc) to explore the final stages of merozoite release. Given the recent demonstration for a role in actin I in merozoite dispersal (Das et al., 2017) and the availability of inducible-knockdown lines, these provide the second source of parasites to study with these compounds. Interesting, previous studies (from 2012) in our laboratory, using three sulphated GAGs (including Arabic sulphate) explored their effect on erythrocyte invasion in enzyme-treated erythrocytes (neuraminidase, trypsin or chymotrypsin) using a two-colour flow cytometry assay (Theron et al., 2010). These studies provided some preliminary evidence that Arabic sulphate inhibition of invasion was not affected by any treatment, but that by sulphated glycogen was mediated through a chymotrypsin-sensitive invasion process. This research offers another interesting route in using the six sulphated GAGs as research tools in the investigation of erythrocyte invasion.

To develop the next generation of heparin mimetics either to study merozoite invasion and egress or as an adjunct therapy, key lessons were learnt as part of this study. First, the size (MW) of the mimetic is important. Work described here for the LMWH is an example of this effect in erythrocyte invasion – with this work correlating generally with previous work reported by Boyle et al. (2010 and 2017). Size is not everything however, chondroitin sulphate C is a large sulphated GAG and has low invasion blocking activity – but this does lead on to the next lesson, sulphation is important and where it is sulphated appears important. Chondroitin sulphate C lacks N-sulphation, shown in this study and in data in Boyle et al. (2017) when looking at different CMH to be important in blocking invasion. Variations for some of the sulphated GAGs, and the apparent absence of merozoite clusters using the highly sulphated dextran sulphate, in our study and previous reports also suggests that the optimum level of sulphation may be different for different GAG structures. Investigating this will be hard. It will require varied sulphating of a range of GAGs, with each then having its anti-plasmodial activity recorded (luciferase assay and potentially imaging study). An opportunity to simplify this approach is available based on work by a PhD colleague, Anthony Devlin, in the Skidmore laboratory. His research is exploring how Attenuated Total Reflectance Fourier Transformed Infrared Spectroscopy (ATR-FTIR) can be used to detect and quantify different types of bond vibrations which allows for the description of structures such as N and O-sulphation (Devlin et al., deposited in BioRxiv). By generating ATR-FTIR spectra for a large number of GAGs (Figure 6.2A) the information about the peaks (vibrations of different bonds within the molecule) position and height can be captured and analysed by principal components analysis (Figure 6.2B). In this figure – the first two PC separate out common GAGs by their structural component (types of glycosidic bonds) as well as the presence of 2-O-sulphated, 6-O-sulphated and N-sulphated components. This same approach has been used to analyse many of the CMH and sulphated GAGs libraries used in chapter five. Plotting the first three PC in a 3D plot

distributes the compounds (Figure 6.3). This data provides an interesting start. First, three very low potent compounds cluster in a space together (MS5; Hydroxypropyl methyl cellulose sulphate; MS14; pectin sulphate; MS15, gum mastic sulphate). If this ATR-FTIR library were expanded, and the method is designed for high throughput screening and other compounds

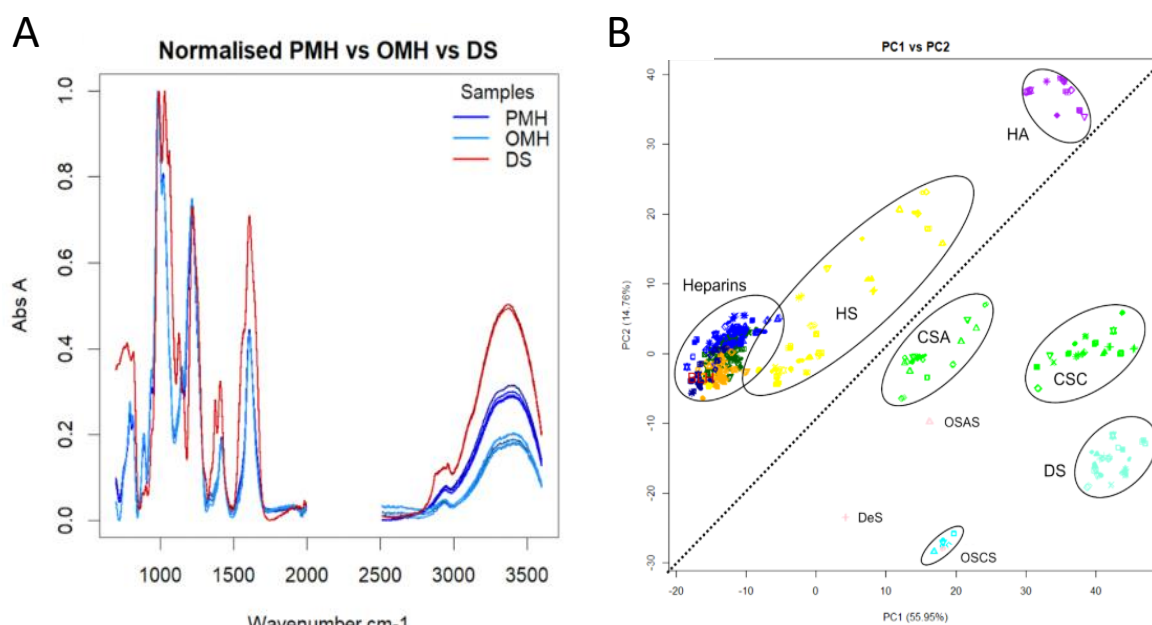


Figure 6.2 **ATR-FTIR of sulphated GAGs.** (A) FTIR spectra of porcine (PMH) and ovine (OMH) mucosal heparin compared to dermatan sulphate (DS). (B) PCA of transformed spectra with PC1 and PC2 providing a 2D separation of common GAG structures by glycosidic bond and sulphation pattern (Source: Devlin et al., 2019 submitted to bioRxiv).

fell into this space – then these may not be of interest as they share spectral features typical of low potency compounds. Using mass spectroscopy or nuclear magnetic resonance, the structures within these low potency compounds could be identified and excluded in future searches. The data for the more potent compounds is less clear. CMH9, agarose sulphate, Arabic sulphate and propylene glycol alginic sulphate are distributed across space – and while it may be that being positioned higher in the space is important, CMH7 clusters more closely

with low potency CMH. Larger libraries and exploring other PC (there are 16 of them) may provide a screen for potential compounds to test as well as a means to look for common substructures in potent heparin mimetics.

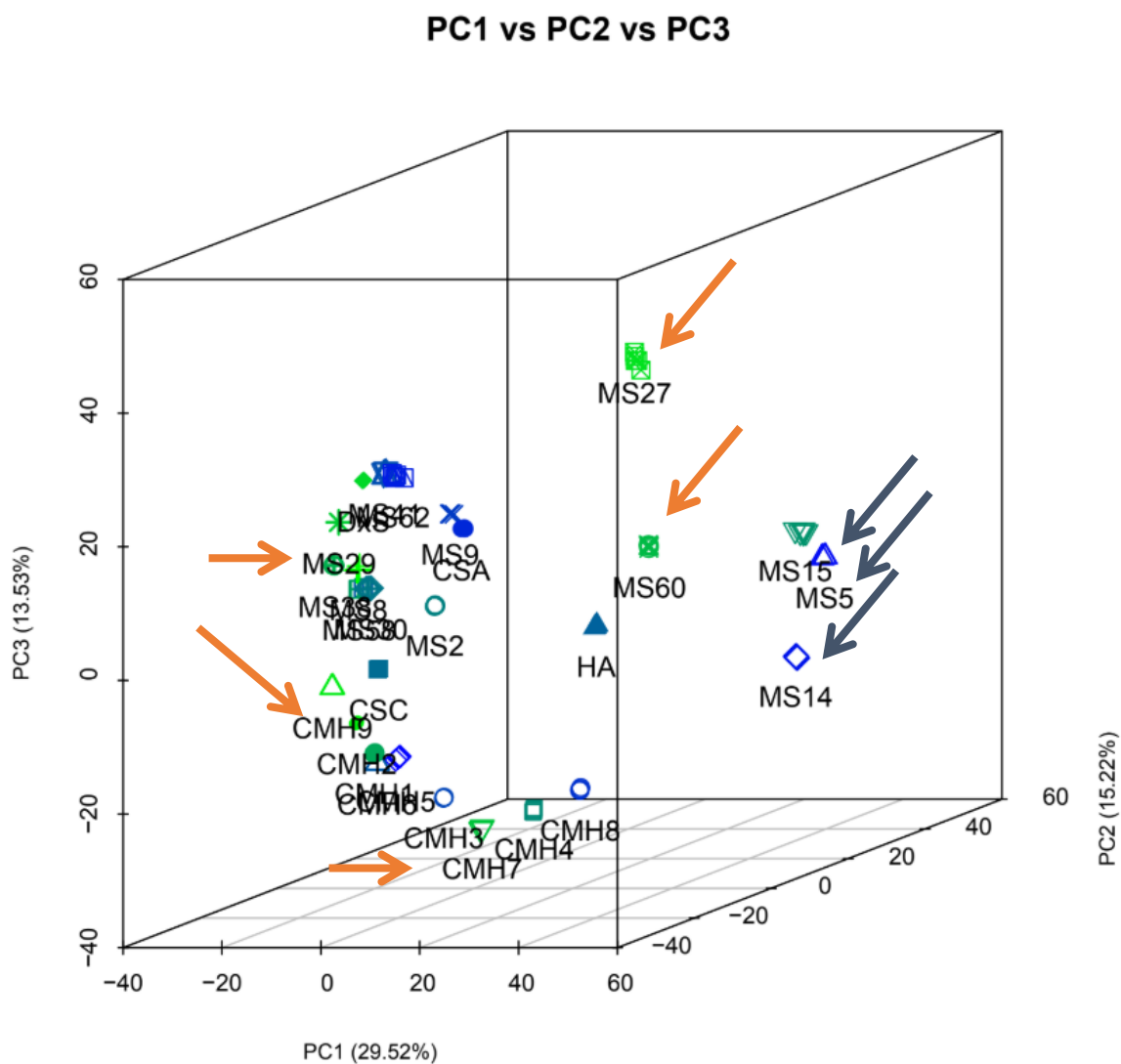


Figure 6.3 **Principle components analysis of ATR-FITR of CMH and sulphated GAGs.** 3D plot of compounds PC1 to PC3 data. Compounds highlighted in orange arrows are potent inhibitors (CMH7 and 9; MS 27, agarose sulphate; MS29, Arabic sulphate; MS60 propylene glycol alginic sulphate). Compounds with a blue arrow are not potent (MS5, Hydroxypropyl methyl cellulose sulphate; MS14; pectin sulphate; MS15, gum mastic sulphate).

The Sevuparin phase I/IIa trial showed how a low anticoagulation low molecular weight heparin could be employed in a trial to demonstrate safety and initial efficacy. Sevuparin was tolerated well in adult males and also showed a significant but short-lived blocking of reinvasion and de-sequestration, when compared to the control arm of the trial (Leitgeb et al., 2017) Sevuparin in the phase IIa trial, was used in combination with atovaquone and proguanil (Malanil) and compared to atovaquone and proguanil alone. This was done as the rapid onset of artemisinin combination therapy was considered likely to obscure the reinvasion phenotype being measured. There was no significant difference in the trial arms on blocking of reinvasion and de-sequestration after 8 hours - where parasite clearance time in both groups were similar (53 hrs in sevuparin/drug and 51 hrs in drug), the parasitaemia reduction over 24 or 48 hrs were similar, with sevuparin/drug (24 hrs - 87.44%, 48hrs -99.96%) and drug alone (24hrs -84.64%, 48 hrs -99.78%). It would seem that even the slower acting atovaquone and proguanil would mask any additional protective effect of the Sevuparin. This is important when we think about how clinical trials for heparin mimetic adjunct therapies would be designed. Any adjunct therapy would have to be as safe as and more clinically effective than the current treatment for it to be considered for future use – and the current frontline treatment for malaria are the artemisinin combination therapies. In addition, the adjunct therapy would be of real value for severe malaria, where it is needed to offset the immediate life-threatening pathology to allow the drug time to reduce the parasite burden and reduce the development of additional pathology. Severe malaria is mainly associated with young children and understanding how to do a trial of heparin mimetic in children with severe malaria would be very difficult. The previous trials of heparin did so at a time when the leading antimalarials (aminoquinolines and antifolates) were failing and thus the standard of care was low – this is not true currently with the artemisinin combination therapies.

Perhaps one route forward for heparin mimetics as an adjunct therapy is if they are not first considered to be used as a drug that blocks erythrocyte invasion or disrupting resetting or de-sequestering infected erythrocytes. Instead, the potential for heparin or a heparin mimetic in reducing histone-mediated coagulation and vascular leakage in cerebral malaria could be where new opportunities arise. Cerebral malaria is linked to infected erythrocytes sequestering in the microvessels of the brain (Taylor et al., 2014), with localised coagulopathy and leak of fluid from the blood into the brain that can lead to brain swelling. A recent report (Moxon et al, prerelease in bioRxiv) links these effects to the presence of histones (Figure 6.4) released either from sequestered parasites or from damaged endothelium.

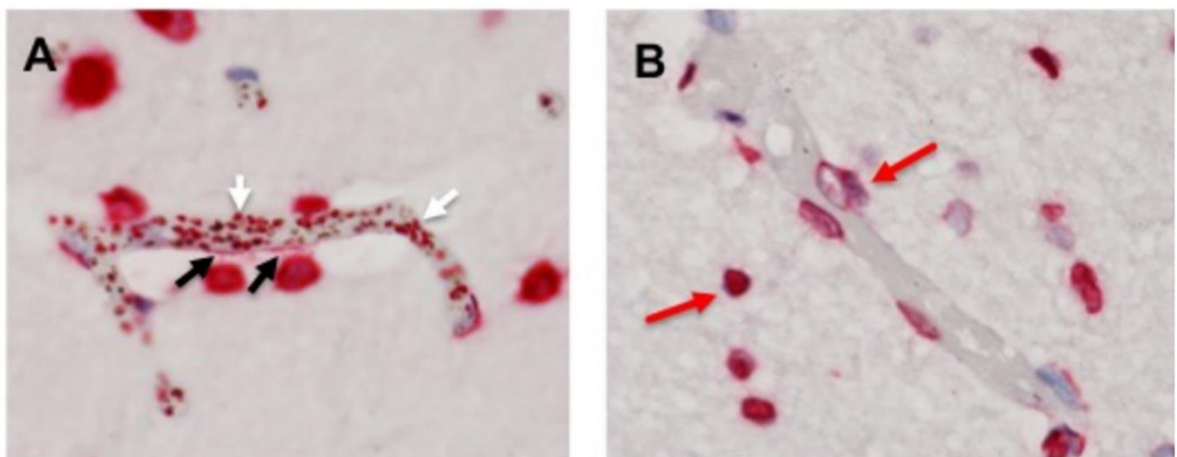


Figure 6.4 **Histone staining of brain microvessel endothelium.** (A) Histone staining (red) of a cerebral malaria case. The black arrows show staining of the internal face of the blood vessel. The large red puncta are human cells, with the white arrows showing the multiple small red puncta of infected erythrocytes sequestered within the brain micro blood vessel. (B) Sample from a non cerebral malaria case does not show staining of the epithelium of the blood vessel or sequestered infected erythrocytes (Source: Moxon et al. www.biorxiv.org/content/biorxiv/early/2019/03/20/563551.full.pdf).

Histones have previously been linked with other inflammatory conditions, eg. sepsis (Wildhagen et al., 2014), where treatment with an antithrombin affinity-depleted heparin (low anticoagulation) offers protection from more serious complications (and death). This principle was also shown in the Moxon et al. study, where a non-anticoagulant heparin (N-acetylated to remove the key N-sulphation on D Glucosamine used at 200 µg/ml) prevented histone-mediated toxicity of a cultured human brain microvascular endothelial cell line and protected it from leakage (Moxon et al., prerelease in bioRxiv). Whilst this demonstrates the potential for non-anticoagulant heparin as a potential therapy – the current concentration evaluated for human brain microvascular endothelial cell lines is likely a 10-fold higher concentration that could likely be safely delivered to a child. Demonstrating that there is a concentration-dependent effect and that the concentration of the heparin/heparin mimetic could be greatly reduced and still be effective would be useful. This suggests further research to gain a greater understanding of what aspects of heparin, chemically modified heparin or sulphated GAGs could contribute to binding plasma histones away so that they do not cause endothelial pathology. Testing sulphated GAG binding to histones could be rapidly screened in surface plasmon resonance assays, with this screening supported by the ATR-FTIR to look for important structural features, with the potency of the sequestering effect tested *in vitro* using human brain microvascular endothelial cell lines to monitor cell death and their barrier function against leakage. There is a mouse model for cerebral malaria – using *P. berghei* infection of certain mouse lines (White et al., 2010), although its use would have to be initially tested as the pathology of this cerebral model doesn't require infected erythrocyte sequestration in the brain. Importantly, moving into a human trial would need to consider how to safely and effectively evaluate a potent histone-binding mimetic in conjunction with a rapid-acting combination therapy drug.

REFERENCES

- A. M. Dondorp, C. Ince, P. Charunwatthana, J. Hanson, A. van Kuijen, M. A. Faiz, . . . N. P. J. Day. (2008). Direct *in vivo* assessment of microcirculatory dysfunction in severe falciparum malaria. *The Journal of Infectious Diseases*, 197(1), 79-84.
- Achan, J., Talisuna, A. O., Erhart, A., Yeka, A., Tibenderana, J. K., Baliraine, F. N., . . . D'Alessandro, U. (2011). Quinine, an old anti-malarial drug in a modern world: role in the treatment of malaria. *Malaria Journal*, 10(1), 144.
- Adams, Y., Smith, S., Schwartz-Albiez, R., & Andrews, K. (2005). Carrageenans inhibit the *in vitro* growth of *plasmodium falciparum* and cytoadhesion to CD36. *Parasitology Research*, 97(4), 290-294.
- Adjalley, S. H., Lee, M. C. S., & Fidock, D. A. (2010). A method for rapid genetic integration into *plasmodium falciparum* utilizing mycobacteriophage Bxb1 integrase. *Methods in Molecular Biology* (Clifton, N.J.), 634, 87.
- Albisetti, M., & Andrew, M. (2001). Low molecular weight heparin in children. *European Journal of Pediatrics*, 161(2), 71–77.
- Allen, S. J., O'Donnell, a Alexander, N. D., & Clegg, J. B. (1996). Severe malaria in children in Papua New Guinea. *QJM : Monthly Journal of the Association of Physicians*, 89(10), 779–788.
- Amaratunga, C., Lim, P., Suon, S., Sreng, S., Mao, S., Sopha, C., Fairhurst, R. M. (2016). Dihydroartemisinin–piperaquine resistance in *Plasmodium falciparum* malaria in Cambodia: a multisite prospective cohort study. *The Lancet Infectious Diseases*, 16(3), 357–365.
- Anna M Leitgeb, Prakaykaew Charunwatthana, Ronnatrai Rueangveerayut, Chirapong Uthaisin, Kamolrat Silamut, Kesinee Chotivanich, . . . Arjen M Dondorp. (2017). Inhibition of

merozoite invasion and transient de-sequestration by sevuparin in humans with *plasmodium falciparum* malaria. PLoS One, 12(12), e0188754.

Aquino, R. S., & Park, P. W. (2016). Glycosaminoglycans and infection. *Frontiers in Bioscience (Landmark Edition)*, 21(6), 1260-1277.

Arama, C., & Troye-Blomberg, M. (2014). The path of malaria vaccine development: challenges and perspectives. *Journal of Internal Medicine*, 275(5), 456–466.

Ariey, F., Witkowski, B., Amaratunga, C., Beghain, J., Langlois, A. C., Khim, N., ... Ménard, D. (2014). A molecular marker of artemisinin-resistant *Plasmodium falciparum* malaria. *Nature*, 505(7481), 50–55.

Baker, D. A., Stewart, L. B., Large, J. M., Bowyer, P. W., Ansell, K. H., Jiménez-Díaz, M. B., ... Osborne, S. A. (2017). A potent series targeting the malarial cGMP-dependent protein kinase clears infection and blocks transmission. *Nature communications*, 8(1), 430.

Baker, D. A., Stewart, L. B., Large, J. M., Bowyer, P. W., Ansell, K. H., Jiménez-Díaz, M. B., ... Osborne, S. A. (2017). A potent series targeting the malarial cGMP-dependent protein kinase clears infection and blocks transmission. *Nature Communications*, 8(1).

Bannister, L. H. et al. (2003). *Plasmodium falciparum* apical membrane antigen 1 (PfAMA-1) is translocated within micronemes along subpellicular microtubules during merozoite development. *Journal of Cell Science*, 116(18), 3825–3834.

Bannister, L. H., Hopkins, J. M., Dluzewski, A. R., Margos, G., Williams, I. T., Blackman, M. J., ... Mitchell, G. H. (2003). *Plasmodium falciparum* apical membrane antigen 1 (PfAMA-1) is translocated within micronemes along subpellicular microtubules during merozoite development. *Journal of Cell Science*, 116(18), 3825-3834.

Barragan A, Fernandez V, Chen Q, von Euler A, Wahlgren M (2000) The duffy-binding-like domain 1 of *Plasmodium falciparum* erythrocyte membrane protein 1 (PfEMP1) is a heparan sulfate ligand that requires 12 mers for binding. *Blood* 95: 3594–3599.

- Barragan, A., Spillmann, D., Kremsner, P. G., Wahlgren, M., & Carlson, J. (1999). *Plasmodium falciparum*: Molecular background to strain-specific rosette disruption by glycosaminoglycans and sulfated glycoconjugates. *Experimental Parasitology*, 91(2), 133-143.
- Barsoum, R. S. (2000). Malarial acute renal failure. *Journal of the American Society of Nephrology : JASN*, 11(11), 2147–2154.
- Bartoloni, A., & Zammarchi, L. (2012). Clinical Aspects of Uncomplicated and Severe Malaria. *Mediterranean Journal of Hematology and Infectious Diseases*, 4(1), 2012026.
- Bastos, M. F., Albrecht, L., Kozlowski, E. O., Lopes, S. C. P., Blanco, Y. C., Carlos, B. C., . . . Costa, F. T. M. (2014). Fucosylated chondroitin sulfate inhibits *plasmodium falciparum* cytoadhesion and merozoite invasion. *Antimicrobial Agents and Chemotherapy*, 58(4), 1862-1871.
- Baum, J., Chen, L., Healer, J., Lopaticki, S., Boyle, M., Triglia, T., . . . Cowman, A. F. (2009). Reticulocyte-binding protein homologue 5 – an essential adhesin involved in invasion of human erythrocytes by *plasmodium falciparum*. *International Journal for Parasitology*, 39(3), 371-380.
- Beeson, J. G., Rogerson, S. J., & Brown, G. V. (2002). Evaluating specific adhesion of *Plasmodium falciparum*-infected erythrocytes to immobilised hyaluronic acid with comparison to binding of mammalian cells. *International Journal for Parasitology*, 32(10), 1245–1252. doi:10.1016/s0020-7519(02)00097-8.
- Bei, A. K., Desimone, T. M., Badiane, A. S., Ahouidi, A. D., Dieye, T., Ndiaye, D., . . . Duraisingh, M. T. (2010). A flow cytometry-based assay for measuring invasion of red blood cells by *plasmodium falciparum*. *American Journal of Hematology*, 85(4), 234.
- Binks, R. H., & Conway, D. J. (1999). The major allelic dimorphisms in four *plasmodium falciparum* merozoite proteins are not associated with alternative pathways of erythrocyte invasion. *Molecular & Biochemical Parasitology*, 103(1), 123-127.
- Blackman, M. J., & Holder, A. A. (1992). Secondary processing of the *plasmodium falciparum* merozoite surface protein-1 (MSP1) by a calcium-dependent membrane-bound serine protease:

Shedding of MSP133 as a noncovalently associated complex with other fragments of the MSP1. *Molecular and Biochemical Parasitology*, 50(2), 307-315.

Boyle, M. J., Richards, J. S., Gilson, P. R., Chai, W., & Beeson, J. G. (2010). Interactions with heparin-like molecules during erythrocyte invasion by *plasmodium falciparum* merozoites. *Blood*, 115(22), 4559-4568.

Boyle, M. J., Skidmore, M., Dickerman, B., Cooper, L., Devlin, A., Yates, E., . . . Beeson, J. G. (2017). Identification of heparin modifications and polysaccharide inhibitors of *plasmodium falciparum* merozoite invasion that have potential for novel drug development. *Antimicrobial Agents and Chemotherapy*, 61(11).

Boyle, M. J., Wilson, D. W., & Beeson, J. G. (2013). New approaches to studying *plasmodium falciparum* merozoite invasion and insights into invasion biology. *International Journal for Parasitology*, 43(1), 1-10..

Brabin, B. J., Bates, I., Cuevas, L. E., Haan, R. J. De, Ph, D., Phiri, A. I., ... Hensbroek, M. B. Van. (2015). Severe Anaemia in Malawian Children.

Brito, A. S., Arimatéia, D. S., Souza, L. R., Lima, M. A., Santos, V. O., Medeiros, V. P., . . . Chavante, S. F. (2008). Anti-inflammatory properties of a heparin-like glycosaminoglycan with reduced anti-coagulant activity isolated from a marine shrimp. *Bioorganic & Medicinal Chemistry*, 16(21), 9588-9595.

Burns, A. L., Dans, M. G., Balbin, J. M., F de Koning-Ward, T., Gilson, P. R., Beeson, J. G., ... Wilson, D. W. (2019). Targeting malaria parasite invasion of red blood cells as an antimalarial strategy. *FEMS microbiology reviews*, 43(3), 223–238.

Burrows, J. N., Duparc, S., Gutteridge, W. E., Hooft van Huijsduijnen, R., Kaszubska, W., Macintyre, F., ... Wells, T. N. C. (2017). New developments in anti-malarial target candidate and product profiles. *Malaria Journal*, 16(1).

Burrows, J. N., van Huijsduijnen, R. H., Möhrle, J. J., Oeuvray, C., & Wells, T. N. (2013). Designing the next generation of medicines for malaria control and eradication. *Malaria journal*, 12, 187.

Butcher, G. A., Parish, C. R., & Cowden, W. B. (1988). Inhibition of growth in vitro of *Plasmodium falciparum* by complex polysaccharides. *Transactions of the Royal Society of Tropical Medicine and Hygiene*, 82(4), 558–559.

Carlson J, Ekre HP, Helmby H et al. (1992). Disruption of *Plasmodium falciparum* erythrocyte rosettes by standard heparin and heparin devoid of anticoagulant activity. *Am J Trop Med Hyg*;46:595–602.

Choukri Ben Mamoun, Ilya Y. Gluzman, Sophie Goyard, Stephen M. Beverley, & Daniel E. Goldberg. (1999). A set of independent selectable markers for transfection of the human malaria parasite *plasmodium falciparum*. *Proceedings of the National Academy of Sciences of the United States of America*, 96(15), 8716-8720.

Clark, D., Su, S., & Davidson, E. (1997). Saccharide anions as inhibitors of the malaria parasite. *Glycoconjugate Journal*, 14(4), 473-479.

Cohen, J., Nussenzweig, V., Nussenzweig, R., Vekemans, J., & Leach, A. (2010). From the circumsporozoite protein to the RTS, S/AS candidate vaccine. *Human Vaccines*, 6(1), 90–96.

Cotter, C., Sturrock, H.J., Hsiang, M.S., Liu, J.X., & Feachem, R. (2013). The changing epidemiology of malaria elimination: new strategies for new challenges. *The Lancet*, 382, 900-911.

Cowman, A. F., Berry, D., & Baum, J. (2012). The cellular and molecular basis for malaria parasite invasion of the human red blood cell. *The Journal of Cell Biology*, 198(6), 961–71.

Cowman, A. F., Morry, M. J., Biggs, B. A., Cross, G. A., & Foote, S. J. (1988). Amino acid changes linked to pyrimethamine resistance in the dihydrofolate reductase-thymidylate synthase gene of *Plasmodium falciparum*. *Proceedings of the National Academy of Sciences of the United States of America*, 85(23), 9109–9113.

Cowman, A. F., Tonkin, C. J., Tham, W.-H., & Duraisingh, M. T. (2017). The Molecular Basis of Erythrocyte Invasion by Malaria Parasites. *Cell Host & Microbe*, 22(2), 232–245.

Crabb, B. S., Triglia, T., Waterkeyn, J. G., & Cowman, A. F. (1997). Stable transgene expression in *plasmodium falciparum*. *Molecular & Biochemical Parasitology*, 90(1), 131-144.

Crandall, I. E., Szarek, W. A., Vlahakis, J. Z., Xu, Y., Vohra, R., Sui, J., & Kisilevsky, R. (2007). Sulfated cyclodextrins inhibit the entry of plasmodium into red blood cells. *Biochemical Pharmacology*, 73(5), 632-642.

Cui, L., Cui, L., Miao, J., Wang, J., & Li, Q. (2008). *Plasmodium falciparum*: Development of a transgenic line for screening antimalarials using firefly luciferase as the reporter. *Experimental Parasitology*, 120(1), 80-87.

Dahl, E. L., & Rosenthal, P. J. (2007). Multiple antibiotics exert delayed effects against the *Plasmodium falciparum* apicoplast. *Antimicrobial agents and chemotherapy*, 51(10), 3485–3490.

Danny W Wilson, Christopher D Goodman, Brad E Sleebs, Greta E Weiss, Nienke WM de Jong, Fiona Angrisano, . . . James G Beeson. (2015). Macrolides rapidly inhibit red blood cell invasion by the human malaria parasite, *plasmodium falciparum*. *BMC Biology*, 13(1), 52.

Danny W. Wilson, Christine Langer, Christopher D. Goodman, Geoffrey I. McFadden, & James G. Beeson. (2013). Defining the timing of action of antimalarial drugs against *plasmodium falciparum*. *Antimicrobial Agents and Chemotherapy*, 57(3), 1455-1467.

Das, S., Hertrich, N., Perrin, A., Withers-Martinez, C., Collins, C., Jones, M., . . . Blackman, M. (2015). Processing of *plasmodium falciparum* merozoite surface protein MSP1 activates a spectrin-binding function enabling parasite egress from RBCs. *Cell Host & Microbe*, 18(4), 433-444.

Das, S., Lemgruber, L., Tay, C. L., Baum, J., & Meissner, M. (2017). Multiple essential functions of *plasmodium falciparum* actin-1 during malaria blood-stage development. *BMC Biology*, 15(1), 70-16.

Das, S., Saha, B., Hati, A. K., & Roy, S. (2018). Evidence of Artemisinin-Resistant *Plasmodium falciparum* Malaria in Eastern India. *New England Journal of Medicine*, 379(20), 1962–1964.

- De Koning-Ward, T. F., Waters, A. P., & Crabb, B. S. (2001). Puromycin-N-acetyltransferase as a selectable marker for use in *Plasmodium falciparum*. *Molecular and Biochemical Parasitology*, 117(2), 155–160.
- Del Giudice, G., Verdini, a S., Pinori, M., Pessi, a, Verhave, J. P., Tougne, C., ... Engers, H. D. (1987). Detection of human antibodies against *Plasmodium falciparum* sporozoites using synthetic peptides. *Journal of Clinical Microbiology*, 25(1), 91–6.
- Dellicour, S., Tatem, A. J., Guerra, C. a, Snow, R. W., & ter Kuile, F. O. (2010). Quantifying the number of pregnancies at risk of malaria in 2007: a demographic study. *PLoS Medicine*, 7(1), e1000221.
- Devlin, A., Mycroft-West, C., Guerrini, M., Yates, E., & Skidmore, M. (2019). Analysis of solid-state heparin samples by ATR-FTIR spectroscopy. *bioRxiv*, , 538074.
- Dickerman, B. K., Elsworth, B., Cobbold, S. A., Nie, C. Q., McConville, M. J., Crabb, B. S., & Gilson, P. R. (2016). Identification of inhibitors that dually target the new permeability pathway and dihydroorotate dehydrogenase in the blood stage of *Plasmodium falciparum*. *Scientific Reports*, 6(1).
- Dionísio, M., & Grenha, A. (2012). Locust bean gum: Exploring its potential for biopharmaceutical applications. *Journal of pharmacy & bioallied sciences*, 4(3), 175–185.
- Dolan, S. A., Miller, L. H., & Wellems, T. E. (1990). Evidence for a switching mechanism in the invasion of erythrocytes by *Plasmodium falciparum*. *The Journal of clinical investigation*, 86(2), 618–624.
- Dolan, S. A., Proctor, J. L., Alling, D. W., Okubo, Y., Wellems, T. E., & Miller, L. H. (1994). Glycophorin B as an EBA-175 independent *Plasmodium falciparum* receptor of human erythrocytes. *Molecular and Biochemical Parasitology*, 64(1), 55–63.
- Dondorp, A. M., Nosten, F., Yi, P., Das, D., Phyto, A. P., Tarning, J., ... White, N. J. (2009). Artemisinin resistance in *Plasmodium falciparum* malaria. *The New England journal of medicine*, 361(5), 455–467.

Drew, D. R., & Beeson, J. G. (2015). PfrH5 as a candidate vaccine for *Plasmodium falciparum* malaria. *Trends in Parasitology*, 31(3), 87–88.

Dunkman, A. A., Buckley, M. R., Mienaltowski, M. J., Adams, S. M., Thomas, S. J., Kumar, A., ... Soslowsky, L. J. (2014). The injury response of aged tendons in the absence of biglycan and decorin. *Matrix biology : journal of the International Society for Matrix Biology*, 35, 232–238.

Dvorin, J. D., Martyn, D. C., Patel, S. D., Grimley, J. S., Collins, C. R., Hopp, C. S., ... Duraisingh, M. T. (2010). A plant-like kinase in *Plasmodium falciparum* regulates parasite egress from erythrocytes. *Science (New York, N.Y.)*, 328(5980), 910–912.

Elabbadi, N., M. Ancelin, and H. Vial. (1992). Use of radioactive ethanolamine incorporation into phospholipids to assess *in vitro* antimalarial activity by the semiautomated microdilution technique. *Antimicrob. Agents Chemother* 36:50–55.

Efficacy and Safety of the RTS,S/AS01 Malaria Vaccine during 18 Months after Vaccination: A Phase 3 Randomized, Controlled Trial in Children and Young Infants at 11 African Sites. (2014). *PLoS Medicine*, 11(7), e1001685.

Embury, S. H., Matsui, N. M., Ramanujam, S., Mayadas, T. N., Noguchi, C. T., Diwan, B. A., . . . Cheung, A. T. W. (2004). The contribution of endothelial cell P-selectin to the microvascular flow of mouse sickle erythrocytes *in vivo*. *Blood*, 104(10), 3378-3385.

English, M., Muambi, B., Mithwani, S., & Marsh, K. (1997). Lactic acidosis and oxygen debt in African children with severe anaemia. *QJM: Monthly Journal of the Association of Physicians*, 90, 563–569.

Evans, S. G., Morrison, D., Kaneko, Y., & Havlik, I. (1998). The effect of curdlan sulphate on development *in vitro* of *plasmodium falciparum*. *Transactions of the Royal Society of Tropical Medicine and Hygiene*, 92(1), 87-89.

Falade, C., Mokuolu, O., Okafor, H., Orogade, A., Falade, A., Adedoyin, O., ... Callahan, M. V. (2007). Epidemiology of congenital malaria in Nigeria: a multi-centre study. *Tropical Medicine & International Health*, 12(11), 1279–1287.

- Feachem, R. G., Phillips, A. A., Hwang, J., Cotter, C., Wielgosz, B., Greenwood, B. M., ... Snow, R. W. (2010). Shrinking the malaria map: progress and prospects. *Lancet* (London, England), 376(9752), 1566–1578.
- Fidock, D. a, Nomura, T., Talley, a K., Cooper, R. a, Dzekunov, S. M., Ferdig, M. T., ... Wellems, T. E. (2000). Mutations in the *P. falciparum* digestive vacuole transmembrane protein PfCRT and evidence for their role in chloroquine resistance. *Molecular Cell*, 6(4), 861–71.
- Fidock, D. A., Nkrumah, L. J., Ghosh, P., Hatfull, G. F., Jacobs, W. R., Moura, P. A., & Muhle, R. A. (2006). Efficient site-specific integration in *plasmodium falciparum* chromosomes mediated by mycobacteriophage Bxb1 integrase. *Nature Methods*, 3(8), 615-621.
- Fraser, J. R. E., Laurent, T. C., & Laurent, U. B. G. (1997). Hyaluronan: its nature, distribution, functions and turnover. *Journal of Internal Medicine*, 242(1), 27–33.
- Fry, M., & Pudney, M. (1992). Site of action of the antimalarial hydroxynaphthoquinone, 2-[trans-4-(4'-chlorophenyl)cyclohexyl]-3-hydroxy-1,4-naphthoquinone (566C80). *Biochemical Pharmacology*, 43(7), 1545–1553.
- Gabius HJ. 2009; The sugar code: Fundamentals of glycosciences. Wiley-VCH; John Wiley distributor, Chichester, UK.
- Gachot, B., & Ringwald, P. (1998). Severe malaria. *La Revue Du Praticien*, 48(3), 273–278.
- Gadalla, N. B., Tavera, G., Mu, J., Kabyemela, E. R., Fried, M., Duffy, P. E., ... Wellems, T. E. (2015). Prevalence of *Plasmodium falciparum* anti-malarial resistance-associated polymorphisms in pfcr, pfmdr1 and pfnhe1 in Muheza, Tanzania, prior to introduction of artemisinin combination therapy. *Malaria Journal*, 14(1), 129.
- Gaillard, T., Madamet, M., & Pradines, B. (2015). Tetracyclines in malaria. *Malaria Journal*, 14(1), 445.
- Gardner, M., Hall, N., Fung, E., White, O., Berriman, M., Hyman, R., ... Barrell, B. (2002). Genome sequence of the human malaria parasite *Plasmodium falciparum*. *Nature*, 419, 498–511.

- Gemma, S., Giovani, S., Brindisi, M., Tripaldi, P., Brogi, S., Savini, L., ... Blackman, M. J. (2012). Quinolylhydrazones as novel inhibitors of *Plasmodium falciparum* serine protease PfSUB1. *Bioorganic & Medicinal Chemistry Letters*, 22(16), 5317–5321.
- Genton, B., D’Acremont, V., Rare, L., Baea, K., Reeder, J. C., Alpers, M. P., & Müller, I. (2008). *Plasmodium vivax* and mixed infections are associated with severe malaria in children: a prospective cohort study from Papua New Guinea. *PLoS Medicine*, 5(6), e127.
- Gerd R. Hetzel, & Christoph Sucker. (2005). The heparins: All a nephrologist should know. *Nephrology, Dialysis, Transplantation : Official Publication of the European Dialysis and Transplant Association - European Renal Association*, 20(10), 2036-2042.
- Gerotziapas, G. T., Petropoulou, A. D., Verdy, E., Samama, M. M., & Elalamy, I. (2007). Effect of the anti-factor xa and anti-factor IIa activities of low-molecular-weight heparins upon the phases of thrombin generation. *Journal of Thrombosis and Haemostasis*, 5(5), 955-962.
- Gill, J., Chitnis, C. E., & Sharma, A. (2009). Structural insights into chondroitin sulphate A binding Duffy-binding-like domains from *Plasmodium falciparum*: implications for intervention strategies against placental malaria. *Malaria journal*, 8, 67.
- Glushakova, S., Busse, B. L., Garten, M., Beck, J. R., Fairhurst, R. M., Goldberg, D. E., & Zimmerberg, J. (2017). Exploitation of a newly-identified entry pathway into the malaria parasite-infected erythrocyte to inhibit parasite egress. *Scientific Reports*, 7(1), 12250-13.
- Goodman, C. D., Su, V., & McFadden, G. I. (2007). The effects of anti-bacterials on the malaria parasite *Plasmodium falciparum*. *Molecular and Biochemical Parasitology*, 152(2), 181–191.
- Gray, E., Mulloy, B., & Barrowcliffe, T.W. (2008). Heparin and low-molecular-weight heparin. *Thrombosis and haemostasis*, 99 5, 807-18.
- Graewe, S., Rankin, K. E., Lehmann, C., Deschermeier, C., Hecht, L., Froehlke, U., ... Heussler, V. (2011). Hostile takeover by Plasmodium: reorganization of parasite and host cell membranes during liver stage egress. *PLoS pathogens*, 7(9), e1002224.

- Greenwood, B. M., Fidock, D. a, Kyle, D. E., Kappe, S. H. I., Alonso, P. L., Collins, F. H., & Duffy, P. E. (2008). Review series Malaria : progress , perils , and prospects for eradication, 118(4).
- Guerra, C. a., Snow, R. W., & Hay, S. I. (2006). Mapping the global extent of malaria in 2005. *Trends in Parasitology*, 22(8), 353–358.
- Gupta, K., Gupta, P., Solovey, A., & Hebbel, R. P. (1999). Mechanism of interaction of thrombospondin with human endothelium and inhibition of sickle erythrocyte adhesion to human endothelial cells by heparin. *Biochimica Et Biophysica Acta (BBA) - Molecular Basis of Disease*, 1453(1), 63-73.
- Hadley, T. J., Klotz, F. W., Pasvol, G., Haynes, J. D., McGinniss, M. H., Okubo, Y., & Miller, L. H. (1987). Falciparum malaria parasites invade erythrocytes that lack glycophorin A and B (MkMk). Strain differences indicate receptor heterogeneity and two pathways for invasion. *The Journal of clinical investigation*, 80(4), 1190–1193.
- Hafalla, J. C., Silvie, O., & Matuschewski, K. (2011). Cell biology and immunology of malaria. *Immunological Reviews*, 240(1), 297–316.
- Halbroth, B. R., & Draper, S. J. (2015). *Recent Developments in Malaria Vaccinology*. *Advances in Parasitology* (Vol. 88). Elsevier Ltd.
- Hasenkamp, S., Wong, E. H., & Horrocks, P. (2012). An improved single-step lysis protocol to measure luciferase bioluminescence in *Plasmodium falciparum*. *Malaria journal*, 11, 42.
- Hati, A. K., Das, S., Roy, S., & Saha, B. (2018). Evidence of artemisinin-resistant *plasmodium falciparum* malaria in eastern india. *The New England Journal of Medicine*, 379(20), 1962-1964.
- Havlik, I., Looareesuwan, S., Vannaphan, S., Wilairatana, P., Krudsood, S., Thuma, P. E., ... Kaneko, Y. (2005). Curdlan sulphate in human severe/cerebral *Plasmodium falciparum* malaria. *Transactions of the Royal Society of Tropical Medicine and Hygiene*, 99(5), 333–340.

Havlik, I., Rovelli, S., & Kaneko, Y. (1994). The effect of curdlan sulphate on in vitro growth of *Plasmodium falciparum*. *Transactions of the Royal Society of Tropical Medicine and Hygiene*, 88(6), 686–687. doi:10.1016/0035-9203(94)90230-5.

Heddini, A., Pettersson, F., Kai, O., Shafi, J., Obiero, J., Chen, Q., ... Marsh, K. (2001). Fresh isolates from children with severe *Plasmodium falciparum* malaria bind to multiple receptors. *Infection and immunity*, 69(9), 5849–5856.

Helen M. Kyriacou, Katie E. Steen, Ahmed Raza, Monica Arman, George Warimwe, Peter C. Bull, . . . J. Alexandra Rowe. (2007). In vitro inhibition of *plasmodium falciparum* rosette formation by curdlan sulfate. *Antimicrobial Agents and Chemotherapy*, 51(4), 1321-1326.

Hill, a. V. S. (2011). Vaccines against malaria. *Philosophical Transactions of the Royal Society B: Biological Sciences*, 366(1579), 2806–2814.

Hirsh, J. (1998). Low-Molecular-Weight Heparin : A Review of the Results of Recent Studies of the Treatment of Venous Thromboembolism and Unstable Angina. *Circulation*, 98(15), 1575–1582.

Hirsh, J., Warkentin, T. E., Shaughnessy, S. G., Anand, S. S., Halperin, J. L., Raschke, R., . . . Dalen, J. E. (2001). Heparin and low-molecular-weight heparin mechanisms of action, pharmacokinetics, dosing, monitoring, efficacy, and safety. *Chest*, 119(1), 94S.

Holder, A. A., Blackman, M. J., Burghaus, P. A., Chappel, J. A., Ling, I. T., McCallum-Deighton, N., & Shai, S.(1992). A malaria merozoite surface protein (MSP1)-structure, processing and function. *Memórias Do Instituto Oswaldo Cruz*, 87(suppl 3), 37–42.

Holmes, M. W., Bayliss, M. T., & Muir, H. (1988). Hyaluronic acid in human articular cartilage. Age-related changes in content and size. *The Biochemical journal*, 250(2), 435–441.

Hopwood, J. J., & Robinson, H. C. (1973). The molecular-weight distribution of glycosaminoglycans. *The Biochemical journal*, 135(4), 631–637.

Horrocks, P., & Lanzer, M. (1998). Transfection of plasmodium: A new chapter in the molecular analysis of malaria. *Parasitology International*, 47(2), 101-106.

- Hu, S., Jiang, W., Li, S., Song, W., Ji, L., Cai, L., & Liu, X. (2015). Fucosylated chondroitin sulphate from sea cucumber reduces hepatic endoplasmic reticulum stress-associated inflammation in obesity mice. *Journal of Functional Foods*, 16, 352-363.
- Huang, N., Wu, M.-Y., Zheng, C.-B., Zhu, L., Zhao, J.-H., & Zheng, Y.-T. (2013). The depolymerized fucosylated chondroitin sulfate from sea cucumber potently inhibits HIV replication via interfering with virus entry. *Carbohydrate Research*, 380, 64–69.
- Hulett, M. D., Freeman, C., Hamdorf, B. J., Baker, R. T., Harris, M. J., & Parish, C. R. (1999). Cloning of mammalian heparanase, an important enzyme in tumor invasion and metastasis. *Nature Medicine*, 5(7), 803–809.
- Hviid, L., & Jensen, A. T. R. (2015). PfEMP1 – A Parasite Protein Family of Key Importance in *Plasmodium falciparum* Malaria Immunity and Pathogenesis. *Advances in Parasitology*, 51–84.
- Idro, R., Jenkins, N. E., & Newton, C. R. J. C. (2005). Pathogenesis, clinical features, and neurological outcome of cerebral malaria. *The Lancet. Neurology*, 4(12), 827–40.
- Iozzo, R. V., & San Antonio, J. D. (2001). Heparan sulfate proteoglycans: heavy hitters in the angiogenesis arena. *The Journal of clinical investigation*, 108(3), 349–355.
- Jacob D. Johnson, Richard A. Denull, Lucia Gerena, Miriam Lopez-Sanchez, Norma E. Roncal, & Norman C. Waters. (2007). Assessment and continued validation of the malaria SYBR green I-based fluorescence assay for use in malaria drug screening. *Antimicrobial Agents and Chemotherapy*, 51(6), 1926-1933.
- James, M. A., & Alger, N. E. (1981). *Plasmodium berghei*: Effect of carrageenan on the course of infection in the A/J mouse. *International Journal for Parasitology*, 11(3), 217-220.
- Trowbridge, J. M., & Gallo, R. L. (2002). Dermatan sulfate: New functions from an old glycosaminoglycan. *Glycobiology*, 12(9), 125R.

Jeremy N Burrows, Stephan Duparc, Winston E Gutteridge, Rob Hooft van Huijsduijnen, Wiweka Kaszubska, Fiona Macintyre, . . . Timothy N C Wells. (2017). New developments in anti-malarial target candidate and product profiles. *Malaria Journal*, 16(1).

Jin Woo Jang, Ju Yeon Kim, Jung Yoon, Soo Young Yoon, Chi Hyun Cho, Eun Taek Han, . . . Chae Seung Lim. (2014). Flow cytometric enumeration of parasitemia in cultures of *plasmodium falciparum* stained with SYBR green I and CD235A. *TheScientificWorldJournal*, 2014, 536723.

Jin, L., Abrahams, J. P., Skinner, R., Petitou, M., Pike, R. N., & Carrell, R. W. (1997). The anticoagulant activation of antithrombin by heparin. *Proceedings of the National Academy of Sciences of the United States of America*, 94(26), 14683–14688.

Kain, K. C., Orlandi, P. A., Haynes, J. D., Sim, K. L., & Lanar, D. E. (1993). Evidence for two-stage binding by the 175-kD erythrocyte binding antigen of *Plasmodium falciparum*. *The Journal of experimental medicine*, 178(5), 1497–1505.

Kantele, A., & Jokiranta, T. S. (2011). Review of cases with the emerging fifth human malaria parasite, *Plasmodium knowlesi*. *Clin Infect Dis*, 52(11), 1356–62.

Kishimoto, T. K., Viswanathan, K., Ganguly, T., Elankumaran, S., Smith, S., Pelzer, K., . . . Sasisekharan, R. (2008). Contaminated heparin associated with adverse clinical events and activation of the contact system. *The New England Journal of Medicine*, 358(23), 2457-2467.

Klein, E. Y. (2013). Antimalarial drug resistance: A review of the biology and strategies to delay emergence and spread. *International Journal of Antimicrobial Agents*, 41(4), 311-317.

Klonis, N., Crespo-Ortiz, M. P., Bottova, I., Abu-Bakar, N., Kenny, S., Rosenthal, P. J., & Tilley, L. (2011). Artemisinin activity against *Plasmodium falciparum* requires hemoglobin uptake and digestion. *Proceedings of the National Academy of Sciences of the United States of America*, 108(28), 11405–11410.

Kobayashi, K., Takano, R., Takemae, H., Sugi, T., Ishiwa, A., Gong, H., . . . Kato, K. (2013). Analyses of interactions between heparin and the apical surface proteins of *plasmodium falciparum*. *Scientific Reports*, 3(1), 3178.

- Köwitsch, A., Zhou, G., & Groth, T. (2018). Medical application of glycosaminoglycans: A review. *Journal of Tissue Engineering and Regenerative Medicine*, 12(1), e41.
- Krishna, S., Uhlemann, a, & Haynes, R. (2004). Artemisinins: mechanisms of action and potential for resistance. *Drug Resistance Updates*, 7(4-5), 233–244.
- Kulane, Asli & Ekre, H.P. & Perlmann, Peter & Rombo, Lars & Wahlgren, Mats & Wahlin, Birgitta. (1992). Effect of Different Fractions of Heparin on *Plasmodium falciparum* Merozoite Invasion of Red Blood Cells in Vitro. *The American journal of tropical medicine and hygiene*. 46. 589-94.
- L J Smeijsters, N M Zijlstra, F F Franssen, & J P Overdulve. (1996). Simple, fast, and accurate fluorometric method to determine drug susceptibility of *plasmodium falciparum* in 24-well suspension cultures. *Antimicrobial Agents and Chemotherapy*, 40(4), 835-838.
- L Xiao, C Yang, P S Patterson, V Udhayakumar, & A A Lal. (1996). Sulfated polyanions inhibit invasion of erythrocytes by plasmodial merozoites and cytoadherence of endothelial cells to parasitized erythrocytes. *Infection and Immunity*, 64(4), 1373-1378.
- Lagerberg, R. (2008). Malaria in Pregnancy: A Literature Review. *Journal of Midwifery & Women's Health*, 53(3), 209–215.
- Lambros, C., & Vanderberg, J. P.(1979). Synchronization of *Plasmodium falciparum* Erythrocytic Stages in Culture. *The Journal of Parasitology*, 65(3), 418.
- Leitgeb, A. M., Blomqvist, K., Cho-Ngwa, F., Samje, M., Nde, P., Titanji, V., & Wahlgren, M. (2011). Low anticoagulant heparin disrupts *plasmodium falciparum* rosettes in fresh clinical isolates. *The American Journal of Tropical Medicine and Hygiene*, 84(3), 390-396.
- Lindahl, U., Lidholt, K., Spillmann, D., & Kjellén, L. (1994). More to “heparin” than anticoagulation. *Thrombosis Research*, 75(1), 1–32.
- Linhardt, R. J., Avci, F. Y., Toida, T., Kim, Y. S., & Cygler, M. (2006). CS lyases: structure, activity, and applications in analysis and the treatment of diseases. *Advances in pharmacology* (San Diego, Calif.), 53, 187–215.

Lunyin Yu, Hari G. Garg, Boyangzi Li, Robert J. Linhardt and Charles A. Hales. (2010) Antitumor Effect of Butanoylated Heparin with Low Anticoagulant Activity on Lung Cancer Growth in Mice and Rats”, *Current Cancer Drug Targets* 10: 229.

Lwin, K. M., Imwong, M., Suangkanarat, P., Jeeyapant, A., Vihokhern, B., Wongsan, K., ... Nosten, F. (2015). Elimination of *Plasmodium falciparum* in an area of multi-drug resistance. *Malaria Journal*, 14(1), 319.

Lyon, J. A., Carter, J. M., Thomas, A. W., & Chulay, J. D. (1997). Merozoite surface protein-1 epitopes recognized by antibodies that inhibit *plasmodium falciparum* merozoite dispersal. *Molecular & Biochemical Parasitology*, 90(1), 223-234.

Lyon, J. A., Thomas, A. W., Hall, T., & Chulay, J. D. (1989). Specificities of antibodies that inhibit merozoite dispersal from malaria-infected erythrocytes. *Molecular & Biochemical Parasitology*, 36(1), 77-85.

Lyth, O., Vizcay-Barrena, G., Wright, K. E., Haase, S., Mohring, F., Najer, A., ... Baum, J. (2018). Cellular dissection of malaria parasite invasion of human erythrocytes using viable *Plasmodium knowlesi* merozoites. *Scientific Reports*, 8(1).

MacKintosh, C. L., Beeson, J. G., & Marsh, K. (2004). Clinical features and pathogenesis of severe malaria. *Trends in Parasitology*, 20(12), 597–603.

Maitland, K. (2015). Management of severe paediatric malaria in resource-limited settings. *BMC Medicine*, 13(1), 42.

Maitland, K., & Newton, C. R. J. C. (2005). Acidosis of severe falciparum malaria: Heading for a shock? *Trends in Parasitology*, 21(1), 11–16.

Mamoun, C. B., Gluzman, I. Y., Goyard, S., Beverley, S. M., & Goldberg, D. E. (1999). A set of independent selectable markers for transfection of the human malaria parasite *plasmodium falciparum*. *Proceedings of the National Academy of Sciences*, 96(15), 8716-8720. doi:10.1073/pnas.96.15.8716

- Mandal, S. (2014). Epidemiological aspects of vivax and falciparum malaria: Global spectrum. *Asian Pacific Journal of Tropical Disease*, 4(Suppl 1), S13–S26.
- Marcum, J. A., McKenney, J. B., Galli, S. J., Jackman, R. W., & Rosenberg, R. D. (1986). Anticoagulant active heparin-like molecules from mast cell-deficient mice. *American Journal of Physiology-Heart and Circulatory Physiology*, 250(5), H879–H888.
- Marin-Mogollon, C., Salman, A. M., Koolen, K. M. J., Bolscher, J. M., van Pul, Fiona J A, Miyazaki, S., . . . Khan, S. M. (2019). A *P. falciparum* NF54 reporter line expressing mCherry-luciferase in gametocytes, sporozoites, and liver-stages. *Frontiers in Cellular and Infection Microbiology*, 9, 96.
- Mark A Skidmore, Khairul Mohd Fadzli Mustaffa, Lynsay C Cooper, Scott E Guimond, Edwin A Yates, & Alister G Craig. (2017). A semi-synthetic glycosaminoglycan analogue inhibits and reverses *plasmodium falciparum* cytoadherence. *PloS One*, 12(10), e0186276.
- Marques, J., Vilanova, E., Mourão, P. A. S., & Fernández-Busquets, X. (2016). Marine organism sulfated polysaccharides exhibiting significant antimalarial activity and inhibition of red blood cell invasion by plasmodium. *Scientific Reports*, 6(1), 24368.
- Marrelli, M. T., Honório, N. A., Flores-Mendoza, C., Lourenco-de-Oliveira, R., Marinotti, O., & Kloetzel, J. K. (1999). Comparative susceptibility of two members of the anopheles oswaldoi complex, an. oswaldoi and an. konderi, to infection by *plasmodium vivax*. *Transactions of the Royal Society of Tropical Medicine and Hygiene*, 93(4), 381-384.
- Martin Smilkstein, Nongluk Sriwilaijaroen, Jane Xu Kelly, Prapon Wilairat, & Michael Riscoe. (2004). Simple and inexpensive fluorescence-based technique for high-throughput antimalarial drug screening. *Antimicrobial Agents and Chemotherapy*, 48(5), 1803-1806.
- Mary Lynn Baniecki, Dyann F. Wirth, & Jon Clardy. (2007). High-throughput plasmodium falciparum growth assay for malaria drug discovery. *Antimicrobial Agents and Chemotherapy*, 51(2), 716-723.
- Maurel, P., Rauch, U., Flad, M., Margolis, R. K., & Margolis, R. U. (1994). Phosphacan, a chondroitin sulfate proteoglycan of brain that interacts with neurons and neural cell-adhesion

molecules, is an extracellular variant of a receptor-type protein tyrosine phosphatase. *Proceedings of the National Academy of Sciences*, 91(7), 2512–2516.

Moxon, C. A., Alhamdi, Y., Storm, J., Toh, J. M., Ko, J. Y., Murphy, G., . . . Toh, C. (2019). Parasite histones mediate leak and coagulopathy in cerebral malaria. *bioRxiv*, , 563551

O'Donnell, R. A., Freitas-Junior, L. H., Preiser, P. R., Williamson, D. H., Duraisingh, M., McElwain, T. F., . . . Crabb, B. S. (2002). A genetic screen for improved plasmid segregation reveals a role for Rep20 in the interaction of *Plasmodium falciparum* chromosomes. *The EMBO journal*, 21(5), 1231–1239.

Menendez, C., Fleming, a. F., & Alonso, P. L. (2000). Malaria-related anaemia. *Parasitology Today*, 16(00), 469–476.

Miller, R. S., Wongsrichanalai, C., Buathong, N., McDaniel, P., Walsh, D. S., Knirsch, C., & Ohrt, C. (2006). Effective treatment of uncomplicated *Plasmodium falciparum* malaria with azithromycin-quinine combinations: a randomized, dose-ranging study. *The American Journal of Tropical Medicine and Hygiene*, 74(3), 401–6.

Mitchell, G. H., Hadley, T. J., McGinniss, M. H., Klotz, F. W., & Miller, L. H. (1986). Invasion of erythrocytes by *plasmodium falciparum* malaria parasites: Evidence for receptor heterogeneity and two receptors. *Blood*, 67(5), 1519-1521.

Mitchell, G., Hadley, T., McGinniss, M., Klotz, F., & Miller, L. (1986). Invasion of erythrocytes by *Plasmodium falciparum* malaria parasites: evidence for receptor heterogeneity and two receptors. *Blood*, 67(5), 1519-1521.

Mohd Ridzuan Mohd Abd Razak, Umi Rubiah Sastu, Nor Azrina Norahmad, Abass Abdul-Karim, Amirrudin Muhammad, Prem Kumar Muniandy, . . . Noor Rain Abdullah. (2016). Genetic diversity of *plasmodium falciparum* populations in malaria declining areas of sabah, east malaysia. *PLoS One*, 11(3), e0152415.

Moorthy, V. S., & Okwo-Bele, J.-M. (2015). Final results from a pivotal phase 3 malaria vaccine trial. *The Lancet*, 6736(15), 15–17.

Munir M, Husada T, Rampengan TH, Mustadjab I, Wulur FH. Paediatr Indones. (1976). Heparin in the treatment of cerebral malaria (a preliminary report). Paediatr Indones. Nov-Dec;16(11-12):489-95.

Muralidharan, V., & Striepen, B. (2015). Teaching old drugs new tricks to stop malaria invasion in its tracks. BMC Biology, 13(1), 72.

Mvé-Ondo, B., Nkoghe, D., Arnathau, C., Rougeron, V., Bisvigou, U., Mouele, L. Y., ... Ollomo, B. (2015). Genetic diversity of *Plasmodium falciparum* isolates from Baka Pygmies and their Bantu neighbours in the north of Gabon. Malaria Journal, 14(1), 395.

N Elabbadi, M L Ancelin, & H J Vial. (1992). Use of radioactive ethanolamine incorporation into phospholipids to assess in vitro antimalarial activity by the semiautomated microdilution technique. Antimicrobial Agents and Chemotherapy, 36(1), 50-55.

Nasamu, A. S., Glushakova, S., Russo, I., Vaupel, B., Oksman, A., Kim, A. S., ... Goldberg, D. E. (2017). Plasmeepsins IX and X are essential and druggable mediators of malaria parasite egress and invasion. Science, 358(6362), 518–522.

Nelson DL, Lehninger AL, Cox MM. (2008); Lehninger principles of biochemistry. Macmillan, New York, USA.

Newton, C. R. J. C., & Krishna, S. (1998). Severe Falciparum Malaria in Children: Current Understanding of Pathophysiology and Supportive Treatment. Pharmacology & Therapeutics, 79(1), 1–53.

Nguansangiam, S., Day, N. P. J., Hien, T. T., Mai, N. T. H., Chaisri, U., Riganti, M., ... Pongponratn, E. (2007). A quantitative ultrastructural study of renal pathology in fatal *Plasmodium falciparum* malaria. Tropical Medicine & International Health : TM & IH, 12(9), 1037–1050.

Orlandi, P. A., Klotz, F. W., & Haynes, J. D. (1992). A malaria invasion receptor, the 175-kilodalton erythrocyte binding antigen of *Plasmodium falciparum* recognizes the terminal Neu5Ac(alpha 2-3)Gal- sequences of glycophorin A. The Journal of cell biology, 116(4), 901–909.

Orton, L. C., & Omari, A. a a. (2008). Drugs for treating uncomplicated malaria in pregnant women. *Cochrane Database of Systematic Reviews (Online)*, (4), CD004912.

Othman, A. S., Marin-Mogollon, C., Salman, A. M., Franke-Fayard, B. M., Janse, C. J., & Khan, S. M. (2017). The use of transgenic parasites in malaria vaccine research. *Expert Review of Vaccines*, 16(7), 685-697.

Pancake, S. J. (1992). Malaria sporozoites and circumsporozoite proteins bind specifically to sulfated glycoconjugates. *The Journal of Cell Biology*, 117(6), 1351–1357.

Pavão, M. S. G. (2002). Structure and anticoagulant properties of sulfated glycosaminoglycans from primitive chordates. *Anais Da Academia Brasileira De Ciencias*, 74(1), 105-112.

Perrimon, N., & Bernfield, M. (2000). Specificities of heparan sulphate proteoglycans in developmental processes. *Nature*, 404(6779), 725–728.

Pino, P., Caldelari, R., Mukherjee, B., Vahokoski, J., Klages, N., Maco, B., ... Soldati-Favre, D. (2017). A multistage antimalarial targets the plasmepsins IX and X essential for invasion and egress. *Science*, 358(6362), 522–528.

Pisano C, Aulicino C, Vesci L et al. (2005) Under sulphated, low-molecular weight glycol-split heparin as an antiangiogenic VEGF antagonist. *Glycobiology*;15:1c–6c.

Polanowska-Grabowska, R., Wallace, K., Field, J. J., Chen, L., Marshall, M. A., Figler, R., ... Linden, J. (2010). P-Selectin–Mediated platelet-neutrophil aggregate formation activates neutrophils in mouse and human sickle cell disease. *Arteriosclerosis, Thrombosis, and Vascular Biology*, 30(12), 2392-2399.

Policy, M., & Committee, A. (2013). Malaria Policy Advisory Committee to the WHO: conclusions and recommendations of March 2013 meeting. *Malaria Journal*, 12(March), 213.

Potchen, M. J., Kampondeni, S. D., Seydel, K. B., Birbeck, G. L., Hammond, C. a, Bradley, W. G., ... Taylor, T. E. (2012). Acute brain MRI findings in 120 Malawian children with cerebral malaria: new insights into an ancient disease. *American Journal of Neuroradiology*, 33(9), 1740–1746.

- Powell AK, Yates EA, Fernig DG, et al. (2004); Interactions of heparin/heparan sulfate with proteins: appraisal of structural factors and experimental approaches. *Glycobiology* 14: 17R–30R.
- Premji, Z., Hamisi, Y., Shiff, C., Minjas, J., Lubega, P., & Makwaya, C. (1995). Anaemia and *Plasmodium falciparum* infections among young children in an holoendemic area, Bagamoyo, Tanzania. *Acta Tropica*, 59(1), 55–64.
- Price, R. N., Tjitra, E., Guerra, C. a., Yeung, S., White, N. J., & Anstey, N. M. (2007). Vivax malaria: Neglected and not benign. *American Journal of Tropical Medicine and Hygiene*, 77(SUPPL. 6), 79–87.
- Rabenstein, D. L. (2002). Heparin and heparan sulfate: structure and function. *Natural Product Reports*, 19(3), 312–331.
- Rajeev K. Mehlotra, Hisashi Fujioka, Paul D. Roepe, Omar Janneh, Lyann M. B. Ursos, Vanessa Jacobs-Lorena, . . . Peter A. Zimmerman. (2001). Evolution of a unique *plasmodium falciparum* chloroquine-resistance phenotype in association with pfcrt polymorphism in papua new guinea and south america. *Proceedings of the National Academy of Sciences of the United States of America*, 98(22), 12689-12694.
- Rampengan TH. (1991). Cerebral malaria in children. Comparative study between heparin, dexamethasone and placebo. *Paediatr Indones*. Jan-Feb;31(1-2):59-66.
- Recuenco, F. C., Kobayashi, K., Ishiwa, A., Enomoto-Rogers, Y., Fundador, N. G. V., Sugi, T., . . . Kato, K. (2014). Gellan sulfate inhibits *plasmodium falciparum* growth and invasion of red blood cells in vitro. *Scientific Reports*, 4(1), 4723.
- Reed, M. B., Saliba, K. J., Caruana, S. R., Kirk, K., & Cowman, a F. (2000). Pgh1 modulates sensitivity and resistance to multiple antimalarials in *Plasmodium falciparum*. *Nature*, 403(6772), 906–909.
- Renu Goonewardene, Johanna Daily, David Kaslow, Terrence J. Sullivan, Patrick Duffy, Richard Carter, . . . Dyann Wirth. (1993). Transfection of the malaria parasite and expression

of firefly luciferase. Proceedings of the National Academy of Sciences of the United States of America, 90(11), 5234-5236.

Rieckmann KH, Campbell GH, Sax LJ, Mrema JE. (1978). Drug sensitivity of *Plasmodium falciparum* : an in-vitro microtechnique. Lancet 1(8054): 22–23.

Robert Kisilevsky, Ian Crandall, Walter A. Szarek, Shridhar Bhat, Christopher Tan, Lee Boudreau, & Kevin C. Kain. (2002). Short-chain aliphatic polysulfonates inhibit the entry of plasmodium into red blood cells. Antimicrobial Agents and Chemotherapy, 46(8), 2619-2626.

Rogerson, S. J., Reeder, J. C., Al-Yaman, F., and Brown, G. V. (1994). Sulfated glycoconjugates as disrupters of *Plasmodium falciparum* erythrocyte rosettes. American Journal of Tropical Medicine and Hygiene 51, 198–203.

Rowe A, Berendt AR, Marsh K et al. (1994). *Plasmodium falciparum*: a family of sulphated glycoconjugates disrupts erythrocyte rosettes. Exp Parasitol;79:506–16.

Saiwaew, S., Sritabal, J., Piaraksa, N., Keayarsa, S., Ruengweerayut, R., Utaisin, C., . . . Craig, A. (2017). Effects of sevuparin on rosette formation and cytoadherence of *plasmodium falciparum* infected erythrocytes. PLoS One, 12(3)

Sandra Hasenkamp, Adam Sidaway, Oliver Devine, Richard Roye, & Paul Horrocks. (2013). Evaluation of bioluminescence-based assays of anti-malarial drug activity. Malaria Journal, 12(1), 58.

Schantz-Dunn, J., & Nour, N. M. (2009). Malaria and pregnancy: a global health perspective. Reviews in Obstetrics & Gynecology, 2(3), 186–92.

Schlagenhauf, P., Blumentals, W. a, Suter, P., Regep, L., Vital-Durand, G., Schaerer, M. T., . . . Adamcova, M. (2012). Pregnancy and fetal outcomes after exposure to mefloquine in the pre- and periconception period and during pregnancy. Clinical Infectious Diseases: An Official Publication of the Infectious Diseases Society of America, 54(11), e124–31.

Shi, Y. P., Hasnain, S. E., Sacci, J. B., Holloway, B. P., Fujioka, H., Kumar, N., . . . Lal, a a. (1999). Immunogenicity and in vitro protective efficacy of a recombinant multistage

Plasmodium falciparum candidate vaccine. Proceedings of the National Academy of Sciences of the United States of America, 96(4), 1615–20.

Shukla, D., Liu, J., Blaiklock, P., Shworak, N. W., Bai, X., Esko, J. D., ... Spear, P. G. (1999). A Novel Role for 3-O-Sulfated Heparan Sulfate in Herpes Simplex Virus 1 Entry. *Cell*, 99(1), 13–22.

Sim, B., Chitnis, C., Wasniowska, K., Hadley, T., & Miller, L. (1994). Receptor and ligand domains for invasion of erythrocytes by *Plasmodium falciparum*. *Science*, 264(5167), 1941–1944.

Sinka, M. E., Bangs, M. J., Manguin, S., Rubio-Palis, Y., Chareonviriyaphap, T., Coetzee, M., ... Hay, S. I. (2012). A global map of dominant malaria vectors. *Parasites & Vectors*, 5(1), 69.

Skidmore, M. A., Dumax-Vorzet, A. F., Guimond, S. E., Rudd, T. R., Edwards, E. A., Turnbull, J. E., ... Yates, E. A. (2008). Disruption of rosetting in *Plasmodium falciparum* Malaria with chemically modified heparin and low molecular weight derivatives possessing reduced anticoagulant and other serine protease inhibition activities. *Journal of Medicinal Chemistry*, 51(5), 1453-1458.

Skidmore, M. A., Kajaste-Rudnitski, A., Wells, N. M., Guimond, S. E., Rudd, T. R., Yates, E. A., & Vicenzi, E. (2015). Inhibition of influenza H5N1 invasion by modified heparin derivatives. *MedChemComm*, 6(4), 640-646.

Smith, A. D., Bradley, D. J., Smith, V., Blaze, M., Behrens, R. H., Chiodini, P. L., & Whitty, C. J. M. (2008). Imported malaria and high risk groups: observational study using UK surveillance data 1987-2006. *BMJ (Clinical Research Ed.)*, 337(jul03_2), a120.

Smitskamp, H., & Wolthuis, F. H. (1971). New concepts in treatment of malignant tertian malaria with cerebral involvement. *British medical journal*, 1(5751), 714–716.

Snow, R. W., Trape, J. F., & Marsh, K. (2001). The past, present and future of childhood malaria mortality in Africa. *Trends in Parasitology*, 17(12), 593–597.

Stern, R., Asari, A., & Sugahara, K. (2006). Hyaluronan fragments: An information-rich system. *European Journal of Cell Biology*, 85(8), 699–715.

Suzanne L. Fleck, Berry Birdsall, Jeffrey Babon, Anton R. Dluzewski, Stephen R. Martin, William D. Morgan, . . . Anthony A. Holder. (2003). Suramin and suramin analogues inhibit merozoite surface protein-1 secondary processing and erythrocyte invasion by the malaria parasite *plasmodium falciparum*. *Journal of Biological Chemistry*, 278(48), 47670-47677.

Tang, F., Chen, F., & Li, F. (2013). Preparation and potential in vivo anti-influenza virus activity of low molecular-weight κ -carrageenans and their derivatives. *Journal of Applied Polymer Science*, 127(3), 2110-2115. doi:10.1002/app.37502

Tangpukdee, N., Thanachartwet, V., Krudsood, S., Luplertlop, N., Pornpininworakij, K., Chalermrut, K., ... Wilairatana, P. (2006). Minor liver profile dysfunctions in *Plasmodium vivax*, *P. malariae* and *P. ovale* patients and normalization after treatment. *The Korean Journal of Parasitology*, 44(4), 295–302.

Telen, M. J., Batchvarova, M., Shan, S., Bovee-Geurts, P. H., Zennadi, R., Leitgeb, A., . . . Lindgren, M. (2016). Sevuparin binds to multiple adhesive ligands and reduces sickle red blood cell-induced vaso-occlusion. *British Journal of Haematology*, 175(5), 935-948.

Theron, M., Hesketh, R. L., Subramanian, S., & Rayner, J. C. (2010). An adaptable two-color flow cytometric assay to quantitate the invasion of erythrocytes by *plasmodium falciparum* parasites. *Cytometry. Part A: The Journal of the International Society for Analytical Cytology*, 77(11), 1067-1074.

Thomas, O., Lybeck, E., Strandberg, K., Tynngård, N., & Schött, U. (2015). Monitoring low molecular weight heparins at therapeutic levels: Dose-responses of, and correlations and differences between aPTT, anti-factor xa and thrombin generation assays. *PLoS ONE*, 10(1).

Tilley, L., Dixon, M. W. A., & Kirk, K. (2011). The *Plasmodium falciparum*-infected red blood cell. *The International Journal of Biochemistry & Cell Biology*, 43(6), 839–842.

Trager, W., & Jensen, J. (1976). Human Malaria Parasites in Continuous Culture. *Science*, 193(4254), 673-675.

- Trampuz, A., Jereb, M., Muzlovic, I., & Prabhu, R. M. (2003). Clinical review: Severe malaria. *Critical Care (London, England)*, 7(4), 315–323.
- Tun, K. M., Imwong, M., Lwin, K. M., Win, A. A., Hlaing, T. M., Hlaing, T., ... Woodrow, C. J. (2015). Spread of artemisinin-resistant *Plasmodium falciparum* in Myanmar: a cross-sectional survey of the K13 molecular marker. *The Lancet Infectious Diseases*, 15(4), 415–421.
- Tun, K. M., Imwong, M., Lwin, K. M., Win, A. A., Hlaing, T. M., Hlaing, T., ... Woodrow, C. J. (2015). Spread of artemisinin-resistant *plasmodium falciparum* in myanmar: A cross-sectional survey of the K13 molecular marker. *The Lancet Infectious Diseases*, 15(4), 415-421.
- Uchimura, K. (2014). Keratan Sulfate: Biosynthesis, Structures, and Biological Functions. *Glycosaminoglycans*, 389–400.
- Udomsangpetch R , Wåhlin B , Carlson J , Berzins K , Torii M , Aikawa M , Perlmann P , Wahlgren M , 1989 . Plasmodium falciparum -infected erythrocytes form spontaneous erythrocyte rosettes . *J Exp Med* 169: 1835 – 1840
- Ullah, I., Sharma, R., Biagini, G. A., & Horrocks, P. (2017). A validated bioluminescence-based assay for the rapid determination of the initial rate of kill for discovery antimalarials. *The Journal of Antimicrobial Chemotherapy*, 72(3), 717.
- Van Dijk, M. R., Vinkenoog, R., Ramesar, J., Vervenne, R. A. W., Waters, A. P., & J. Janse, C. (1997). Replication, expression and segregation of plasmid-borne DNA in genetically transformed malaria parasites. *Molecular & Biochemical Parasitology*, 86(2), 155-162.
- Viswanathan, K., Guerrini, M., Buhse, L., Torri, G., Venkataraman, G., Al-Hakim, A., . . . Lansing, J. C. (2008). Oversulfated chondroitin sulfate is a contaminant in heparin associated with adverse clinical events. *Nature Biotechnology*, 26(6), 669-675.
- Volpi, N. (2007). Analytical aspects of pharmaceutical grade chondroitin sulfates. *Journal of Pharmaceutical Sciences*, 96(12), 3168–3180.
- Von Itzstein, M., Plebanski, M., Cooke, B. M., & Coppel, R. L. (2008). Hot, sweet and sticky: the glycobiology of *Plasmodium falciparum*. *Trends in Parasitology*, 24(5), 210–218.

Walenga, J. M., Jeske, W. P., Prechel, M. M., Bacher, P., & Bakhos, M. (2004). Decreased prevalence of heparin-induced thrombocytopenia with low-molecular-weight heparin and related drugs. *Seminars in Thrombosis and Hemostasis*, 30(S 1), 69-80.

Walker, N. F., Nadjm, B., & Whitty, C. J. M. (2014). *Malaria. Medicine*, 42(2), 100–106.

Wang, W., Zhang, P., Hao, C., Zhang, X., Cui, Z., & Guan, H. (2011). *In vitro* inhibitory effect of carrageenan oligosaccharide on influenza A H1N1 virus. *Antiviral research*, 92 2, 237-46.

Warkentin, T. E., Levine, M. N., Hirsh, J., Horsewood, P., Roberts, R. S., Gent, M., & Kelton, J. G. (1995). Heparin-induced thrombocytopenia in patients treated with low-molecular-weight heparin or unfractionated heparin. *N Engl J Med*, 332(20), 1330-1336.

Watt, G., Jongsakul, K., & Ruangvirayuth, R. (2002). A pilot study of N-acetylcysteine as adjunctive therapy for severe malaria. *QJM : Monthly Journal of the Association of Physicians*, 95(5), 285–90.

Weatherall, D. J., Miller, L. H., Baruch, D. I., Marsh, K., Doumbo, O. K., Casals-Pascual, C., & Roberts, D. J. (2002). Malaria and the red cell. *Hematology / the Education Program of the American Society of Hematology. American Society of Hematology. Education Program*, 35–57.

Weigel, P. H., & DeAngelis, P. L. (2007). Hyaluronan Synthases: A Decade-plus of Novel Glycosyltransferases. *Journal of Biological Chemistry*, 282(51), 36777–36781.

Weiss, G. E., Gilson, P. R., Taechalertpaisarn, T., Tham, W., de Jong, Nienke W M, Harvey, K. L., . . . Crabb, B. S. (2015). Revealing the sequence and resulting cellular morphology of receptor-ligand interactions during *plasmodium falciparum* invasion of erythrocytes. *PLoS Pathogens*, 11(2), e1004670.

White, J., Lindgren, M., Liu, K., Gao, X., Jendeberg, L., & Hines, P. (2019). Sevuparin blocks sickle blood cell adhesion and sickle-leucocyte rolling on immobilized I-selectin in a dose dependent manner. *British Journal of Haematology*, 184(5), 873-876.

White, N. J., Pukrittayakamee, S., Hien, T. T., Faiz, M. A., Mokuolu, O. a., & Dondorp, A. M. (2014). Malaria. *The Lancet*, 383(9918), 723–735.

Wildhagen, Karin C. A. A, García de Frutos, P., Reutelingsperger, C. P., Schrijver, R., Aresté, C., Ortega-Gómez, A., . . . Nicolaes, G. A. F. (2014). Nonanticoagulant heparin prevents histone-mediated cytotoxicity in vitro and improves survival in sepsis. *Blood*, 123(7), 1098-1101.

Wickramasinghe, S. N., & Abdalla, S. H. (2000). Blood and bone marrow changes in malaria. *Best Practice & Research Clinical Haematology*, 13(2), 277–299.

Wong, E. H., Hasenkamp, S., & Horrocks, P. (2011). Analysis of the molecular mechanisms governing the stage-specific expression of a prototypical housekeeping gene during intraerythrocytic development of *P. falciparum*. *Journal of Molecular Biology*, 408(2), 205-221.

Woodrow, C. J. (2005). Artemisinins. *Postgraduate Medical Journal*, 81(952), 71–78.

WHO., 2012. World Malaria Report. Available at https://www.who.int/malaria/publications/world_malaria_report_2012/report/en/

WHO., 2018. World Malaria Report. Available at <https://www.who.int/malaria/publications/world-malaria-report-2018/report/en/>

Yimin Wu, C. David Sifri, Hsien-Hsien Lei, Xin-zhuan Su, & Thomas E. Wellems. (1995). Transfection of *plasmodium falciparum* within human red blood cells. *Proceedings of the National Academy of Sciences of the United States of America*, 92(4), 973-977.

Yoshida, T., Yasuda, Y., Mimura, T., Kaneko, Y., Nakashima, H., Yamamoto, N., & Uryu, T. (1995). Synthesis of curdlan sulfates having inhibitory effects in vitro against AIDS viruses HIV-1 and HIV-2. *Carbohydrate Research*, 276(2), 425-436.

Yuan, H., Song, J., LI, X., LI, N., & Dai, J. (2006). Immunomodulation and antitumor activity of κ -carrageenan oligosaccharides. *Cancer Letters*, 243(2), 228–234.

Yvonne Adams, Craig Freeman, Reinhard Schwartz-Albiez, Vito Ferro, Christopher R. Parish, & Katherine T. Andrews. (2006). Inhibition of *plasmodium falciparum* growth *in vitro* and adhesion to chondroitin-4-sulfate by the heparan sulfate mimetic PI-88 and other sulfated oligosaccharides. *Antimicrobial Agents and Chemotherapy*, 50(8), 2850-2852.

Appendix 1 (chapter 5) showing growth inhibition data (luciferase growth inhibition assay) and PC1 of sulphated GAGs at three concentration in (Dd2^{luc} and NF54^{luc}) strains (Pages: 216-218).

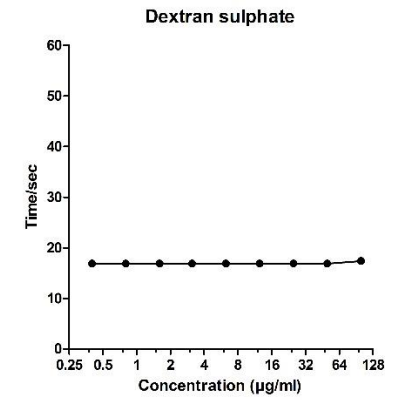
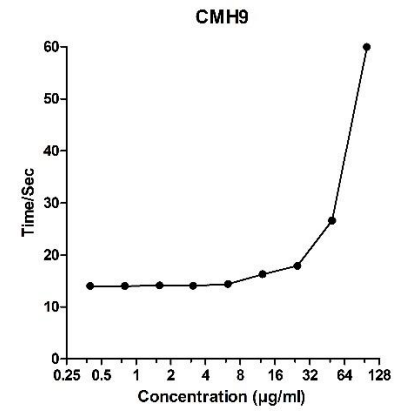
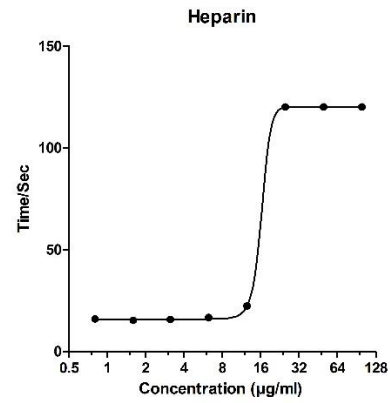
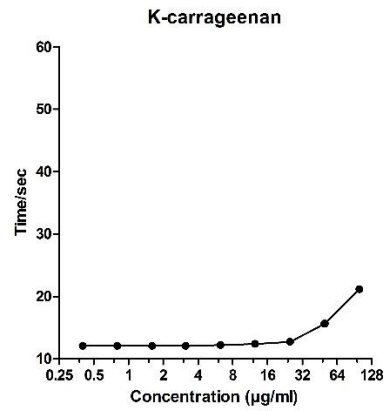
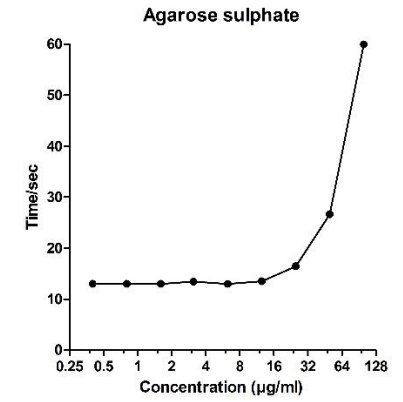
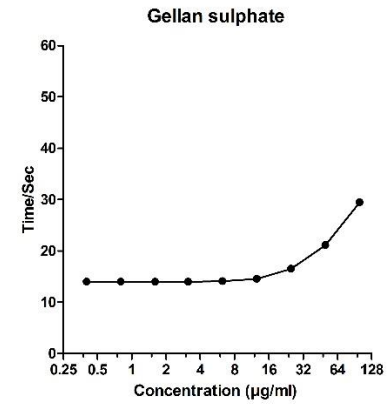
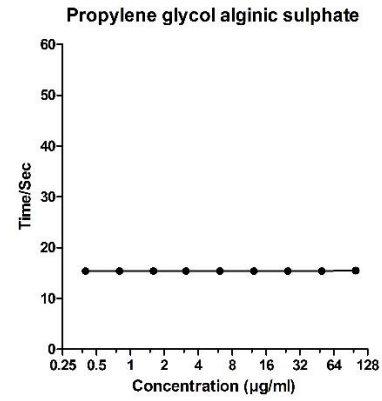
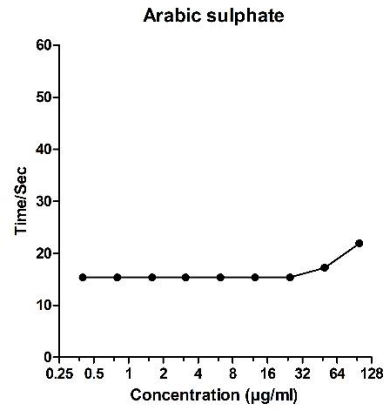
Appendix II (chapter 5) showing aPTT and PT data of sulphated of Sulphated GAG (Pages:219-220).

GAG	Strain	% Mean normalized growth when exposed to the following concentration of GAG (ug/ml)			PC1		Strain	% Mean normalized growth when exposed to the following concentration of GAG (ug/ml)			PC1
		100.0	33.3	11.1				100.0	33.3	11.1	
Ghatti sulphate	Dd2 ^{luc}	8.9	61.7	84.3		21.1	NF54 ^{luc}	1.8	45.4	79.9	37.6
(Hydroxypropyl)methyl cellulose sulphate	Dd2 ^{luc}	66.1	69.2	73.1		-20.5	NF54 ^{luc}	98.5	106.5	103.1	-76.7
Gellan sulphate	Dd2 ^{luc}	0.7	8.3	72.1		63.9	NF54 ^{luc}	1.2	1.3	24.3	83.9
Xanthan sulphate	Dd2 ^{luc}	20.0	67.4	83.6		9.9	NF54 ^{luc}	14.7	64.9	79.5	16.6
Locust Bean Gum sulphate	Dd2 ^{luc}	98.4	91.9	93.7		-64.4	NF54 ^{luc}	84.6	95.1	97.5	-57.9
Pectin sulphate	Dd2 ^{luc}	39.1	85.3	108.5		-23.1	NF54 ^{luc}	75.2	84.8	93.8	-43.6
Gum Mastic	Dd2 ^{luc}	17.0	53.9	67.0		26.0	NF54 ^{luc}	33.3	82.2	102.9	-15.1
Carboxymethyl cellulose sulphate	Dd2 ^{luc}	115.0	115.8	110.9		-96.8	NF54 ^{luc}	112.8	111.1	104.9	-90.3
Agarose sulphate	Dd2 ^{luc}	0.3	11.3	72.1		62.4	NF54 ^{luc}	1.2	3.4	52.1	73.3
Arabic sulphate	Dd2 ^{luc}	0.7	22.0	88.9		49.9	NF54 ^{luc}	1.0	7.1	61.3	68.0
Amylose sulphate	Dd2 ^{luc}	10.3	73.9	91.2		10.3	NF54 ^{luc}	1.4	47.3	69.6	40.2
Hypromellose sulphate	Dd2 ^{luc}	70.4	95.0	98.8		-48.1	NF54 ^{luc}	64.9	79.3	94.7	-33.1
Glycogen Type II sulphate	Dd2 ^{luc}	95.0	98.0	99.2		-67.6	NF54 ^{luc}	82.9	94.2	93.2	-54.6
Pullulan sulphate	Dd2 ^{luc}	17.1	48.9	91.5		20.7	NF54 ^{luc}	1.7	28.8	66.0	52.7
Levan sulphate	Dd2 ^{luc}	2.7	35.6	101.5		35.9	NF54 ^{luc}	1.5	11.6	64.7	63.8
Paramylon sulphate	Dd2 ^{luc}	101.0	100.0	101.3		-73.8	NF54 ^{luc}	82.8	97.2	104.4	-60.2
Fucogalactan sulphate	Dd2 ^{luc}	17.8	43.6	83.9		26.0	NF54 ^{luc}	2.2	57.0	80.8	30.0

K-carrageenan	Dd2 ^{luc}	11.9	18.0	56.1		55.3		NF54 ^{luc}	1.2	2.8	40.6		77.5
Welan sulphate	Dd2 ^{luc}	1.2	55.3	84.1		30.5		NF54 ^{luc}	1.0	29.3	57.5		55.7
Propylene glycol alginic sulphate	Dd2 ^{luc}	14.0	19.9	76.6		45.8		NF54 ^{luc}	0.8	1.4	21.9		84.9
Tara sulphate	Dd2 ^{luc}	30.2	92.8	117.9		-24.5		NF54 ^{luc}	1.1	37.4	51.6		52.6
DEXTRAN sulphate	Dd2 ^{luc}	11.4	30.4	46.0		51.4		NF54 ^{luc}	0.5	14.2	71.4		60.7
Chondroitin Sulphate A	Dd2 ^{luc}	86.8	89.9	92.2		-54.4		NF54 ^{luc}	98.3	91.3	115.7		-71.3
Chondroitin Sulphate C	Dd2 ^{luc}	108.0	100.3	109.7		-81.8		NF54 ^{luc}	119.3	103.7	112.4		-92.9
Hyaluronic acid	Dd2 ^{luc}	97.2	110.3	104.5		-78.6		NF54 ^{luc}	110.8	126.9	120.2		-103.7
Heparin	Dd2 ^{luc}	4.9	37.4	87.3		37.9		NF54 ^{luc}	7.9	42.6	67.9		39.1
CMH1	Dd2 ^{luc}	16.0	34.2	75.8		35.9		NF54 ^{luc}	8.8	39.1	68.6		40.4
CMH2	Dd2 ^{luc}	27.0	60.2	84.3		9.2		NF54 ^{luc}	58.2	84.3	88.8		-29.5
CMH3	Dd2 ^{luc}	89.0	100.6	97.7		-64.5		NF54 ^{luc}	76.3	86.3	94.8		-45.6
CMH4	Dd2 ^{luc}	8.2	45.4	112.0		22.4		NF54 ^{luc}	36.4	65.4	81.2		0.2
CMH5	Dd2 ^{luc}	117.5	116.0	116.4		-100.5		NF54 ^{luc}	100.0	104.7	101.8		-76.2
CMH6	Dd2 ^{luc}	102.6	103.0	98.2		-75.7		NF54 ^{luc}	101.6	102.5	101.6		-75.9
CMH7	Dd2 ^{luc}	12.3	30.6	51.1		48.9		NF54 ^{luc}	12.2	53.0	64.8		30.7
CMH8	Dd2 ^{luc}	81.9	95.7	99.0		-56.8		NF54 ^{luc}	91.8	105.8	101.1		-70.8
CMH9	Dd2 ^{luc}	0.3	2.5	55.9		73.3		NF54 ^{luc}	0.2	0.2	13.3		88.9
Heparin	Dd2 ^{luc}	3.6	32.5	77.8		45.1		NF54 ^{luc}	7.9	42.6	67.9		39.1
ARIXTRA	Dd2 ^{luc}	18.3	110.5	106.2		-23.0		NF54 ^{luc}	26.4	87.3	94.5		-10.6

REVAPARIN	Dd2 ^{luc}	52.9	93.4	88.1		-31.1		NF54 ^{luc}	11.5	56.2	67.2		28.4
ENOXAPARIN	Dd2 ^{luc}	65.1	108.8	103.7		-54.5		NF54 ^{luc}	21.3	67.3	72.5		12.7
TINZAPARIN	Dd2 ^{luc}	1.3	50.3	85.4		33.2		NF54 ^{luc}	0.3	24.8	57.5		58.9
DALTEPARIN	Dd2 ^{luc}	23.1	89.8	106.0		-13.6		NF54 ^{luc}	7.5	51.9	67.4		33.8
Heparin	Dd2 ^{luc}	4.9	37.4	87.3		37.9		NF54 ^{luc}	7.9	42.6	67.9		39.1

PT



aPTT

